UNIVERSITÄTSKLINIKUM HAMBURG-EPPENDORF

Kopf- und Neurozentrum
Klinik und Poliklinik für Mund-, Kiefer- und Gesichtschirurgie

Univ.-Prof. Dr. med. Dr. med. dent. Martin Gosau

Aktivierung, Funktionalisierung sowie Evaluierung resorbierbarer Biomaterialien auf Seidenbasis im Bereich der Regeneration und Wundheilung in der Mund-, Kiefer- und Gesichtschirurgie

Dissertation

zur Erlangung des Doktorgrades Dr. rer. biol. hum.
an der Medizinischen Fakultät der Universität Hamburg

vorgelegt von:

Sandra Fuest
aus Aachen

Hamburg 2024

Angenommen von der
Medizinischen Fakultät der Universität Hamburg am: **12.12.2024**

Veröffentlicht mit Genehmigung der
Medizinischen Fakultät der Universität Hamburg:

Prüfungsausschuss, der/die Vorsitzende: **Univ.-Prof. Dr. Dr. Ralf Smeets**

Prüfungsausschuss, zweite/r Gutachter/in: **Univ.-Prof. Dr. Dr. Thomas Beikler**

Prüfungsausschuss, dritte/r Gutachter/in: **Univ.-Prof. Dr. Dr. Alexander Eckert**

Für meine Eltern

Mit Geduld und Zeit wird aus
dem Maulbeerbaum ein Seidenkleid.

Karl Simrock

Gender Disclaimer

„Das in dieser Arbeit gewählte generische Maskulinum bezieht sich zugleich auf die männliche, die weibliche und andere Geschlechteridentitäten.“

Danksagung

An dieser Stelle möchte ich mich bei all den Menschen bedanken, die mich während der Zeit meiner Dissertation und der Erstellung dieser Arbeit unterstützt und begleitet haben.

Danken möchte ich in erster Linie Univ.-Prof. Dr. Dr. Ralf Smeets, der mich als mein Doktorvater und Mentor stets in all meinen Ideen bestärkt hat und immer ein offenes Ohr für meine Fragen und Probleme hatte. Durch seine enorme Geduld und sein Vertrauen in mich hat er meinen beruflichen Werdegang maßgeblich mitgestaltet und dafür bin ich ihm sehr dankbar. Darüber hinaus hat er es mir ermöglicht, mich national und international zu vernetzen, wovon ich persönlich sehr profitiert habe. Ein weiterer Dank gilt den beiden weiteren Mitgliedern meines Thesis-Komitees, Univ.-Prof. Dr. Dr. Thomas Beikler und Prof. Dr. Christian Apel, die mich stets bei meinem Vorhaben unterstützt haben und immer hilfreiche Ratschläge für mich hatten.

Weiterhin möchte ich mich bei allen Co-Autoren der im Rahmen dieser Doktorarbeit entstandenen Publikationen für die gute wissenschaftliche Zusammenarbeit bedanken. Ein besonderer Dank gilt PD Dr. Dr. Franz Ricklefs, Audrey Laure Céline Grust und Dr.-Ing. Alexander Kopp für den stets hilfreichen Austausch und das Vertrauen in mich. M.Sc. Thomas Derra danke ich für die hilfreiche Unterstützung bei der Erstellung der Grafiken im Rahmen dieser Dissertation.

Meinen Kollegen der Mund-, Kiefer- und Gesichtschirurgie und der Sektion für Regenerative Orofaziale Medizin danke ich für den konstruktiven wissenschaftlichen und privaten Austausch. Insbesondere danken möchte ich Univ.-Prof. Dr. Dr. Martin Gosau für die gute Aufnahme ins Team.

Mein Dank geht außerdem an meine beiden lieben Freundinnen M.Sc. Leonie Früh und M.Sc. Vanessa Klein, welche mir in vielen Punkten und stressigen Zeiten die nötige Ruhe und Unterstützung gegeben haben und immer ein offenes Ohr für meine Fragen und Probleme hatten.

Mein größter Dank gilt mit Abstand meinen Eltern, die mir stets in all meinen Lebenssituationen zur Seite stehen und immer ermöglichen jeden Weg einzuschlagen, der sich mir eröffnet. Ohne euch wäre das alles nicht möglich, danke dafür!

Publikationsliste

Fuest, S., Smeets, R., Gosau, M., Aavani, F., Knipfer, C., Grust, A. L. C., Kopp, A., Becerikli, M., Behr, B., & Matthies, L. (**2023**).

Layer-by-Layer Deposition of Regenerated Silk Fibroin–An Approach to the Surface Coating of Biomedical Implant Materials. ACS biomaterials science & engineering, 9(12), 6644–6657.

- **Submission history:**
- Received: 26 June 2023
- Revised: 29 October 2023
- Accepted: 2 November 2023
- Published online: 20 November 2023

Schäfer, S., Smeets, R., Köpf, M., Drinic, A., Kopp, A., Kröger, N., Hartjen, P., Assaf, A. T., Aavani, F., Beikler, T., Peters, U., Fiedler, I., Busse, B., Stürmer, E. K., Vollkommer, T., Gosau, M., & **Fuest, S.** (**2022**).

Antibacterial properties of functionalized silk fibroin and sericin membranes for wound healing applications in oral and maxillofacial surgery. Biomaterials advances, 135, 212740.

- **Submission history:**
- Received: 9 November 2021
- Revised: 13 February 2022
- Accepted: 25 February 2022
- Available online: 17 March 2022

Schäfer, S., Aavani, F., Köpf, M., Drinic, A., Stürmer, E. K., **Fuest, S.**, Grust, A. L. C., Gosau, M., & Smeets, R. (**2023**).

Silk proteins in reconstructive surgery: Do they possess an inherent antibacterial activity? A systematic review. Wound repair and regeneration: official publication of the Wound Healing Society [and] the European Tissue Repair Society, 31(1), 99–110.

- **Submission history:**
- Received: 31 May 2022
- Revised: 25 August 2022
- Accepted: 6 Septemeber 2022
- Published: 15 September 2022

Fuest, S., Salviano-Silva, A., Maire, C. L., Xu, Y., Apel, C., Grust, A. L. C., Delle Coste, A., Gosau, M., Ricklefs, F. L., & Smeets, R. (**2024**).

Doping of casted silk fibroin membranes with extracellular vesicles for regenerative therapy: a proof of concept. Scientific reports, 14(1), 3553.

- **Submission history:**
- Received: 15 December 2023
- Revision received: 15 January 2024
- Accepted: 7 February 2024
- Published: 12 February 2024

Zusammenfassung

Innovative Biomaterialkonzepte nehmen heutzutage eine immer einflussreichere Rolle im medizinischen Sektor ein. Dabei zählen zu den wichtigsten Anforderungen eine exzellente Biokompatibilität, Non-Toxizität, gute mechanische Eigenschaften und im besten Fall eine Resorbierbarkeit nach erfolgreicher Implantation. Da diese Eigenschaften von synthetischen Materialien oder Metallwerkstoffen nicht oder nur teilweise erfüllt werden, rücken Biomaterialien natürlichen Ursprungs vermehrt in den Fokus der aktuellen Forschung. Besonders im breit gefächerten Arbeitsgebiet der Mund-, Kiefer- und Gesichtschirurgie gehört der Einsatz von regenerativen Biomaterialien nach Traumata, chirurgischen Eingriffen oder ästhetischen Anwendungen zum Standardverfahren, um die Regeneration und Wundheilung nachhaltig zu fördern und zu optimieren.

Im Rahmen dieser Dissertation wurden Seidenproteine von den Kokons des Maulbeerseidenpinners Bombyx mori (*B. mori*) umfassend charakterisiert und evaluiert. Dazu wurden die beiden Proteine Fibroin und Sericin durch einen schonenden Löseprozess isoliert und im Anschluss versatil in Formen wie Membranen oder Vliese überführt. Die Vorteile von Seidenfibroin als Biomaterial sind seine hohe Festigkeit, Feuchtigkeitsspeicherung, Flexibilität, Biokompatibilität, Bioresorbierbarkeit, Sauerstoffdurchlässigkeit und hämostatische Fähigkeit. Des Weiteren ist die Degradations- und Freisetzungskinetik von Produkten aus Seidenfibroin exakt steuerbar. Der Grundstein dieser Arbeit liegt auf der experimentellen *in-vitro*-Studie, welche sich mit reiner Fibroinlösung als innovative Beschichtungstechnik von Implantatmaterialien auseinandersetzt und diese in Hinblick auf die Minimierung möglicher Fremdkörperabstoßungsreaktionen hin untersucht. Ein weiterer Schwerpunkt liegt auf der Beurteilung des antibakteriellen Verhaltens von Seidenstrukturen in der oralen Wundheilung. Hier werden Seidenmembranen und –vliese mittels Gentamicin und Silber funktionalisiert und in Verbindung mit dem oralen Mikrobiom gebracht, um eine spätere klinische Anwendung als Wundauflage in der Mund-, Kiefer- und Gesichtschirurgie zu realisieren. Da sich die Kombination von Additiven und seidenfibroinhaltigen Trägerstrukturen als vielversprechender Ansatz für den Bereich der Wundheilung und Regeneration herauskristallisiert hat, wird in einem letzten Schritt eine gezogene Fibroinmembran mit Extrazellulären Vesikeln (EVs) funktionalisiert, um die Regeneration im Kopf-Hals-Bereich mit Hilfe eines bioaktiven resorbierbaren Materials nachhaltig zu verbessern.

Abstract

Innovative biomaterial concepts are playing an increasingly influential role in the medical sector today. The most important requirements include excellent biocompatibility, non-toxicity, good mechanical properties and, in the best case, absorbability after successful implantation. As these properties are not or only partially fulfilled by synthetic materials or metal materials, biomaterials of natural origin are increasingly becoming the focus of current research. The use of regenerative biomaterials after trauma, surgical interventions or aesthetic applications is a standard procedure, particularly in the broadly diversified field of oral and maxillofacial surgery, in order to sustainably promote and optimise regeneration and wound healing.

As part of this dissertation, silk proteins from the cocoons of the mulberry silkworm Bombyx mori (*B. mori*) were comprehensively characterised and evaluated. For this purpose, the two proteins fibroin and sericin were isolated by a gentle dissolution process and subsequently versatilised into forms such as membranes or nonwovens. The advantages of silk fibroin as a biomaterial are its high strength, moisture retention, flexibility, biocompatibility, bioresorbability, oxygen permeability and haemostatic ability. Furthermore, the degradation and release kinetics of silk fibroin products can be precisely controlled. The cornerstone of this work is the experimental in-vitro study, which deals with pure fibroin solution as an innovative coating technique for implant materials and examines it with regard to the minimisation of possible foreign body rejection reactions. Another focus is on the evaluation of the antibacterial behaviour of silk structures in oral wound healing. Here, silk membranes and fleeces are functionalised using gentamicin and silver and brought into contact with the oral microbiome in order to realise a later clinical application as a wound dressing in oral and maxillofacial surgery. As the combination of additives and silk fibroin-containing carrier structures has emerged as a promising approach for the area of wound healing and regeneration, the final step will be to functionalise a pulled fibroin membrane with extracellular vesicles (EVs) in order to sustainably improve regeneration in the head and neck area with the help of a bioactive resorbable material.

Abbildungsverzeichnis

Tabellenverzeichnis

Abkürzungsverzeichnis

Beta – β

Bombyx mori – *B. mori*

Colony Forming Unit – CFU

Desoxyribonukleinsäure – DANN

Enzyme-linked-immunosorbet assay – ELISA

Extrazelluläre Vesikel – EV

Extrazellulärmatrix – EZM

Fluoresceindiacetat – FDA

Fourier-Transform-Infrarotspektroskopie – FTIR

Fötales Rinderserum – FBA

Gingiva-Fibroblasten – GF

Glutaraldehydlösung – GA

Guided Bone Regeneration – GBR

Guided Tissue Regeneration – GTR

Gute Herstellungspraxis – GMP

Kohlenstoffdioxid – CO_2

Layer-by-Layer – LbL

Optische Dichte – OD

Partielle Thromboplastinzeit – PTT

Plasmaelektroylische Oxidation – PEO

Poly(ethylene oxide) – PEO

Poly-Methyl-Metha-Crylat – PMMA

Polyvinylalkohol – PVA

Propidiumjiodid – PI

Rasterelektronenmikroskopie – REM

Reaktive Sauerstoffspezies – ROS

Real Time Quantitative PCR – qrt-PCR

Sauerstoff – O_2

Silbernanopartikeln – AGNPs

Silbernitratlösung – $AGNO_3$

Staphylococcus aureus – S. aureus

Ultra-Violett – UV

Voll-entsalztes-Wasser – VE-Wasser

Water vapor transmission – WVT

Zone of inhibition – ZOI

Inhaltsverzeichnis

1 Einleitung

Seide ist eine natürliche Hochleistungsfaser und gewinnt als innovatives Biomaterial seit einigen Jahren vor allem im Bereich der biomedizintechnischen Forschung immer mehr an Bedeutung (Jindal *et al.*, 2014; Fitzpatrick *et al.*, 2021; Parivatphun *et al.*, 2022). Besonders die Seide der domestizierten Maulbeerspinnerraupe *B. mori*, welche sich ausschließlich von den Blättern des Maulbeerbaumes ernährt, ist kommerziell breit verfügbar und findet am häufigsten Anwendung in der Medizintechnik. Als resorbierbare Alternative zu herkömmlichen Materialien wie Kollagen oder Bio-Polymeren vereint Seide zahlreiche Vorteile wie eine versatile Weiterarbeitung und exzellente Biokompatibilität bei sehr guter mechanischer Festigkeit (Santin *et al.*, 1999; Zuo, Dai and Wu, 2006; Seo *et al.*, 2007; Kopp, Schunck, *et al.*, 2020; Jaya Prakash, Wang and Kandasubramanian, 2023). Produziert von bestimmten Insekten- und Spinnentierarten hat Seide bereits eine lange Tradition in der Textilindustrie (Naskar, R. R. Barua, *et al.*, 2014). Dabei besteht Rohseide aus zwei parallelen Fibroinfasern (hydrophob und wasserunlöslich), welche von einer kompakten, äußeren Schicht aus Seidensericin (wasserlösliches Protein) ummantelt wird (Zhou *et al.*, 2001; Altman *et al.*, 2003; Jin *et al.*, 2005; Kopp, Schunck, *et al.*, 2020). Die aus den Kokons des *B. mori* gewonnene Seide besitzt nicht nur enorme Zugfestigkeiten von bis zu 740 MPa, sondern weist darüber hinaus weitere biologische Schlüsselkomponenten wie eine verminderte Immunogenität und eine einstellbare biologische Degradation auf (Shao and Vollrath, 2002; Zuo, Dai and Wu, 2006; Kopp *et al.*, 2019a; Kopp, Schunck, *et al.*, 2020). Abbildung 1 stellt schematisch die Wertschöpfungskette des *B. mori* und die anschließende Überführung der Seidenkokons in die Medizintechnik dar. In der Biomedizinischen Technik kann Seide sowohl im unveränderten, natürlichen Zustand als auch in verändertem, regenerierten Zustand zur Anwendung kommen (Koh *et al.*, 2015a; Kopp, Schunck, *et al.*, 2020). Neben Nahtmaterialien oder Wundverbänden kann Seide als weitere Komponente im Bereich des *Tissue Engineering* eingesetzt werden (Kundu *et al.*, no date; Wray *et al.*, 2011; Zhu *et al.*, 2011; Kasoju and Bora, 2012a; Farè *et al.*, 2013; Kuboyama *et al.*, 2013; Koh *et al.*, 2015a; Kopp, Schunck, *et al.*, 2020). Nach der Regeneration und Verarbeitung von Seide in reines Fibroin können daraus verschiedenste 2D- und 3D-Modelle (unter anderem Filme, Schäume und makroporöse Schwämme) hergestellt werden, welche ein breites Anwendungsspektrum abdecken und insbesondere als Ersatz menschlichen Gewebes wie Knorpel, Hornhaut, Knochen oder Haut angewendet werden (Nazarov, Rina; Jin, Hyoung-Joon; kaplan, 2004; Yang *et al.*, 2007; Chao *et al.*, 2010; Harkin *et al.*, 2011a; Zhu *et al.*, 2014; Bhardwaj *et al.*, 2015; Koh *et al.*, 2015a; Kopp, Schunck, *et al.*, 2020; Kopp, Smeets, *et al.*, 2020, 2020).

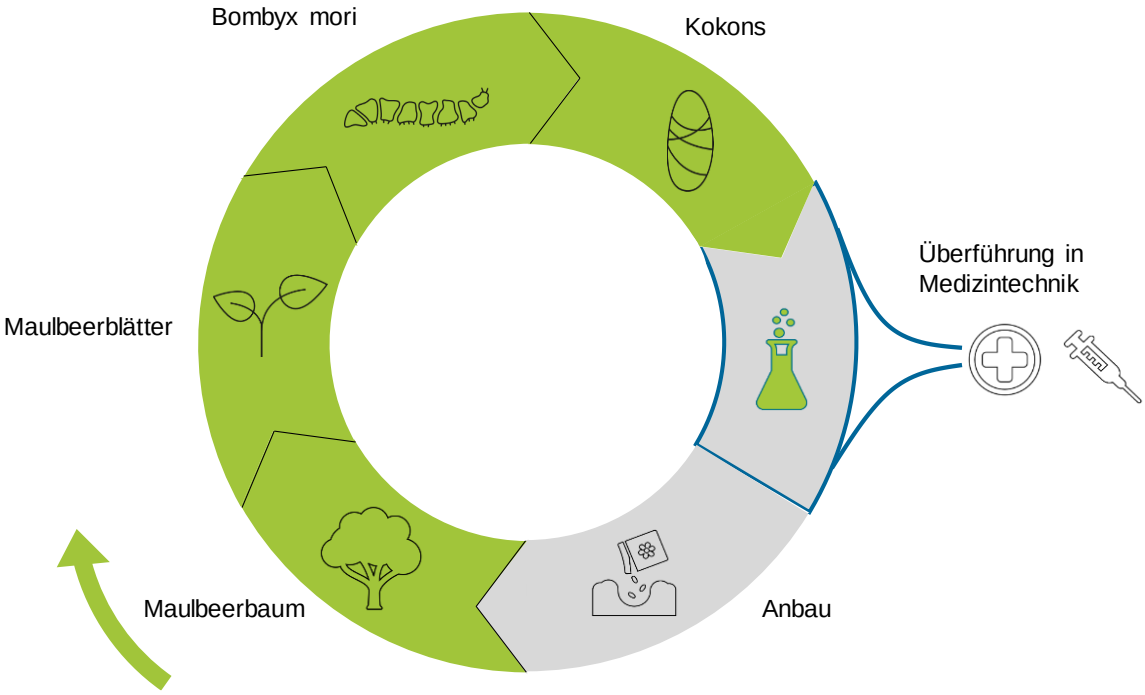

Abbildung 1: Eigene Darstellung der Wertschöpfungskette von Seidenkokons des Maulbeerseidenspinners *B. mori* in Anlehnung an Fibrothelium GmbH (*Fibrothelium GmbH*, 2022).

Besonders aufgrund des immerwährenden Fortschritts im Bereich der modernen Medizin nimmt der Bereich der Regeneration und Wundheilung sowie die Wiederherstellung der Funktionalität von verloren gegangenem Gewebe eine zunehmend wichtigere Rolle ein (Chouhan and Mandal, 2020).

Vor allem Defekte im Bereich der Rekonstruktion von Weichgewebe oder Knochen, z.B. nach einer Tumor-/ Traumaoperation, weisen aufgrund der Morbidität des Patientenkollektivs eine hohe Prävalenz für eine verlangsamte oder ausbleibende Geweberegeneration auf. Aktuelle Präparate zeigen sich sowohl im Handling, der Stabilität, als auch in der Stimulation der Geweberegeneration nicht für jede Indikation ideal, sodass letztendlich oft ein autologes Transplantat, d.h. die Entnahme gesunden Gewebes an anderer Stelle im Körper, der Goldstandard bleibt. Deshalb sollen auf Basis von funktionalisiertem Seidenfibroin, welches sich im Körper auflöst (resorbiert) und durch stimuliertes Zielgewebe ersetzt wird, verschiedene Produkte für die Regeneration und Wundheilung getestet werden, welche durch geeignete Herstellungsverfahren selbstexpandierend wirken und eine individuell anwendungsbezogene Porosität bzw. Stabilität, sowie stimulierende Eigenschaften aufweisen (Wenk, Merkle and Meinel, 2011; Kasoju and Bora, 2012a; Wang and Zhang, 2013; Sun *et al.*, 2014; Luo *et al.*, 2015; Thangavel *et al.*, 2017; Wang, Liu and Fan, 2017; Cheng *et al.*, 2018; Smeets, Henningsen, *et al.*, 2022).

Zur Beantwortung der Forschungsfrage dieser kumulativen Dissertation wurden vier Studien publiziert, welche sich mit der Charakterisierung von Seidenfibroin sowohl in Form einer wässrigen Lösung als auch in unterschiedlichen Ausprägungen mit verschiedensten Funktionalisierungen beschäftigen.

In Fuest et. al. 2023 lag der Schwerpunkt auf der Biologisierung von verschiedenen Implantatoberflächen mittels regeneriertem Seidenfibroin als zukunftsorientierte Möglichkeit zur Optimierung der Osseointegration im Weichgewebsinterface (Fuest *et al.*, 2023). Basierend auf ausgewählten Prozessparametern konnte in dieser experimentellen *in-vitro*-Studie eine gleichmäßige und homogene Schicht aus Seidenfibroin auf verschiedenen Implantatmaterialien (Titan, Magnesium und Poly-Methyl-Metha-Crylat (PMMA)) durch eine sogenannte *Layer-by-Layer* Beschichtungstechnik erzielt werden und diese mikroskopisch und in der Zellkultur charakterisiert und evaluiert werden (Fuest *et al.*, 2023).

In Schaefer et. al. (Schäfer *et al.*, 2022) wurden Vliese und Membranen auf Seidenbasis antibakteriell mit Silberionen und Gentamicin beladen und für den Einsatz in der Mund-, Kiefer- und Gesichtschirurgie/ Oralchirurgie/ Implantologie evaluiert. Aus Seidenfibroin gegossene Membranen und elektrogesponnene Vliese wurden auf ihre Biokompatibilität und antibakterielle Wirksamkeit gegen typische Erreger der Mundflora (u.a. *Streptococcus mutans*) untersucht (Schäfer *et al.*, 2022). Im Rahmen eines systematischen Reviews wurde die Fragestellung untersucht, ob die beiden Seidenproteine Fibroin und Sericin intrinsische antibakterielle Eigenschaften besitzen oder wie das Biomaterial entsprechend funktionalisiert werden kann, um diese Eigenschaften langfristig zu erzielen (Schäfer *et al.*, 2023).

In einer weiterführenden Studie nach Fuest et. al. 2024 (Fuest *et al.*, 2024) lag der Fokus auf der Erforschung einer *proof-of-concept*-Verbundstruktur in Form einer Fibroin-Membran und Extrazellulären Vesikeln (EVs) aus einer immortalisierten Gingivafibroblasten-Zelllinie für den regenerativen Ansatz im Kopf-Hals-Bereich. Hierbei lag das Hauptaugenmerk auf der Evaluierung der Möglichkeit, native EVs in ein resorbierbares Biomaterial einzubetten und dies zu charakterisieren.

Publikationsübergreifend werden im Rahmen dieser Dissertation die Ergebnisse in Bezug auf die zugehörigen Forschungsfragen umfangreich evaluiert und diskutiert. Im Anschluss daran wird ein Fazit gezogen und Empfehlungen für die zukünftige Arbeit gegeben.

2 Grundlagen

2.1 Seidenarten

Seide wird von den unterschiedlichsten Insekten- und Spinnenarten produziert, um Netze oder Kokons für den Metamorphosezyklus herzustellen (Harkin *et al.*, 2011b). Die Kokonseide des Maulbeerseidenspinners *B. mori* gehört zu den bekanntesten Seidenarten weltweit und stammt aus der Familie der *bombycidae*, welche gemeinsam mit der Familie der *saturniidae* zu den am häufigsten verwendeten Seidenarten gehört (Harkin *et al.*, 2011b; Meng, Zhu and Chen, 2017). Domestiziert wurde die Seidenraupe vom Wildseidenspinner *Bombyx mandarina*, der vor allem im Norden Indiens, Nordchina, Korea, Japan und den fernöstlichen Regionen Russlands zu finden ist. Das Alleinstellungsmerkmal des *B. mori* liegt in der einfachen Zucht der Raupen und Ernährung durch die Blätter des Maulbeerbaums.

Der Metamorphosezyklus des Seidenspinners vom Ei zum ausgebildeten Kokon beginnt mit dem Legen der Eier (Naskar, R.R. Barua, *et al.*, 2014; Li *et al.*, 2023). Dabei legt der weibliche Falter zwischen 300-400 Eier, die er bereits beim Schlupf aus dem Kokon im Hinterleib trägt und die während der Puppenruhe heranreifen. Das Weibchen signalisiert seine Paarungsbereitschaft durch Austreten eines Duftmoleküls aus dem Hinterleib. Nach erfolgreicher Partnersuche erfolgt die Befruchtung der Eier durch das Faltermännchen (Omenetto and Kaplan, 2010; Wang, Liu and Fan, 2017). Die Eier werden anschließend für rund zehn Tage inkubiert bis die Larven schlüpfen, welche dann für ca. 30 Tage ausschließlich mit den Blättern des Maulbeerbaums gefüttert werden. Sobald die Larven sich zu einer Raupe entwickelt haben, beginnt die Seidenproduktion und damit der Aufbau der Kokons. Bemerkenswert ist, dass die Spinndrüsen mehr als die Hälfte des Körpergewichts der Raupe ausmachen. Durch gezielte Kopfbewegungen beim Austreten des Materials legt der *B. mori* Windung für Windung einen Faden um seinen Körper. Dabei spannt die Raupe zuerst elastische Haltefäden, dann schlingt sie den Faden in der Form einer „Acht“ um ihre eigene Achse. Dieser Vorgang wiederholt sich bis zu 230.000 Mal, bis die Struktur des Kokons vollständig ausgebildet ist (Drinic, 2019).

Der Kokon selbst besteht dabei nur aus einem einzigen Faden, der je nach Größe eine Länge zwischen 700-1500 Metern annehmen kann (Ude *et al.*, 2014; Drinic, 2019). Um den Kokon vollständig auszubilden dauert es zwei bis drei Tage. Der Kokon bietet in erster Linie Schutz vor Fressfeinden und Witterungsverhältnissen. Nach 15-20 Tagen ist der Falter ausgewachsen und produziert ein chemisches Lösungsmittel, mit dem er den Kokon lokal zerfressen und schlüpfen kann. Danach beginnt der Zyklus von neuem (Takeda, 2009; Anitha,

2011; Ude *et al.*, 2014; Colomban and Jauzein, 2018; Drinic, 2019). Abbildung 2 stellt den Methamorphosezyklus des *B. mori* vom Ei bis zum Falter noch einmal grafisch dar.

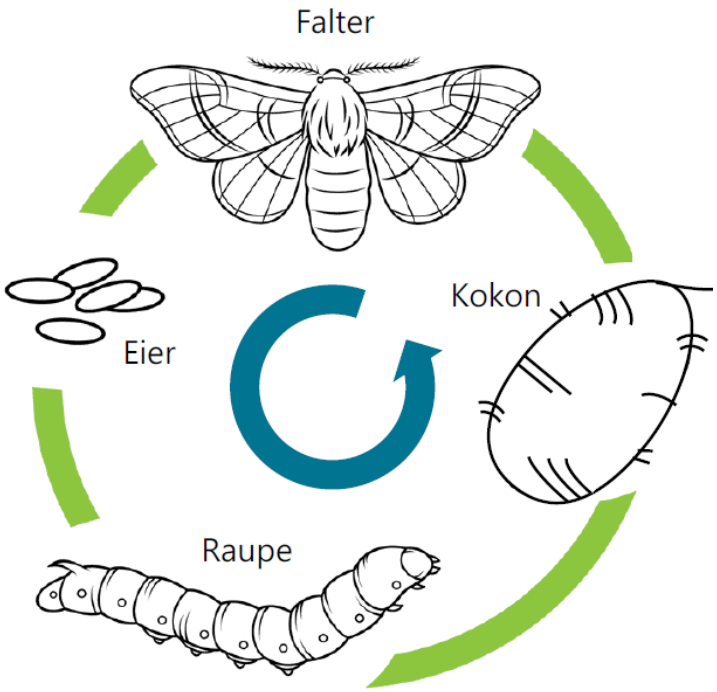

Abbildung 2: Eigene Darstellung des Lebenszyklus des *B. mori* angelehnt an (Omenetto and Kaplan, 2010; Wang *et al.*, 2017).

2.2 Synthese und Morphologie der Seide des *B. mori*

Das verspinnbare Seidenmaterial wird zuerst durch dünne Ausführungsgänge zu der im Kopfbereich gelegenen Spinnwarze und von dort aus dem Körper geleitet. Das Spinnorgan selbst besteht dabei aus zwei großen Drüsen, die seitlich unter dem Nahrungskanal angelegt sind (s. Abb. 3 (A)). Der Drüsenapparat besteht aus einem vielfach gewundenen Schlauch, der in die drei Segmente untergliedert werden kann (Nwekwo, 2015; Drinic, 2019):

- *Posterior* (15 cm, 500 Sekretionszellen, Fibroin-Ausscheidung)
- *Median* (7 cm, 300 Sektetionszellen, Sericin-Ausscheidung)
- *Anterior* (2 cm, 25 Sekretionszellen, Sericin-Ausscheidung)

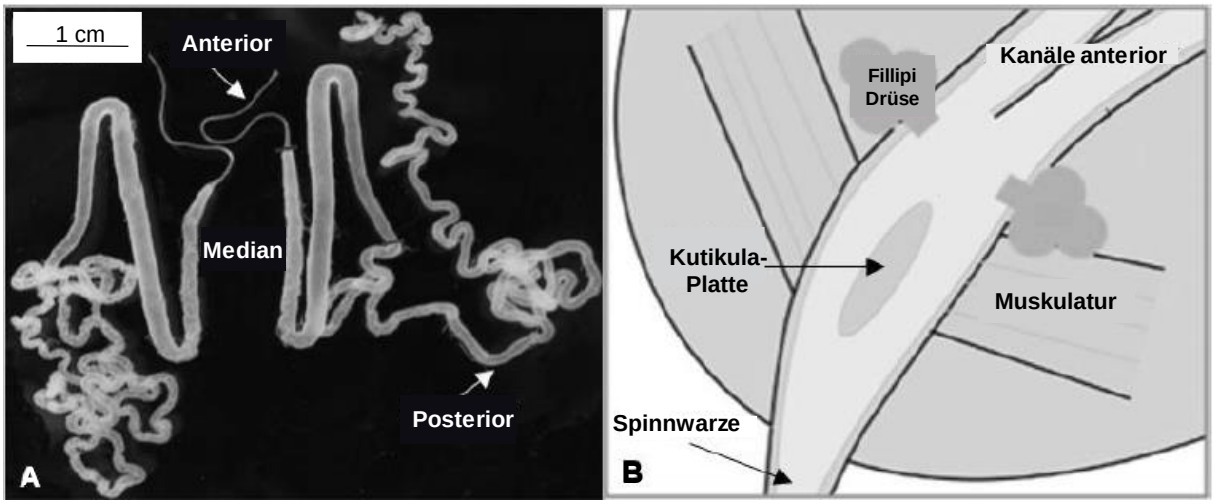

Abbildung 3: Aufbau des Drüsenapparats: (A) Aufbau der einzelnen Drüsensegmente; (B) Schematischer Aufbau der Spinndüse (Fang *et al.*, 2015).

In den *posterioren* Segmenten werden die *heavy*- und *light-chain*-Abschnitte des Fibroins und das Glykoprotein P25 synthetisiert, welches die Selbstassemblierung des Fibroins und den intrazellulären Transport unterstützt (Asakura *et al.*, 2007; Drinic, 2019). Das Protein Fibroin wird anschließend in den *median*-Abschnitt weitergeleitet. Hier werden die ersten Sericin-Proteine synthetisiert. Dabei wird die Synthese des Sericins durch das *anteriore* Segment ergänzt und kleidet das Fibroin bei dem eigentlichen Spinnvorgang aus (Naskar, R. R. Barua, *et al.*, 2014; Fang *et al.*, 2015; Drinic, 2019). Der Spinnkanal selbst wird aus der Drüse *anterior* und der Spinndüse zusammengesetzt. Die *anterioren* Kanäle münden in einem großen Kanal, in welchem die zwei sogenannten Filippi-Drüsen liegen (s. Abb. 3 (B)). Die genaue Funktion derer ist umstritten, es wird angenommen, dass diese die Umgebungstemperatur einstellen, um die einzelnen synthetisierten Seiden-Bestandteile zusammenzufügen. Der eigentliche Spinndruck wird über eine dorsal und ventral gelegene Muskulatur reguliert. Zentral im Lumen befindet sich die *Kutikula*-Platte (Sutherland *et al.*, 2010; Wang *et al.*, 2016; Drinic, 2019). Entlang des Segments *anterior* wird der pH-Wert der Spinnlösung durch eine Vielzahl von Protonenpumpen gehemmt, welche eine moderate Ionenkonzentration im Lumen erzeugen und den Wasseranteil regulieren (Andersson, Johansson and Rising, 2016). Durch die hohe Viskosität kann ein kontinuierlicher Spinnprozess ohne Kapillaraufbruch gewährleistet werden (Sutherland *et al.*, 2010).

Die Struktur der Seide besteht aus zwei natürlichen Proteinen. Neben zwei parallel verlaufenden Fibroinfasern wird die Seidenfaser von Sericin, einem kleberartigen Protein, zusammengehalten und erhält dadurch seine Form und Struktur (Cao and Wang, 2009; Koh *et al.*, 2015b). Der Rohseidenfaden weist einen Durchmesser zwischen 15-25 µm auf. Die prozentualen Anteile an Proteinen in jeder einzelnen Seidenfaser betragen zwischen 70 –

80 % bei Fibroin und 20 – 50 % bei Sericin (Sobajo *et al.*, 2008; Kopp *et al.*, 2019a). Während Sericin einen hydrophilen und amorphen Charakter hat und wasserlösliche Eigenschaften besitzt, weist Seidenfibroin eine nanofibrillenartige hydrophobe Proteinstruktur auf, welche aus drei Komponenten besteht, die für Flexibilität, Elastizität und Integrität sorgen (Cao and Wang, 2009; Hardy and Scheibel, 2010; Naskar, R.R. Barua, *et al.*, 2014). Neben dem hydrophoben *heavy chain* (*h.c.*) Fibroin, welches unter anderem für die Ausbildung der Beta-Faltblattstruktur verantwortlich ist, wird die Struktur ergänzt durch das *light chain* (*l.c.*) Fibroin und das P25-Glycoprotein (P25). Das *l.c.* Fibroin ist in seinem molekularen Aufbau hydrophil und über eine Disulfid-Brückenbindung mit dem *h.c.* Fibroin verbunden (Molverhältnis zwischen *h.c.* – *l.c.* – P25: 6:6:1) (Tanaka, Inoue and Mizuno, 1999; Horan *et al.*, 2005; Cao and Wang, 2009; Hardy and Scheibel, 2010; Naskar, R.R. Barua, *et al.*, 2014). In Abbildung 4 ist der Aufbau der Fibroin-Komposition noch einmal schematisch dargestellt.

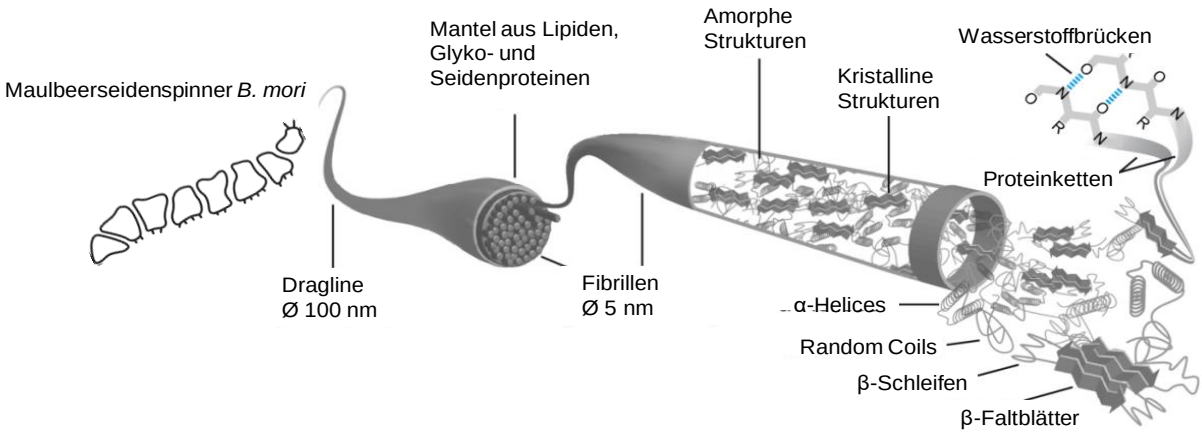

Abbildung 4: Eigene Darstellung der Fibroin-Komposition in Anlehnung an Lang 2015 (Gregor Lang, 2015).

2.1.2 Materialeigenschaften der Seide

Seide weist im Vergleich zu anderen biologischen Materialien zahlreiche positive mechanische und biologische Eigenschaften auf, detailliert aufgelistet in Tabelle 1. Die Seidenfaser weist eine Zugfestigkeit von 300 – 740 MPa auf und zeigt sich mit diesen mechanischen Kennwerten robuster als Kevlar (Poly-Paraphenylen-Terephthalamid) oder Nylon (Hardy and Scheibel, 2010; Kundu *et al.*, 2013a; Koh *et al.*, 2015b; Kopp *et al.*, 2019a; Kopp, Schunck, *et al.*, 2020). Dabei wird die Festigkeit und Steifigkeit der Seide hauptsächlich durch die Beta-Faltblattstruktur bestimmt, dessen Bestandteile in erster Linie Wasserstoffbrückenbindungen, *Van-der-Vaals*-Kräfte sowie hydrophobe Wechselwirkungen sind (Koh *et al.*, 2015a; Shen *et al.*, 2018; Yin *et al.*, 2021; Yu *et al.*, 2021; Smeets, Tauer, *et al.*, 2022). Darüber hinaus

variieren die mechanischen Werte je nach Varianz der Eigenschaften des Kokons, da diese als natürliches Produkt immer anders ausfallen. Nach Studien von Liivak et. al. 1998 (Liivak *et al.*, 1998) besteht eine log-lineare Beziehung zwischen der Struktur einer einzelnen Seidenfaser und seinen mechanischen Eigenschaften (Liivak *et al.*, 1998). Ausgehend von diesen beeindruckenden mechanischen Eigenschaften kann die Familie der Seidenproteine für eine ganze Reihe von Materialoptionen versatil verwendet werden (Altman *et al.*, 2003). Wichtig zu erwähnen ist jedoch, dass die mechanischen Kennwerte in regenerierten Seidenfibroin-Strukturen deutlich niedriger sind als dies bei Rohseide der Fall ist. Der Grund hierfür liegt in der mangelnden Ausbildung der Sekundärstruktur (Beta (β) – Faltblätter) sowie einer instabileren Proteinstruktur insgesamt (Cao and Wang, 2009; Kundu *et al.*, 2013a; Kopp, Smeets, *et al.*, 2020). Gerade in regenerierten Seidenstrukturen findet sich vermehrt die sogenannte Silk I-Konfiguration wieder, in welcher amorphe Bereiche sowie nicht erkennbare β-Faltblatt-Bereiche dominieren (Kopp *et al.*, 2019a; Kopp, Schunck, *et al.*, 2020; Kopp, Smeets, *et al.*, 2020). Die mechanische Festigkeit von regenerierten Seidenstrukturen resultiert jedoch aus den kristallinen Bereichen und der Sekundärstruktur der Polypeptidketten (Silk II-Konfiguration) (Kopp, Smeets, *et al.*, 2020). Diese kann unter anderem durch eine chemische Nachbehandlung (Alkohole wie zum Beispiel Ethanol (C_2H_5OH) oder Methanol (CH_3OH)) erzielt werden, in welcher die Sekundärstruktur in die β-Faltblattanordnung konvertiert wird und sich bisher nicht vernetzte Polypeptidketten zu kristallinen Bereichen umwandeln. Diese Nachbehandlung resultiert in wasserunlöslichen Fibroinstrukturen, wodurch sich die Steifigkeit und Bruchrate erhöht (Kim *et al.*, 2003; Bayraktar *et al.*, 2005; Ha, Tonelli and Hudson, 2005; Danielle N Rockwood *et al.*, 2011; Numata, 2014; Kopp *et al.*, 2019a; Kopp, Smeets, *et al.*, 2020; Schäfer *et al.*, 2022; Fuest *et al.*, 2023). Alternative Methoden wie die Einwirkung von Wasserdampf über einen gewissen Zeitraum erhöhen ebenfalls den Kristallinitätsgrad des Fibroins und überführen die Seiden in einen wasserunlöslichen Zustand (Chen *et al.*, 2006; Jiang *et al.*, 2007; Kopp, Smeets, *et al.*, 2020; Fuest *et al.*, 2023). Um die mechanischen Eigenschaften von Fibroin für regenerative Anwendungen zu optimieren, bieten der Literatur zufolge die Additivierung natürliche Polymere wie Hyaluronsäure, Chitosan und Alginate immer mehr Alternativen (Um *et al.*, 2001; D.-H. Roh *et al.*, 2006; Garcia-Fuentes *et al.*, 2008; Lu *et al.*, 2008; Arnon *et al.*, 2015; Srivastava *et al.*, 2015). Darüber hinaus können hygroskopische Weichmacher (*Plasticizers*) wie Sorbitol, Glycerol und Glucose die Stabilität des Fibroins mit einhergehender Flexibilität deutlich erhöhen (Srivastava *et al.*, 2015).

Seide und im besonderen Fibroin als Biomaterial erweist sich als äußerst biokompatibles Protein (Altman *et al.*, 2003). Ein Biomaterial ist dabei „*…jede Substanz (außer einem Arzneimittel) oder Kombination von Substanzen synthetischen oder natürlichen Ursprungs, die jederzeit als Ganzes oder als Teil eines Systems verwendet werden kann, das ein Gewebe,*

ein Organ oder eine Funktion des Körpers behandelt, ergänzt oder ersetzt“ (Recum and Laberge, 1995; Cao and Wang, 2009). Seidenfibroin wurde besonders wegen seiner kontrollierbaren proteolytischen (pH-neutralen) Abbaubarkeit, seiner Fülle an versatilen Formen und seiner Biokompatibilität vor allem im biomedizinischen Bereich umfassend untersucht (Horan *et al.*, 2005; Wang *et al.*, 2008; Biggi *et al.*, 2020). Resultierend konnte festgestellt werden, dass es sich um ein biologisches, harmloses und ungiftiges, nicht zytotoxisches Naturmaterial handelt (Wadbua *et al.*, 2010; Kasoju and Bora, 2012c; Li and Li, 2014; Wong, Chan and Chrzanowski, 2014; Chen *et al.*, 2018). Neben einer ausgewiesenen Biokompatibilität stimulieren aus Seidenfibroin hergestellte Medizinprodukte die Interaktion des Gewebes, ohne dabei schädliche Reaktionsprodukte zu erzeugen. Darüber hinaus zeigt sich Fibroin als äußerst permeabel und durchlässig für Wasserdampf und Sauerstoff. Mit der einhergehenden thermischen Stabilität (bis zu 250 °C) kann Seide als Trägerstruktur hohen Temperaturen standhalten und so für medizinische Anwendungen sterilisiert werden (Um *et al.*, 2001; Min *et al.*, 2004; Amiraliyan, Nouri and Kish, 2009; Cao and Wang, 2009; Hofmann *et al.*, 2014; Koh *et al.*, 2015a; Wang *et al.*, 2015). Trotz dieser durchaus positiven Datenlage birgt Seidenfibroin auch einige Nachteile, unter anderem ein leicht sprödes Verhalten, Fragmentierungsprobleme sowie Schwierigkeiten bei der Herstellung eines einheitlichen skalierbaren Herstellungsprozesses verschiedener Seidenprodukte (Lamboni *et al.*, 2015; Chen *et al.*, 2018; Sultan, Lee and Kim, 2018).

Tabelle 1: Eigene Darstellung der biologischen und mechanischen Merkmale von Seide in Anlehnung an (Frich *et al.*, 1997; Pins *et al.*, 1997; Vollrath and Knight, 2001; Fu, Shao and Fritz, 2009; Omenetto and Kaplan, 2010; Koh *et al.*, 2015b).

Biologische Merkmale					
Biokompatibilität			Geringe Immunogenität		
Permeabel für O_2 und H_2O-Dampf			Einstellbare Degradation		
Bioaktiv			Zytokompatibilität		
Mechanische Merkmale					
Material	E-Modul [GPa]	Festigkeit [MPa]	Dehnbarkeit [%]	Zähigkeit [MJm^{-3}]	Referenz
B. Mori	10-17	300-740	28	150	Koh et. al. 2015
Nylon	1,8-5	430-950	18	80	Fu et. al. 2009
Kevlar	130	3600	2,7	50	Fu et. al. 2009
Baustahl	200	1500	0,8	6	Omenetto et. al. 2010
Kollagen	0,0018-0,046	0,9-7,4	24-68	-	Koh et. al. 2015, Pins et. al. 1997

2.1.3 Fibroinrekombination und Designausprägungen

Die Struktur der Rohseide birgt zahlreiche Vorteile und wird bereits seit vielen Jahren in der Medizin als chirurgisches Nahtmaterial eingesetzt (Altman *et al.*, 2003). Für eine bedarfsgerechte Anwendung können die beiden Seidenproteine Fibroin und Sericin durch verschiedenste Verfahren initial getrennt sowie individuell und patientenspezifisch weiterverarbeitet werden. Die Basis dafür bildet der sogenannte „*Degumming*"-Prozess, in welchem die beiden Proteine voneinander getrennt werden. Im Anschluss daran wird die reine Fibroin-Watte mittels „*Ajisawa´s reagent*" gelöst, einem proteinschonenden Lösemittel auf Wasser- und Salzbasis (Ajisawa, 1997; Kopp *et al.*, 2019a, 2019b; Kopp, Smeets, *et al.*, 2020). Andere *Degumming*-Methoden auf Enzym- und Säurebasis werden im Rahmen dieser Dissertation nicht weiterverfolgt, da diese den Löseprozess enorm verlängern und die mechanischen Eigenschaften der Seide erheblich verschlechtern (Chopra and Gulrajani, 1994; Ajisawa, 1997; Khan and Tsukada, 2014). In einem weiteren Schritt entsteht über einen Dialyseprozess die fertige, rekombinierte Fibroinlösung zum weiteren individuellen Gebrauch (Danielle N. Rockwood, Gil, *et al.*, 2011; Huang *et al.*, 2018; Sultan, Lee and Kim, 2018). In

Abbildung 5 ist die Prozesskette vom Kokon zur Lösung noch einmal grafisch dargestellt. Weiteren Studien von Wöltje et. al. (Wöltje *et al.*, 2021) zufolge kann eine reine Fibroinlösung mittlerweile innerhalb von vier Stunden hergestellt werden.

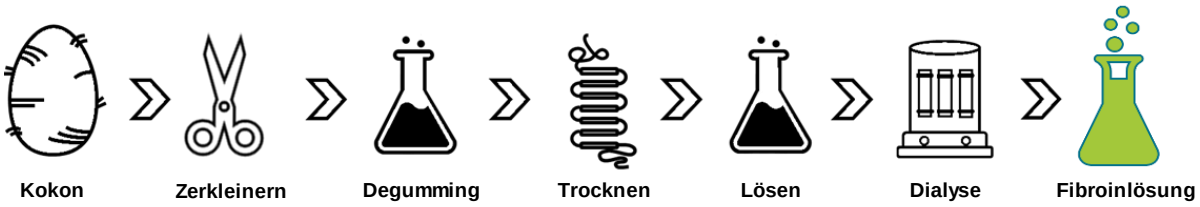

Abbildung 5: Eigene Darstellung der Prozesskette vom Seidenkokon zur fertigen Fibroinlösung in Anlehnung an (*Fibrothelium GmbH*, 2022).

Durch die vielseitigen Gestaltungsmöglichkeiten der Seide sind eine Reihe von Ausprägungen für die Anwendung in der Biomedizinischen Technik entstanden (Thurber, Omenetto and Kaplan, 2015; Patil, Reagan and Bohara, 2020; Sun *et al.*, 2021).
Die morphologische Variabilität von Fibroin ermöglicht es, neben Seidenlösungen auch Fasern, 3D-Scaffolds, Hydrogele oder nanoporöse Vliese sowie Membranen/ Folien entstehen zu lassen, siehe Abbildung 6. Diese können dabei individuell funktionalisiert oder beladen werden. Der Fokus dieser Doktorarbeit liegt neben der Charakterisierung der Fibroinlösung auch auf den Strukturen Membran und nanoporöses Vlies. Diese werden unter anderem im Folgenden näher erläutert:

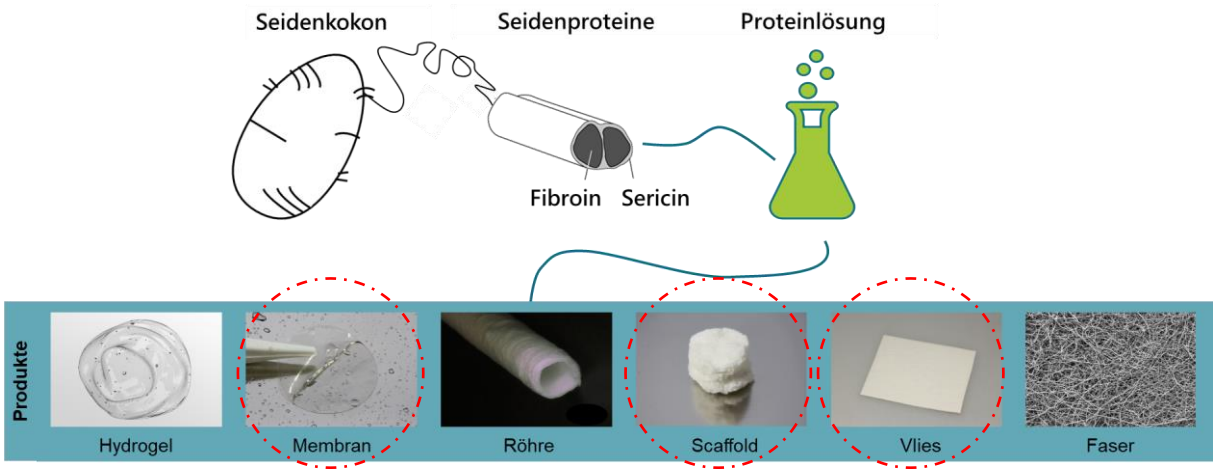

Abbildung 6: Eigene Darstellung der versatilen Weiterverarbeitungsmöglichkeiten von Seidenfibroin in Anlehnung an Fibrothelium GmbH (*Fibrothelium GmbH*, 2022).

- **Fibroinlösung:**

Die Fibroinlösung stellt eine wichtige Grundlage für die Weiterverarbeitung zu verschiedensten seidenbasierten Strukturen dar (Tao, Kaplan and Omenetto, 2012; Baumann, 2017). Bedingt durch das schonende Herstellungsverfahren unter Raumtemperatur ist es möglich, eine pH-neutrale Fibroinlösung zu generieren. Diese Bedingungen werden genutzt, um sensitive Medikamente in Seidenimplantate zu inkorporieren (Karageorgiou *et al.*, 2006; Baumann, 2017). Darüber hinaus können auch andere organische (Proteine, Enzyme, Zellen) und anorganische Stoffe (u.a. Laserfarbstoffe) in die Fibroinlösungen eingebracht werden, um beispielsweise die Biointegration von photonischen und elektronischen Sensoren zu optimieren (Kundu *et al.*, 2013a; Baumann, 2017). Aber auch nicht-funktionalisierte Fibroinlösungen erweisen sich als vielversprechende Möglichkeit als Beschichtungsmaterial für Implantate zu fungieren und können die körpereigene Immunantwort nachweislich verringern (Fuest *et al.*, 2023).

- **Membranen/ Folien:**

In der Medizintechnik wird das Biomaterial Seide als Membran oder Folie genutzt. Sie bieten aufgrund Ihrer porenlosen Struktur eine Barrierefunktion und können somit okklusiv oder semi-okklusiv gestaltet werden (Sultan, Lee and Kim, 2018). Die einfachste Methode, eine Seidenmembran herzustellen, stellt das Abgießen der Seidenlösung in ein planes Gefäß mit anschließender Trocknung dar. Um homogenere Membrandicken zu generieren, kann alternativ auf maschinelle Geräte wie ein Filmziehrakel oder spezielle Gießvorrichtungen zurückgegriffen werden. Zusätzlich kann die Dicke der Folie durch die Seidenkonzentration angepasst werden und erlaubt darüber hinaus eine poröse Gestaltung (Danielle N. Rockwood, Gil, *et al.*, 2011). Seidenmembranen finden ihren Nutzen vor allem in Wundmodellen der Haut, und glänzen mit Eigenschaften wie einer guten Wundheilungsrate und geringer inflammatorischer Antwort (Sugihara *et al.*, 2000, 2008). In der Hals-, Nasen-, Ohrenheilkunde gibt es aktuelle Studien, die Fibroin Membranen als Trommelfellersatz evaluieren (Kim *et al.*, 2010). Die Vorteile für diese Indikation liegen im transparenten, elastischen und adhäsiven Verhalten der Fibroinmembran. Im mund-, kiefer- und gesichtschirurgischen Bereich sind Seidenmembranen unter anderem im Bereich der *Guided-Bone-Regeneration* (GBR) und *Guided-Tissue-Regeneration* (GTR) einsetzbar. In einem präklinischen Knochendefekt-Modell an New-Zealand-White-Rabbits erwiesen sich Oberflächen-modifizierte Seidenmembranen (bioaktiviert mit β-TCP/Hydroxylapatit-Keramik) als äußerst regenerationsfördernd und zeigten eine gute Knochenreifung für β-TCP (Smeets, Knabe, *et al.*, 2017). In einer klinischen Studie mit n= 71 Patienten erzielte die Behandlung von Spalthautentnahmestellen mit einer Membran

auf Seidenbasis eine 17,65 % verbesserte Heilungs- und Reepithelisierungsrate verglichen mit den Standardpräparaten (Zhang *et al.*, 2017). Für Seidenmembranen gibt es diverse weitere Anwendungsmöglichkeiten, entweder in Ihrer reinen Form ohne additive Zusätze oder als Komposite mit Polyvinylalkohol (PVA) oder antibakteriellen Substanzen wie Silbernanopartikeln (AgNPs) (Patil, Reagan and Bohara, 2020; Schäfer *et al.*, 2022). Die Biofunktionalisierung von Seidenmembranen mittels EVs zur Optimierung der Regenerationsfähigkeit wurde im Rahmen dieser Doktorarbeit untersucht (Fuest *et al.*, 2024).

- **Nanoporöse Vliese:**

Abhängig vom Herstellungsverfahren können je nach Anwendungsfall nanoporöse Vliese mittels Elektrospinning hergestellt werden. Im Elektrospinnverfahren werden Polymerfasern im Nanometerbereich aus Fibroinlösung durch die Einwirkung eines elektromagnetischen Feldes erzeugt. Besonders im Bereich des *Tissue Engineering* werden Trägerstrukturen für die Zellmigration zur unterstützenden Regeneration von beschädigtem Gewebe eingesetzt (Kopp, Smeets, *et al.*, 2020). Die Verspinnbarkeit von Seidenfibroin stellt bislang allerdings eine Herausforderung dar. Gerade die Viskosität hat einen großen Einfluss auf die Morphologie der Faser, die Größe der Faser und die mechanischen Eigenschaften (He *et al.*, 2008). Diese ist abhängig von den einzelnen Bestandteilen in der Lösung. Ist die Viskosität zu gering, erhöht sich das Risiko eines Kapillaraufbruchs während des Elektrospinning-Prozess aufgrund der zu niedrigen Oberflächenspannung. Mittels zusätzlicher Komponenten wie Gelatine oder Poly-(ethylene-oxide) (PEO) konnte eine verspinnbare Viskosität der Seidenlösung erreicht werden (Wang *et al.*, 2004; Zaitoon and Lim, 2020). Weitere Additive (Zusatzstoffe) wie beispielsweise EVs, antibakterielle Substanzen, Nanopartikel oder Medikamentenwirkstoffe können darüber hinaus individuell der Spinnlösung beigemischt werden (Kasoju, Bhonde and Bora, 2009; Wang *et al.*, 2018). Die strukturellen Vorteile nanoporöser Vliese liegen in der großen spezifischen Oberfläche, die mit einer verbesserten Zelladhäsion und -proliferation einhergehen (Unger *et al.*, 2004). Ein einzigartiger Vorteil ergibt sich aus den geringen Faserdurchmessern mit einhergehender hoher Porosität, wodurch die Durchlässigkeit für Nebenprodukte und Nährstoffe sowie das Einwachsverhalten in das umliegende Zellgewebe optimiert werden können (Ayutsede, Jonathan; Gandhi, Milind; Ko, Frank; Micklus, Michael; sukigara, 2003; Kim *et al.*, 2003; Chen *et al.*, 2006; Amiraliyan, Nouri and Kish, 2009; Cao and Wang, 2009). Aufgrund der versatilen Variationsmöglichkeiten der nanoporösen Vliese durch die einstellbaren Prozessparameter können Wundauflagen und Trägergerüste für regenerative medizinische Indikationen realisiert werden (Cao and Wang, 2009; Haghi, A.; Zaikov, 2011).

- **3D-Scaffolds:**

Für die dreidimensionale Gestaltung von Proteinen auf Seidenbasis gibt es kaum „Limitationen“. So können 3D-Scaffolds unter anderem durch die Zugabe von porogenen räumliche Strukturen annehmen, welche im Anschluss jedoch in zum Teil aufwendigen Dialyseschritten ausgewaschen und entgast werden müssen (Nazarov, Jin and Kaplan, 2004; Sultan, Lee and Kim, 2018; Patil, Reagan and Bohara, 2020). Den einfachsten und zeitsparendsten Weg stellt die sogenannte „*freeze-thawing*“ Methode dar, bei welchem sich das poröse Seidengeflecht über mehrmalige Tau- und Gefrierprozesse ausbildet. Das gemeinsame Ziel aller Herstellungsverfahren besteht in der Ausbildung einer realitätsnahen Extrazellulärmatrix-Struktur (EZM-Struktur) mit einhergehend variablen Porengrößen und Dichten. Durch die Zugabe von organischen und anorganischen Stoffen als Komposite können ähnliche *blended/ hybrid materials* geschaffen werden, welche in ihren Bestandteilen jedoch untereinander kompatibel sein müssen, da inhomogene Gemische entstehen können, die eine gegenteilige Wirkung aufweisen (Kundu *et al.*, 2013a). Das Ziel des 3D-Konstruktes liegt aufgrund der großen Oberfläche in einer begünstigten Zelladhäsion und Gewebeintegration (Sultan, Lee and Kim, 2018). Durch die poröse Oberflächenstruktur und Interkonnektivität weisen 3D-Scaffolds sehr gute Bedingungen für proliferierende Zellen auf (Danielle N. Rockwood, Gil, *et al.*, 2011; Danielle N. Rockwood, Preda, *et al.*, 2011; Patil, Reagan and Bohara, 2020). Im Bereich der Wundheilung und Regeneration konnte Seide im Zusammenhang mit Alginaten als eine Art Wundschwamm die Regenerationszeit der Wunde von zwölf auf sechs Tage reduzieren und erzeugte im Vergleich zu konventionellen Produkten eine signifikant höhere Reepithelialisierung (D. H. Roh *et al.*, 2006). In einer weiteren präklinischen Studie konnte gezeigt werden, dass verschiedene 3D-Scaffold Typen (Salz/ Wasser oder Saccharose/ Hexafluoroisopropanol) in der Zellkultur-Testung mit Chondrozyten suffiziente Knorpelmatrix ausbildeten und gleichzeitig unterschiedliche Degradationszeiträume aufzeigten (Makaya *et al.*, 2009).

2.1.4 Seidensericin:

Wie bereits im Kapitel „*Synthese und Morphologie der Seide des B. mori*“ (S. 5) erwähnt, besteht der Rohseidenfaden aus den zwei Fibroinsträngen und einer Ummantelung aus Sericin, welche die Fibroinfasern zusammenhält und dem Kokon seine Struktur und Festigkeit verleiht (Meinel and Kaplan, 2012; Nguyen *et al.*, 2019). Studien zufolge konnte belegt werden, dass Sericin bemerkenswerte biologische Eigenschaften aufweist, welche allerdings in Kombination mit Fibroin zu allergischen Reaktionen führt (Thurber, Omenetto and Kaplan, 2015; Gautam, Jain and Kapoor, 2017; Gholipourmalekabadi *et al.*, 2020). Aufgrund seiner

exzellenten Gerinnungs- und Feuchthalteeigenschaften wird Sericin besonders in kosmetischen Präparaten wie Cremes oder Gelen verwendet. Hinzu kommen Studien zufolge ein antioxidatives Verhalten, eine antikarzinogene Wirkung sowie herausragende UV-Schutzeigenschaften (Aramwit, Siritientong and Srichana, 2012; Lamboni *et al.*, 2015). Silva et. al. 2022 beschreibt darüber hinaus die Verbesserung der Osteoblastenproliferation und damit einhergehenden Knochenregeneration unter Anwendung von Seidensericin (Noosak *et al.*, 2022; Silva *et al.*, 2022).

2.2 Seide in der Mund-, Kiefer- und Gesichtschirurgie

Besonders nach schweren Traumata oder Tumoren im Gesichtsbereich mit einhergehendem Verlust von Hart- und Weichgewebe resultiert dies in erheblichen funktionellen und ästhetischen Beeinträchtigungen für den Patienten (Zhang and Yelick, 2018; Emara and Shah, 2021; Smeets *et al.*, 2023). Zur Wiederherstellung von fehlendem Gewebe kommen Transplante zum Einsatz, die überwiegend autolog, allogen oder xenogen sind (Smeets *et al.*, 2023):

- Autolog: vom eigenen Organismus stammend
- Allogen: von einem Individuum gleicher Spezies stammend
- Xenogen: von anderen Lebewesen stammend

Autolog bezeichnet dabei Transplantate, die von derselben Person stammen (Rentsch *et al.*, 2012; Smeets, Henningsen, *et al.*, 2017). Bei allogenen Transplantaten handelt es sich bei Spender und Empfänger nicht um dieselbe Person, aber um dieselbe Spezies (Smeets, Henningsen, *et al.*, 2017). Kommen xenogene Transplantate zum Einsatz, sind diese üblicherweise vom Rind oder Schwein (Smeets *et al.*, 2014; Smeets, Henningsen, *et al.*, 2017). All diese Ansätze stellen zwar nach wie vor den Goldstandard dar, weisen aber auch Komplikationen auf, unter anderem Abstoßungsreaktionen und Infektionen, die eine erhöhte Morbidität und verlängerte Krankenhausaufenthalte mit sich bringen (Smeets *et al.*, 2023). Die Herausforderung besteht also nicht nur in der Entwicklung innovativer Werkstoffkonzepte, welche kostengünstig und skalierbar produziert werden können, sondern auch in der Verträglichkeit und defektfüllenden Funktionalität des Materials (Smeets *et al.*, 2023). Zudem muss die Herstellung solcher Materialien den Richtlinien des Arzneimittelgesetzes unterliegen und die Bedingungen der Guten Herstellungspraxis (GMP) erfüllen. Zur Qualitätssicherung gelten regelmäßige Kontrollen *post implantationem* als unerlässlicher Nachweis.
Die Weiterentwicklung geeigneter Biomaterialtechnologie für die Hart- und Weichgeweberegeneration zur Umgehung der oben aufgeführten Problematiken ist aktueller

Stand der Forschung in der Mund-, Kiefer- und Gesichtschirurgie. Der Schwerpunkt liegt dabei auf den folgenden Themenfeldern, siehe Abbildung 7.

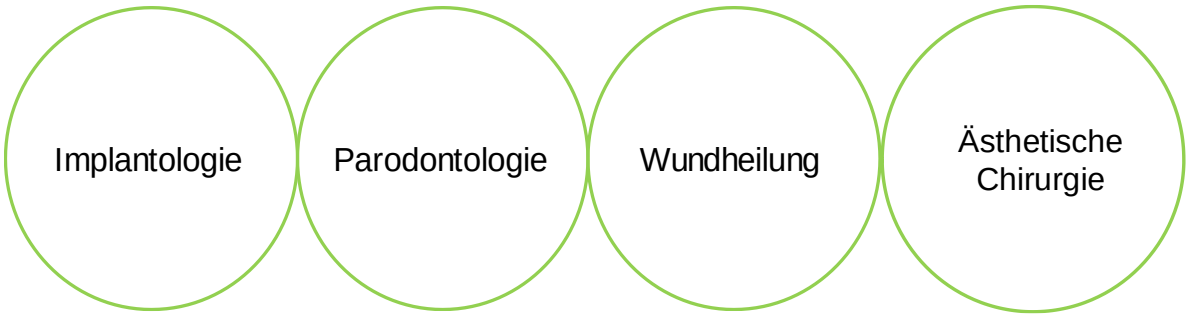

Abbildung 7: Eigene Darstellung der aktuellen Forschungsschwerpunkte von innovativen Biomaterialtechnologien in der Mund-, Kiefer- und Gesichtschirurgie.

Im implantologischen Bereich, u.a in der orofazialen Rekonstruktion, gilt das sogenannte „*All-in-one-Prinzip*“, welches besagt, dass Hart- und Weichgewebe gemeinsam regeneriert oder rekonstruiert werden müssen (Zhang and Yelick, 2018; Smeets *et al.*, 2023). Obwohl somit eine optimale Durchblutung des Gewebes sichergestellt werden kann, zeigen Studien, dass Weichgewebe im Vergleich zum Hartgewebe eine schnellere Wachstums- und höhere Migrationsrate aufweist. Dies bringt nicht nur ein schnelleres Einwachsen von Bindegewebe in den jeweiligen Defekt mit sich, sondern sorgt auch dafür, das eine erfolgreiche Knochenheilung und Knochenneubildung verhindert wird (Zhang and Yelick, 2018; Smeets *et al.*, 2023). Um dieses Problem zu verhindern, werden vor Implantation dentaler Implantate inerte Barriere-Membranen (*Guided Bone Regeneration (GBR)/ Guided Tissue Regeneration (GTR)*) unter die Schleimhaut und auf den Kieferknochen (Defektspalt) gelegt. Diese verhindern nicht nur das Einwachsen von Bindegewebe, sondern stabilisieren auch eingebrachtes partikuläres Material durch Schaffung eines Hohlraums (Smeets, Henningsen, *et al.*, 2022; Smeets *et al.*, 2023). Besonders die Barriere- und Leitfunktion ist von sehr wichtiger Bedeutung, um ein Absinken der Membran in den Kieferdefekt, zu verhindern und im Sinne eines Platzhalters zu fungieren (Toffler, 2014; Lu *et al.*, 2015; Smeets, Knabe, *et al.*, 2017). Die Anwendung von seidenbasierten Membranen zur Rekonstruktion von Kieferkammdefekten und für die *GBR/ GTR* stellt eine innovative Materialtechnologie dar, indem sie nicht nur die oben aufgeführten Risiken fast gänzlich ausschließt, sondern darüber hinaus mit weiteren Biomaterialien funktionalisiert werden kann. Der aktuelle Forschungsschwerpunkt liegt hierbei auf einem vollständig resorbierbaren Augmentations-Kit, welches neben einer resorbierbaren Membran auf Fibroin-Basis kombiniert wird mit einem Versteifungselement aus Magnesium und resorbierbaren Magnesium Pins zur Fixierung der Membran am jeweiligen Defekt. Gerade in dieser Kombinationsvariante soll Magnesium als stützende Struktur für mehr Formstabilität sorgen. Magnesium kommt bereits als natürliches Element im humanen Organismus vor und ist für viele physiologische Abläufe verantwortlich

(Saris *et al.*, 2000; Kim *et al.*, 2014). Durch die Freisetzung von Magnesium Ionen können Entzündungs -und Abstoßungsreaktionen gelindert und der Knochenaufbau unterstützt werden (Saris *et al.*, 2000; Kim *et al.*, 2014). Jüngste Studien haben zudem bewiesen, dass Magnesium als Knochenersatzmaterial eingestuft werden kann. So zeigten sich neben hohen Mineralablagerungsraten auch eine erhöhte Knochenmasse und eine verbesserte Neubildung des Knochengewebes in Verbindung mit Magnesium (Saris *et al.*, 2000; Witte *et al.*, 2005; Kopp *et al.*, 2019a).

Im Bereich parodontaler Defekte kommen Okklusivmembranen ebenfalls zu Anwendung, um zu verhindern, dass die umgebende Mukosa in die Defektstelle eindringen kann (Gamal and Iacono, 2013; Zhang and Yelick, 2018; Emara and Shah, 2021; Smeets *et al.*, 2023). Die modifizierbaren Eigenschaften des Seidenfibroins bringen auch für den Bereich der Wundheilung und ästhetischen Chirurgie entscheidende Vorteile mit sich, die im Kapitel 2.3 *„Anforderungen der Seide an Regenerations- und Wundheilungsprozesse“* (S. 17) näher erläutert werden.

2.3 Anforderungen an Seide bei Regenerations- und Wundheilungsprozessen

Die Regeneration einer Wunde stellt einen physiologischen Prozess dar. Dabei setzt, abhängig vom Ausmaß der Wunde, ein individueller und sequenzieller Heilungsprozess ein, welcher unterschiedlich lange andauern kann (Flanagan, 2000; Koh and DiPietro, 2011; Srivastava *et al.*, 2015; Gonzalez *et al.*, 2016; Singh, Young and McNaught, 2017; Patil, Reagan and Bohara, 2020). Die Nutzung einer geeigneten Wundabdeckung zum Schutz vor Keimen und extensiver Austrocknung stellt demnach ein seit Jahrhunderten anerkanntes Prinzip dar (Wigger-Alberti *et al.*, 2009; Shah, 2011; Broussard and Powers, 2013; Farahani and Shafiee, 2021). Allerdings gibt es je nach Wundsituation verschiedenste Anforderungen an das zu benutzende Material. Im Bereich der natürlichen Biomaterialien gibt es bereits seit Jahren diverse Polymere, welche neben einer ausreichenden Biokompatibilität eine einfachen Herstellung und Handhabung vereinen (Ninan *et al.*, 2015; Üstündağ Okur *et al.*, 2019; Juncos Bombin, Dunne and McCarthy, 2020; Patil, Reagan and Bohara, 2020; Wang *et al.*, 2023). Neben Chitosan und verschiedenen Polysacchariden wie Stärke oder Alginate finden auch Kollagen und proteinbasierte Materialien weitverbreitet Anwendung (D.-H. Roh *et al.*, 2006; Lu *et al.*, 2008; Rouabhia and Allaire, 2010; Patil, Reagan and Bohara, 2020). Um Gewebedefekte entsprechend gut versorgen zu können, sind neben einer exzellenten Biokompatibilität auch gute mechanische Verhältnisse sowie ein entsprechendes Degradationsverhalten von großer Bedeutung (Agarwal, Wendorff and Greiner, 2008; Wang *et al.*, 2010; Huang *et al.*, 2012, 2018; Patil, Reagan and Bohara, 2020). Um die Regeneration des Defekts so optimal wie möglich zu gestalten, sollte der Gewebeersatz möglichst der Extrazellulärmatrix des natürlichen Gewebes entsprechen und darüber hinaus die Zell-Interaktion durch eine makro- oder

nanoporöse Struktur unterstützen (Gil *et al.*, 2011; Li *et al.*, 2013; Huang *et al.*, 2018). Weitere Anforderungen für den Bereich Wundheilung und Regeneration sind in der folgenden Abbildung 8 noch einmal schematisch dargestellt. Obwohl die Palette an Materialkonzepten vielfältig scheint, sind einige dieser Werkstoffe aufgrund ihrer Verarbeitungsmöglichkeiten, strukturellen Degradation oder Immunogenität für den uneingeschränkten Einsatz in der Regeneration und Wundheilung limitiert (Lehmann *et al.*, 2022; Smeets, Henningsen, *et al.*, 2022). Seidenfibroin schafft hier aufgrund seiner exzellenten mechanischen Eigenschaften mit einhergehender einstellbarer Degradierbarkeit einen entscheidenden Vorteil zur Optimierung innovativer Materialkonzepte (Smeets, Henningsen, *et al.*, 2022). Besonders im Bereich der Wundheilung konnten Studien belegen, dass Fibroin die Leukozytenanzahl und die Dauer der Entzündung essentiell verringert hat (Gholipourmalekabadi *et al.*, 2020). Fibroin beschleunigt die Proliferation humaner Zellen sowohl *in vitro* als auch *in vivo*, was eine Deckung der Defektstelle mit einhergehender Neovaskularisierung von nativem Gewebe zur Folge hat (Napavichayanun and Aramwit, 2017; Chouhan and Mandal, 2020; Patil, Reagan and Bohara, 2020; Schäfer *et al.*, 2022). Park et al. 2018 haben in einer Studie die Korrelation zwischen einer beschleunigten Wundheilung und einer vermehrten Ausschüttung des Transkriptionsfaktors NF-κB im Zusammenhang mit Seidenfibroin gezeigt (Park *et al.*, 2018). Hierbei wird deutlich, wie eng der Prozess der Wundheilung mit der Ausbildung von Wachstums- und Proliferations-stimulierenden Faktoren zusammenhängt (Chouhan and Mandal, 2020). Die Funktionalität von Seidenfibroin im Bereich der Regeneration und Wundheilung hat demnach also positive Auswirkungen auf die Proliferation und Interaktion mit dem umliegenden Gewebe (Brown and Badylak, 2014; Hodgkinson and Bayat, 2014; Sultan, Lee and Kim, 2018; Patil, Reagan and Bohara, 2020; Schäfer *et al.*, 2022; Smeets, Henningsen, *et al.*, 2022). Die beim protelolytischen Abbau des Fibroins entstehenden Peptidfragmente zeigen sich Studien wie Yamada et. al. 2004 zufolge ebenfalls Proliferations-stimulierend (Yamada *et al.*, 2004).

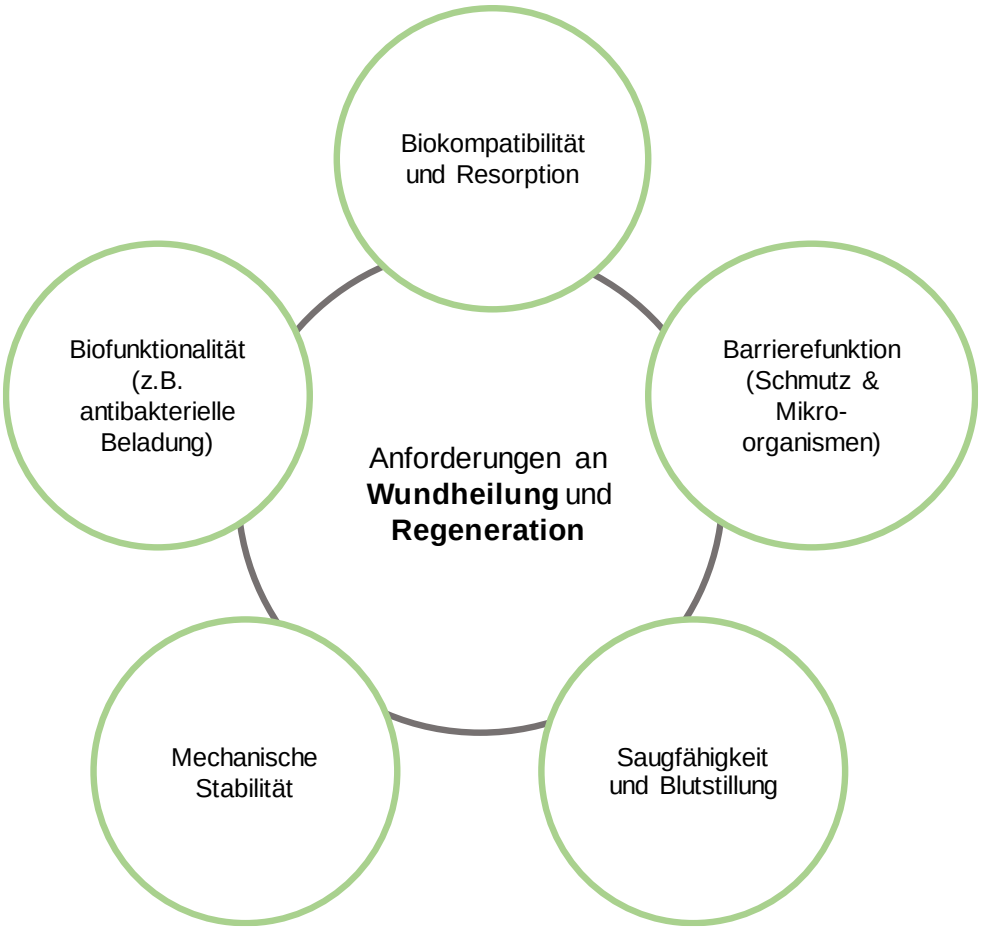

Abbildung 8: Eigene Darstellung der Anforderungen an Wundheilung und Regeneration in Anlehnung an (Huang *et al.*, 2018; Patil, Reagan and Bohara, 2020).

3 Zielstellung dieser Doktorarbeit

Das übergeordnete Ziel dieser Dissertation lag in der „Funktionalisierung und Charakterisierung von Biomaterialien auf Seidenfibroin-Basis für eine spätere Anwendung im Bereich der Regeneration und Wundheilung in der Mund-, Kiefer- und Gesichtschirurgie“.
Um einen besseren Überblick über die Forschungsschwerpunkte geben zu können, wurden in Abbildung 9 ein Schaubild erstellt, welches die Forschungsfrage dieser Dissertation einmal grafisch darstellt und darüber hinaus 3 inkrementelle Hypothesen verfasst, die als Leitfaden der in dieser Arbeit fokussierten Schwerpunkte dienen:

Hypothese 1: Kann Seidenfibroin als Beschichtung auf Implantatmaterialien aufgetragen werden und inwieweit beeinflusst diese Fremdkörperabstoßungsreaktionen? (Veröffentlichung I)

Hypothese 2: Besitzen Strukturen auf Seidenbasis ein inhärentes antibakterielles Verhalten und können antibakteriell beladene Seidenmatrices eine wichtige Rolle in der Wundheilung einnehmen? (Veröffentlichung II und III)

Hypothese 3: Können Fibroin Membranen mittels EVs funktionalisiert werden, um die Regenerative Medizin im Kopf-Hals-Bereich zu optimieren? (Veröffentlichung IV)

Die Basis aller Publikationen bildet der Isolationsprozess des Seidenfibroins gemäß der PureSilk® (*Fibrothelium GmbH*, 2022) Technologie aus den Kokons des Maulbeerseidenspinners *B. mori*. Ein Schwerpunkt lag dabei zu Beginn auf der Charakterisierung von regeneriertem Seidenfibroin als Layer-by-Layer Beschichtung von Implantatmaterialien, um die Fremdkörperabstoßungsreaktion besser regulieren und u.a. die Osteogenese stimulieren zu können (Fuest *et al.*, 2023). Nachdem die Funktionalität von Seidenfibroin als Lösung belegt werden konnte, wurde in einem nächsten Schritt die Ausbildung verschiedener Seidenstrukturen fokussiert und der Schwerpunkt auf die Funktionalisierung jener Strukturen gelegt, um die Regenerationsfähigkeit und Wundheilung zu verbessern und damit einhergehend bakterielle Infektionen im Bereich der Zahnheilkunde wie eine periimplantäre Mukositits oder eine Periimplantitis zu vermindern. Zur Anwendung kamen hier in einem ersten Schritt antibakterielle Substanzen und EVs (Schäfer *et al.*, 2022, 2023; Fuest *et al.*, 2024) zur Optimierung der Regeneration und der Wundheilung in der Mund-, Kiefer- und Gesichtschirurgie. Abbildung 9 stellt die durchgeführten Arbeiten und daraus resultierenden Veröffentlichungen dieser Dissertation noch einmal grafisch dar.

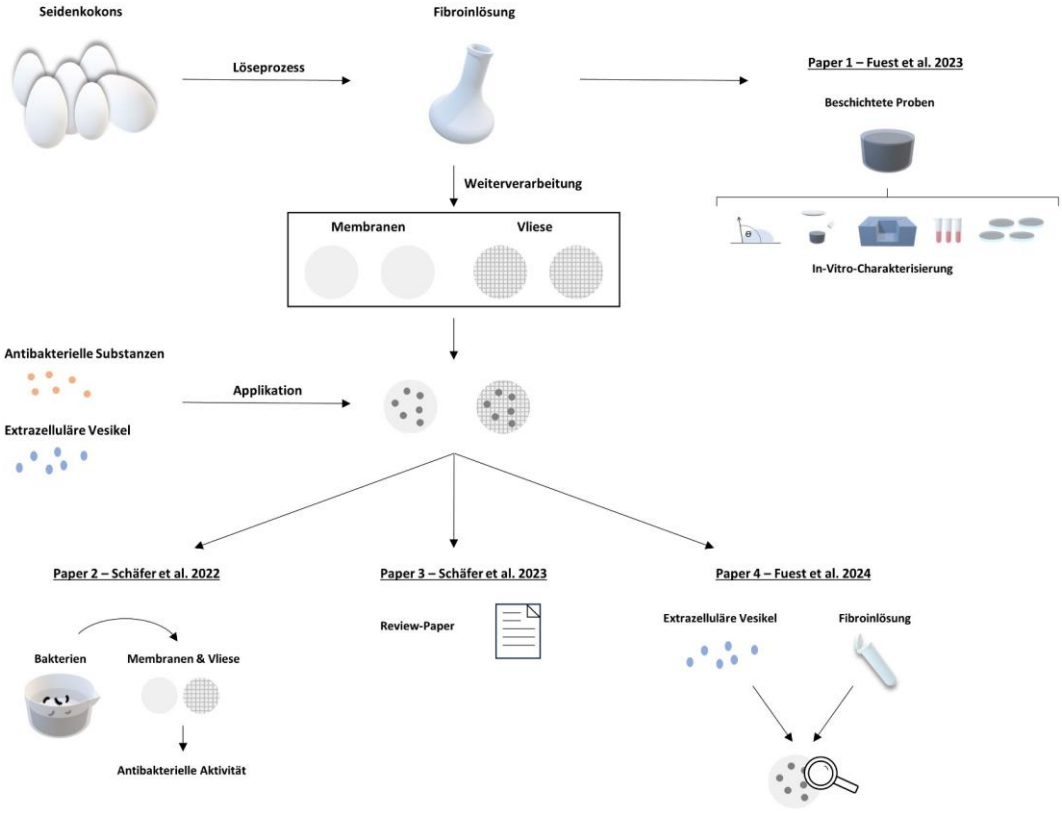

Abbildung 9: Eigene Darstellung der im Rahmen dieser Dissertation durchgeführten Arbeiten und daraus resultierenden Veröffentlichungen.

3.1 Veröffentlichung I: „Layer-by-Layer Deposition of Regenerated Silk Fibroin─An Approach to the Surface Coating of Biomedical Implant Materials.“

Fuest, S., Smeets, R., Gosau, M., Aavani, F., Knipfer, C., Grust, A. L. C., Kopp, A., Becerikli, M., Behr, B., & Matthies, L. (**2023**). *Layer-by-Layer Deposition of Regenerated Silk Fibroin ─ An Approach to the Surface Coating of Biomedical Implant Materials*. ACS biomaterials science & engineering, 9(12), 6644–6657.

Beschichtungstechniken bieten große Vorteile für moderne Therapiekonzepte. Das übergeordnete Ziel dieser Studie lag in der Charakterisierung von Seidenfibroin-basierten Beschichtungen auf den Implantatwerkstoffen Titan (Ti6-AL-4V), Magnesium (WE43) und Polymeren (Poly-Methyl-Metha-Crylat (PMMA)), die häufig für orthopädische und andere knochenbezogene Implantate verwendet werden. Diese Art der Oberflächenmodifikation durch funktionale Beschichtungen wird als innovative Möglichkeit in Betracht gezogen, um unter anderem die Osseointegration und Weichgeweberegeneration von Implantatmaterialien nachhaltig zu verbessern. Hierfür wurden die Kokons des Maulbeerspinners *B. mori* in einem schonenden Verfahren in eine wässrige Fibroinlösung überführt und im Anschluss daran die regenerierte Fibroinlösung mittels *Dip-Coating* Verfahren auf die Oberfläche der Implantatmaterialien aufgetragen. Die Werkstoffe Titan und Magnesium wurden vorab mittels Plasmaelektroylischer Oxidation (PEO) in einen superhydrophilen Zustand überführt, um eine bessere Adhäsion des Fibroins an der Oberfläche zu gewährleisten. Mit Hilfe von Rasterelektronenmikroskopie (REM), Kontaktwinkelmessung und Fourier-Transform-Infrarotspektroskopie (FTIR) wurde die aufgebrachte Schicht untersucht und im Rahmen von Zyto- und Hämokompatibilitätstestungen evaluiert (s. Abbildung 10). Die Charakterisierung der drei Probengruppen ergab, dass die zusätzliche PEO-Behandlung auf den Titan- und Magnesiumproben zu deutlich kleineren Kontaktwinkeln führte, was für eine Benetzbarkeit und Hydrophilie spricht. Die FTIR Analyse ergab einen höheren Gehalt an β-Faltblättern nach zusätzlicher Nachbehandlung der Seidenschichten. Die Bewertung der Hämokompatibilität wurde durch die zusätzliche Seidenfibroin-Schicht nicht verändert; darüber hinaus zeigten die Zytokompatibilitätstestungen, dass Fibroin eine signifikante entzündungsfördernde Reaktion hervorruft, welche bei einer Reihe von physiologischen Prozessen, einschließlich der Osteogenese eine wichtige Rolle spielt.

Die dargestellten Ergebnisse zeigen, dass die Beschichtung von Implantatmaterialien mittels Seidenfibroin ein großes Potenzial für den Einsatz als Medizinprodukt aufweisen (Fuest *et al.*, 2023).

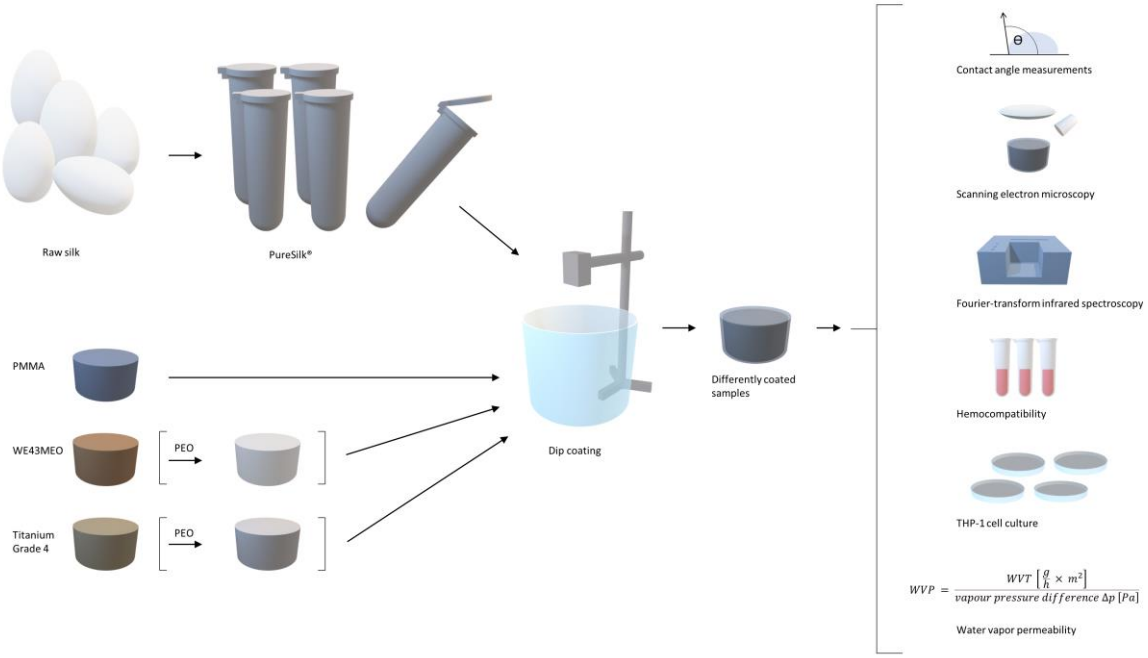

Abbildung 10: Eigene Darstellung des Versuchsaufbaus und der experimentell durchgeführten Versuche in Fuest et. al. 2023 (Fuest *et al.*, 2023).

3.2 Veröffentlichung II: „Antibacterial properties of functionalized silk fibroin and sericin membranes for wound healing applications in oral and maxillofacial surgery.“

Schäfer, S., Smeets, R., Köpf, M., Drinic, A., Kopp, A., Kröger, N., Hartjen, P., Assaf, A. T., Aavani, F., Beikler, T., Peters, U., Fiedler, I., Busse, B., Stürmer, E. K., Vollkommer, T., Gosau, M., & **Fuest, S.** (**2022**). *Antibacterial properties of functionalized silk fibroin and sericin membranes for wound healing applications in oral and maxillofacial surgery.* Biomaterials advances, 135, 212740.

Die optimale Versorgung oraler Wunden mit geeigneten antibakteriellen Verbänden stellt bis heute eine enorme Herausforderung dar. Ziel dieser Studie lag deshalb in der Charakterisierung und Evaluierung von Membranen und Vliesen auf Seidenproteinbasis, welche mit den antibakteriellen Substanzen Silbernitratlösung ($AgNO_3$) und Gentamicin funktionalisiert wurden. Zu Beginn wurden die Proteine Fibroin und Sericin aus den Kokons des *B. mori* voneinander getrennt und mittels eines speziellen Gießverfahrens und Elektrospinning zu Membranen und Vliesen weiterverarbeitet und mit antibakteriellen Substanzen beladen. Im Anschluss daran wurden die Probekörper mittels künstlichem Speichel versehen und mit einem anaeroben Bakterienstamm kultiviert. Die antibakterielle Wirkung wurde im Anschluss anhand der Lebendbakterienzahl und der Gesamtbakterienzahl ermittelt. Darüber hinaus wurde die Zytokompatibilität mittels direkter und indirekter Testreihen (Zellproliferation (XTT) und Zytotoxizität (LDH)) bestimmt und die Probekörper unter dem REM charakterisiert, siehe Abbildung 11.

Die mikroskopischen Aufnahmen stellten die glatte Membranstruktur und die verwobene Struktur der Vliese gegenüber.

Die Ergebnisse wiesen auf ein signifikant geringeres Wachstum der Bakterienkolonien und eine geringere DNA-Zahl für gegossene Membran mit Silbernitratlösung hin, mit einer Verringerung der Bakterienzahl um 3 logarithmische Werte (99,9 %) im Colony-Forming-Unit (CFU) und Real Time Quantitative PCR (qrt-PCR) - Assay im Vergleich zu unbehandelten Kontrollmembranen und mit Gentamicin funktionalisierten Membranen und Vliese ($p < 0,001$). Ebenso erbrachten Gentamicin-behandelte Vliese im Vergleich zu silberbehandelten Vliesen und der Kontrollgruppe ($p < 0,001$) signifikant niedrigere DNA- und Koloniewachstumszahlen. Zusammenfassend lässt sich sagen, dass Membranen mit Silber im Vergleich zu Vliesen mit Gentamicin eine um 1 log höhere antibakterielle Aktivität aufweisen, während Vliese mit Gentamicin eine bessere Zytokompatibilität für L929-Zellen zeigen.

Somit konnte gezeigt werden, dass die Beladung von Seidenstrukturen mit antibakteriellen Substanzen erfolgreich war und eine antibakterielle Wirksamkeit erzielt werden konnte was einen Grundstein für die erfolgreiche Anwendung von Seidenmaterialien in der oralen Wundheilung darstellt (Schäfer *et al.*, 2022).

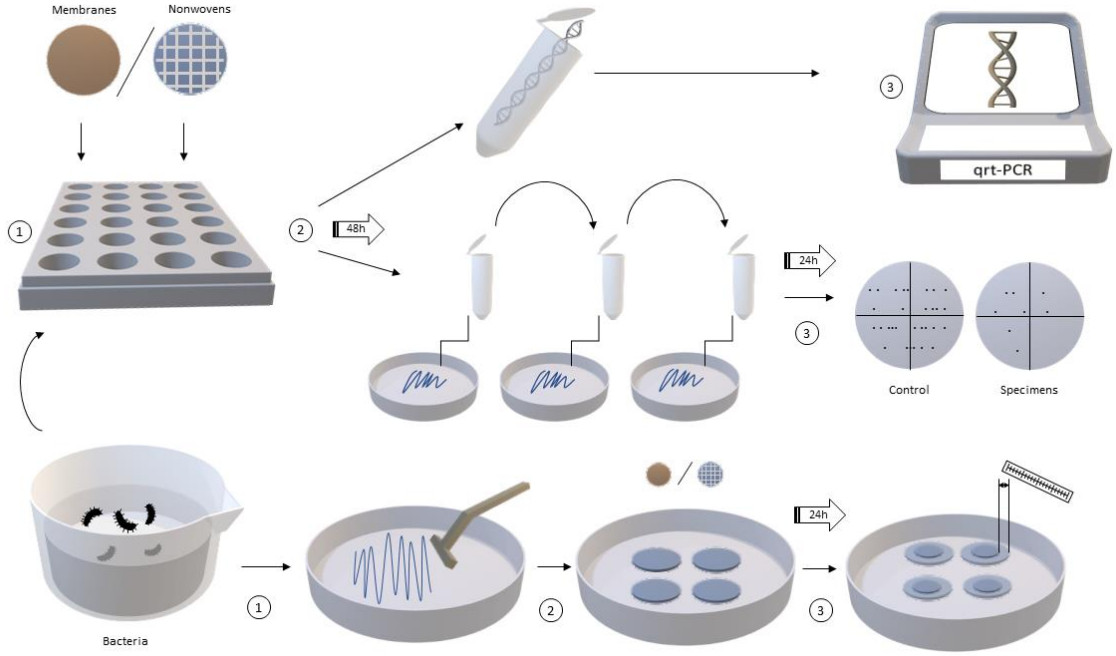

Abbildung 11: Darstellung des antibakteriellen Versuchsaufbaus aus Schäfer et. al. 2022 (Schäfer *et al.*, 2022).

3.3 Veröffentlichung III: „Silk proteins in reconstructive surgery: Do they possess an inherent antibacterial activity? A systematic review.“

Schäfer, S., Aavani, F., Köpf, M., Drinic, A., Stürmer, E. K., **Fuest, S.**, Grust, A. L. C., Gosau, M., & Smeets, R. (**2023**). *Silk proteins in reconstructive surgery: Do they possess an inherent antibacterial activity? A systematic review.* Wound repair and regeneration: official publication of the Wound Healing Society [and] the European Tissue Repair Society, 31(1), 99–110.

Der Sektor der rekonstruktiven Chirurgie beinhaltet ein breites Spektrum an chirurgischen Verfahren und regenerativen Ansätzen zur Behandung unterschiedlichster Gewebearten. Da jeder chirurgische Eingriff nicht nur ein erhöhtes Risiko einer Infektion mit sich bringt, sondern auch eine finanzielle Belastung für den Patienten darstellt, wird gerade im kieferchirurgischen Bereich an innovativen Materialkonzepten geforscht, die neben einer exzellenten Biokompatibilität weitere Vorteile wie eine einstellbare Abbaubarkeit und eine minimale Immunogenität mit einhergehenden antibakteriellen Eigenschaften mit sich bringen. Diese Voraussetzungen können mit dem Biomaterial Seide erfüllt werden. Das Ziel dieses systematischen Reviews lag in der Erstellung einer systematischen Übersicht zu folgender Forschungsfrage: Besitzen Seidenproteine (Fibroin & Sericin) eine intrinsische antibakterielle Eigenschaft und wie können diese so modifiziert werden, dass eine solche Eigenschaft erzielt wird (Schäfer *et al.*, 2023)?

Die in diese Recherche eingeschlossenen Search-Terms lauten (Schäfer *et al.*, 2023):

(Seidenfibroin) ODER (Seidensericin) ODER (Seidenprotein) UND (antibakteriell) ODER (antimikrobiell) ODER (bakterientötend)

Einschlusskriterien waren hier (s. Abbildung 12):

1- Originalarbeiten (präklinisch und klinisch)
2- Indikation: klinische Anwendung
3- Bestandteil der zu untersuchenden Materialien Fibroin oder Sericin
4- Schwerpunkt liegt auf antibakterieller Analyse
5- Kontrollgruppe ohne antibakterielle Funktionalisierung

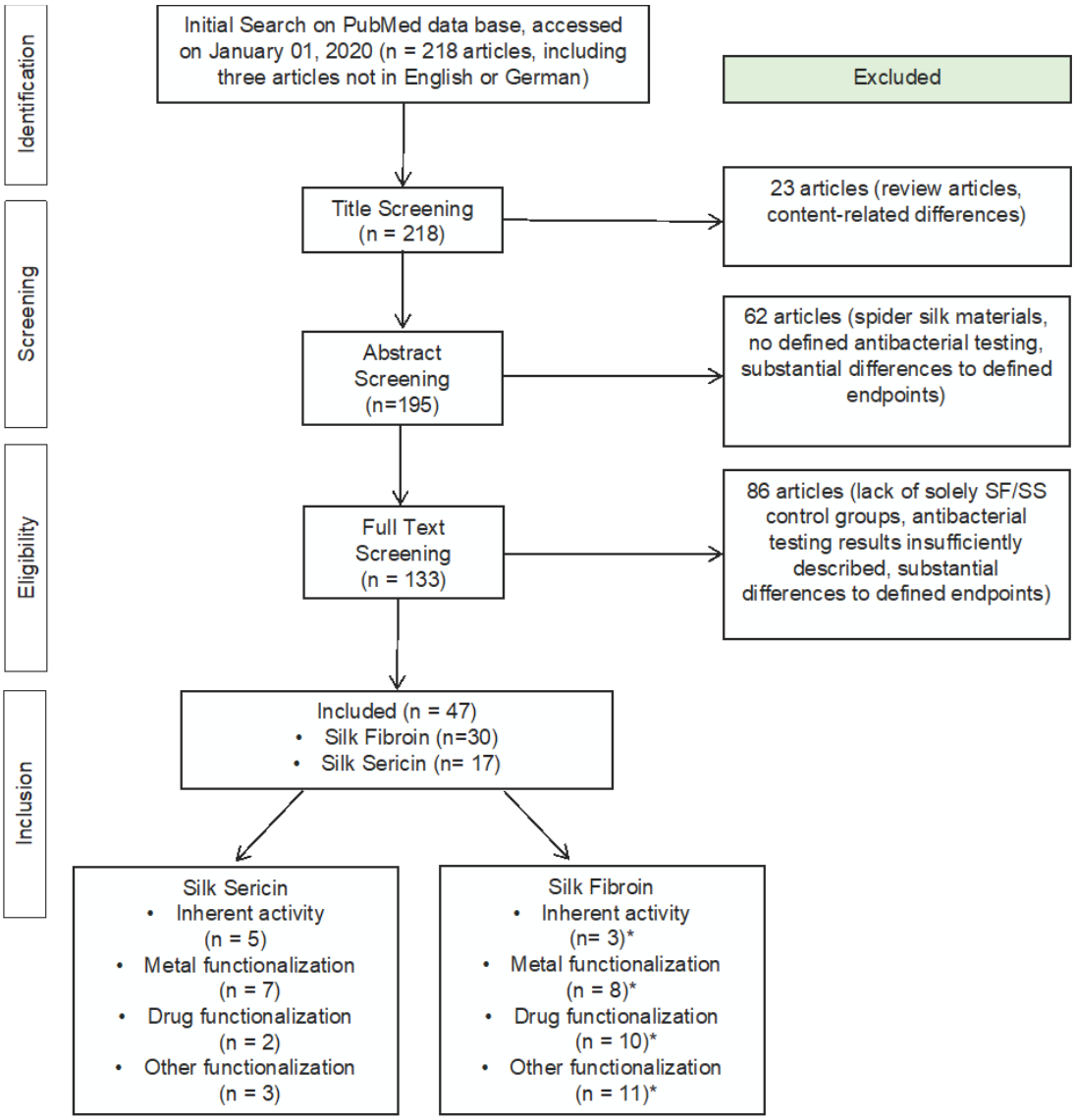

Abbildung 12: Flussdiagramm gemäß der PRISMA Richtlinien für systematische Reviews (Page *et al.*, 2021; Schäfer *et al.*, 2023).

3.4 Veröffentlichung IV: „Doping of casted silk fibroin membranes with extracellular vesicles for regenerative therapy – a proof of concept.“

Fuest, S., Salviano-Silva, A., Maire, C. L., Xu, Y., Apel, C., Grust, A. L. C., Delle Coste, A., Gosau, M., Ricklefs, F. L., & Smeets, R. (**2024**). *Doping of casted silk fibroin membranes with extracellular vesicles for regenerative therapy: a proof of concept.* Scientific reports, 14(1), 3553.

Bioaktive Materialkonzepte für den gezielten Einsatz sind seit Jahren ein wichtiger Forschungsschwerpunkt in der regenerativen Medizin. Ziel dieser Studie war es, eine *proof-of-concept*-Verbundstruktur in Form einer Membran aus natürlichem Seidenfibroin (SF) und extrazellulären Vesikeln (EVs) aus dem Überstand einer immortalisierten Gingiva-Fibroblasten (GF)-Zelllinie zu untersuchen. EVs haben vielfältige Fähigkeiten, auf ihre Zielzellen einzuwirken, und können daher sowohl in der Physiologie als auch in der Regeneration eine entscheidende Rolle spielen. Als Trägermaterial werden pH-neutrale, abbaubare Membranen auf Seidenfibroinbasis verwendet, die hervorragende zell- und gewebespezifische Eigenschaften aufweisen. Durch einen alkoholbasierten, schonenden Löseprozess können die Kokons des B. mori in eine wässrige Lösung überführt werden. Im Anschluss daran wird die reine Fibroinlösung mit den EVs funktionalisiert und im Anschluss in die Form einer Membran überführt, grafisch dargestellt auch in Abbildung 13.

Die Charakterisierung der Vesikel ergab einen Größenbereich zwischen 120-180 nm und eine hohe Expression der üblichen EV-Marker (z.B. CD9, CD63 und CD81), gemessen mittels Nanopartikel-Tracking-Analyse (NTA) und Einzel-EV-Flow-Analyse (IFCM). Eine anfängliche Integration der EVs in die SF-Membran wurde mit Hilfe der Raster- und Transmissionselektronenmikroskopie (SEM und TEM) analysiert und die Vesikel wurden erfolgreich nachgewiesen, auch wenn sie nicht homogen in der Membran verteilt waren. Die Proliferation von L929-Zellen war auf den mit EVs funktionalisierten Membranen erhöht ($p>0,05$). Durch direkte und indirekte Tests konnte die Zytokompatibilität der Membranen mit und ohne EVs nachgewiesen werden und zeigte signifikante Unterschiede im Vergleich zur toxischen Kontrolle ($p<0,05$).

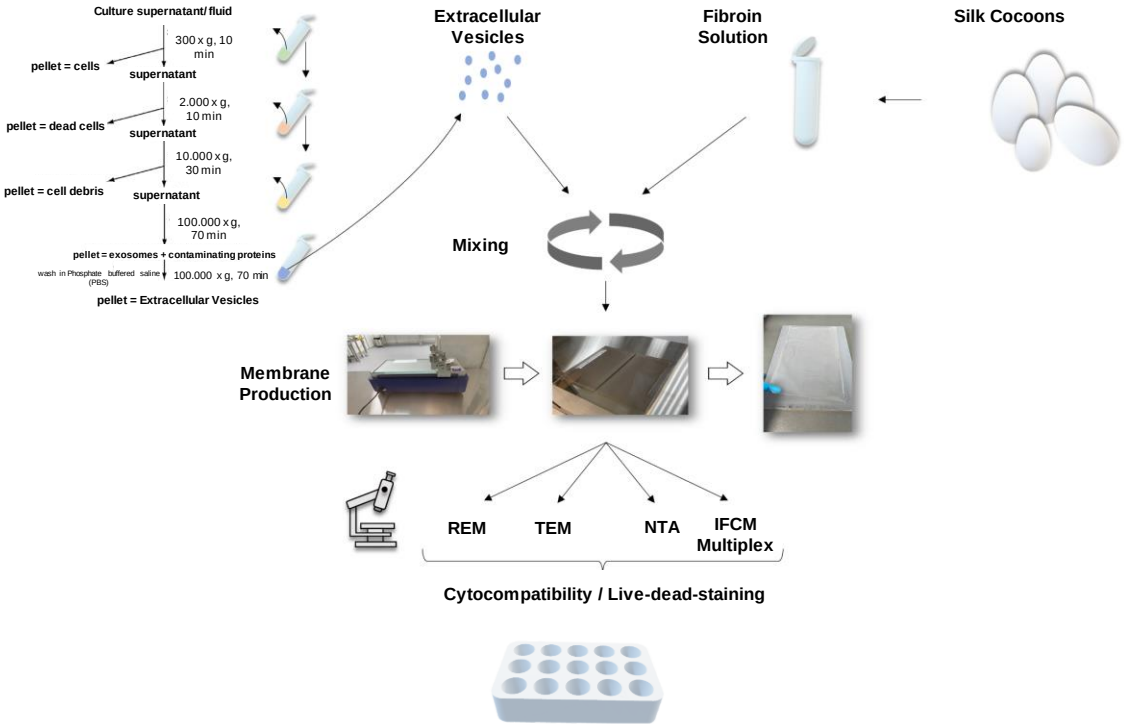

Abbildung 13: Eigene Darstellung der durchgeführten Experimente in Fuest et. al. 2024 (Fuest *et al.*, 2024).

Tabelle 2: Eigene Darstellung der in dieser Dissertation verwendeten Materialien und Methoden.

<table>
<tr><th colspan="2">Fibroinisolation</th><th>Sericinisolation</th></tr>
<tr><td colspan="2">Die Seidenfibroin-Lösung wurde gemäß der PureSilk® Technologie hergestellt. Die beiden Proteine Fibroin und Sericin wurden durch den Degumming Prozess voneinander getrennt und die reine Fibroin-Watte mittels Ajisawa´s reagent in eine lösliche Form überführt. Das gelöste Fibroin wurde mit Hilfe eines Extraktionsverfahrens innerhalb von acht Stunden vollständig gegen Voll-entsalztes-Wasser (VE-Wasser) dialysiert. Die für diese Studie verwendete Fibroinkonzentration wurde auf 1 g/ml eingestellt und bei 4 °C gelagert.</td><td>Entbastungsprozess von B. mori-Seidenkokons mittels 8 M Harnstofflösung (1:44.414). Die Sericin-Harnstofflösung wurde in Dialysemembranen (MWCO 3,5 kDa) überführt und 48 Stunden lang dialysiert.
Flexible Strukturen aus Sericin wurden durch Zugabe von Glycerin zu der Sericin-Lösung hergestellt.</td></tr>
<tr><th colspan="3">Weiterverarbeitungsformen</th></tr>
<tr><th colspan="2">Vliese</th><th>Membranen</th></tr>
<tr><td colspan="2">Herstellung: Elektrospinnverfahren werden Polymerfasern im Nanometerbereich aus Fibroinlösung durch die Einwirkung eines elektromagnetischen Feldes erzeugt.
Funktionalisierung: Tauchprozess in AgNO3-Lösung oder Gentamicin.</td><td>Herstellung: Abgießen der Seidenlösung in ein planes Gefäß mit anschließender Trocknung. Um homogenere Membrandicken erzielen zu können, kann alternativ auf maschinelle Geräte wie einem Filmziehrakel oder speziellen Gießvorrichtungen zurückgegriffen werden.
Funktionalisierung: Fibroinlösung vorab mit Gentamicin oder Silbernitrat gemischt und letztere für 1 h mit Ultra-Violettem (UV) Licht bestrahlt. Alternative Funktionalisierung der Seidenlösung mittels Extrazellulärer Vesikel</td></tr>
<tr><th colspan="3">Nachbehandlungsmethoden</th></tr>
<tr><td colspan="3">Kristallisierung der Fibroin-Strukturen mittels Ethanolbad (70 v%) für 1 h und alternativ einer 30-Minütigen Wasserdampfbehandlung bei 70 °C mit anschließender Trocknung.</td></tr>
<tr><th>Veröffentlichung I: Layer-by- Layer (Fuest et. al. 2023)</th><th>Veröffentlichung II/ III: Antibakterielle Seide (Artikel + Review) (Schäfer et. al. 2022, 2023)</th><th>Vedröffentlichung IV: Vesikel/ Seide (Fuest et. al. 2024)</th></tr>
<tr><td>Probekörper:
Titan (Ti Grade 4, ø 9 mm, Meotec GmbH, Deutschland)
Magnesium (WE43MEO, ø 9 mm, Meotec GmbH, Deutschland)
PMMA (Acrylglas-Rundstab ø 8 mm, B&T Metall, Deutschland)
PEO-Modifkation durch von Titan und Magnesium durch Anlegen eines Gleichstroms und Ausbildung einer Oxidschicht.
Beschichtungstechnik mittels DipMator-Software für 10 Sek. in 5 Gew.-% SF Lösung.
Kontaktwinkelmessung in Anlehnung an DIN ISO 55660-2, Auswertung mittels Image Access (Imagic Bildverarbeitung AG, Glattbrugg, Schweiz)
REM-Analyse mittels Philips XL30, Sputtertechnik durch Sputter Coater S150B (Edwards, Crawly, Englang)
FTIR Messungen mit einem Nicolet Nexus 470 Spektrometer (Thermo Fisher Scientific, Waltham, MA, USA)
Zellkultur-Testungen: Hämokompatibilitätsmessung im Chandler-Loop-System (CORMED, Rüthen, Deutschland); Besiedlung von THP-1 Zellen in Vollmediummit anschließender Fixierung der Zellen auf der Oberfläche mittels 3%iger Glutaraldehydlösung (GA). Die Sekretion von TNF-α wurde mittels ELISA-Sandwich-Kit gemäß den Angaben des Herstellers (Quantikine, R&D Systems, Minneapolis, MN, USA) evaluiert.
Statistik: Es wurde ein zweiseitiger t-Test für ungepaarte Stichproben mit GraphPad Prism (Version 8.4.0; GraphPad Software) durchgeführt. Die Daten sind mit (*) für ein Signifikanzniveau p < 0,05 gekennzeichnet.</td><td>Artikel:
REM-Analyse mittels Crossbeam 340 (Zeiss, Oberkochen, Deutschland)
Sputtertechnik durch Sputter Coater S150B (Edwards, Crawly, Englang)
Bestimmung der Gesamtlebendkeimzahl:
Inkubation der Proben 24 Stunden lang in künstlichem Speichel (a-Amylase 1 mg/mL, Mucin 0,85 mg/mL und Rinderserumalbumin (BSA) 0,4 mg/mL).
Herstellung der einer flüssigen Bakterienmischkultur durch anaerobe Färbungen von früh kolonisierenden Streptococcus mutans (Streptococcus mutans, DSM 20523, Deutsche Sammlung von Mikroorganismen und Zellkulturen GmbH, Leibnitz, Deutschland), mäßig kolonisierenden Actinomyces naeslundii (Actinomyces naeslundii, DSM 17233, Deutsche Sammlung von Mikroorganismen und Zellkulturen GmbH, Leibnitz, Deutschland), Fusobacterium nucleatum (Fusobacterium nucleatum, DSM 15643, Deutsche Sammlung von Mikroorganismen und Zellkulturen GmbH, Leibnitz, Deutschland) und der spät kolonisierende Porphyromonas gingivalis (Porphyromonas gingivalis, DSM 20709, Deutsche Sammlung von Mikroorganismen und Zellkulturen GmbH, Leibnitz, Deutschland). Die Anzahl der lebensfähigen Bakterien wurde durch Beimpfen von Blutagarplatten in Verdünnungen von 1:100, 1:1000 und 1:10.000 getestet und die Kolonie bildende Einheit (KBE) gemessen. Gesamtanzahl der bakteriellen DNA wurde mittels Polymerase-Kettenreaktion (PCR) gemessen (innuPREP DNA Isolation Kit, Analytik Jena AG, Jena, Deutschland); die DNA-Menge mittels qrt-PCR (CFX96 Touch Real-Time PCR Detection System, Bio-Rad Laboratories, Berkeley, Kalifornien, USA) mittels eubakteriellem 16S-rRNA-Primer. Die direkte antibakterielle Aktivität wurde mittels Hemmhoftest (Agar-Diffusionstest) bestimmt. Die statistische Analyse der antibakteriellen Tests wurde mit SAS 7.4 (SAS Institute Inc., Cary, North Carolina, USA) durchgeführt. Die Zytokompatibilität wurde in Anlehnung an die deutsche Fassung der EN ISO 10993.5: 2009/-12: 2012 durchgeführt.

Review:
Search-Terms:
(Seidenfibroin) ODER (Seidensericin) ODER (Seidenprotein) UND (antibakteriell) ODER (antimikrobiell) ODER (bakterientötend)
Einschlusskriterien:
1- Originalarbeiten (präklinisch und klinisch)
2- Indikation: klinische Anwendung
3- Bestandteil der zu untersuchenden Materialien Fibroin oder Sericin
4- Schwerpunkt liegt auf antibakterieller Analyse 5- Kontrollgruppe ohne antibakterielle Funktionalisierung</td><td>Vesikelisolation:
immortalisierte humane Zahnfleischfibroblasten (P10866, Innoprot, Derio (Bizkaia), Spanien) durch Ultrazentrifugation gewonnen.
Vesikelcharakterisierung: Vesikeltracking mittels Nanoparticle Tracking Analysis (NTA) und Imaging Flow Cytometry (IFCM). Die phänotypische Charakterisierung erfolgt mittels MACSPlex Exosome Kit (Miltenyi). REM Analyse mittels Crossbeam 340, Zeiss, Oberkochen, Deutschland. Gold-Sputterprozess erfolgt mittels Sputter Coater S150B, Edwards, London, England. TEM Analyse mittels TEM LEO 906 (Carl Zeiss, Oberkochen, Deutschland). Die Zytokompatibilität wurde in Anlehnung an die deutsche Fassung der EN ISO 10993.5: 2009/-12: 2012 durchgeführt.
Statistik: Auswertung mittels SPSS 21 (IBM, Armonk, NY, USA). **p < 0,05 bedeutet einen signifikanten Unterschied für alle getesteten Gruppen.</td></tr>
</table>

5 Gesamtdiskussion

Seide als Biomaterial natürlichen Ursprungs erhält in der orofazialen Medizin seit Jahren immer mehr Aufmerksamkeit (Kopp *et al.*, 2019a; Kopp, Schunck, *et al.*, 2020; Molinnus *et al.*, 2021; Smeets, Henningsen, *et al.*, 2022; Fuest *et al.*, 2023, 2024; Smeets *et al.*, 2023). Seidenmaterialien lassen sich aufgrund ihrer versatilen Formgebung ideal als Trägermaterialien für verschiedenste klinische Applikationen funktionalisieren (Schäfer *et al.*, 2022; Fuest *et al.*, 2024). Aber auch Fibroin in Form einer regenerierten Lösung als Beschichtungsmaterial stellt eine sinnvolle Alternative zu herkömmlichen Beschichtungen dar. Allem voraus geht die Überführung der Seidenkokons des *B. mori* in eine wässrige Fibroinlösung. Dieser Vorgang beinhaltet bei allen hier aufgeführten Publikationen stets die gleiche Prozessroute unter Verwendung des Lösemittels „*Ajisawa´s reagent*“, welches durch seine Bestandteile Wasser, Ethanol und Calcium einen sehr schonenden Löseprozess im Vergleich zu toxischen Alternativen wie Lithiumbromid oder Ameisensäure darstellt (Ajisawa, 1997). Der Entbastungsprozess, bei dem die beiden Proteine Fibroin und Sericin mittels Natriumcarbonat (Na_2CO_3) voneinander getrennt werden, erwies sich wie auch in der Literatur beschrieben als erfolgreich. Einen milderen Trennprozess konnte die Studie von Yamada et. al. 2001 zeigen, welche die beiden Proteine sowohl in 8 M Harnstoff als auch in 0,05 % Na_2CO_3 erhitzte und mittels SDS-Page eine intaktere Fibroinstruktur auf molekularer Ebene beim Löseprozess mit 8 M Harnstoff evaluierte (Yamada *et al.*, 2001). Mittels unterschiedlicher Kristallisierungsmethoden ist es möglich, die Proteinkonformation der wasserlöslichen Seide I in eine wasserunlösliche Seide II Struktur umzuwandeln (Fuest *et al.*, 2023). Die Struktur der Seide I gilt als weniger komprimierte Struktur, weist dadurch aber auch einen sehr instabilen Charakter auf. Mit Hilfe von organischen Lösemitteln oder thermischen Behandlungen kann die Proteinstruktur der Seide umgewandelt werden und es entsteht eine sogenannte β-Faltblattstruktur (Seide II). Nach Angaben der Literatur beeinflusst die Konzentration der Behandlungslösung die Geschwindigkeit der Kristallisation (Wang *et al.*, 2005; Terada *et al.*, 2016). Alkoholkonzentrationen von 90% oder 100% verlangsamen die Kristallisation extrem (Wang *et al.*, 2005; Terada *et al.*, 2016). Aus diesem Grund wurde in der Studie nach Fuest et. al. 2023 eine 70 Vol% Ethanolkonzentration verwendet (Fuest *et al.*, 2023). Vergleichend dazu wurde als weitere Methode die Nachbehandlung mittels temperaturgesteuerter Behandlung gemäß Hu et. al. 2011 mittels Wasserdampf etabliert (Hu *et al.*, 2011). Diese Technik stellt eine schonendere und wirksamere Methode, wenn auch zeitaufwendigere Methode zur Kontrolle der molekularen Struktur und des Kristallisationsgrades dar. Die Wassermoleküle mit ihrer vergleichsweise kleinen Größe dringen in die Ansammlung der Seidenproteinketten ein und „*plastifizieren*“ die Proteinstruktur zu einem Netzwerk mit höherer Kettenbeweglichkeit bei gleichbleibender Flexibilität der Fibroin-Strukturen (Tanaka, Inoue and Mizuno, 1999; Guo *et al.*, 2019; Fuest *et al.*, 2023). Weiteren Studien zufolge können auch

Ultraviolettes Licht (UV-Licht) oder Glycerol zur Ausbildung des Kritsallisationsgrades bei gleichbleibender Flexibilität der Seidenstruktur beitragen (Wang *et al.*, 2015).

Seidenfibroin erfüllt als innovatives Biomaterial die meisten Anforderungen von konventionellen Beschichtungsmaterialien und bietet somit eine einfache, vielseitige und leichte Beschichtung von Implantatmaterialien mit dem Ziel, diese zu funktionalisieren und die Interaktion von Zellen und Gewebe positiv zu beeinflussen (Fuest *et al.*, 2023). Obwohl verschiedene Techniken entwickelt wurden, Seidenfibroin auf Substratoberflächen aufzutragen und diese zu charakterisieren (Guo *et al.*, 2019; Saha, Pramanik and Biswas, 2019), fehlen bis heute systematische Bewertungskriterien einer einheitlichen Seidenfibroin-Beschichtung durch Layer-by-Layer (LbL) auf relevanten Implantatmaterialien (Saha, Pramanik and Biswas, 2019). Trotz zahlreicher Fortschritte bei den Beschichtungsmaterialien wurde beobachtet, dass nach der Implantation schwere allergische Reaktionen auftreten können (Luthringer, Feyerabend and Römer, 2014). Die Anwendung von reinem Fibroin als Beschichtung auf den Implantatmaterialien Titan, Magnesium und PMMA wurde von Fuest et. al. 2023 charakterisiert (Fuest *et al.*, 2023) und evaluierte u.a. ihre Eigenschaften im Hinblick auf Fremdkörperreaktionen. Es konnte beobachtet werden, dass die Benetzungseigenschaften der beiden metallischen Werkstoffe durch eine vorhergehende PEO-Modifizierung optimiert werden konnten und eine hydrophilere Oberfläche erzielt werden konnte, die sich für Magnesium von 73° auf 18° und für Titan von 58° auf 17° reduzierten. Besonders im Biomedizinischen Bereich hat sich gezeigt, dass Oberflächenmodifikationen wie PEO die Verträglichkeit von Blut erhöhen (Tang, Thevenot and Hu, 2008). Vergleichende Ergebnisse zeigten auch Mingo et. al. und Echeverry-Rendón et. al. (Echeverry-Rendón *et al.*, 2017; Mingo *et al.*, 2018). In der vorliegenden Studie wurde die LbL-Methode verwendet, um etablierte Implantatmaterialien mit Seidenfibroin zu beschichten. Die Gruppe von Saha et al. hat die Beschichtung von Seidenfibroin auf TiO2-Nanoröhrchen (Titan Grad 4 Legierung) durchgeführt (Saha, Pramanik and Biswas, 2019). Hier wurden Kontaktwinkel von 83° bis 90° gemessen. Die LbL-Methode konnte erfolgreich für Seidenfibroin-Beschichtungen auf Materialoberflächen etabliert werden. Es kann die Hypothese abgeleitet werden, dass die Schichtdicke des Fibroins mit steigender Anzahl an Tauchgängen zunimmt. Allerdings erwiesen sich die Schichtdicken nicht immer als homogen auf der Oberfläche verteilt und erzielten Schichtdicken von durchschnittlich ~ 2,22 µm bzw. 5,14 µm für Magnesium und Titan. Die dünnste Schicht wurde für PMMA erzielt mit ca. 0,41 µm und zum Teil unbeschichteten Bereichen. Diese Daten passten mit den Daten aus der Literatur überein, siehe u.a. Guo et. al. 2019 und Ghumatkar et. al. 2016 (Ghumatkar *et al.*, 2016; Guo *et al.*, 2019). Die PEO-modifizierten Proben zeigten ein besseres Beschichtungsverhalten als die nicht modifizierten Proben. Besonders die Poren der PEO-Schicht füllten sich mit Fibroin und erzielten in den Bereichen höhere Schichtdicken. Die Untersuchung der Hämokompatibilität wurde in erster

Linie zur Beurteilung der Blutgerinnung durchgeführt, die von einer Reihe proteolytischer Faktoren abhängt. Dieser Prozess umfasst intrinsiche und extrinsische Gerinnungsreaktionen (Monroe and Hoffman, 2006; Fuest *et al.*, 2023). Die gemessene Thromboplastinzeit (PTT-Zeit) zeigte sich auf den unbehandelten Magnesiumproben leicht erhöht als auf den PEO-behandelten Proben, was auch mit anderen Studien nach Kzhyshkowska et. al. 2015 und Bridges et. al. 2008 übereinstimmt (Bridges and García, 2008; Kzhyshkowska *et al.*, 2015; Fuest *et al.*, 2023). Aufgrund der hohen Korrosionsneigung von reinen Magnesiumlegierungen wird vermutet, dass große Mengen an Magnesiumionen dem Blutfluss ausgesetzt sind und dies eine mögliche Hämolyse, sprich einem Platzen der Blutkörperchen, zur Folge haben kann (Bunn, Ransil and Chao, 1971; Gailani and Renné, 2007; Fuest *et al.*, 2023).

Mittels Rasterelektronenmikroskopie wurde unter anderem die Anzahl adhärenter Zellen (u.a. die monozytäre undifferenzierte humane monozytäre Leukämiezelllinie (THP-1)) auf den verschiedenen beschichteten Implantatoberflächen analysiert. Ziel der Studie nach Fuest et. al. 2023 war es in erster Linie, die Beschichtung aus Fibroin dahingehend zu modifizieren, dass Monozyten durch Anhaftung an der Oberfläche zu Makrophagen differenzieren können (Fuest *et al.*, 2023). Seidenfibroin wurde verwendet, weil es so angepasst werden kann, dass es die Freisetzung von Zytokinen unterdrückt oder fördert, und weil es unter physiologischen Bedingungen in wässriger Umgebung verarbeitet werden kann. Außerdem wurde bereits in mehreren in-vitro-Studien gezeigt, dass die Zellfunktionalität mittels Seidenfibroin erhalten werden kann (Panilaitis *et al.*, 2003; Reeves *et al.*, 2015; Fuest *et al.*, 2023). Weitergehend wurde mit einem *Enzyme-linked-immunosorbet assay* (ELISA) das entzündliche Potenzial von Seidenfibroin als Beschichtung quantifiziert, da Makrophagen eine entscheidende Rolle im Immunsystem des Menschen spielen (Fuest *et al.*, 2023). Das Immunsystem stellt einen unerlässlichen Bestimmungsfaktor für die Verträglichkeit und Zytokompatibilität von Biomaterialien im Körper dar (Panilaitis *et al.*, 2003; Gardner *et al.*, 2013; Brown and Badylak, 2014). Nach der Implantation von Biomaterialien stimulieren Makrophagen das Gewebe, um die Wundheilung zu gewährleisten, andererseits lösen sie Abbauprozesse und Entzündungsreaktionen aus (Franz *et al.*, 2011; Brown and Badylak, 2014; Sheikh *et al.*, 2015; Fuest *et al.*, 2023). Dabei wirkt TNF-α als proinflammatorisches Zytokin, das von M1-ähnlichen Makrophagen sezerniert wird. Hier wird die Rekrutierung und Differenzierung von mesenchymalen Vorläuferzellen für die Knochenheilung gefördert sowie die Knochenbildung und den Knochenumbau gesteuert (Rasouli, Barhoum and Uludag, 2018; Fuest *et al.*, 2023). Bemerkenswert ist, dass die koordinierte Interaktion zwischen der Osteoimmunreaktion und der Osteogenese, die durch Makrophagen vermittelt wird, eine zentrale regulatorische Rolle in allen Phasen der Knochenreparatur spielt (Rasouli, Barhoum and Uludag, 2018; Fuest *et al.*, 2023). Die Studie nach Fuest et. al. 2023 zeigt, dass TNF-α nach der Fibroin-Beschichtung auf allen getesteten Substratmaterialien signifikant erhöht war. Auf Fibroin-beschichteten,

PEO-oberflächenmodifizierten Titan- und Magnesium-Proben erreichten die TNF-α-Zytokine Werte von 260 pg/ml bzw. 250 pg/ml. Die höchste Menge wurde bei beschichtetem PMMA (~ 400 pg/ml) festgestellt. Ohne Fibroin-Beschichtung waren diese Konzentrationen deutlich geringer. Ein Grund für dieses Verhalten könnte auf Fibroin-Proteine zurückzuführen sein, die sich von der Beschichtung ablösen und eine Aktivierung der Zellen im Medium bewirken (Panilaitis *et al.*, 2003; Fuest *et al.*, 2023).

Summa summarum kann festgestellt werden, dass eine Oberflächenmodifikation mit Seidenfibroin die Biokompatibilität von Implantatmaterialien nachweislich verbessert und die Osteogenese stimuliert. Vergleichende Ergebnisse wurden in den Studien von Guo et. al. 2019, Melke et.al. 2016 und Yoo et. al. 2016 festgestellt (Melke *et al.*, 2016; Yoo *et al.*, 2016; Guo *et al.*, 2019).

Nachdem die Publikation nach Fuest et. al. 2023 (Fuest *et al.*, 2023) erfolgreich gezeigt hat, dass regeneriertes Seidenfibroin in seiner flüssigen Form für eine spätere Anwendung im Biomedizinischen Bereich aufgrund einer hervorragenden Biokompatibilität angewendet werden kann, wurde sich im Rahmen dieser Doktorarbeit die versatile Formgebung der Seide zu Nutze gemacht und diese für verschiedenste klinische Applikationen funktionalisiert.

Dazu zählen neben Wachstumsfaktoren auch antibakterielle Stoffe oder Extrazelluläre Vesikel (EVs) in ihrer spezifischen Funktion (Schäfer *et al.*, 2022, 2023). Hanken et. al. 2016 publizierte eine Studie, in welcher Prä-Adipozyten über Wachstumsfaktoren ausdifferenziert werden konnten, welche an Seidenmembranen gekoppelt waren (Hanken *et al.*, 2016). Darüber hinaus können neben Antibiotika auch metallische Nanopartikel angewendet werden (Yerra and Dadala, 2022), welche antimikrobielle Eigenschaften mit sich bringen und die Entzündungsantwort verringern (Ramadass *et al.*, 2019; Zhang *et al.*, 2019; Wang *et al.*, 2020). Besonders Gentamicin, ein Aminoglykosid-Antibiotikum, wird in großem Maße zur akuten Behandlung bakterieller Haut- und Weichteilinfektionen eingesetzt (Rosen *et al.*, 1991; Gruessner *et al.*, 2001; Kwong *et al.*, 2020; Schäfer *et al.*, 2022). Sideratou et al. 2022 charakterisierte antibiotika-beladene 3D-Seidenscaffolds zur späteren Behandlung dentaler Infektionen wie z.B. einer Periimplantitis (Sideratou *et al.*, 2022).

Eine weitere Studie nach Zhou et. al. 2017 schaffte es, antibakterielle Wirkstoffe (AgNPs und Gentamicin) mit einer Seidenfibroin/ Chitosan-Dentalimplantatbeschichtung zu kombinieren, welche zum einen die Biofilmbildung und das Bakterienwachstum deutlich hemmte und zum anderen das Wachstum von knochenbildenden Zellen (Osteoblasten) vermehrt unterstützte (Zhou *et al.*, 2017; Schäfer *et al.*, 2022). Besonders offene Wunden, welche bei chirurgischen Eingriffen entstehen können, stellen ein großes Risiko für eine Infektion mit Mikroorganismen wie Bakterien oder Pilzen und Viren dar (Schäfer *et al.*, 2023). Innovative Biomaterialkonzepte wie Seidenproteine könnten eine ideale Präventionsmaßnahme bieten und die bakterielle Besiedlung nachweislich vermindern (Schäfer *et al.*, 2023). Im Rahmen eines systematischen

Reviews nach Schäfer et. al. 2023 wurde evaluiert, dass Fibroin in 16,67 % und Sericin in 35,29 % (Verhältnis 6:17) der entsprechenden Studien eine inhärente antibakterielle Aktivität aufweist (Schäfer *et al.*, 2023). Besonders bemerkenswert war dabei, dass die Interaktion und Wirksamkeit von Sericin gegen Bakterienzellen nicht nur dosisabhängig ist, sondern auch von den strukturellen Merkmalen nach der Herstellung abhängt. Letzteres ist besonders in Hinblick auf die beabsichtigte Anwendung eine unvermeidliche Überlegung. Strukturen wie Membranen oder Vliese aus Sericin sind aufgrund der variablen Verteilung des Molekulargewichtes im trockenen Stadium zerbrechlich (Makvandi *et al.*, 2020; Schäfer *et al.*, 2022, 2023). In dieser Hinsicht gibt es einige Herausforderungen bei der Anwendung von Sericin für die Regeneration von Weichgewebe oder Knochen, wie z. B. bei der GBR oder der GTR, die ein Gerüst oder eine okklusive Membran erfordern, um vorübergehend Platz, Unterstützung und Führung für die Adhäsion und Proliferation von Wirtszellen zu bieten (Makvandi *et al.*, 2020; Smeets, Henningsen, *et al.*, 2022; Schäfer *et al.*, 2023). Ein von Yang et. al. 2017 getestetes Sericin-Nanokomposit-Hydrogel hemmte nachweislich das Bakterienwachstum, in dem es Bakterien an der Hydrogeloberfläche adsorbiert hat (Yang *et al.*, 2017; Schäfer *et al.*, 2023). Im Gegensatz dazu ist Fibroin nicht als Polymer mit bakterizider Wirkung bekannt. So führten Zhang et al. eine mehrteilige Studie durch, in der eine neuartige Fibroin-Folie/ ein neuartiger Fibroin-Verband für die Wundheilung untersucht und mit kommerziellen Wundverbänden verglichen wurde. Die Studie umfasste eine *In-vitro*-Bewertung, bei der die Fibroin Folie aufgrund ihrer einzigartigen nichtporösen Struktur das Eindringen von Bakterien mechanisch verhindern konnte, sowie ein *In-vivo*-Modell eines Hautdefekts bei Kaninchen, bei dem sich zeigte, dass die Fibroin-Folie die durchschnittliche Wundheilungszeit effektiv verkürzt und die Hautregeneration im Vergleich zu einer kommerziellen Wundauflage verbessert. Eine anschließende Bewertung in einem Schweinemodell bestätigte die langfristige Sicherheit und Wirksamkeit der Folie bei Hautdefekten in voller Dicke. Darüber hinaus reduzierte die Seidenfibroinfolie in einer randomisierten klinischen Einzelblindstudie mit 71 Patienten signifikant die Wundheilungszeit und das Auftreten unerwünschter postoperativer Infektionen (Zhang *et al.*, 2017; Schäfer *et al.*, 2023). Bei genauer Durchsicht der aktuellen Literatur konnte in fünf von 30 untersuchten Studien eine Indikation für die antibakterielle Wirkung von Fibroin festgestellt werden. Drei Studien schrieben Fibroin jedoch die beste oder eine ähnliche antibakterielle Aktivität im Vergleich zur Kontrollgruppe zu. Zwei dieser Studien untersuchten genetisch veränderte Seidenraupen, die antibakterielle Peptide produzieren, und eine Studie berichtete über eine ähnliche antibakterielle Aktivität von reinem Fibroin im Vergleich zu Polypropylen + Fibroin. Von den anderen beiden Studien untersuchte eine Studie von Arpaçay et al. 2016 antimikrobielle Implantatbeschichtungen für eine verbesserte Knochenregeneration (Arpaçay and Türkan, 2016). Sie wiesen Levofloxacin-beschichteten Implantaten die beste antibakterielle Wirkung gegen die Biofilmbildung von *Staphylococcus aureus* zu. Allerdings

wurde auch bei den ausschließlich mit Fibroin beschichteten Implantaten im Vergleich zu den unbeschichteten eine geringere Biofilmbildung beobachtet, wobei eine geringere Anzahl koloniebildender Einheiten festgestellt wurde (Arpaçay and Türkan, 2016; Schäfer *et al.*, 2023).

Es gibt eine Reihe von neuartigen Ansätzen, Wirkstoffe wie Polymere, Lipide, Antibiotika oder metallische Nanopartikel direkt an die Seidenproteine zu binden (Lv *et al.*, 2016; Song *et al.*, 2016; Zhou *et al.*, 2018; Jo *et al.*, 2019; Khan *et al.*, 2019; Tian *et al.*, 2019). Im Rahmen der Veröffentlichung von Schäfer et. al. 2022 lag der Schwerpunkt auf der Charakterisierung und Evaluierung von Seidenfibroin- und Sericinmembranen und Vliese für die intraorale Wundheilung, welche mit den antibakteriellen Substanzen Gentamicin und Silber additiviert wurden. Die unterschiedlichen Ausprägungen der Seidenproteine zur Anwendung in der intraoralen Wundheilung wurden zu Beginn mittels REM analysiert. Die Fibroinvliese zeigten sich durch eine stark ineinander verschlungene Faserstruktur im Vergleich zu der glatten Oberfläche der gegossenen Membranen auf Fibroin- und Sericinbasis. Die Querschnittsaufnahme der Vliese zeigte eine homogene und gleichmäßig verteilte Faserverbindung innerhalb der gesamten Dicke (Schäfer *et al.*, 2022). Die Membranen zeigten sich dagegen amorph in ihrer Struktur mit vereinzelten aufeinander geschichteten Bereichen, welche als Schneide-Artefakte identifiziert werden konnten. Die gegossenen Membranen wiesen hingegen eine raue Oberflächentopographie auf; dies kann bedingt durch die Funktionalisierung mit Silber und Gentamicin hervorgerufen werden (Schäfer *et al.*, 2022).

Besonders nanofaserige Seidenstrukturen zeigten gemäß der Literatur eine verbesserte Anheftung und Vermehrung von Fibroblasten und Keratinozyten und optimierten den Heilungsprozess von Wunden in Schleimhautgeweben (Kasoju and Bora, 2012b; Gholipourmalekabadi *et al.*, 2020). Eine Studie nach Tang et. al. 2015 untersuchte die Wundheilungsfähigkeit von elektrogesponnenen Fibroinvliesen auf der Wangenschleimhaut in Rattenmodellen (Tang *et al.*, 2015). Diese verbessern nachweislich den Heilungsprozess und optimieren zudem die entzündungshemmende Wirtsreaktion (Tang *et al.*, 2015). Vergleichende Ergebnisse zeigte eine weitere *in-vivo* Studie von Ge et. al. 2012, in welcher Gerüststrukturen auf Fibroinbasis auf bukkale Defekte in der Ratte getestet wurden (Ge *et al.*, 2012). Um die Wundheilung signifikant zu verbessern muss eine ausreichende Biokompatibilität des defektfüllenden Materials gewährleistet sein, um die Zellen des geschädigten Gewebes ideal zu versorgen (Schäfer *et al.*, 2022). Die exzellente Biokompatibilität von Seide konnte bereits in zahlreichen Studien dargelegt werden, auch im Rahmen dieser Doktorarbeit, u.a. in Schäfer et. al. 2022 und Fuest et. al. 2024 (Schäfer *et al.*, 2022; Fuest *et al.*, 2024). Mit Ausnahme der silberbeladenen Membran zeigten alle mit Gentamicin-funktionalisierenden und Kontrollmembranen eine ausreichende Zytokompatibilität sowohl in den indirekten Testungen (XTT, LDH) als auch in den direkten

Testungen (*Live-dead-staining*). Die in Schäfer et. al. 2022 verwendete Dosis von 10 mg/ ml Gentamicin für L929-Mausfibroblasten stellt eine tolerierbare Anwendungsdosis dar und zeigt vergleichende Ergebnisse zu Stevanovic et. al. 2020, die eine gute Verträglichkeit zwischen Zellen und Gentamicin bei einer Menge unter 50 mg/ ml darstellen konnten (Stevanović *et al.*, 2020; Schäfer *et al.*, 2022). Im Gegensatz dazu zeigten sich die silberbeladenen Membranen und Vliese, welche mit 100 mg/ L AgNPs funktionalisiert waren, zytotoxisch in der Zellkultur (Schäfer *et al.*, 2022). Zurückzuführen ist dieses Verhalten auf den oxidativen Stress, der durch die Silberionen auf die Zelle ausgeführt wird. Vergleichende Ergebnisse konnte Panda et. al. 2011 erzielen (Panda *et al.*, 2011; Schäfer *et al.*, 2022). In der Tat erzeugen AgNPs ein hohes Maß an intrazellulären reaktiven Sauerstoffspezies (ROS). Diese beeinträchtigen die Aktivität von antioxidativen Enzymen, was zu apoptotischen Signalwegen in der Zelle führen kann (Panda *et al.*, 2011; Piao *et al.*, 2011; Schäfer *et al.*, 2022). Hinzu kommt, dass AgNPs an funktionelle Gruppen von Zellproteinen binden und anschließend physiochemische Wechselwirkungen innerhalb der Zellen auslösen (Składanowski *et al.*, 2016; Schäfer *et al.*, 2022). Vergleichende Studien berichten über eine sichere, nicht zytotoxische Anwendung von AgNPs bei Konzentrationen von ≤ 25 mg/ L (He *et al.*, 2017; Lv *et al.*, 2018; Schäfer *et al.*, 2022). Der Schwerpunkt der Studie nach Schäfer et. al. 2022 lag jedoch auf der Charakterisierung der Membranen und Vliese in Hinblick auf die antibakteriellen Eigenschaften von funktionalisierten Seidenmembranen und Vliesen. Besonders die Verwendung von Silber als antibakterielle Substanz wird in der regenerativen Medizin schon seit Jahrzehnten untersucht (Klasen, 2000; Lv *et al.*, 2016; Schäfer *et al.*, 2022). Die antibakterielle Wirkung von Silber beruht auf einer Störung der Membranpermeabilität, die zu einem Verlust von intrazellulären K^+-Ionen, ATP und Phospholipiden führt. Darüber hinaus verursachen AgNPs oxidative Schäden, indem sie ROS erzeugen und anschließend intrazelluläre Metaboliten durch permeabilisierte Membranen entweichen (Gopinath *et al.*, 2017; Schäfer *et al.*, 2022).
Das Aminoglykosid-Antibiotikum Gentamicin besitzt einen Wirkmechanismus, der auf einem sauerstoffabhängigen Eintritt in die Bakterienzelle und der Stagnation der bakteriellen Proteinsynthese durch Bindung an die 30S ribosomale Untereinheit beruht (Gopinath *et al.*, 2017; Schäfer *et al.*, 2022). Dieser Prozess führt zum Zerfall der Zytoplasmamembran (Serio *et al.*, 2018; Schäfer *et al.*, 2022). Um das antibakterielle Potenzial von AgNPs und Gentamicin zu beurteilen, wurde im Rahmen dieser Doktorarbeit eine qrt-PCR, ein CFU-Assay und ein Agar-Diffusionstest (Hemmhoftest, Zone of inhibition (ZOI)) durchgeführt. Die getesteten Bakterienstämme wurden in Anlehnung an die Übersichtsarbeit von Curtis et. al. 2020 gewählt. Hier kamen die gram-positiven, fakultativ anaeroben, frühen Kolonisatoren *Actinomyces naeslundii* und *Streptococcus mutans* zur Anwendung, welche die häufigsten Bakterienstämme in der gesunden oralen Mikroflora darstellen (Piao *et al.*, 2011; Curtis, Diaz and Van Dyke, 2020; Schäfer *et al.*, 2022). Zusätzlich wurden zwei anaerobe, gram-negative

Bakterienspezies mit einbezogen: *Fusobacterium nucleatum*, welche die zweithäufigste intraorale Mikrobe bei gesunden Patienten darstellt, sowie die mit Parodontitis assoziierte Bakterienart *Porphyromonas gingivalis* (Curtis, Diaz and Van Dyke, 2020; Schäfer *et al.*, 2022). Durch die Anwendung von künstlichem Speichelmedium konnten optimale Wachstumsbedingungen für die Bakterienkulturen gewährleistet werden, welche äquivalent zu den klinischen Bedingungen in der Mundhöhle waren (Schäfer *et al.*, 2022). Die beste antibakterielle Aktivität wurde für die silberbeladenen Membranen (AgNPs) beobachtet; die qrt-PCR Ergebnisse zeigen die niedrigste bakterielle DNA-Zahl im Vergleich zu allen anderen anderen Materialgruppen, was auf ein reduziertes bakterielles Adhäsionspotenzial um 3 log-Stufen im Vergleich zu den Kontrollmembranen und Vliesen hindeutet (Schäfer *et al.*, 2022).

In vergleichenden Ergebnissen hinsichtlich einer ausreichenden antibakteriellen Aktivität konnte von Chandrasekaran et al. 2015 gezeigt werden, dass silberbeladene Fibroinfasern eine >90%ige Hemmung der Bakterienstämme *Pseudomonas aeruginosa* und *Staphylococcus aureus* aufweisen, die besonders mit Hautinfektionen assoziiert sind (Chandrasekaran *et al.*, 2015; Schäfer *et al.*, 2022).

Bei den getesteten Fibroin- und Sericin Vliesen zeigte sich die beste antibakterielle Aktivität bei den mit Gentamicin beladenen Vliesen, besonders in Hinblick auf die Anzahl lebensfähiger Bakterien und die Gesamtkeimzahl, welche sich mit einer 2log-Reduktion verdeutlichte. Mittels Hemmhoftest konnte eine direkte antibakterielle Aktivität von 7–8 mm ZOI nachgewiesen werden (Schäfer *et al.*, 2022).

Die verschiedenen Ergebnisse zwischen Fibrion- und Sericin Membranen und elektrogesponnenen Fibroin Vliesen könnte an den unterschiedlichen Herstellungsprozessen liegen. Die Funktionalisierung der Membranen wurde bereits vor dem eigentlichen Gussverfahren durchgeführt, sprich die $AgNO_2$ oder Gentamicin wurde in die Seidenlösung inkorporiert. Ein äquivalentes Vorgehen wurde in Fuest et. al. 2024 durchgeführt, auch hier wurden die EVs bereits vor Ausbildung der finalen Fibroinstruktur in die Seidenlösung inkorporiert (Fuest *et al.*, 2024). Im Gegensatz dazu wurden die antibakteriellen Wirkstoffe bei den Fibroin-Vliesen erst nach dem Elektrospinnprozess eingearbeitet. Eine weitere mögliche Erklärung für die geringere antibakterielle Aktivität kann die Auswaschung und/ oder Wechselwirkung von Silberionen (Ag-Ionen) mit Bestandteilen des künstlichen Speichels (z. B. BSA), Kultivierungsmedien (z. B. Hemin, Cystein, Pepsin usw.) oder dem PBS, das im Testverfahren verwendet wurde, sein (Schäfer *et al.*, 2022). Ando et al. 2010 begründen die Beeinträchtigung der antibakteriellen Aktivität von Silber auf Bestandteile der Kulturmedien, welche fötales Rinderserum (FBS) enthielten (ANDO *et al.*, 2010; Schäfer *et al.*, 2022).

In vielen Fällen kann der Einschluss von Additiven durch die interne Konformation der Polymerketten beeinflusst werden, was unter anderem in einer Studie von Besheli et al. 2017 belegt werden konnte, indem die Beladung mittels Antibiotika optimiert wurde und der Gehalt

der Seide II Struktur (ß-Faltblätter) erhöht wurde (Hassani Besheli *et al.*, 2017; Schäfer *et al.*, 2022). Dies kann durch verschiedene Nachbehandlungsmethoden wie Alkohole oder Wasserdampf möglich gemacht werden, siehe Fuest et. al. 2023 (Fuest *et al.*, 2023). Einige Studien schreiben den Seidenproteinen Fibroin und Sericin eine inhärente bakterizide Aktivität zu. Diese Thematik wurde bereits in Schäfer et. al. 2023 ausführlich recherchiert und im Rahmen eines systematischen Reviews diskutiert (Schäfer *et al.*, 2023). Bakhsheshi-Rad et. al. 2020 beispielsweise fanden heraus, dass Sericin Verbände bei *Escherichia coli* und *Staphylococcus aureus* im Hemmhoftest einen ZOI von 3-3,5 mm hervorriefen (Bakhsheshi-Rad *et al.*, 2020; Schäfer *et al.*, 2022). Gilotra et. al. 2018 konnte im Rahmen der durchgeführten Studie eine positive Korrelation zwischen der Hemmung des Koloniewachstums und der Sericin Konzentration in der Seidenstruktur feststellen (Gilotra *et al.*, 2018; Schäfer *et al.*, 2022). Die inhärente antibakterielle Eigenschaft von Fibroin wird hauptsächlich seiner Barrierefunktion als Wundverband zugeschrieben und wurde bereits von Zhang et. al. 2017 erfolgreich im Rahmen von in-vitro und in-vivo Modellen bewiesen (Zhang *et al.*, 2017; Schäfer *et al.*, 2022). Zusätzlich wird den Kokons des B. mori eine antimikrobielle Wirkung zugeschrieben, da antimikrobielle Peptide (z.B. Seroine) im Fibroin einen natürlichen Schutz der Seidenraupe gegen externe Krankheitserreger darstellen (Guo *et al.*, 2016; Schäfer *et al.*, 2022). Zusammenfassend konnte die im Rahmen dieser Dissertation durchgeführte Studie nach Schäfer et. al. 2022 keine antimikrobielle Aktivität aufweisen, weder die mit Fibroin noch die mit Sericin additivierten Strukturen. Allerdings können sie als gute mechanische Barriere fungieren, wie der Hemmhoftest gezeigt hat (Schäfer *et al.*, 2022). Für eine Anwendung in der Wundheilung im Bereich der Mund-, Kiefer- und Gesichtschirurgie zeigen sich Membranen auf Seidenbasis als ein vielversprechendes Substrat, es sollten hier jedoch weitere Studien u.a. in-vivo folgen.

Neben antibakteriellen Substanzen haben sich auch Extrazelluläre Vesikel (EVs) in den letzten Jahren als ein wichtiger Mediator herauskristallisiert, um die Förderung der Regeneration verschiedenster Gewebearten im Bereich der MKG-Chirurgie zu progressieren. Diese membranartigen Partikel, die von einer Bi-Lipid-Membran umschlossen sind, tragen eine vielfältige Ladung aus Proteinen, Lipiden, Nukleinsäuren und anderen bioaktiven Molekülen. Diese Ladung kann auf Empfängerzellen übertragen werden und so deren Verhalten und Funktionen beeinflussen (Fuest *et al.*, 2024). EVs aus mesenchymalen Stammzellen zeigen immunmodulatorische Eigenschaften, die das Risiko von negativen Immunantworten reduzieren und die positiven regenerativen Eigenschaften erhalten. Bereits seit einigen Jahren gelten EVs als Hoffnungsträger in der Diagnostik und Anti-Tumortherapie (Momen-Heravi *et al.*, 2013; Gardiner *et al.*, 2016; Li *et al.*, 2017; Colao *et al.*, 2018; Alcaraz, Compañ and Guillén, 2019). Auch in verschiedenen *in vitro* sowie *in vivo* Studien konnte nachgewiesen werden, dass EVs unter anderem die Angiogenese und die Reepithelisierung von defektem Gewebe

nachhaltig verbessern konnten (Z. Qian *et al.*, 2020; Zhang *et al.*, 2020; Liu *et al.*, 2021). Die wohl größte Herausforderung von EVs besteht in der schnellen Ausscheidung und daraus resultierenden raschen Verdauung durch Fresszellen (Makrophagen) (Witwer *et al.*, 2013). Die Immobilisierung der EVs in ein geeignetes Trägermaterial aus Seidenfibroin, welches eine längerfristige und kontrollierte Freisetzung der EVs am Wirkungsort ermöglicht, ist aktuell Stand der Forschung, und wird von der Arbeitsgruppe unter anderem im Sachhilfeantrag der Deutschen Forschungsgemeinschaft mit der Projektnummer 516860159 „*EVs zur Funktionalisierung von Polymeren – neue biohybride Materialien für die Regenerative Medizin im Kopf-Hals-Bereich*“ untersucht (AP 94/3-1 | RI 2616/ 5-1 | SM 214/8-1) (Fuest *et al.*, 2024). Weitere Arbeitsgruppen konnten bereits zeigen, dass die Inkorporierung von EVs in eine biomaterial-basierte Trägerstruktur wie z.B. ein Hydrogel oder ein 3D-Scaffolds effektivere Ergebnisse erzielte als die direkte Injektion der EVs in den jeweiligen Defekt (Liu *et al.*, 2017; Shi *et al.*, 2017; Xu *et al.*, 2018; Han *et al.*, 2019; Zhang *et al.*, 2020). Kyung Kim et. al. 2021 konnte in einem Kleintierversuch belegen, dass die Beschichtung eines 3D-Scaffolds auf Seidenbasis mit EVs eine proliferierende Wirkung auf das Wachstum von mesenchymalen Stammzellen mit sich brachte und zudem die osteogene Differenzierung förderte (Kyung Kim *et al.*, 2021). Im Hinblick auf die Behandlung von Defekten im Kopf-Hals-Bereich zeigten Qian et al. 2020, dass die Applikation von Seidenfasern, auf deren Oberflächen Liposomen mit eingekapseltem Leptin aufgelagert wurden, zu einer verbesserten Regeneration der Mundschleimhaut und Förderung der Gefäßbildung führte (C. Qian *et al.*, 2020). Im Rahmen dieser Dissertation wurde eine weitere Studie mit Fokus auf regenerative Therapieansätze durchgeführt. Die Studie nach Fuest et. al. 2024 (Fuest *et al.*, 2024) beschäftigte sich mit der Inkorporierung von EVs einer immortalisierten GF-Zelllinie in eine Fibroinstruktur. Die hier verwendete Struktur einer gezogenen Fibroinmembran, in der die EVs bereits in die Proteinlösung eingearbeitet sind, stellt somit einen innovativen Ansatz dar, die biologische native Funktion der EVs zu erhalten und sie darüber hinaus mit einem neuartigen Biomaterial zu vereinen (Fuest *et al.*, 2024). Die Lösung des Fibroins aus den Kokons des B. mori erfolgte auch in dieser Studie gemäß der PureSilk® Technologie unter Benutzung des schonenden Lösemittels „*Ajisawa´s reagent*“ (Schäfer *et al.*, 2022; Fuest *et al.*, 2023). Insbesondere bei regenerativen Ansätzen ist es wichtig, ein geeignetes Gerüst zu erzeugen, das an der Zielstelle implantiert werden kann, und eine geeignete Mikroumgebung zu schaffen, die dem Wirtsgewebe sehr ähnlich ist, um die gewünschten zellulären Reaktionen auszulösen (Kundu *et al.*, 2013b). Die Fibroinmembran in dieser Studie wurde auf einer PTFE Platte mittels Filmziehrakel gezogen, wodurch eine homogene Schichtdicke des Fibroins von 200 µm in feuchtem Zustand und 40 µm nach 24-stündiger Trocknung erzielt werden konnte (Fuest *et al.*, 2024). Zusätzlich konnten durch die Zugabe von Glycerol die flexiblen und transparenten Eigenschaften der Seide bei gleichzeitiger Wasserunlöslichkeit aufrechterhalten werden. Dies

konnte bereits in Studien von Srivastava et. al. 2015 erfolgreich gezeigt werden, und auch die Publikation nach Fuest et. al. 2023 im Rahmen dieser Dissertation hat gezeigt, dass flexiblere und transparentere Strukturen durch geeignete Nachbehandlungsmethoden wie der Einfluss von Wasserdampf erzielt werden können, die die Seidenstrukturen in einen unlöslichen Zustand überführen (Srivastava *et al.*, 2015; Fuest *et al.*, 2023). Die Inkorporierung der EVs wurde hier, genauso wie in Schäfer et. al. 2022, bereits nach Herstellung der Fibroinlösung und vor Überführung in eine versatile Struktur durchgeführt, um ein homogeneres Release-Verhalten der EVs aus dem Trägermaterial erzielen zu können. Die Größe der GF-EVs aus der Studie nach Fuest et. al. 2024 zeigten einen erwarteten Größenbereich von 120-180 nm (Fuest *et al.*, 2024). Die multimodale Proteinanalyse ergab außerdem eine hohe Expression gängiger EV-Marker, einschließlich CD9 und CD63, sowie erhöhte Werte von CD105, CD29, CD142 und CD44 auf unseren EVs. Diese Marker, die mit einer Reihe von zellulären Prozessen in Verbindung gebracht werden, unterstreichen die vielfältigen Funktionen der EVs der GF. Das Vorhandensein von CD105, CD29, CD142 und CD44 auf EV-Oberflächen deutet auf mögliche Beiträge zur interzellulären Kommunikation, zur Gewebehomöostase und zu Reaktionen auf physiologische Signale hin (Fuest *et al.*, 2024). Ein bemerkenswerter Befund ist die signifikante Häufigkeit von CD81 auf GF-EVs, was auf seine potenzielle Bedeutung bei der Erleichterung von Interaktionen mit Zielzellen hinweist. Diese erhöhte Präsenz von CD81 deutet auf eine entscheidende Rolle bei der interzellulären Kommunikation und dem Transport von Gütern hin. Die Eigenschaften und das molekulare Profil der GF-EVs, wie sie in dieser Studie ermittelt wurden, unterstreichen ihr Potenzial für Biomaterialanwendungen. Die Vielseitigkeit ihrer Funktionen in Verbindung mit den identifizierten spezifischen Markern deutet auf eine vielversprechende Rolle bei der Beeinflussung des Zellverhaltens, der Aufrechterhaltung der Gewebehomöostase und der Reaktion auf physiologische Signale hin (Fuest *et al.*, 2024). Die größte Herausforderung, eine kontrollierte Freisetzung von EVs zu erzielen und sie über einen längeren Zeitraum am Wirkort zu halten, kann durch die Einbindung in ein geeignetes Biomaterial ermöglicht werden. Frühere Studien haben bereits gezeigt, dass sich die Integration von EVs in verschiedene Trägerstrukturen als effizienter erwiesen hat als eine direkte Applikation in den jeweiligen Defekt (Li *et al.*, 2017; Shi *et al.*, 2017; Xu *et al.*, 2018; Han *et al.*, 2019; Zhang *et al.*, 2020; Song *et al.*, 2022; Fuest *et al.*, 2024). Shi et. al. 2017 hat beispielsweise festgestellt, dass hybride 3D-Gerüststrukturen aus Seide und Chitosan, welche mit EVs aus gingivalen mesenchymalen Stammzellen beladen waren, eine verbesserte Wundheilung bei diabetischen Ratten zeigten (Shi *et al.*, 2017; Fuest *et al.*, 2024). Die Schwierigkeit besteht darin, die EVs homogen in der Fibroinstruktur zu verteilen. Dies war in Fuest et. al. 2024 nicht möglich, wie mittels TEM deutlich gezeigt werden konnte. Hier könnten makroporöse Strukturen wie elektrogesponnene Vliese oder 3D-Scaffolds besser geeignet sein, damit sich die EVs besser in das Biomaterial einbetten und

innerhalb der Porenstruktur anhaften (Zhang *et al.*, 2012; Wang *et al.*, 2022; Fuest *et al.*, 2024). Zukünftige Forschungsansätze sollte daher untersuchen, welche Fibroinstrukturen eine sinnvollere Alternative als bioaktiver Zellträger darstellen, um ein ideales und homogen verteiltes Freisetzungsverhalten für eine spätere Anwendung im Bereich der Regeneration und Wundheilung gewährleisten zu können (Fuest *et al.*, 2024). Die hier gezogenen Membranen wurden mittels REM auf ihre Oberflächenbeschaffenheit und ihren Querschnitt hin untersucht und zeigten sich in ihrer Struktur vergleichbar mit der Studie von Schäfer et. al. 2022 (Schäfer *et al.*, 2022). Die Biokompatibilität der Membranen zeigte keinerlei zytotoxische Auffälligkeiten, weder in der funktionalisierten Gruppe noch in der Kontrollgruppe, wie bereits durch zahlreiche Arbeiten der Arbeitsgruppe belegt werden konnte (Kopp, Schunck, *et al.*, 2020; Kopp, Smeets, *et al.*, 2020; Schäfer *et al.*, 2022; Fuest *et al.*, 2023). Die höheren Lebensfähigkeitswerte deuten darauf hin, dass diese Proben in der Lage sind, die durch die Kontrollsubstanz induzierten toxischen Wirkungen abzuschwächen. Generell deuten diese Ergebnisse darauf hin, dass L929-Zellen im Vergleich zu MC3T3-Zellen anfälliger für die toxischen Wirkungen von SF mit EVs und ohne EVs sein könnten. Dieser interessante Effekt wurde auch von anderen beschrieben, die die zytotoxischen Wirkungen verschiedener Materialien auf diese beiden Zelllinien verglichen (Brackett *et al.*, 2010; Wang *et al.*, 2013; Shin, Ko and Kim, 2016; Fuest *et al.*, 2024). Daher kann es von Vorteil sein, mehr als eine Zelllinie in die Bewertung potenzieller zytotoxischer Wirkungen von Materialien oder Medizinprodukten einzubeziehen. Dieses Ergebnis legt nahe, dass Seidenfibroin mit EVs und Seidenfibroin ohne EVs möglicherweise Verbindungen oder Faktoren enthalten, die das zelluläre Überleben fördern und der Toxizität entgegenwirken (Fuest *et al.*, 2024). Diese Ergebnisse deuten darauf hin, dass weitere Untersuchungen über die Zusammensetzung und den Wirkmechanismus von SF mit EVs und SF ohne EVs erforderlich sind. Die funktionalisierten und nicht funktionalisierten Fibroinmembranen zeigten in den ersten 5 Tagen eine gute Proliferation (Fuest *et al.*, 2024). Ab dem 5. Tag wird der Spitzenwert überschritten und die Zahl der Zellen nimmt ab. Andererseits zeigen Studien nach Mandal et. al. 2009, dass die Proliferation in Seidenstrukturen besonders von deren Porosität und Porengröße abhängig ist (Mandal and Kundu, 2009). In einem nächsten Schritt soll auch die Freisetzungskinetik der EVs aus dem Trägermaterial analysiert werden, die vermutlich durch die Porosität der SF-Struktur eingestellt werden kann. Da es sich bei der hier verwendeten Membran um eine porenfreie Fibroinstruktur handelt, könnte dies ein limitierender Faktor für eine stärkere Proliferation der Zellen sein (Mandal and Kundu, 2009; Jiang *et al.*, 2021). Darüber hinaus ist der Test von der Position der Vesikel in der Membran abhängig. Aufgrund des Schrumpfungsprozesses der Membran während des Trocknens ist es jedoch möglich, dass sich ein Teil der Vesikel an der Oberfläche der Membran festgesetzt hat und sich positiv auf die Proliferation der Zellen auswirkt. Da sowohl auf den reinen als auch auf den funktionalisierten Fibroinmembranen eine

zelltypspezifische Morphologie und eine hohe Zelldichte bei der Lebend-/Totfärbung festgestellt wurde, kann davon ausgegangen werden, dass die reine Fibroinstruktur ein hohes Potenzial für die Verwendung als bioaktives Material besitzt und Anwendung im Bereich der Mund-, Kiefer- und Gesichtschirurgie finden kann (Fuest *et al.*, 2024).

6 Fazit und Ausblick

Im Rahmen der vorliegenden Dissertation wurde die Fragestellung untersucht, in wieweit Seide als resorbierbares Biomaterial Anwendung für in der Regenerativen Medizin und Wundheilung im mund-, kiefer- und gesichtschirurgischen Bereich finden kann. Hierzu wurden vier Publikationen veröffentlicht, die sich mit der Charakterisierung von Seidenfibroin als Lösung und in versatilen Formen mit funktioneller Beladung beschäftigt. In einem ersten Schritt wurde die reine Fibroinlösung als Beschichtungsmaterial auf verschiedenen Implantatoberflächen charakterisiert und eine geeignete Nachbehandlungsmethodik entwickelt, durch welche mittels thermischer Verfahren die Stabilität der Seide bei gleichbleibenden biologischen und mechanischen Eigenschaften optimiert werden kann. Dementsprechend können zukünftige Implantate genau auf die Bedürfnisse der Patienten zugeschnitten werden und einen schnelleren Heilungsprozess mit weniger Komplikationen fördern. In einem weiteren Schritt wurde nun die Fibroinlösung durch etablierte Verfahren wie Elektrospinning oder Gießprozesse in Vliese und Membranen überführt und mittels antibakterieller Substanzen und EVs versehen. Die Beladung der Seidenstrukturen erwies sich als erfolgreich und es konnte gezeigt werden, dass eine Inkorporierung sowohl in die Lösung als auch nach Ausbildung einer Struktur möglich war. Die antibakterielle Aktivität von Silber und Gentamicin rief eine Eindämmung der bakteriellen DNA-Zahl und des Koloniewachstums der getesteten oralen Mikroben hervor. Die Beladung mittels EVs zeigte einen vielversprechenden Ansatz in der regenerativen Therapie im Kopf-Hals-Bereich. Die EVs konnten erfolgreich in das Trägermaterial Seide inkorporiert werden und eine erhöhte Proliferation der Zellen konnte in Verbindung mit einer entsprechenden Zytokompatibilität gewährleistet werden.

In künftigen Studien sollte an der Optimierung der Seidenstrukturen gearbeitet werden, um eine homogenere Verteilung der additiven Zusätze zu gewährleisten und so ein gezielteres Freisetzungsverhalten der Vesikel und antibakteriellen Zusätze realisieren zu können. Auch verschiedenste Dosis-Wirkungs-Profile könnten zum Tragen kommen, um für die jeweilige Seidenstruktur die ausreichende Anzahl an Additiven ermitteln zu können. Darüber hinaus sind weiterführende *in-vitro* und *in-vivo* Studien in Klein- oder Großtiermodellen gerade Stand der Forschung im Rahmen der Arbeitsgruppe, in welchen unter anderem Seidenmembranen für eine spätere Anwendung in der GBR/ GTR-Therapie evaluiert werden. Darüber hinaus wurde sich im Rahmen dieser Dissertation ausschließlich auf die beiden Strukturen Membran und Vlies fokussiert, hier sollten weiterführende Studien auch 3D-Strukturen oder Hydrogele auf Seidenbasis Anwendung finden, um möglicherweise ein optimierteres Release-Verhalten der additiven Zusätze gewährleisten zu können. Zu diesem Zweck könnte die Wirksamkeit der bioaktiven Seiden-Matrices und des Seiden-Gels in verschiedenen *Potency-Assays* (Zytokompatibilität, Zellproliferation und -migration und *in-vitro*-Angiogenese) geprüft werden.

Außerdem könnten die induzierten Wundheilungs-prozesse in humanen oralen und kutanen 3D-*in-vitro* und *ex-vivo*-Wundmodellen, welches die *in-vivo*-Situation widerspiegelt, analysiert werden. Besonders in Hinblick zur langfristigen Vermeidung von Tierversuchen bieten alternative Forschungsmodelle hier einen vorteilhaften Ansatz für die Bewertung von innovativen Materialkonzepten.

Zusammenfassend bietet Seide als Biomaterial vielversprechende Möglichkeiten für den Bereich der Wundheilung und Regeneration in der Mund-, Kiefer- und Gesichtschirurgie. Obwohl es bereits verschiedene Techniken und Methoden gibt, um Strukturen aus Seide herzustellen und ggf. zu funktionalisieren, ist eine weiterführende Forschung erforderlich, um Seidenproteine noch anpassungsfähiger zu gestalten und optimieren zu können.

7 Erklärung des Eigenanteils an den Publikationen

Veröffentlichung I:

Fuest, S., Smeets, R., Gosau, M., Aavani, F., Knipfer, C., Grust, A. L. C., Kopp, A., Becerikli, M., Behr, B., & Matthies, L. (**2023**). *Layer-by-Layer Deposition of Regenerated Silk Fibroin—An Approach to the Surface Coating of Biomedical Implant Materials.* ACS biomaterials science & engineering, 9(12), 6644–6657.

CRediT authorship contribution statement:

Conceptualization, S.F., A.K. and R.S.; **methodology, validation and formal analysis, S.F.** and A.K.; resources, R.S., M.G. and B.B.; **data curation S.F.** and M.B.**; data curation and writing—original draft,** L.M. and **S.F.;** writing—review and editing, L.M., F.A., A.L.C.G. and C.K.; supervision, L.M., R.S. and M.G.

All authors have read and agreed to the published version of the manuscript.

Veröffentlichung II:

Schäfer, S., Smeets, R., Köpf, M., Drinic, A., Kopp, A., Kröger, N., Hartjen, P., Assaf, A. T., Aavani, F., Beikler, T., Peters, U., Fiedler, I., Busse, B., Stürmer, E. K., Vollkommer, T., Gosau, M., & **Fuest, S.** (**2022**). *Antibacterial properties of functionalized silk fibroin and sericin membranes for wound healing applications in oral and maxillofacial surgery.* Biomaterials advances, 135, 212740.

CRediT authorship contribution statement:

Schäfer S: bacterial analysis; design and planning of experiments; data collection; data analysis and interpretation of results; drafted the manuscript.
Smeets R: interpretation and critical revision; approval of the article.
Köpf M: idea and concept of the study; design and planning of experiments; interpretation of results; critical revision and approval of the
article.
Drinic A: development of fabrication and functionalization methods for silk protein membranes as well as sample production; critical revision and approval of the article.
Kopp A: critical revision and approval of the article.
Kröger N: critical revision and approval of the article.
Hartjen P: cytocompatibility analysis; critical revision and approval of the article.
Assaf AT: interpretation; critical revision and approval of the article.
Aavani F: interpretation; critical revision and approval of the article.
Beikler T: critical revision and approval of the article.

Peters U: data collection, data analysis/interpretation.
Fiedler I: SEM analysis; data collection, critical revision and approval of the article.
Busse B: SEM analysis; data collection.
Stürmer EK: critical revision and approval of the article.
Vollkommer T: critical revision and approval of the article.
Gosau M: interpretation and critical revision; approval of the article.
Fuest S: interpretation; critical revision of the manuscript; approval of the article.

All authors have read and agreed to the published version of the manuscript.

Veröffentlichung III:

Schäfer, S., Aavani, F., Köpf, M., Drinic, A., Stürmer, E. K., **Fuest, S.**, Grust, A. L. C., Gosau, M., & Smeets, R. (**2023**). *Silk proteins in reconstructive surgery: Do they possess an inherent antibacterial activity? A systematic review.* Wound repair and regeneration: official publication of the Wound Healing Society [and] the European Tissue Repair Society, 31(1), 99–110.

CRediT authorship contribution statement:

Sogand Schäfer: design and planning of the review; data collection; data analysis and interpretation of results; drafted the manuscript. Farzaneh Aavani: interpretation; critical revision and approval of the article. Marius Köpf: interpretation; critical revision and approval of the article. Aleksander Drinic: interpretation; critical revision and approval of the article. Ewa K. Stürmer: critical revision and approval of the article. **Sandra Fuest: critical revision of the manuscript; approval of the article**. Audrey Laure Céline Grust: critical revision and approval of the article. Martin Gosau: critical revision; approval of the article. Ralf Smeets: interpretation and critical revision; approval of the article.

All authors have read and agreed to the published version of the manuscript.

Veröffentlichung IV:

Fuest, S., Salviano-Silva, A., Maire, C. L., Xu, Y., Apel, C., Grust, A. L. C., Delle Coste, A., Gosau, M., Ricklefs, F. L., & Smeets, R. (**2024***). Doping of casted silk fibroin membranes with extracellular vesicles for regenerative therapy: a proof of concept.* Scientific reports, 14(1), 3553.

CRediT authorship contribution statement:

Conceptualization, S.F., C.A. and R.S.; **methodology, validation and formal analysis, S.F.**, A.S.S., C.L.M., Y.X. and A.D.C.; project administration and resources, R.S., F.L.R. and C.A..; **data**

curation S.F., A.S.S. and Y.X.; **writing—original draft, S.F.**, F.L.R and C.A..; writing—review and editing, R.S., A.L.C.G. and M.G; supervision, C.A., F.L.R, R.S. and M.G.

All authors have read and agreed to the final version of the manuscript.

8 Veröffentlichungen I-IV

ACS Biomaterials SCIENCE & ENGINEERING

pubs.acs.org/journal/abseba Article

Layer-by-Layer Deposition of Regenerated Silk Fibroin—An Approach to the Surface Coating of Biomedical Implant Materials

Sandra Fuest, Ralf Smeets, Martin Gosau, Farzaneh Aavani, Christian Knipfer, Audrey Laure Céline Grust, Alexander Kopp, Mustafa Becerikli, Björn Behr, and Levi Matthies*

Cite This: *ACS Biomater. Sci. Eng.* 2023, 9, 6644–6657 Read Online

ACCESS | Metrics & More | Article Recommendations

ABSTRACT: Biomaterials and coating techniques unlock major benefits for advanced medical therapies. Here, we explored layer-by-layer (LbL) deposition of silk fibroin (SF) by dip coating to deploy homogeneous films on different materials (titanium, magnesium, and polymers) frequently used for orthopedic and other bone-related implants. Titanium and magnesium specimens underwent preceding plasma electrolytic oxidation (PEO) to increase hydrophilicity. This was determined as surface properties were visualized by scanning electron microscopy and contact angle measurements as well as Fourier transform infrared spectroscopy (FTIR) analysis. Finally, biological in vitro evaluations of hemocompatibility, THP-1 cell culture, and TNF-α assays were conducted. A more hydrophilic surface could be achieved using the PEO surface, and the contact angle for magnesium and titanium showed a reduction from 73 to 18° and from 58 to 17°, respectively. Coating with SF proved successful on all three surfaces, and coating thicknesses of up to 5.14 μm (±SD 0.22 μm) were achieved. Using FTIR analysis, it was shown that the insolubility of the material was achieved by post-treatment with water vapor annealing, although the random coil peak (1640−1649 cm^{-1}) and the α-helix peak (at 1650 cm^{-1}) were still evident. SF did not change hemocompatibility, regardless of the substrate, whereas the PEO-coated materials showed improved hemocompatibility. THP-1 cell culture showed that cells adhered excellently to all of the tested material surfaces. Interestingly, SF coatings induced a significantly higher amount of TNF-α for all materials, indicating an inflammatory response, which plays an important role in a variety of physiological processes, including osteogenesis. LbL coatings of SF are shown to be promising candidates to modulate the body's immune response to implants manufactured from titanium, magnesium, and polymers. They may therefore facilitate future applications for bioactive implant coatings. However, further in vivo studies are needed to confirm the proposed effects on osteogenesis in a physiological environment.

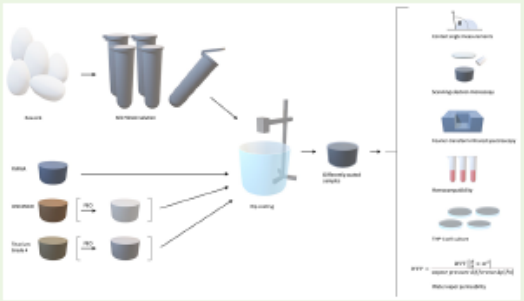

KEYWORDS: *silk fibroin, layer-by-layer, coating, implant, foreign body reaction*

1. INTRODUCTION

The application of materials for the fabrication of implants has been widely increasing in the last few decades. Innovative biomaterials such as ceramics, metals, and their alloys as well as polymers are increasingly coming to the fore.[1] Following implant insertion in the human body, various interactions occur between the host tissue and the facilitated (bio)material.[2] It is known that the protein−biomaterial interaction serves as a signal for inflammatory cells, which then initiate foreign body reactions. The surface chemistry and topography of implants determine the composition and severity of those reactions in the human body.[3,4] Severe forms of the body's inflammatory response can manifest themselves in skin reactions such as eczema or impaired wound healing, among many other symptoms based on local or systemic effects. To prevent such undesirable consequences, biomaterial-based implants can be surface-modified using various methods.[5] Surface modification of a biomaterial can be done by morphological surface modification or, alternatively, by changing material properties, for example, by adding new materials to the surface or facilitating coating techniques.[6,7] Surface coatings are among the most promising approaches to impart desirable properties to implants, such as enhancement of implant healing. A coating can generally be defined as an area that is in close or direct contact with the surface of a material and whose properties are different from

Received: June 26, 2023
Revised: October 29, 2023
Accepted: November 2, 2023
Published: November 20, 2023

https://doi.org/10.1021/acsbiomaterials.3c00852
ACS Biomater. Sci. Eng. 2023, 9, 6644−6657

those of the base material or substrate. In detail, these near-surface areas can be created either by altering, that is, changing the surface composition or by depositing the same or a different material on the substrate surface.[8]

A dedicated surface coating of dynamically loaded areas of an implant can, for example, minimize wear debris and thus reduce the risk of allergic reactions. Generally, coating materials should possess specific properties such as biocompatibility, nontoxicity, low immunogenicity, and degradability, that is, bioabsorption if needed. Of note, for osteoconduction and osseointegration of implant materials, coordinated interaction between the osteoimmune response and osteogenesis, which is mediated by macrophages, plays a central regulatory role in all stages of bone repair.[9] In the case of applying a biomaterial coating, both the coating material itself and the coating technique determine the implant's and related therapy's success rate.[10] Polysaccharides and lipid-based waxes are the most widely used coatings in biomaterial engineering because of their commercially available formulations. As a new alternative, proteins show a good barrier against O_2 and CO_2 and display desirable adherence to hydrophilic surfaces. Furthermore, they exhibit satisfactory mechanical properties. In particular, they exhibit a good water vapor barrier as well as better resistance to external agents since they can be cross-linked by physical (heating) or chemical (alcohol) treatments.[11]

Several coating techniques are available for processing biomaterials, including chemical or physical vapor deposition, sol−gel technique, spray technique, electrophoretic deposition technique, and dip technique, among others. However, not all of them are suitable for processing protein-based biopolymers because of their extreme processing conditions in terms of stress, temperature, and other ambient conditions as well as their relatively high costs.[12,13] Dipping methods are well-established techniques for the easy deposition of thin films on substrates. If done properly, such films can be homogeneously and uniformly applied as well as functionalized by subsequent post-treatment steps.[14] Dipping processes can also be utilized to develop immersive layer-by-layer (LbL) assemblies, also called "dip assembly". This technique is typically performed by immersing a substrate into a solution several times, followed by intermediate washing steps to remove the unbound material.[15−17] In general, the driving forces of the LbL assembly technique are electrostatic interactions between oppositely charged species, but the process can also be influenced by charge transfer interactions, van der Waals interactions, hydrogen bonding, and hydrophobic interactions. The main force or stabilizing interaction in alternate LbL film assembly is perceived to be electrostatic interactions between oppositely charged species.[18,19] The assembly of thin films has been of considerable interest because of its ability to exert nanometer control of film thickness and a plethora of useable materials to choose from for coating planar and particulate substrates.[18] The LbL procedure is inexpensive, facile, and very versatile as the coatings can be formed on virtually any substrate in almost any shape and size.[20,21] A huge advantage against conventional coating techniques is further the fact that it is possible to embed agents with desirable functions into these coatings, for example, pharmacological drugs, nutrients, and proteins.[18,22]

In recent years, silk fibroin (SF) from the silkworm *Bombyx mori* has been extensively studied for its use in the textile industry, biomedical engineering, and drug delivery systems.[23] This natural polymer exhibits properties such as biocompatibility, controllable biodegradability, low toxicity, fullness, strength, and elasticity as well as water vapor and oxygen permeability.[24,25] Due to their thermal stability up to 250 °C, SF-based structures can also withstand high temperatures in vivo and in sterilization processes.[26−29] Despite considerable research in the field, there are few approved (medical) products made from SF. Although versatile processing possibilities exist, the production of the fibroin solution from the cocoons has thus far been largely carried out mostly with the aid of the expensive and harmful solvent lithium bromide.[30,31] The earliest method to achieve a SF solution free of toxic solvents on a salt and alcohol base was the so-called Ajisawa's reagent.[24,32,33] Furthermore, Ajisawa's reagent made out of $CaCl_2$ and an ethanol-based reactant is not only cheaper than lithium bromide but would also greatly simplify the scalability options for industrial processes.[34]

It is well known that SF proteins can build different conformational structures:

- Silk I: good water solubility, formed by α-helix and β-sheet
- Silk II: main structural conformation of SF, rich in β-sheet, good resistance to water solubility, and high mechanical properties
- Random coil: usually exists in the solution of SF[35]

As a novel biomaterial, SF also meets most requirements of conventional coating systems and thus outperforms them in many properties. SF provides a simple, versatile, and lightweight coating for scaffolds or implants that can be used for further biofunctionalization.[36] In vitro studies have shown that silk has antimicrobial properties, enabling it to act as an important clinical mediator in the field of surface coatings.[37−40] Due to its antimicrobial properties, SF can reduce the adhesion and proliferation of bacteria on substrate surfaces and thus prevent biofilm formation.[1,38] Disadvantages of SF include brittleness, fragmentation, and difficulty in producing uniform thickness as a coating depending on the methods and parameters chosen for application.[41] Various techniques such as electrophoretic deposition of SF on titanium substrates have been developed to address and evaluate these shortcomings.[12] Even though the LbL assembly technique is one of the most widespread and often facilitated coating processes for SF in the literature, systematic approaches to evaluate, develop, and provide uniform SF coatings by LbL on relevant implant materials are to this day still missing. According to the literature, the solvent lithium bromide was often used, and new post-treatment techniques, for example, by means of water vapor annealing (WVA), took place almost exclusively for protein-based coatings in the food sector.[42,43] This study focused on the coating of silk-fibroin-based implant materials using the LbL method. The challenges included achieving a homogeneously distributed surface on the implant materials. The fibroin solution was prepared using the salt-based solvent Ajisawa, and after coating, a gentle alternative to alcohol-based crystallization methods was established using WVA. The fibroin layer was homogeneously distributed on the implant surfaces and showed no negative manifestations in hemocompatibility tests. The cytocompatibility showed an increase in TNF-α levels, which can be interpreted as a possible factor in stimulating osteogenesis and potentially ameliorating implant osteoconduction and osseointegration.

2. MATERIALS AND METHODS

2.1. SF Solution. For an SF aqueous solution, fibroin was separated from sericin by degumming in hot alkali solution before dissolving it in a

https://doi.org/10.1021/acsbiomaterials.3c00852
ACS Biomater. Sci. Eng. 2023, 9, 6644−6657

proprietary nontoxic solvent system based on Ajisawa's reagent. The dissolved fibroin was fully dialyzed against VE water within 8 h by using tailored extraction processing. The fibroin concentration used in this study was adjusted to 1 g/mL and stored at 4 °C. To calculate the dilution factor of the SF solution, the volumes of the solution before and after dialysis were expressed as a ratio, see eq 1.

$$\text{Dilution factor} = \frac{\text{solution quantity before dialysis[mL]}}{\text{solution quantity after dialysis[mL]}} \quad (1)$$

To determine the SF concentration of the dialyzed solution, the dilution factor determined according to eq 2 was used.

$$\text{Fibroin concentration[wt \%]} = \frac{\text{concentration before dialysis [wt]}}{\text{dialysis factor}} \quad (2)$$

If higher concentrations of SF were required, then the solution was heated to 70 °C. If low concentrations were desired, then the SF solution was diluted with ddH_2O.

2.2. Material Preparation, Dip-Coating, and Post-treatment. Three established biomaterials used for medical implants were examined:

- Titanium (Ti grade 4, ø 9 mm, Meotec, Aachen, Germany)
- Magnesium (WE43MEO, ø 9 mm, Meotec, Aachen, Germany)
- PMMA (Acryl glass round bar, ø 8 mm, B&T Metall, Schwindegg, Germany)

First, magnesium, titanium, and PMMA samples were embedded in SamplKwick powder and Liquid Fast Cure Acrylic resin (BUEHLER, Lake Bluff, IL, USA). Second, one side of the samples was first ground flat in a grinding machine (Tegramin-20, Struers, Willich, Germany) with a #80 grit. The epoxy resin was sanded down from the other side until this side of the samples also showed a flat shape. Subsequently, one of the sides was sanded smoother with different grain sizes (#120, #320, #1200, #2000, and #4000) until a shiny and scratch-free surface was obtained. The samples proceeded to an experimental dip-coating setup (Fibrothelium, Aachen, Germany). To this end, the materials were placed in isopropanol (70 wt %) for 1 h for cleaning and dust removal and immersed in a 5 wt % SF solution for 10 s at a time. In the next step, the samples were dipped in purified water to remove the unbound material. The samples were then hung for 1 h to dry and sealed with aluminum foil to prevent the samples from being contaminated. In this way, three samples each were coated with either one or five layers with self-developed software for automation called DipMator. To convert the dried SF layers on the different materials from a hydrophilic to a hydrophobic state, a gentle post-treatment was required. This was achieved via crystallization of SF by treatment with 70% ethanol (EtOH) or WVA for 30 min. Ultimately, the titanium and magnesium samples underwent plasma electrolytic oxidation (PEO) surface modification (Meotec, Aachen, Germany).[44] By applying a direct current, a uniform oxide layer was formed on the materials, which itself served as a rotating anode during electrochemical processing. The resulting PEO layers were ~15−16 μm in thickness for the magnesium and ~17−19 μm in thickness for the titanium samples.

2.3. Contact Angle Measurements. To determine hydrophilic and hydrophobic surface properties, the contact angles were measured based on DIN 55660-2. Herein, the imaging of a lying drop was used to measure the intersection between the drop contour and the projection of the surface. In the case of complete wetting, the contact angle amounts to 0°. Between 0 and 90°, the substrate was considered wettable, and above 90°, it was not wettable. The measurements were carried out at 22 °C and a humidity of 38% RH. For each drop, 5 μL of purified water was applied to the tested surface and then analyzed using imaging software Image Access (Imagic Bildverarbeitung, Glattbrugg, Switzerland) to determine the contact angle.

2.4. Surface Behavior and Layer Thickness. For the evaluation of SF on coated surfaces, samples were examined with an XL30 SEM microscope (Philips, Amsterdam, the Netherlands). The surfaces of the samples were provided with a very thin layer of precious metal (sputtered). The coating material gold is called a sputter target and was deposited as a thin layer with a thickness of 2−20 nm on the sample surface. With the Sputter Coater S150B (Edwards, Crawly, England), the samples were coated.

For the optical assessment of the layer thickness, the specimens were embedded in epoxy resin (Epoclear—Schmitz-Metallographie GmbH, Herzogenrath, Germany) and dried for 24 h followed by sanding down (grain size #4000) from one side until the samples showed a flat shape. Micrographs of the coated samples treated with water vapor were taken. The layer thickness was determined with the help of the computer program Image Access. Representative pictures were taken with magnifications of 1000-fold and 5000-fold, and the layer thickness was taken with a 2000-fold magnification.

2.5. Solubility Testing and FTIR Analysis. Attenuated total reflectance Fourier transform infrared (FTIR) was used to study the conformation and morphology of the SF coatings by using a Nicolet Nexus 470 spectrometer (Thermo Fisher Scientific, Waltham, MA, USA) with a resolution of 4 cm^{-1}. A total of 64 scans were coadded to produce full spectra ranging from 1450 to 1700 cm^{-1}.

2.6. Hemocompatibility. All examinations from the blood collection to the final analysis were carried out within less than 2 h after drawing. Whole blood samples were drawn from healthy volunteers in sodium citrate or EDTA-containing vials for analyses of coagulation and hemolysis or hematology, respectively. A total of five specimens (cylinders of D 7.0 mm × L 6.0 mm) of the same group were placed in 40 cm polyvinyl chloride tubes (3/8 in. × 3/32 in.) precoated with a "Ph.i.s.i.o." (Phosphorylcholine inert surface) coating (CORMED, Rüthen, Germany), a special polymer layer which hinders plasma protein deposition and platelet adhesion. After 4 mL of blood was added, the tube was circularly bent, and both ends were tightly closed by heat-shrink tubing. Tubes loaded with blood but without any specimen served as negative controls. Circular tubes were turned in a 38 °C water bath for 60 min (resulting in a blood temperature of 37 °C). Blood analyses were performed by a standard clinical equipment in the Institute of Clinical Chemistry, Transfusion and Laboratory Medicine, BG University Hospital Bergmannsheil, Ruhr-University Bochum, Germany. Coagulation measurements were performed using the ACL Top system (Werfen GmbH, Munich, Germany), while the blood cell counts were assessed with the DXH system (Beckman Coulter, Brea, California, USA). Free hemoglobin levels were determined using the HemoCue Hb 801 system (HemoCue AB, Ängelholm, Sweden). All measurements were performed following the manufacturer's instructions.

2.7. THP-1 Cell Culture. Samples of the material groups magnesium, titanium, and PMMA were colonized with undifferentiated THP-1 cells (3.6×10^5, RPMI, 10% serum, 1% penicillin/streptomycin, 50 μmol β-mercapto-EtOH; according to ATCC specifications) in full medium and preincubated for 45 min. Then, 1.7 mL of full medium was added to the samples and incubated (37 °C, 5% CO_2, and 95% RH) for 12 h. Subsequently, the test specimens were coated with a 3% glutaraldehyde (GA) solution for fixation, and the liquid was replaced by PBS. For degradation analysis of the silk-based coating materials, undifferentiated THP-1 cells were applied to the SF membranes and incubated for 4 days in full medium. The following day, the SF membranes were fixed with a 3% GA solution. The degradation behavior of the membranes was checked by means of SEM. Secretion of TNF-α, a pivotal messenger of inflammation, was measured using an ELISA sandwich kit according to the manufacturer's instructions (Quantikine, R&D Systems, Minneapolis, MN, USA).

2.8. Water Vapor Permeability. The water vapor transmission (WVT) through a material layer was determined by using the ASTM E96/E96-M standard. The following eq 3 was used to calculate the permeation quantity of water vapor over a certain period. Both the temperature and humidity were kept constant for each test.

$$\text{WVT} = \frac{\text{weight loss } \Delta g[g]}{\text{time[h]} \times \text{material area} A[m^2]} \quad (3)$$

The water vapor permeability (WVP) is defined by the time rate of water vapor transfer through a material induced by a vapor pressure

https://doi.org/10.1021/acsbiomaterials.3c00852
ACS Biomater. Sci. Eng. 2023, 9, 6644−6657

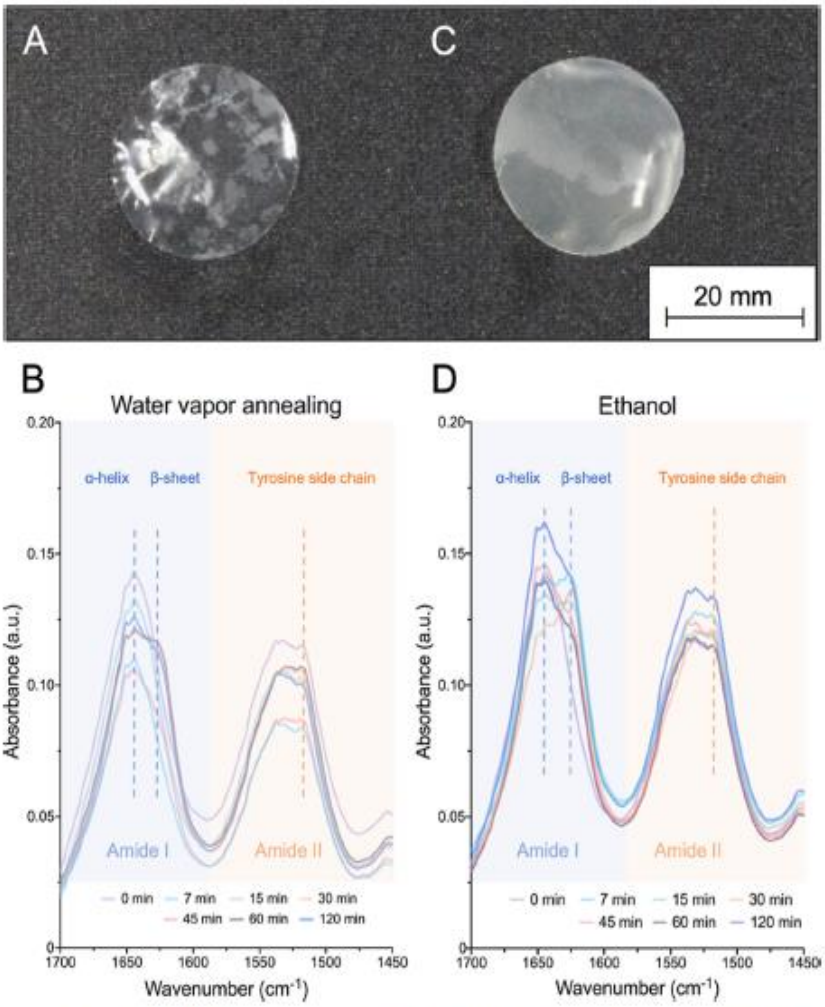

Figure 1. Crystallinity of differently treated SF membranes detected by FTIR. (A,B) Water vapor-annealed; (C,D) EtOH-treated; the macroscopic transparency difference between water vapor-annealed and EtOH-treated membranes is visibly distinct (A vs C). $n = 5$ samples tested.

difference between two specific surfaces and was calculated from WVT according to eq 4.

$$\text{Permeability} = \frac{\text{WVT}\left[\frac{g}{h} \times m^2\right]}{\text{vaporpressure difference } \Delta p[\text{Pa}]} \quad (4)$$

An EZ-Cup vapometer (Thwing Albert, West Berlin, NJ, USA) was used to perform the measurement.[45] The cup was filled up to three-quarters with ddH_2O. The membrane, without post-treatment, was cut to size and placed between the neoprene seals. The inner diameter of the permeation was 6.5 cm. Finally, the Teflon seal was applied, and the cup was closed using the flange ring. The controlled ambient conditions were realized by a climatic chamber. The temperature was 37 °C, and the humidity was 25 RH % to achieve physiologically similar ambient temperatures. A laboratory balance was placed in the climatic chamber, and the test time was 24 h. A camera was mounted in the climatic chamber to take pictures of the measurements every hour.

2.9. Statistical Analysis. If not otherwise specified, $n = 5$ samples were tested. For statistical analyses, SPSS 22 software (version 22.0; IBM Corp., Armonk, NY, USA) and GraphPad Prism (version 8.4.0; GraphPad Software, LaJolla, CA, USA) were employed. Quantitative characteristics are presented as mean ± standard deviation (SD). The normal distribution of the data was tested with the Shapiro–Wilk test. Herein, either a two-tailed t-test for unpaired samples or an ordinary one-way analysis of variance (ANOVA) and Tukey's multiple comparison test on normally distributed data, while the Mann–Whitney test or Kruskal–Wallis test and Dunn's multiple comparison test for nonparametric-distributed data, were applied. Data are indicated with (*) for a level of significance $p < 0.05$.

3. RESULTS

3.1. Crystallization Kinetics of SF. To increase the stability of SF membranes and counteract rapid dissolution after implant insertion, post-treatments to initiate β-sheet formation within the films and hence imply water insolubility are of importance when considering implant application of SF layers by LbL. To study different postprocessing treatments and evaluate parameters such as optical density without restraints, single SF films without an underlying substrate material were tested and analyzed. As expected, it was observed that untreated membranes would rapidly dissolve in water compared with membranes treated with WVA or EtOH. After just a few seconds, the untreated membranes began to decompose, beginning in the middle and heading toward peripheral areas. Figure 1A,B shows membranes treated by the WVA method, while samples of C and D were post-treated with EtOH. Both groups of post-treated membranes withstood water immersion over a minimum time of 60 min and did not dissolve visibly to

https://doi.org/10.1021/acsbiomaterials.3c00852
ACS Biomater. Sci. Eng. 2023, 9, 6644–6657

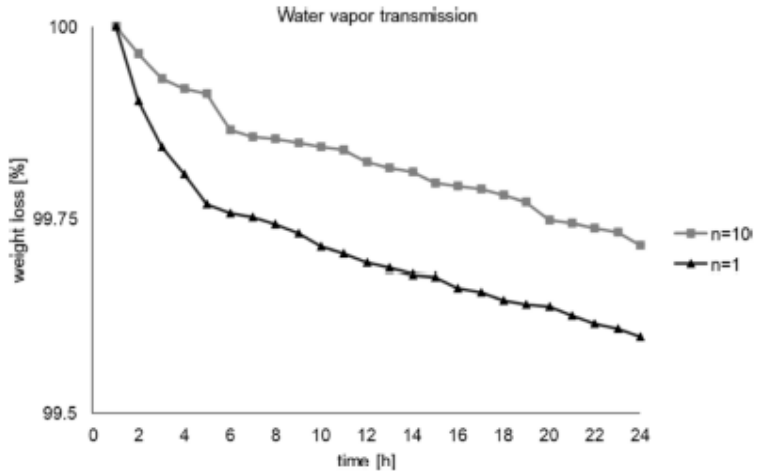

Figure 2. Measurement of WVT and permeability. The determination of mass change was a function of time. Within 24 h, 0.29% of mass was lost through ten layers of SF, compared to 0.40% in one layer of SF. $n = 3$ experiments conducted.

that point. A clear difference could be visualized after drying the post-treated membranes. While the water vapor-annealed membranes showed a transparent and clear structure, the EtOH-treated ones appeared fragile, yellowish, faded, and matt. However, the choice of post-treatment had only little influence on their brittleness.

To better understand the interactions between proteins and water molecules, water solubility, and comparison of both post-treated membranes as well as the molecular structure of the reconstituted SF, FTIR analysis was performed at 45 °C. To this end, silk films were prepared from high concentrations of regenerated SF in aqueous solution (~10 wt %). Figure 1B shows typical FTIR spectra revealing structural changes during WVA from 0 to 120 min. The amide I (1600−1700 cm^{-1}) and amide II (1450−1600 cm^{-1}) regions were selected to demonstrate the formation of the β-sheet crystals. Initially, the samples were in a noncrystalline state, and no peak was observed in the wavenumber region of 1600−1640 cm^{-1} (0 min), which is the main absorbance region of the β-sheet crystal in amide I. When the annealing time increased, the β-sheet crystal peak appeared gradually, centered at 1630 cm^{-1}. It should be noted that there is no uniform formation of a peak with increasing time, but the curves between 30 and 120 min have a significantly higher absorption spectrum. The random coil peaks (1640−1649 cm^{-1}) and the α-helix peak (centered at 1650 cm^{-1}) were still evident, although the SF membranes were already water insoluble after 7 min post-treatment. The silk I indicator 1652 cm^{-1} α-helix was significantly higher than other peaks, such as the random coil peaks and the β-sheet peak. The tyrosine side chain absorbance in the amide II region also shifted from 1515 cm^{-1}, indicating the packing of the beginning β-sheet crystals during the WVA process. Similar behavior was observed for EtOH-post-treated membranes, as seen in Figure 1D. The absorption spectrum here reached maximum values of 1.6×10^{-1} au in comparison to the water vapor-annealed ones with 1.4×10^{-1} au. A more pronounced peak was detected in the β-sheets in the range of 1626 cm^{-1}, and already from 15 min post-treatment time, the curves built up almost uniformly on each other. The random coil peaks and the α-helix peak decreased simultaneously and shifted more to the region around 1660 cm^{-1}. Also, the tyrosine side chain absorbance in the amide II region shifted from 1515 cm^{-1}, indicating the packing of dense β-sheet crystals during EtOH treatment.

In summary, water vapor-annealing post-treatment provided an effective method for insolubilizing SF and thus the potential for the application of durable LbL coatings. The process allowed us to sufficiently control the β-sheet content of silk films, avoiding brittleness and solvent-induced protein inactivity. The water vapor method exhibited lower absorption spectra and led to the desired result after only a few minutes. Compared to the chemical post-treatment with EtOH, higher peaks in the silk I structure were detected, indicating the potential for better resistance and longevity when applied as a coating on implant substrates. As post-treatment with water vapor appeared to be less detrimental to the stability of the SF films, we chose to utilize WVA for subsequent experiments.

3.2. WVP of SF Films. Besides the insolubility of the films, the potential transmissivity of SF LbL coatings for water and other small molecules was tested to evaluate the protective character of the coated substrates in terms of corrosion/degradation. Figure 3 depicts the mass decrease (evaporation loss) within the vapometer over time in dependence of membrane thickness. Within 24 h, 0.74 g (0.29%) of water vapor permeated through the ten-layer ($n = 10$) SF coating membrane. The one-layer SF membrane ($n = 1$) lost 1.03 g (0.40%) of water vapor within 24 h. On average, the mass decreased by 0.03 g (±SD 0.03 g) at $n = 10$ per hour. The mass change per hour at $n = 1$ was on average 0.04 g (±SD 0.06 g). The $n = 10$ SF membrane exhibited a WVT of 9.31 g/(h*m^2), whereas the $n = 1$ SF membrane demonstrated a WVT of 12.93 g/(h*m^2), see Figure 2.

To determine the permeability, the pressure difference Δp from the saturation vapor pressure and the difference in relative humidity (RH) between the vapometer and the climate chamber were recorded. Thus, the saturation vapor pressure of water at the specified temperature was 47.45 hPa. The air humidity in the vapometer was indicated with 100 RH %. Out of this, for ten layers, a permeation of 27.7×10^{-6} g/(h*m^2*Pa) was determined. For one fibroin layer, a permeation of 38.5×10^{-6} g/(h*m^2*Pa) was calculated.

3.3. Surface Characteristics. As hydrophilicity plays an important role in physiological environments, water drop contact angle measurements were conducted on all tested

https://doi.org/10.1021/acsbiomaterials.3c00852
ACS Biomater. Sci. Eng. 2023, 9, 6644−6657

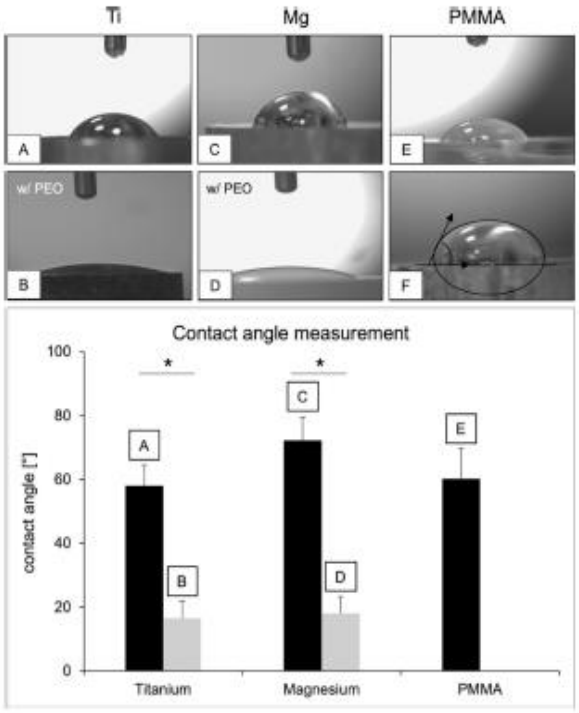

Figure 3. Contact angle measurement. (A) Titanium w/o PEO treatment and (B) titanium w/PEO treatment; (C) magnesium w/o PEO treatment and (D) magnesium w/PEO treatment; (E) PMMA w/o PEO treatment; and (F) schematic demonstration of contact angle measurement; $p_{\text{Titanium}} < 0.05$; $p_{\text{Magnesium}} < 0.05$; $n = 5$ samples tested.

materials, namely, unmodified and PEO surface-modified titanium (Ti grade 4), unmodified and PEO surface-modified magnesium (WE43MEO), and polymers (PMMA), without further surface modification, to give a first insight on the potential applicability of a LbL coating from liquid solution. The titanium surfaces, which serve as a reference material with widespread application in orthopedic and other bone-related surgical fields, showed an ellipsoidal shape. A contact angle of 58° was calculated. This angle was the smallest in comparison with the other two materials. Magnesium behaved more hydrophobically in this measurement. The drop on the surface had an almost completely round shape and a repellent behavior toward the surface with a contact angle of 73°. The contact angles measured for PMMA were 60° on average. Due to the rather hydrophobic character of the investigated materials measured here, the contact angle of PEO surface-modified samples was examined in the next step to see whether the wettability of the measured materials was altered. PEO surface modification is clinically already in use for both magnesium and titanium implants to enable specific functionality like slow degradation (magnesium) or the improvement of cell attachment (titanium) and thus showed potential to further improve the wettability and application of SF coatings by LbL coating within our approach. Panels B and D show the contact angle measurement of the PEO surface-modified samples from titanium and magnesium. In summary, surfaces could be wetted much better, and the water droplets were evenly distributed on the surface. The angles of the materials titanium and magnesium after PEO treatment were 17 and 18°, respectively. The standard deviations ranged from 5.2° for the PEO surface-modified materials to 9.6° for PMMA. Statistical analysis revealed significant differences (*), see Figure 3.

3.4. Surface Morphology of Coated SF Samples. To verify whether a uniform coating of the different substrates could be achieved, microsections of each group were analyzed by SEM. Five SF layers were applied to each test specimen. In Figure 4, representative SEM images of the SF-coated magnesium (A–H), titanium (I–P), and PMMA (Q–T) samples for the post-treatment and the PEO groups are shown at different

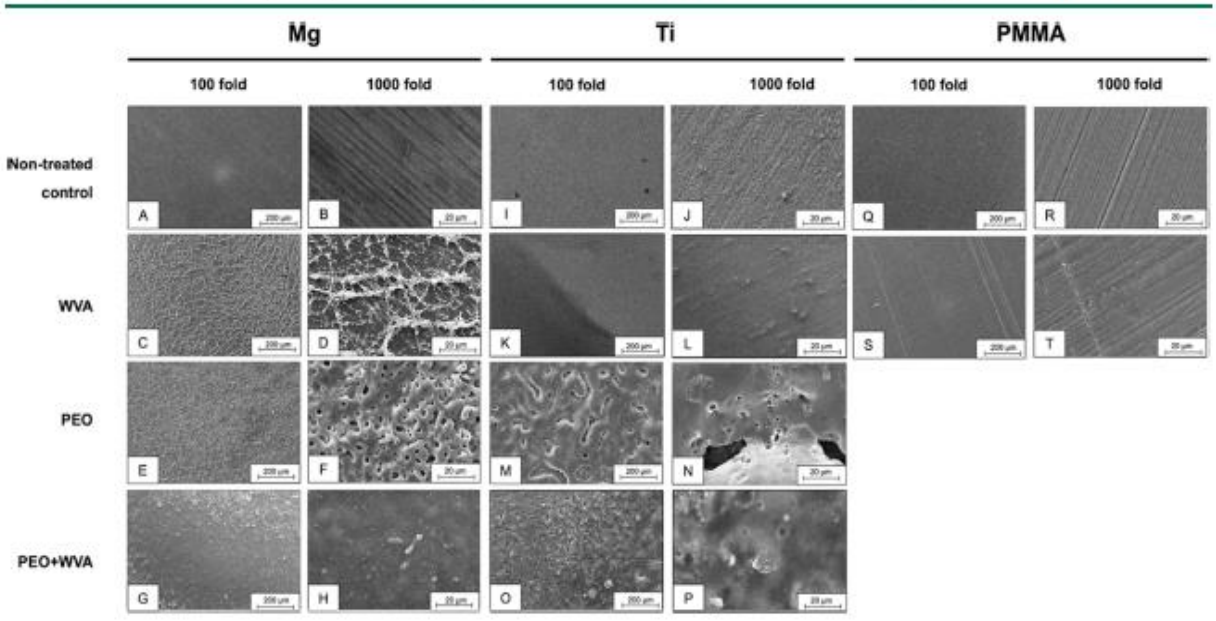

Figure 4. SEM images of SF-coated specimens undergoing different surface treatments. (A–H) Magnesium; (A,B) Mg w/oPEO + SF; (C,D) Mg w/o PEO + SF + WVA; (E,F) Mg + PEO + SF; (G,H) Mg + PEO + SF + WVA; (I–P) titanium grade 4; (I,J) Ti w/o PEO + SF; (K,L) Ti w/o PEO + SF + WVA; (M,N) Ti + PEO + SF; (O,P) Ti + PEO + SF + WVA; (Q–T) PMMA; (Q,R) PMMA + SF; (S,T) PMMA + SF + WVA; $n = 5$ samples tested.

https://doi.org/10.1021/acsbiomaterials.3c00852
ACS Biomater. Sci. Eng. 2023, 9, 6644–6657

magnifications using untreated bare samples serving as controls (top row).

Images A and B show the nontreated magnesium specimens, and C and D show the water vapor post-treated SF-coated magnesium samples. The different formation and state of the SF layers after water vapor treatment can be seen clearly, showing an irregular coating of the surfaces with SF. Sections C and D show the SF magnesium specimens after water vapor post-treatment. Here, a rootlike covering of the surfaces was detected. The SF layer stretched along the surfaces. Again, there seemed to be no homogeneous distribution of the SF layer on the surface. In contrast, a more homogeneous distribution of the SF layer was observed on the PEO surface-modified magnesium samples (panels E−H). In comparison to the uncoated PEO negative control, the SF solution penetrated evenly and completely into the pores and covered the surface uniformly.

In panels I−P, the same optical analysis methods were performed on the titanium groups. A clear difference was seen between the titanium samples post-treated with water vapor and the magnesium samples treated accordingly. The pictures K and L show a more uniform SF coating than the magnesium-treated samples. The same SF layer on titanium seemed to adhere to the surface. The inherent surface irregularities of titanium in the blank state, pictures (I−J), seemed to promote film formation and thus were completely covered and filled by the SF solution. However, certain irregularities on the surface were detected, but using the applied analytical methods, it was not certain whether these were SF aggregations or dust (section L). However, also on the titanium samples, a nonuniform coating was observed when using PEO surface modification as a base layer (pictures M−P). Here, a reduction of the number of pores by SF was seen, but at 100- and 1000-fold magnifications (panels M and N), small pores were still evident.

Treatment with water vapor showed an irregular structure for magnesium but a uniform structure for titanium. This may be attributed to the underlying corrosion effects of magnesium, which prevent the even distribution of SF in the SF layer. Upon PEO surface modification, a more uniform SF layer was achieved on the magnesium samples. The pores were closed uniformly by SF, and a homogeneous surface structure was generated.

Panels Q−T show the micrographs of SF-coated PMMA samples. Here, the post-treatment method of water vapor was also performed. However, for obvious reasons, any kind of metallic conversion coating such as PEO was not possible with PMMA. A clear difference between the post-treatment and the negative control was only seen at a 1000-fold magnification (panels R and T), resulting in an intact SF layer.

To further characterize the interface of the SF coatings, cross sections of the different sample groups were performed and analyzed, with Figure 5 showing all surfaces without and Figure 6 showing all surfaces with PEO surface modification. In Figure 5, sections A−C show the embedded magnesium and SF layers. The upper part of the picture shows the polymeric embedding material including filling particles. At a magnification of 5000-fold (panel C), a uniform and homogeneous distribution of the SF layer can be seen, which seemed completely torn off the magnesium surface due to the embedding and drying process, hence impeding interpretation. The SF layer thickness on magnesium on average was 2.22 μm (±SD 0.49 μm). The titanium samples are displayed in panels D−F. Although a layer thickness of 5.14 μm (±SD 0.22 μm) was achieved, the layer often appeared perforated and lumpy compared to the untreated magnesium sample. The thinnest and most difficult-to-measure

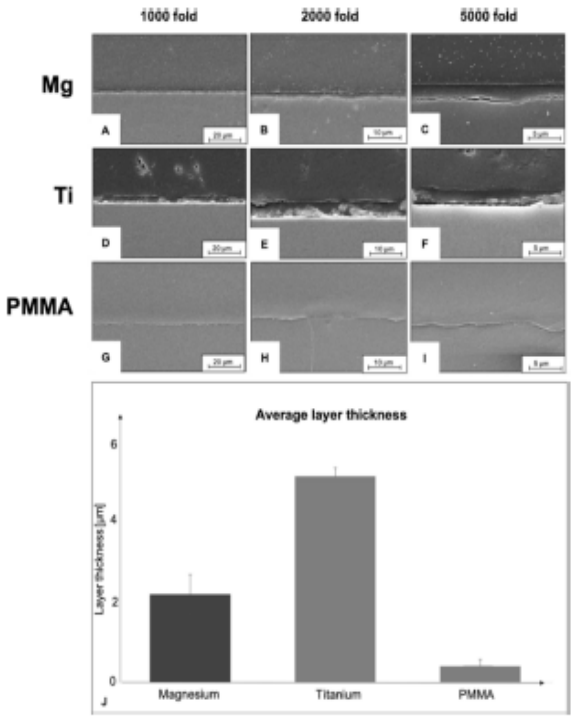

Figure 5. SEM images of the SF layers with WVA on different substrates in cross-section. (A−C) Magnesium; (D−F) titanium; (G−I) PMMA; (J) comparison of the average layer thickness. n = 5 samples tested.

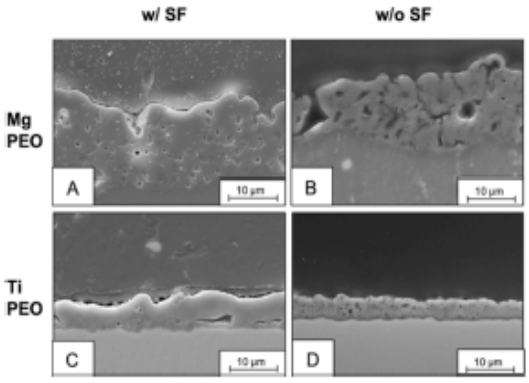

Figure 6. SEM images of the SF layer with WVA and PEO surface modifications in cross-section. (A,B) Mg + PEO with and without SF coating and (C,D) Ti + PEO with and without SF coating. n = 5 samples tested.

SF layer was seen on PMMA. Due to the transparency of the specimen and the embedding material, hardly any SF layer could be determined. The layer showed neither uniformity nor a homogeneous distribution on the surface. For this reason, only a SF layer thickness with an average of 0.41 μm could be measured, see pictures G−I. Independent experiments were conducted five times.

The determination of the coating thickness on the PEO surface-modified magnesium and titanium samples proved challenging. Due to the pores, it was hardly possible to measure an even and homogeneously distributed layer as the pores were filled with SF, while the nonporous flat surface regions showed a lower but homogeneous layer thickness. Figure 6 shows PEO

https://doi.org/10.1021/acsbiomaterials.3c00852
ACS Biomater. Sci. Eng. 2023, 9, 6644−6657

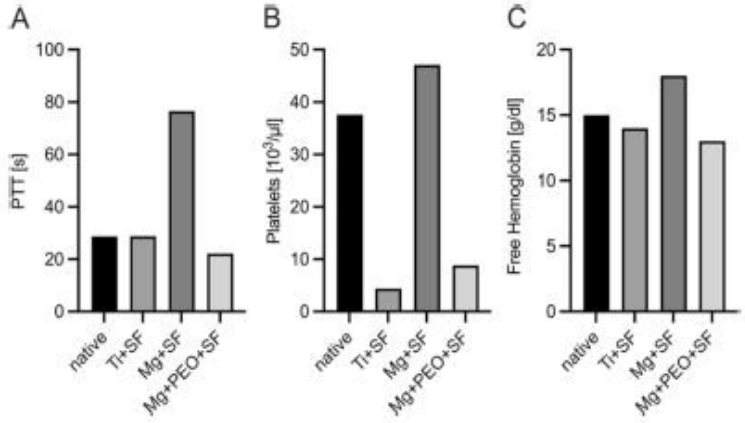

Figure 7. Hemocompatibility evaluation of titanium and untreated and PEO surface-modified magnesium specimens after SF coating and post-treatment with WVA; (A) PTT assay; (B) platelet activation assay; and (C) free hemoglobin assay. $n = 5$ samples tested. The negative control consisted of native blood without additional samples.

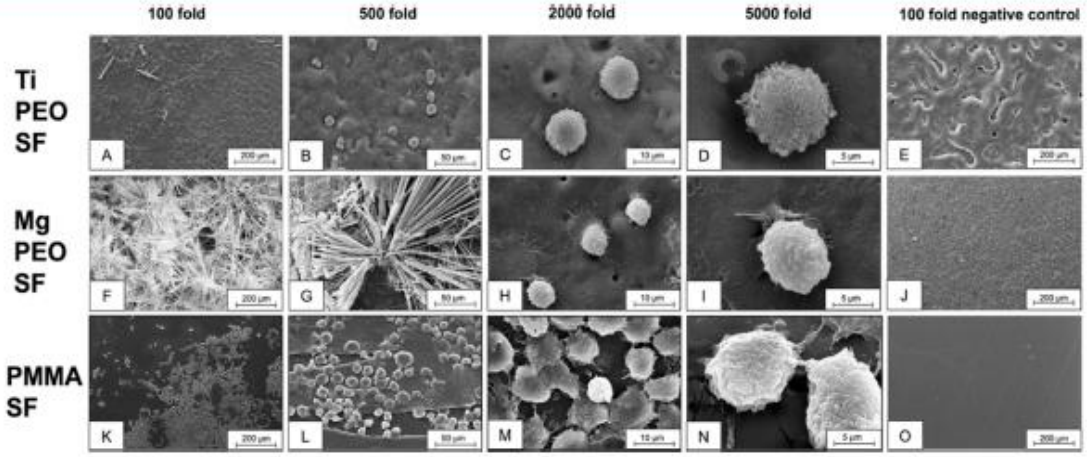

Figure 8. SEM images of THP-1 cell adhesion on the implant surfaces. (A–D) Ti + PEO + SF w/WVA; (E) Ti negative control w/o cells; (F–I) Mg + PEO + SF w/WVA; (J) Mg negative control w/o cells; (K–N) PMMA w/o PEO + SF w/WVA; and (O) PMMA negative control w/o cells. $n = 5$ samples tested.

surface-modified magnesium (A and B) and titanium (C and D) samples, on the left side fibroin-coated and on the right side the corresponding negative control.

3.5. Hemocompatibility Evaluation. To further evaluate hemocompatibility characteristics, PTT, free hemoglobin, and platelet activation tests were performed for groups showing potential clinical use in previous testing, namely, titanium, magnesium, and Mg + PEO after LbL coating with SF (see Figure 7). The results of the PTT assay showed that with spatially native blood, unmodified magnesium implants had a longer clotting time, indicating impaired physiological clotting. In contrast, titanium and magnesium PEO did not alter PTT. The platelet count was reduced in titanium and magnesium PEO specimen-containing blood samples. It was also observed that the platelet count in native blood was low. Furthermore, it was found that free hemoglobin levels were slightly elevated in unmodified magnesium implants, suggesting induction of hemolysis in this group. In general, it can be concluded that magnesium without PEO surface modification showed limited hemocompatibility, whereas magnesium with surface modification by PEO and metallic titanium exhibited hemocompatibility.

3.6. Cellular Adhesion Potential. During SEM evaluation of the different groups, blood cells could be detected on all three different materials; see Figure 8. In sections A–D, adherent cells on SF-coated titanium could be identified. The cells did not show a homogeneous distribution on the surface but settled and nestled on the SF-filled holes attributed to the PEO surface modification (section C). Individually, adherent cells were also detected on the SF-coated magnesium samples (images G and H). However, most of the surface was covered by oxide rods, which made it difficult to detect undifferentiated cells. While the cells on titanium had a nested and uneven cell-typical structure, the cells on the magnesium surface looked brighter and smoother (sections D and H). The oxide rods indicated a reaction of the magnesium surface with the previously surrounding medium (blood). The extent to which this reaction affected the adhesion of cells on the surface could not be determined at this point. The highest count of cells on the different substrates was found for PMMA. The cells did not only adhere excellently on top of the material but also connected interdependently. For all three tested implant materials, negative controls without cells are shown (panels E, J, and O).

https://doi.org/10.1021/acsbiomaterials.3c00852
ACS Biomater. Sci. Eng. 2023, 9, 6644–6657

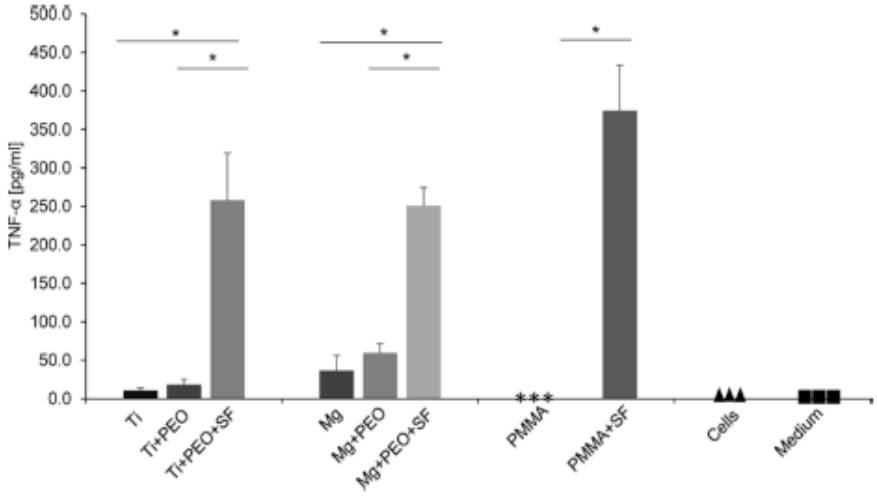

Figure 9. Proinflammatory response caused by macrophage response in the presence and absence of SF w/WVA quantified by TNF-α. For untreated PMMA samples (asterisk), cells (triangle), and culture medium (square), no detectable induction of TNF-α was measured. $n = 5$ samples tested.

3.7. TNF-α Response. Proinflammatory TNF-α cytokines were measured to assess the inflammatory response in the presence of SF as a coating material on the different tested substrates. As shown in Figure 9, compared to the control macrophages (cells and medium only), the SF composites showed a significantly higher concentration of TNF-α within a 12 h period. The number of TNF-α measured for coated titanium and magnesium was 260 L and 250 pg/mL, respectively. The concentration of TNF-α in coated PMMA showed the highest value with almost 400 pg/mL. Significant differences were also observed between the PEO surface-modified and PEO + SF-coated magnesium and titanium samples. Evidently, SF coating increased the concentration of TNF-α in all implant materials ($p < 0.05$).

4. DISCUSSION

After implant insertion, osteoconduction and osseointegration both depend not only on a variety of biological factors but also on the response to the foreign material.[46] Factors impeding osseointegration and implant success include radiation therapy, certain pharmacological agents, or other patient-related factors such as advanced age, osteoporosis, nutritional deficiencies, renal insufficiency, or smoking.[47] With an increasing use of orthopedic implants for joint replacement (predominantly knee and hip) in an aging population, as well as other applications, there is a growing demand for optimal interaction and integration between implant and bone.[48] Biomaterial-mediated inflammation after implant insertion can not only increase the risk of implant failure and influence the overall health of patients but also promote regenerative processes.[49] Macrophages are recognized as significant mediators of implant-associated inflammation. In fact, they possess a key role in establishing a balance between inflammatory and regenerative responses.[50] In recent years, several approaches have been introduced to prevent inordinate material-inflicted inflammatory responses following protein absorption and excessive immune activation.[51] Despite material advancement, it has been observed that they may cause severe allergic reactions after implantation.[52] The focus of the present in vitro study was to develop SF coatings by the LbL method for established implant materials and evaluate their properties with regard to foreign body reactions. In previous work, our group was able to show the suitability of SF scaffolds for implant applications.[33] Accordingly, our goal was to evaluate SF films as coatings for different implant materials and to investigate the wetting behavior of titanium, magnesium, and PMMA during the LbL dip coating.[53] Besides, in the field of biomedical engineering, surface modifications such as PEO have been shown to increase blood compatibility.[54] The measured contact angles for titanium and magnesium without such PEO modification were 58 and 79°, indicating a rather hydrophobic character and undesirable wetting properties for use with any aqueous solution. Significantly lower contact angles and thus good wetting properties, however, could be observed for PEO surface-modified titanium and magnesium. Hence, this indicates that a significant change in contact angle between the bare metallic and the PEO-modified samples is directly related to surface morphology (e.g., roughness) and chemistry. Similar results were observed by Echeverry-Rendón et al.[55] In their study, they reported that after PEO treatment of titanium discs, the contact angle drastically decreased, indicating the super-hydrophilicity of the tested samples. Also, in correspondence with our findings, Mingo et al.[56] observed decreased contact angles after PEO treatment of magnesium-based substrates. The authors suggested that the high surface porosity might promote the penetration of water-based solutions, enhancing wettability. On the other hand, these observations can be attributed to the chemical composition of the surface layer established during PEO surface modification. It was reported that the surface properties of the oxide layer can be customized by varying the PEO electrolyte composition and adding dispersed compounds.[57,58] Such entrapped particles can be incorporated into the surface layer and thus induce specific properties or improve surface performance.[59] For example, Sandhyarani et al. prepared different electrolyte compositions and used these solutions for the PEO surface treatment of metallic zirconium. Accordingly, they indicated that methodically varied concentrations of phosphate-, silicate-, and KOH-based electrolyte systems significantly altered the wettability of the oxide films formed on the surface.[58] In another study, Jiang et al. prepared various electrolyte compositions, such as sodium phosphate, sodium silicate, sodium aluminate, and composite (Na_3PO_4 + Na_2SiO_3 + $NaAlO_2$) electrolytes, and used them for PEO surface

https://doi.org/10.1021/acsbiomaterials.3c00852
ACS Biomater. Sci. Eng. 2023, 9, 6644−6657

modification of pure titanium.[57] Similarly, they proved that the chemical composition of the electrolyte solution drastically affects the physical properties of the fabricated PEO oxide layer.

In the present study, we used the LbL method to coat established implant materials with (titanium and magnesium) and without (PMMA) previous surface passivation by PEO with SF. The group of Saha et al. has shown the coating of SF on TiO_2 nanotubes.[12] They also utilized titanium grade 4 alloys for the electrophoretic disposition of SF, and with regard to hydrophilicity, they found contact angles of 83−90°. In our hands, a contact angle of 58° was measured for Ti, and a contact angle of 73° was measured for magnesium. Elia and colleagues successfully applied a silk electrogel coating on titanium dental implants.[60] Interestingly, they found that during mechanical testing, the adhesive strength of electrogel coatings was comparable to other biologically derived coating systems such as collagen, hydroxyapatite, and chitosan. Both groups were able to achieve a homogeneous coating but concentrated on titanium as an established implant material, whereas PMMA or magnesium were not investigated. The SF backbone consists of the amino acid structure of most hydrophobic (Gly and Ala) chain segments, which generally gives SF a hydrophobic character.[61] Wang et al. described the effects of the adhesive properties of SF on surfaces as a function of the salt content of the SF solution.[18] The experimental setup used for the coating process worked with satisfying performance as the whole surface was covered with layers of SF on most material groups. We hypothesized that the layer thickness of SF would increase with a higher number of dip processes. However, the accuracy and even distribution of SF on the surfaces proved to be challenging. According to the cross sections of the SF-coated samples, it was possible to cover the surface of all materials, but it proved difficult to obtain uniform thickness, at least when considering porosity. While the SF layer thickness of the magnesium and titanium implant materials achieved average values of ∼2.22 and 5.14 μm, respectively, the lowest layer thickness was obtained with the PMMA material (∼0.41 μm), which was consistent with the literature.[62,63] In particular, the PEO-modified samples showed better applicability with SF due to its more hydrophilic and rougher (porous) surface properties. However, pores filled with SF resulted in significantly higher layer thickness in these areas. It was found that PEO surface-modified titanium samples could not be filled with the provided amount of SF solution due to the coarser surface structure and larger pores of the PEO layer, demanding further penetration during the SF LbL coating.

After the SF LbL coating, two different post-treatment techniques were performed to convert the protein conformation of the water-soluble SF of silk I into water-insoluble silk structure II. Silk I has a less compressed structure than silk II but is usually considered very unstable and is converted to silk II (β-sheet) by physiochemical treatments such as mechanical forces, thermal treatment, and immersion in a selected organic solvent, such as alcohol. The first post-treatment was to immerse the silk in organic solvents, in our case, EtOH. Ethanol promotes crystallization by aggregating SF chains, leading to the formation of silk II structures. The rate of crystallization during the chemical treatment is affected by the concentration of the treatment solution. According to the literature, the progress of crystallization is very slow at high concentrations of EtOH solution, such as 90 or 100%.[18,64] The reason for this is the limited mobility of the amorphous SF chains. Therefore, a concentration of 70 vol % EtOH was used in this study. The second method for post-treatment of implants was based on temperature-controlled WVA.[65] WVA is a simple and effective method to control the molecular structure and crystallization of silk biomaterials through physical treatment. Post-treatment with water vapor, although more time-consuming, proved to be a more sensitive and inexpensive alternative to conventional methods. SF is known to require water molecules for crystallization.[62,66] During the post-treatment of silk with water vapor, water molecules play an important role in the amorphous parts of SF. Since the water molecules are comparatively small, they penetrate the silk protein chain network and "plasticize" the system into a water-bound silk network with higher chain mobility, resulting in higher flexibility of the SF structures in contrast to the rather brittle SF textures resulting from EtOH treatment.

After post-treatment of the samples, we performed FTIR analysis to investigate the water insolubility of the post-treated membranes and the molecular structure of SF. Dipping SF films in an EtOH bath to induce crystallization initiated self-assembly and aggregation of SF, resulting in SF microspheres. Compared with the alcohol-treated surfaces of SF, the steam-annealed samples showed significant advantages as the SF layer remained a smooth surface. Upon water annealing, SF interacted with water and reorganized its microdomains into a network dominated by α-helix structures instead of random coil structures. Many β-sheet-rich, fibril-like structures formed in the nodal regions of the network during treatment (white color in SEM). This appearance of post-treated SF structures is consistent with previous reports.[67,68] The water insolubility of the films of SF after steam annealing appears to be due to the formation of a stable silk I structure. When the films were exposed to EtOH, the silk II structure was visible. During annealing with water vapor, the SF chains within the membrane probably self-assembled to form a significant proportion of silk I. After swelling the steam-annealed films in water, the SF films retained their elasticity.[69] Moreover, the SF films annealed in water were more transparent than those treated with EtOH, which is consistent with previously published data.[67,69]

Hemocompatibility evaluation is essential for testing the surface compatibility of biomaterials for implant use. In this study, we performed PTT, platelet activation, and free hemoglobin assays. Blood coagulation can be triggered by a series of proteolytic reactions leading to the formation of fibrin clots; this process includes intrinsic and extrinsic coagulation processes.[70] The result of the PTT assay in the current study can be attributed to the fact that the intrinsic pathway is more easily activated by untreated magnesium implants.[71] Moreover, the present study demonstrated that the PEO surface modification of metallic implant surfaces does not impair PTT, which is in accordance with other studies.[50,51] It was suggested that the inert surface oxide layer reduced the interaction of blood cells and proteins.[72] On the other hand, because of the higher susceptibility to corrosion of untreated magnesium, it is expected that a large amount of magnesium ions will be exposed to blood flow. The interaction of free magnesium ions with the membrane of red blood cells may lead to swelling and rupture of the membrane, potentially resulting in hemolysis.[73,74]

A further essential requirement for biomaterial-based implants is sufficient biocompatibility in vivo, which includes a physiological inflammatory response. To determine the ability of cell-loaded silk films to polarize macrophages, the monocytic undifferentiated human monocytic leukemia cell line (THP-1) was used on the different implant materials. In suspension, THP-1 cells are present as monocytes and become macrophages

https://doi.org/10.1021/acsbiomaterials.3c00852
ACS Biomater. Sci. Eng. 2023, 9, 6644−6657

capable of adhering to surfaces through differentiation. One aim of this study was to use thin layers of SF proteins as the coating material for implants to modulate the release of cytokines and to control the macrophage response to an extent that monocytes can differentiate into macrophages by adhesion to the surfaces. SF was used because it can be tailored to suppress or promote the release of cytokines under physiological conditions and has been previously shown to preserve cell functionality.[75,76] The largest number of adherent cells was detected by SEM on the surface of the coated PMMA. A possible reason for the enormous number of differentiated cells on the surface of PMMA could be the small thickness of the SF layer that could be generated only on this material. Due to an uneven and inhomogeneously distributed SF layer, areas of the PMMA surface remained uncovered. In previous studies, PMMA-induced cellular infiltration and proinflammatory cytokine release suggested that the ratio of total surface area to substrate volume may be an important factor in determining the extent of the inflammatory response.[76,77] Whether the formation and adhesion of cells to the surfaces of implant materials are desirable cannot be determined by this test. Moreover, it needs to be investigated whether cell adhesion and thus differentiation of macrophages on the surfaces also occurred on the samples without SF.

The inflammatory potential of SF as a coating on common biomaterials was quantified by ELISA as macrophages play an important role in the human innate immune system. After the implantation of biomaterials, macrophages stimulate the tissue to ensure wound healing; on the other hand, they trigger degradation processes and inflammatory responses.[3,78,79] Activation of the innate immune response is a useful determinant of biomaterial biocompatibility.[76,78,80] TNF-α is a proinflammatory cytokine that induces the expression of cutaneous and endothelial adhesion molecules and is involved in skin irritation and inflammatory responses to implant materials.[81]

Herein, TNF-α acts as a proinflammatory cytokine, which is secreted by M1-like macrophages, creating the regenerative niche and promoting recruitment and differentiation of mesenchymal progenitor cells for bone healing as well as guiding bone formation and remodeling.[9] Our study shows that TNF-α was significantly increased after SF coating on all tested substrate materials. On SF-coated, PEO surface-modified titanium and magnesium specimens, TNF-α cytokines reached levels of 260 and 250 pg/mL, respectively. The highest amount could be determined with PMMA + SF (~400 pg/mL). These concentrations were significantly reduced without the SF coating. One reason for this behavior could be attributed to fibroin proteins that detach from the coating and cause activation of the cells in the medium.[76] The proinflammatory cytokines can also be understood as biomarkers for the proper differentiation of monocytes to macrophages and the physiological response of macrophages. Despite the potential benefits of PEO on titanium, the layering system has so far only been used in selected applications (e.g., in titanium dental implants), and the wide range of titanium implants, such as orthopedic applications, is not represented. In addition, PEO is not indispensable for titanium in contrast to magnesium, where PEO must always be used to passivate the reactive surface, also with an SF coating on top. Therefore, for titanium implants, the direct use of SF (without PEO) makes economic and functional sense.

The coating of implant materials with SF has been previously shown to improve biocompatibility and osteogenesis, which is in strong accordance with our findings on moderately elevated levels of TNF-α on homogeneously LbL SF-coated substrates.[82−84] The cytokine response to SF particles, as found with inhomogeneously coated PMMA substrates, endorses the benefits of further evaluation of SF film degradation. Additional testing should be performed to determine the proinflammatory response of SF layers as a coating for implant materials and ability to enhance biocompatibility and osteogenesis.[85] Enzymatic degradation experiments should be used to gain an overview of the tunable degradability of SF.[86] Additional investigation will be useful to determine how the crystallization method of SF affects the physiological and mechanical properties and the potential of these coatings in vivo.

5. CONCLUSIONS

In our study, a method for the LbL dip coating of SF for application on different relevant implant materials, namely, titanium, magnesium (with or without PEO surface modification as an intermediate layer), and PMMA, was successfully developed and the resulting SF surfaces were thoroughly characterized. The SF solution was prepared free of toxic solvents, water-based, and biocompatible. SF coatings were brought to an insoluble state by applying WVA as the post-treatment method, thereby controlling the thermal stability and degradation of such protein-based biomaterials. The adsorption process applied was shown to be stable and reproducible as SF layers with thicknesses of up to 5 μm could be achieved. Homogeneous SF films could be established on titanium and magnesium using PEO surface modification as pretreatment; however, the LbL coating of PMMA with SF proved to be challenging. Different biomedical parameters such as hemocompatibility and biocompatibility were tested for the final specimen groups. SF coatings generally showed induction of TNF-α for all implant materials, indicating a proinflammatory response, which has previously been shown to play a pivotal role in a plethora of physiologic processes, including stimulation of osteogenesis. Thus, the LbL coating of SF shows great potential for application as a coating for most common and even upcoming implant materials and should be further tested in vivo to validate its applicability for biomedical use.

■ ASSOCIATED CONTENT

Data Availability Statement

The data that support the findings of this study are available from the corresponding author upon reasonable request.

■ AUTHOR INFORMATION

Corresponding Author

Levi Matthies − *Department of Oral and Maxillofacial Surgery, University Medical Center Hamburg-Eppendorf, D-20246 Hamburg, Germany; Mildred Scheel Cancer Career Center HaTriCS4, University Medical Center Hamburg-Eppendorf, D-20246 Hamburg, Germany;* orcid.org/0000-0001-7168-4428; Email: l.matthies@uke.de

Authors

Sandra Fuest − *Department of Oral and Maxillofacial Surgery, Division of Regenerative Orofacial Medicine, University Medical Center Hamburg-Eppendorf, D-20246 Hamburg, Germany*

https://doi.org/10.1021/acsbiomaterials.3c00852
ACS Biomater. Sci. Eng. 2023, 9, 6644−6657

Ralf Smeets – *Department of Oral and Maxillofacial Surgery, Division of Regenerative Orofacial Medicine, University Medical Center Hamburg-Eppendorf, D-20246 Hamburg, Germany; Department of Oral and Maxillofacial Surgery, University Medical Center Hamburg-Eppendorf, D-20246 Hamburg, Germany*

Martin Gosau – *Department of Oral and Maxillofacial Surgery, University Medical Center Hamburg-Eppendorf, D-20246 Hamburg, Germany*

Farzaneh Aavani – *Department of Oral and Maxillofacial Surgery, Division of Regenerative Orofacial Medicine, University Medical Center Hamburg-Eppendorf, D-20246 Hamburg, Germany*

Christian Knipfer – *Department of Oral and Maxillofacial Surgery, University Medical Center Hamburg-Eppendorf, D-20246 Hamburg, Germany*

Audrey Laure Céline Grust – *Department of Oral and Maxillofacial Surgery, University Medical Center Hamburg-Eppendorf, D-20246 Hamburg, Germany*

Alexander Kopp – *Fibrothelium GmbH, D-52068 Aachen, Germany*

Mustafa Becerikli – *Department of Plastic Surgery, BG University Hospital Bergmannsheil, D-44789 Bochum, Germany*

Björn Behr – *Department of Plastic Surgery, BG University Hospital Bergmannsheil, D-44789 Bochum, Germany*

Complete contact information is available at: https://pubs.acs.org/10.1021/acsbiomaterials.3c00852

Author Contributions

Conceptualization, S.F., A.K., and R.S.; methodology, validation, and formal analysis, S.F. and A.K.; project administration and resources, R.S., M.G., and B.B.; data curation, S.F., L.M., and M.B.; writing—original draft, L.M. and S.F.; writing—review and editing, F.A., A.L.C.G., and C.K.; supervision, L.M., R.S., and M.G.; all authors have read and agreed to the final version of the manuscript.

Funding

L.M. was supported by a fellowship of the Mildred Scheel Cancer Career Center Hamburg of the German Cancer Aid (70113304).

Notes

The authors declare the following competing financial interest(s): The authors declare no competing financial interest. AK is employed at Meotec GmbH, Aachen and Fibrothelium GmbH, Aachen.

■ ACKNOWLEDGMENTS

The authors thank Anke Baranowsky for assistance with cell culture experiments, Marius Köpf for support with queries, and Thomas Derra for technical drawing.

■ ABBREVIATIONS

B. mori	*Bombyx mori*
°C	degree Celsius
$CaCl_2$	calcium chloride
ddH_2O	purified water
ELISA	enzyme-linked immunosorbent assay
EtOH	ethanol
FTIR	Fourier transform infrared spectroscopy
GA	glutaraldehyde
H_2O_2	hydrogen peroxide solution
LbL	layer-by-layer
M1	proinflammatory macrophages
M2	anti-inflammatory macrophages
Na_2CO_3	sodium carbonate
PBS	phosphate-buffered saline
PEO	plasma electrolytic oxidation
PMMA	polymethyl-methacrylate
PTFE	polytetrafluorethylene
RH	relative humidity
SEM	scanning electron microscopy
SF	silk fibroin
THP-1	human monocytic leukemia cell line
TNF-α	tumor necrosis factor α
WVA	water vapor annealing
WVP	water vapor permeability
WVT	water vapor transmission

■ REFERENCES

(1) Olmo, J. A.-D.; Ruiz-Rubio, L.; Pérez-Alvarez, L.; Sáez-Martínez, V.; Vilas-Vilela, J. L. Antibacterial Coatings for Improving the Performance of Biomaterials. *Coatings* **2020**, *10* (2), 139.

(2) Trindade, R.; Albrektsson, T.; Galli, S.; Prgomet, Z.; Tengvall, P.; Wennerberg, A. Osseointegration and foreign body reaction: Titanium implants activate the immune system and suppress bone resorption during the first 4 weeks after implantation. *Clin. Implant Dent. Relat. Res.* **2018**, *20* (1), 82–91.

(3) Sheikh, Z.; Brooks, P.; Barzilay, O.; Fine, N.; Glogauer, M. Macrophages, Foreign Body Giant Cells and Their Response to Implantable Biomaterials. *Materials* **2015**, *8* (9), 5671–5701.

(4) Goodman, S. B.; Yao, Z.; Keeney, M.; Yang, F. The future of biologic coatings for orthopaedic implants. *Biomaterials* **2013**, *34* (13), 3174–3183.

(5) Rendenbach, C.; Fischer, H.; Kopp, A.; Schmidt-Bleek, K.; Kreiker, H.; Stumpp, S.; Thiele, M.; Duda, G.; Hanken, H.; Beck-Broichsitter, B.; Jung, O.; Kroger, N.; Smeets, R.; Heiland, M. Improved in vivo osseointegration and degradation behavior of PEO surface-modified WE43 magnesium plates and screws after 6 and 12 months. *Mater. Sci. Eng., C* **2021**, *129*, 112380.

(6) Qian, Y.; Li, L.; Song, Y.; Dong, L.; Chen, P.; Li, X.; Cai, K.; Germershaus, O.; Yang, L.; Fan, Y. Surface modification of nanofibrous matrices via layer-by-layer functionalized silk assembly for mitigating the foreign body reaction. *Biomaterials* **2018**, *164*, 22–37.

(7) Becerikli, M.; Kopp, A.; Kroger, N.; Bodrova, M.; Wallner, C.; Wagner, J. M.; Dadras, M.; Jettkant, B.; Pohl, F.; Lehnhardt, M.; Jung, O.; Behr, B. A novel titanium implant surface modification by plasma electrolytic oxidation (PEO) preventing tendon adhesion. *Mater. Sci. Eng., C* **2021**, *123*, 112030.

(8) Rasouli, R.; Barhoum, A.; Uludag, H. A review of nanostructured surfaces and materials for dental implants: surface coating, patterning and functionalization for improved performance. *Biomater. Sci.* **2018**, *6* (6), 1312–1338.

(9) Niu, Y.; Wang, Z.; Shi, Y.; Dong, L.; Wang, C. Modulating macrophage activities to promote endogenous bone regeneration: Biological mechanisms and engineering approaches. *Bioact. Mater.* **2021**, *6* (1), 244–261.

(10) Rupp, F.; Liang, L.; Geis-Gerstorfer, J.; Scheideler, L.; Huttig, F. Surface characteristics of dental implants: A review. *Dent. Mater.* **2018**, *34* (1), 40–57.

(11) Lacroix, M.; Vu, K. D. *Edible Coating and Film Materials: Proteins*; Elsevier Ltd, 2013.

(12) Saha, S.; Pramanik, K.; Biswas, A. Silk fibroin coated TiO(2) nanotubes for improved osteogenic property of Ti6Al4V bone implants. *Mater. Sci. Eng., C* **2019**, *105*, 109982.

(13) Karak, N. Biopolymers for paints and surface coatings. In *Biopolymers and Biotech Admixtures for Eco-Efficient Construction Materials*; Pacheco-Torgal, F., Ivanov, V., Karak, N., Jonkers, H., Eds.; Woodhead Publishing, 2016; pp 333–368.

(14) Puetz, J.; Aegerter, M. Dip coating technique. *Sol-gel Technologies for Glass Producers and Users*; Springer, 2004; pp 37−48.
(15) Iler, R. K. Multilayers of colloidal particles. *J. Colloid Interface Sci.* **1966**, *21* (6), 569−594.
(16) Lee, D.; Rubner, M. F.; Cohen, R. E. All-nanoparticle thin-film coatings. *Nano Lett.* **2006**, *6* (10), 2305−2312.
(17) Dubas, S. T.; Schlenoff, J. B. Factors controlling the growth of polyelectrolyte multilayers. *Macromolecules* **1999**, *32* (24), 8153−8160.
(18) Wang, X.; Kim, H. J.; Xu, P.; Matsumoto, A.; Kaplan, D. L. Biomaterial Coatings by Stepwise Deposition of Silk Fibroin. *Langmuir* **2005**, *21* (24), 11335−11341.
(19) Richardson, J. J.; Bjornmalm, M.; Caruso, F. Technology-driven layer-by-layer assembly of nanofilms. *Science* **2015**, *348* (6233), aaa2491.
(20) Kharlampieva, E.; Kozlovskaya, V.; Chan, J.; Ankner, J. F.; Tsukruk, V. V. Spin-assisted layer-by-layer assembly: Variation of stratification as studied with neutron reflectivity. *Langmuir* **2009**, *25* (24), 14017−14024.
(21) Raman, N.; Lee, M. R.; Palecek, S. P.; Lynn, D. M. Polymer multilayers loaded with antifungal β-peptides kill planktonic Candida albicans and reduce formation of fungal biofilms on the surfaces of flexible catheter tubes. *J. Controlled Release* **2014**, *191*, 54−62.
(22) Arnon, H.; Granit, R.; Porat, R.; Poverenov, E. Development of polysaccharides-based edible coatings for citrus fruits: A layer-by-layer approach. *Food Chem.* **2015**, *166*, 465−472.
(23) Li, Z.-H.; Ji, S.-C.; Wang, Y.-Z.; Shen, X.-C.; Liang, H. Silk fibroin-based scaffolds for tissue engineering. *Front. Mater. Sci.* **2013**, *7* (3), 237−247.
(24) Kopp, A.; Smeets, R.; Gosau, M.; Kroger, N.; Fuest, S.; Kopf, M.; Kruse, M.; Krieger, J.; Rutkowski, R.; Henningsen, A.; Burg, S. Effect of process parameters on additive-free electrospinning of regenerated silk fibroin nonwovens. *Bioact. Mater.* **2020**, *5* (2), 241−252.
(25) DeBari, M. K.; King, C. L.; Altgold, T. A.; Abbott, R. D. Silk Fibroin as a Green Material. *ACS Biomater. Sci. Eng.* **2021**, *7* (8), 3530−3544.
(26) Cao, Y.; Wang, B. Biodegradation of silk biomaterials. *Int. J. Mol. Sci.* **2009**, *10*, 1514−1524.
(27) Koh, L. D.; Cheng, Y.; Teng, C. P.; Khin, Y. W.; Loh, X. J.; Tee, S. Y.; Low, M.; Ye, E.; Yu, H. D.; Zhang, Y. W.; Han, M. Y. Structures, mechanical properties and applications of silk fibroin materials. *Prog. Polym. Sci.* **2015**, *46*, 86−110.
(28) Amiraliyan, N.; Nouri, M.; Kish, M. H. Effects of Some Electrospinning Parameters on Morphology of Natural Silk-Based Nanofibers. *J. Appl. Polym. Sci.* **2009**, *113* (1), 226−234.
(29) Min, B. M.; Lee, G.; Kim, S. H.; Nam, Y. S.; Lee, T. S.; Park, W. H. Electrospinning of silk fibroin nanofibers and its effect on the adhesion and spreading of normal human keratinocytes and fibroblasts in vitro. *Biomaterials* **2004**, *25* (7−8), 1289−1297.
(30) Rockwood, D. N.; Preda, R. C.; Yucel, T.; Wang, X.; Lovett, M. L.; Kaplan, D. L. Materials fabrication from Bombyx mori silk fibroin. *Nat. Protoc.* **2011**, *6* (10), 1612−1631.
(31) Wei, Q.; Becherer, T.; Angioletti-Uberti, S.; Dzubiella, J.; Wischke, C.; Neffe, A. T.; Lendlein, A.; Ballauff, M.; Haag, R. Protein interactions with polymer coatings and biomaterials. *Angew. Chem., Int. Ed. Engl.* **2014**, *53* (31), 8004−8031.
(32) Ajisawa, A. Dissolution of silk fibroin with calciumchloride/ethanol aqueous solution Studies on the dissolution of silk fibroin. (IX). *J. Seric. Sci. Jpn.* **1998**, *67* (2), 91−94.
(33) Kopp, A.; Smeets, R.; Gosau, M.; Friedrich, R. E.; Fuest, S.; Behbahani, M.; Barbeck, M.; Rutkowski, R.; Burg, S.; Kluwe, L.; Henningsen, A. Production and characterization of porous fibroin scaffolds for regenerative medical application. *In Vivo* **2019**, *33* (3), 757−762.
(34) Zheng, Z.; Guo, S.; Liu, Y.; Wu, J.; Li, G.; Liu, M.; Wang, X.; Kaplan, D. Lithium-free processing of silk fibroin. *J. Biomater. Appl.* **2016**, *31* (3), 450−463.
(35) Kim, S. H.; Nam, Y. S.; Lee, T. S.; Park, W. H. Silk Fibroin Nanofiber. Electrospinning, Properties, and Structure. *Polym. J.* **2003**, *35* (2), 185−190.
(36) Ziemba, A. M.; Fink, T. D.; Crochiere, M. C.; Puhl, D. L.; Sapkota, S.; Gilbert, R. J.; Zha, R. H. Coating Topologically Complex Electrospun Fibers with Nanothin Silk Fibroin Enhances Neurite Outgrowth in Vitro. *ACS Biomater. Sci. Eng.* **2020**, *6* (3), 1321−1332.
(37) Falguera, V.; Quintero, J. P.; Jiménez, A.; Muñoz, J. A.; Ibarz, A. Edible films and coatings: Structures, active functions and trends in their use. *Trends Food Sci. Technol.* **2011**, *22* (6), 292−303.
(38) Schafer, S.; Smeets, R.; Kopf, M.; Drinic, A.; Kopp, A.; Kroger, N.; Hartjen, P.; Assaf, A. T.; Aavani, F.; Beikler, T.; Peters, U.; Fiedler, I.; Busse, B.; Sturmer, E. K.; Vollkommer, T.; Gosau, M.; Fuest, S. Antibacterial properties of functionalized silk fibroin and sericin membranes for wound healing applications in oral and maxillofacial surgery. *Biomater. Adv.* **2022**, *135*, 212740.
(39) Ramadass, S. K.; Nazir, L. S.; Thangam, R.; Perumal, R. K.; Manjubala, I.; Madhan, B.; Seetharaman, S. Type I collagen peptides and nitric oxide releasing electrospun silk fibroin scaffold: A multifunctional approach for the treatment of ischemic chronic wounds. *Colloids Surf., B* **2019**, *175*, 636−643.
(40) Zhang, D.; Fan, L.; Ma, L.; Liu, J.; Zhou, K.; Song, X.; Sun, M.; Mo, X.; He, C.; Chen, Y.; Wang, H. Helicobacter pylori Ribosomal Protein-A2 Peptide/Silk Fibroin Nanofibrous Composites as Potential Wound Dressing. *J. Biomed. Nanotechnol.* **2019**, *15* (3), 507−517.
(41) Sultan, M. T.; Lee, O. J.; Kim, S. H.; Ju, H. W.; Park, C. H. Silk Fibroin in Wound Healing Process. *Adv. Exp. Med. Biol.* **2018**, *1077*, 115−126.
(42) Xu, W.; Yagoshi, K.; Asakura, T.; Sasaki, M.; Niidome, T. Silk Fibroin as a Coating Polymer for Sirolimus-Eluting Magnesium Alloy Stents. *ACS Appl. Bio Mater.* **2020**, *3* (1), 531−538.
(43) Marelli, B.; Brenckle, M. A.; Kaplan, D. L.; Omenetto, F. G. Silk Fibroin as Edible Coating for Perishable Food Preservation. *Sci. Rep.* **2016**, *6* (1), 25263.
(44) Seo, J.; Lutkenhaus, J. L.; Kim, J.; Hammond, P. T.; Char, K. Effect of the Layer-by-Layer (LbL) Deposition Method on the Surface Morphology and Wetting Behavior of Hydrophobically Modified PEO and PAA LbL Films. *Langmuir* **2008**, *24* (15), 7995−8000.
(45) Lamke, L.; Nilsson, G. E.; Reithner, H. L. The evaporative water loss from burns and the water-vapour permeability of grafts and artificial membranes used in the treatment of burns. *Burns* **1977**, *3* (3), 159−165.
(46) Albrektsson, T.; Johansson, C. Osteoinduction, osteoconduction and osseointegration. *Eur. Spine J.* **2001**, *10*, S96−S101.
(47) Mavrogenis, A. F.; Dimitriou, R.; Parvizi, J.; Babis, G. C. Biology of implant osseointegration. *J. Musculoskelet. Neuronal Interact.* **2009**, *9* (2), 61−71.
(48) Raphel, J.; Holodniy, M.; Goodman, S. B.; Heilshorn, S. C. Multifunctional coatings to simultaneously promote osseointegration and prevent infection of orthopaedic implants. *Biomaterials* **2016**, *84*, 301−314.
(49) Kamath, S.; Bhattacharyya, D.; Padukudru, C.; Timmons, R. B.; Tang, L. Surface chemistry influences implant-mediated host tissue responses. *J. Biomed. Mater. Res., Part A* **2008**, *86* (3), 617−626.
(50) Kzhyshkowska, J.; Gudima, A.; Riabov, V.; Dollinger, C.; Lavalle, P.; Vrana, N. E. Macrophage responses to implants: prospects for personalized medicine. *J. Leukoc. Biol.* **2015**, *98* (6), 953−962.
(51) Bridges, A. W.; Garcia, A. J. Anti-inflammatory polymeric coatings for implantable biomaterials and devices. *J. Diabetes Sci. Technol.* **2008**, *2* (6), 984−994.
(52) Luthringer, B. J.; Feyerabend, F.; Willumeit-Römer, R. Magnesium-based implants: a mini-review. *Magnes. Res.* **2014**, *27* (4), 142−154.
(53) Flemming, R. G.; Murphy, C. J.; Abrams, G. A.; Goodman, S. L.; Nealey, P. F. Effects of synthetic micro-and nano-structured surfaces on cell behavior. *Biomaterials* **1999**, *20* (6), 573−588.
(54) Tang, L.; Thevenot, P.; Hu, W. Surface chemistry influences implant biocompatibility. *Curr. Top. Med. Chem.* **2008**, *8* (4), 270−280.
(55) Echeverry-Rendón, M.; Galvis, O.; Aguirre, R.; Robledo, S.; Castaño, J. G.; Echeverría, F. Modification of titanium alloys surface properties by plasma electrolytic oxidation (PEO) and influence on biological response. *J. Mater. Sci. Mater. Med.* **2017**, *28* (11), 169.

https://doi.org/10.1021/acsbiomaterials.3c00852
ACS Biomater. Sci. Eng. 2023, 9, 6644−6657

(56) Mingo, B.; Arrabal, R.; Mohedano, M.; Llamazares, Y.; Matykina, E.; Yerokhin, A.; Pardo, A. Influence of sealing post-treatments on the corrosion resistance of PEO coated AZ91 magnesium alloy. *Appl. Surf. Sci.* **2018**, *433*, 653−667.
(57) Jiang, H.; Shao, Z.; Jing, B. Effect of electrolyte composition on photocatalytic activity and corrosion resistance of micro-arc oxidation coating on pure titanium. *Procedia Earth Planet. Sci.* **2011**, *2*, 156−161.
(58) S, M.; Prasadrao, T.; Rameshbabu, N. Role of electrolyte composition on structural, morphological and in-vitro biological properties of plasma electrolytic oxidation films formed on zirconium. *Appl. Surf. Sci.* **2014**, *317*, 198−209.
(59) Clyne, T. W.; Troughton, S. C. A review of recent work on discharge characteristics during plasma electrolytic oxidation of various metals. *Int. Mater. Rev.* **2019**, *64* (3), 127−162.
(60) Elia, R.; Michelson, C. D.; Perera, A. L.; Harsono, M.; Leisk, G. G.; Kugel, G.; Kaplan, D. L. Silk electrogel coatings for titanium dental implants. *J. Biomater. Appl.* **2015**, *29* (9), 1247−1255.
(61) Kundu, B.; Rajkhowa, R.; Kundu, S. C.; Wang, X. Silk fibroin biomaterials for tissue regenerations. *Adv. Drug Deliv. Rev.* **2013**, *65* (4), 457−470.
(62) Guo, Y.; Guan, J.; Peng, H.; Shu, X.; Chen, L.; Guo, H. Tightly adhered silk fibroin coatings on Ti6Al4V biometals for improved wettability and compatible mechanical properties. *Mater. Des.* **2019**, *175*, 107825.
(63) Ghumatkar, A.; Budhe, S.; Sekhar, R.; Banea, M. D.; Barros, S. d. Influence of Adherend Surface Roughness on the Adhesive Bond Strength. *Lat. Am. J. Solid. Struct.* **2016**, *13* (13), 2356−2370.
(64) Terada, D.; Yokoyama, Y.; Hattori, S.; Kobayashi, H.; Tamada, Y. The outermost surface properties of silk fibroin films reflect ethanol-treatment conditions used in biomaterial preparation. *Mater. Sci. Eng., C* **2016**, *58*, 119−126.
(65) Hu, X.; Shmelev, K.; Sun, L.; Gil, E. S.; Park, S. H.; Cebe, P.; Kaplan, D. L.; Cebe, P.; Kaplan, D. L. Regulation of Silk Material Structure by Temperature-Controlled Water Vapor Annealing. *Biomacromolecules* **2011**, *12* (5), 1686−1696.
(66) Tanaka, K.; Inoue, S.; Mizuno, S. Hydrophobic interaction of P25, containing Asn-linked oligosaccharide chains, with the H-L complex of silk fibroin produced by Bombyx mori. *Insect Biochem. Mol. Biol.* **1999**, *29* (3), 269−276.
(67) Hu, X.; Kaplan, D.; Cebe, P. Dynamic Protein-Water Relationships during β-Sheet Formation. *Macromolecules* **2008**, *41* (11), 3939−3948.
(68) Qi, Y.; Wang, H.; Wei, K.; Yang, Y.; Zheng, R. Y.; Kim, I. S.; Zhang, K. Q. A Review of Structure Construction of Silk Fibroin Biomaterials from Single Structures to Multi-Level Structures. *Int. J. Mol. Sci.* **2017**, *18* (3), 237.
(69) Jin, H. J.; Park, J.; Karageorgiou, V.; Kim, U. J.; Valluzzi, R.; Cebe, P.; Kaplan, D. L. Water-Stable Silk Films with Reduced β-Sheet Content. *Adv. Funct. Mater.* **2005**, *15* (8), 1241−1247.
(70) Monroe, D. M.; Hoffman, M. What does it take to make the perfect clot? *Arterioscler. Thromb. Vasc. Biol.* **2006**, *26* (1), 41−48.
(71) Kamal, A. H.; Tefferi, A.; Pruthi, R. K. How to interpret and pursue an abnormal prothrombin time, activated partial thromboplastin time, and bleeding time in adults. *Mayo Clin. Proc.* **2007**, *82*, 864−873.
(72) Park, K.; Shim, H. S.; Dewanjee, M. K.; Eigler, N. L. In vitro and in vivo studies of PEO-grafted blood-contacting cardiovascular prostheses. *J. Biomater. Sci., Polym. Ed.* **2000**, *11* (11), 1121−1134.
(73) Gailani, D.; Renné, T. Intrinsic pathway of coagulation and arterial thrombosis. *Arterioscler. Thromb. Vasc. Biol.* **2007**, *27* (12), 2507−2513.
(74) Bunn, H. F.; Ransil, B. J.; Chao, A. The interaction between erythrocyte organic phosphates, magnesium ion, and hemoglobin. *J. Biol. Chem.* **1971**, *246* (17), 5273−5279.
(75) Reeves, A. R. D.; Spiller, K. L.; Freytes, D. O.; Vunjak-Novakovic, G.; Kaplan, D. L. Controlled release of cytokines using silk-biomaterials for macrophage polarization. *Biomaterials* **2015**, *73*, 272−283.
(76) Panilaitis, B.; Altman, G. H.; Chen, J.; Jin, H.-j.; Karageorgiou, V.; Kaplan, D. L. Macrophage responses to silk. *Biomaterials* **2003**, *24* (18), 3079−3085.
(77) Wooley, P. H.; Morren, R.; Andary, J.; Sud, S.; Yang, S. Y.; Mayton, L.; Markel, D.; Sieving, A.; Nasser, S. Inflammatory responses to orthopaedic biomaterials in the murine air pouch. *Biomaterials* **2002**, *23* (2), 517−526.
(78) Brown, B. N.; Badylak, S. F. *Biocompatibility and Immune Response to Biomaterials*; Elsevier Inc., 2014.
(79) Franz, S.; Rammelt, S.; Scharnweber, D.; Simon, J. C. Immune responses to implants - A review of the implications for the design of immunomodulatory biomaterials. *Biomaterials* **2011**, *32* (28), 6692−6709.
(80) Gardner, A. B.; Lee, S. K.; Woods, E. C.; Acharya, A. P. Biomaterials-based modulation of the immune system. *BioMed Res. Int.* **2013**, *2013*, 1−7.
(81) Harkins, A. L.; Duri, S.; Kloth, L. C.; Tran, C. D. Chitosan-cellulose composite for wound dressing material. Part 2. Antimicrobial activity, blood absorption ability, and biocompatibility. *J. Biomed. Mater. Res., Part B* **2014**, *102* (6), 1199−1206.
(82) Guo, Y. Q.; Guan, J.; Peng, H.; Shu, X.; Chen, L.; Guo, H. B. Tightly adhered silk fibroin coatings on Ti6Al4V biometals for improved wettability and compatible mechanical properties. *Mater. Des.* **2019**, *175*, 107825.
(83) Melke, J.; Midha, S.; Ghosh, S.; Ito, K.; Hofmann, S. Silk fibroin as biomaterial for bone tissue engineering. *Acta Biomater.* **2016**, *31*, 1−16.
(84) Yoo, C. K.; Jeon, J. Y.; Kim, Y. J.; Kim, S. G.; Hwang, K. G. Cell attachment and proliferation of osteoblast-like MG63 cells on silk fibroin membrane for guided bone regeneration. *Maxillofac. Plast. Reconstr. Surg.* **2016**, *38* (1), 17.
(85) Hu, K.; Hu, M.; Xiao, Y.; Cui, Y.; Yan, J.; Yang, G.; Zhang, F.; Lin, G.; Yi, H.; Han, L.; Li, L.; Wei, Y.; Cui, F. Preparation recombination human-like collagen/fibroin scaffold and promoting the cell compatibility with osteoblasts. *J. Biomed. Mater. Res., Part A* **2021**, *109* (3), 346−353.
(86) Zhang, L.; Liu, X.; Li, G.; Wang, P.; Yang, Y. Tailoring degradation rates of silk fibroin scaffolds for tissue engineering. *J. Biomed. Mater. Res., Part A* **2019**, *107* (1), 104−113.

https://doi.org/10.1021/acsbiomaterials.3c00852
ACS Biomater. Sci. Eng. 2023, 9, 6644−6657

135 (2022) 212740

Contents lists available at ScienceDirect

Biomaterials Advances

journal homepage: www.journals.elsevier.com/materials-science-and-engineering-c

Antibacterial properties of functionalized silk fibroin and sericin membranes for wound healing applications in oral and maxillofacial surgery

Sogand Schäfer [a,*], Ralf Smeets [a,b], Marius Köpf [c], Aleksander Drinic [c], Alexander Kopp [c], Nadja Kröger [d], Philip Hartjen [b], Alexandre Thomas Assaf [b], Farzaneh Aavani [a], Thomas Beikler [e], Ulrike Peters [e], Imke Fiedler [f], Björn Busse [f], Ewa K. Stürmer [g], Tobias Vollkommer [b], Martin Gosau [b], Sandra Fuest [a]

[a] Department of Oral and Maxillofacial Surgery, Division of Regenerative Orofacial Medicine, University Hospital Hamburg-Eppendorf, 20251 Hamburg, Germany
[b] Department of Oral and Maxillofacial Surgery, University Medical Center Hamburg-Eppendorf, 20251 Hamburg, Germany
[c] Fibrothelium GmbH, Aachen, Germany
[d] Department of Plastic, Reconstructive and Aesthetic Surgery, University Hospital of Cologne, 50937 Cologne, Germany
[e] Department of Periodontics, Preventive and Restorative Dentistry, University Medical Center Hamburg-Eppendorf, 20251 Hamburg, Germany
[f] Department of Osteology and Biomechanics, University Medical Center Hamburg-Eppendorf, 20251 Hamburg, Germany
[g] Department of Vascular Medicine, University Heart Center, Translational Wound Research, University Medical Center Hamburg-Eppendorf, 20251 Hamburg, Germany

ARTICLE INFO

Keywords:
Oral wound healing
Antibacterial wound dressing
Silk protein
Silver
Gentamicin
Electrospinning

ABSTRACT

Oral wounds are among the most troublesome injuries which easily affect the patients' quality of life. To date, the development of functional antibacterial dressings for oral wound healing remains a challenge. In this regard, we investigated antibacterial silk protein-based membranes for the application as wound dressings in oral and maxillofacial surgery. The present study includes five variants of casted membranes, i.e., *i*) membranes-silver nanoparticles (CM-Ag), *ii*) membranes-gentamicin (CM-G), *iii*) membranes-control (without functionalization) (CM-C), *iv*) membranes-silk sericin control (CM-SSC), and *v*) membranes-silk fibroin/silk sericin (CM-SF/SS), and three variants of nonwovens, i.e., *i*) silver nanoparticles (NW-Ag), *ii*) gentamicin (NW-G), *iii*) control (without functionalization) (NW-C). The surface structure of the samples was visualized with scanning electron microscopy. In addition, antibacterial testing was accomplished using agar diffusion assay, colony forming unit (CFU) analysis, and qrt-PCR. Following antibacterial assays, biocompatibility was evaluated by cell proliferation assay (XTT), cytotoxicity assay (LDH), and live-dead assay on L929 mouse fibroblasts. Findings indicated significantly lower bacterial colony growth and DNA counts for CM-Ag with a reduction of bacterial counts by 3log levels (99.9% reduction) in CFU and qrt-PCR assay compared to untreated control membranes (CM-C and CM-SSC) and membranes functionalized with gentamicin (CM-G and NW-G) ($p < 0.001$). Similarly, NW-G yielded significantly lower DNA and colony growth counts compared to NW-Ag and NW-C ($p < 0.001$). In conclusion, CM-Ag represented 1log level better antibacterial activity compared to NW-G, whereas NW-G showed better cytocompatibility for L929 cells. As data suggest, these two membranes have the potential of application in the field of bacteria-free oral wound healing. However, provided that loading strategy and cytocompatibility are adjusted according to the antibacterial agents' characteristic and fabrication technique of the membranes.

* Corresponding author.
E-mail addresses: sog.schaefer@uke.de (S. Schäfer), r.smeets@uke.de (R. Smeets), marius.koepf@fibrothelium.com (M. Köpf), aleksander.drinic@fibrothelium.com (A. Drinic), alexander.kopp@fibrothelium.com (A. Kopp), p.hartjen@uke.de (P. Hartjen), a.assaf@uke.de (A.T. Assaf), t.beikler@uke.de (T. Beikler), u.peters@uke.de (U. Peters), i.fiedler@uke.de (I. Fiedler), b.busse@uke.de (B. Busse), e.stuermer@uke.de (E.K. Stürmer), t.vollkommer@uke.de (T. Vollkommer), m.gosau@uke.de (M. Gosau), s.fuest@uke.de (S. Fuest).

https://doi.org/10.1016/j.bioadv.2022.212740
Received 9 November 2021; Received in revised form 13 February 2022; Accepted 25 February 2022
Available online 17 March 2022

1. Introduction

Wound healing is a complex, highly orchestrated process that includes well-defined overlapping phases known as hemostasis, inflammation, proliferation, and remodeling [1]. Both intra-oral and extra-oral wound healing require an interplay of signaling molecules (e.g., cytokines and growth factors) from blood cells and local tissue cells working in concert to heal the injured site towards a restored barrier function [2].

Depending on the lesion site, wound healing within the oral cavity can be categorized as periodontal healing, dental implant interfaces healing, dental pulp healing, and bone healing [3]. The saliva-filled environment of the oral cavity provides various proteinaceous substances, such as growth factors (epidermal growth factor, vascular endothelial growth factor, and fibroblast growth factors) and histatins, accelerating the wound healing process. Oral wounds have an increased healing potential compared to skin wounds [4]. This is attributed to faster initiation of the inflammatory phase, lower levels of immune mediators, more bone marrow-derived cells, fast re-epithelialization, and rapid fibroblast proliferation [5]. Most importantly, due to favorable anatomical relations, the oral cavity has excellent access to steady blood flow.

Up to now, several approaches have been introduced to heal oral wounds [5–7]. The state-of-the-art in oral and maxillofacial surgery is the utilization of autologous mucocutaneous flaps for or allogenic/xenogeneic grafts, e.g., acellular dermal matrices (ADM), depending on the extent of the soft tissue defect. However, flaps are associated with donor site morbidity and unsatisfactory cosmetic outcomes, whereas ADMs have shown to induce inflammatory reactions, antigenicity, and, additionally, are limited in resources [8,9]. Generally, the healing process of wounds can be accelerated using biomedical engineered structures such as hydrocolloids, films, gauze, hydrogels, foams, and hydrofibers [10]. One of the best-known approaches for oral wound healing is the application of polymer-based membranes [11]. So far, various natural biomaterials have been introduced to promote the oral wound healing process, including collagen [12], alginates [13,14], chitosan [15], and gelatin [16]. Other natural biomaterials such as the silk proteins silk fibroin (SF) and silk sericin (SS) have gained increasing attention due to their remarkable mechanical properties, superior biocompatibility, oxygen, and water vapor permeability, controllable proteolytic degradability, and minimal immunogenicity [17]. Composed of fibroin (70–80%) and sericin (20–30%), the proteins are extracted from the cocoons of the silkworm *Bombyx mori* (*B. mori*) through different well described methods [18]. Silk proteins have shown to complement each phase of the wound healing process, hence, can be broadly used as wound dressings for acute and chronic wound healing [19]. SF interacts with blood components, e.g., platelets and fibrin, initiating the clotting cascade [20]. Additionally, SF and SS materials accelerate the initial inflammatory response, however, they do not prolong this phase. According to in vitro and in vivo studies, SF can significantly decrease the leucocyte count and overall inflammation, which is an advantageous feature in this process [21,22]. Moreover, SF and SS were able to accelerate the proliferation of a variety of human cells in vitro and in vivo, leading to defect site coverage with native tissue and neovascularization [19,20,23]. According to the applicational demand, silk protein-based substances can be manufactured into various forms (e.g., fibers, films, gels, and three-dimensional scaffolds). As an example, the successful utilization of silk proteins as substrates for electrospinning resulted in the fabrication of mechanically advanced membranes for the wound healing process [24]. To further promote biological host responses, prior to electrospinning, different signaling molecules such as growth factors and polypeptides can be incorporated into the silk protein solution [24–26].

Despite the recent progress in oral wound healing, there are some challenging points in the fabrication of membranes for oral wound healing. The oral mucosa is a warm and moist environment which creates an excellent microenvironment for the habitation of bacteria such as *Streptococcus mutans*, *Actinomyces naeslundii*, *Fusobacterium nucleatum* and *Porphyromonas gingivalis*, decreasing the efficacy of the wound healing process. To avoid bacterial growth at the wound site, different antibacterial agents can be incorporated into the wound dressing. Metallic nanoparticles such as silver, magnesium, zinc, or copper have been successfully used to fabricate skin wound dressings with antibacterial activity [27,28]. Silver nanoparticles (AgNPs) in particular are known to contain bacterial growth and display anti-inflammatory properties [29,30]. However, establishing a balance between the antibacterial activity and cytotoxicity potential of AgNPs should be precisely considered. In addition to metal ions, some antibiotics such as penicillins, aminoglycosides, or glycopeptides have been used to modify wound dressings [31,32]. Gentamicin, an aminoglycoside antibiotic, is broadly applied to treat bacterial skin and soft tissue infections [33–35]. A recent investigation by Zhou et al., proposed the idea of combining favorable effects of the two most common antibacterial functional agents AgNPs and gentamicin with an SF/Chitosan dental implant coating. With this approach, the authors could produce antibacterial implant coatings that significantly inhibited bacterial growth, adhesion, and biofilm formation with improved support of preosteoblastic MC3T3 cells and osteoblast growth [36]. Combining the excellent properties of silk materials with antibacterial agents presents an advanced approach in this matter.

In spite of experimental efforts in developing a functional wound dressing for the skin, the application of antibacterial loaded silk protein membranes for oral wound healing has not been evaluated so far. Hence, in this in vitro study, we investigated advanced antibacterial silk protein membranes. Using casting and electrospinning techniques, casted membranes (CM) and nonwovens (NW) had been functionalized with AgNPs and gentamicin prior to our investigation. The aim of this study was the evaluation of antibacterial membranes for wound healing applications in oral and maxillofacial surgery.

2. Materials and methods

2.1. Manufacture of SS/SF membranes

For the manufacture of the fibroin membranes, *B. mori* silk cocoons were used for protein extraction. The procedure was performed according to the PureSilk® technology of the company Fibrothelium GmbH. Briefly, fibroin was separated from sericin by degumming it in a hot alkali solution before dissolving it in a solvent system based on Ajisawa's reagent. The dissolved fibroin was dialyzed against VE water for 48 h. The initial concentration of the resulting fibroin solution was 3 wt%. The solution was then stored at 4 °C.

For the SS substrate, an SS solution was obtained by degumming *B. mori* silk cocoons with 8 M urea solution (1:44.414). The urea solution was heated to 80 °C with the cocons which were degummed for 3 h while being stirred with a magnetic stirrer. After 3 h the cocoons were transferred into a sieve and rinsed with deionized water. The cocoons are then soaked 3 times for 3 min to rinse out residual degumming solution. The SS-urea solution was transferred into dialysis membranes (MWCO 3.5 kDa) and dialyzed against water for 48 h while exchanging the water two times a day. Two structural types of materials based on SS were manufactured: casted membranes (CM) and nonwovens (NW).

For functionalization, three variations of SF-nonwovens (gentamicin, silver, and untreated fibroin controls) and five variations of SS and/or SF-membranes (gentamicin, silver, untreated fibroin controls, SF/SS, and untreated sericin controls) were manufactured (Table 1). First, the SF or SS solution was casted on a PTFE mold. After drying for 24 h at 21 °C under a laminar hood, the final fibroin membrane had a thickness of approximately 0.1–0.2 mm. The thickness was determined by a digital micrometer (Micromar 40 ER, Mahr GmbH, Germany).

For functionalization, the fibroin solution was priorly mixed with gentamicin or silver nitrate (AgNO3). For the $AgNO_3$-functionalized membranes, the mixed solution was UV irradiated for 1 h before casting. SF NWs were electrospun and directly afterwards post-treated in an

Table 1
Functionalization and sample size of SF and SS membranes.

Material (CM/NW)	Sample size/material (n)	Pre-treatment	Fibroin (3 w%)	Sericin (3 w%)	Gentamicin (10 mg/mL)	$AgNO_3$	Post-treatment	Abbreviation
NW	10	–	20 mL	–	–	–	Ethanol (70 v%)	NW-C
NW	10	–	20 mL	–	10 mL	–	Ethanol (70 v%)	NW-G
NW	10	UV irradiation	20 mL	–	–	0.1 g	Ethanol (70 v%)	NW-Ag
CM	10	–	20 mL	–	–	–	Ethanol (70 v%)	CM-SFC
CM	10	–	20 mL	–	10 mL	–	Ethanol (70 v%)	CM-G
CM	10	UV irradiation	20 mL	–	–	0.1 g	Ethanol (70 v%)	CM-Ag
CM	10	–	10 mL	10 mL	–	–	Ethanol (70 v%)	CM-SF/SS
CM	10	–	–	20 ml	–	–	Ethanol (70 v%)	CM-SSC

ethanol bath (70 v%) for 1 h to obtain insolubility. In a next step, the SF NWs were immersed in $AgNO_3$ solution or gentamicin for around 60 min. The $AgNO_3$ treated NWs samples were also UV irradiated.

Flexible SS films were obtained by adding glycerol to the SS solution. In this case the glycerol added, amounted to 30 wt% of the total mass of SS in a defined volume. The solution was then stirred for 5 min to ensure homogeneous mixture of glycerol. Subsequently the SS-glycerol solution was casted onto a PTFE mold and left to dry under a laminar hood at ambient temperature for 48 h. Finally, the dried films were treated with 70 v% ethanol before peeling them off the PTFE sheet. The films were then stored in press-seal bags at ambient temperature until further use.

Finally, all materials were stored in 70 v% ethanol at 4 °C. An overview of functionalization and sample size is given in Table 1.

2.2. Scanning electron microscopy

The surface morphology of the samples was analyzed utilizing scanning electron microscopy (SEM) (Crossbeam 340, Zeiss, Oberkochen, Germany). Prior to imaging, samples were dried under a laminar floor hood for 7 days. A clear cut was performed through the samples' midline with a scalpel for cross-sectional imaging. Samples were then affixed on a sample holder, and subsequently gold-sputtered to provide electron stability (sputter coater S150B, Edwards, London, UK). Imaging was performed in secondary electron (SE) mode at an acceleration voltage of 5 kV, working distance of 5 mm, and at magnifications ranging from 500× to 10.000×.

2.3. Cytocompatibility analysis

Cytocompatibility assessment was proceeded according to our former work [37].

2.3.1. Reference materials (toxic and non-toxic controls)

A polyurethane film containing 0.1% zinc diethyldithiocarbamate (ZDEC) (Hatano Research Institute, Kanagawa, Japan) was used as toxic control substance for all cytocompatibility assays. For the indirect assays, medium that was incubated in the absence of specimens was used as a non-toxic control. For the live-dead staining assay, tissue culture coverslips (TCC) (Sarstedt, Nümbrecht, Germany, Cat. No. 83.1840.002) were used as a non-toxic control material.

2.3.2. Cell culture

L929 mouse fibroblasts were obtained from the European Collection of Cell Culture, ECACC (Salisbury, UK). Cells were cultured in MEM supplemented with 10% fetal bovine serum, glutamine to final concentration of 4 mM and penicillin/streptomycin (100 U/mL each) (all from Life Technologies, Carlsbad, USA), in the following referred to as cell culture medium, at 37 °C, 5% CO_2 and 95% humidity (cell culture conditions). Cells were passaged when they reached approximately 80% confluency.

2.3.3. Extraction

The materials were washed three times for 30 min in 1 mL cell culture medium to remove the storage solution (70 v% ethanol) and to saturate the samples with medium. The materials were then extracted at a ratio of 3 cm^2/mL of cell culture medium for 72 h at 37 °C, 5% CO_2, and 95% humidity (cell culture conditions).

2.3.4. Indirect assay procedure

96-Well plates (Sarstedt, Nümbrecht, Germany) were seeded with 1×10^4 cells/well in 100 µL cell culture medium and incubated under cell culture conditions for 24 h. Thereafter, cell culture medium was discarded and 100 µL of extract was added to each well. Cells were further incubated for 24 h and then subjected to the XTT-assay, while the supernatants were subjected to the LDH-assay.

2.3.5. Viability assay

Cells incubated with the extracts were subjected to an XTT-assay. The "Cell Proliferation Kit II" (XTT) (Roche Diagnostics, Mannheim, Germany) was used according to the manufacturers' instructions. Briefly, the electron-coupling reagent was mixed with XTT labeling reagent (1:50 dilution) and 50 µL of the mixture was added to the cells. After 4 h of incubation under cell culture conditions, substrate conversion was quantified by measuring the absorbance of 100 µL aliquots in a new 96-well plate using a scanning multi-well spectrophotometer (Microplate Reader, Bio-Rad Laboratories, Inc., CA, USA) with filters for 450 nm and 650 nm (reference wavelength).

2.3.6. Cytotoxicity assay

Cytotoxicity was determined using a "LDH-Cytotoxicity Assay Kit II" (BioVision, Milpitas, CA, USA) according to the manufacturers' instructions. Briefly, 10 µL of the cell supernatants were incubated with 100 µL LDH reaction mix for 30 min at room temperature. After addition of stopping solution, absorbances were measured using a scanning multi-well spectrophotometer (Microplate Reader, Bio-Rad Laboratories, Inc., CA, USA) with filters for 450 nm and 650 nm (reference wavelength).

2.3.7. Live-dead staining assay

In order to perform live-dead cell staining on the surfaces of the membrane specimens, 60 µL per mL medium propidium iodide (PI) stock solution (50 µg/mL in PBS) and 500 µL per mL medium fresh fluorescein diacetate (FDA) working solution (20 µg/mL in PBS from 5 mg/mL FDA in acetone stock solution) were added to each well (12 well plate). After a brief incubation for 3 min at room temperature, specimens were rinsed in prewarmed PBS and immediately examined with an upright fluorescence microscope (Nikon ECLIPSE Ti-S/L100, Nikon GmbH, Düsseldorf, Germany) equipped with a filter for parallel detection of red and green fluorescence.

2.3.8. Data evaluation

The mean absorbance of the blank controls without cells was subtracted from the mean absorbances and data was normalized to the negative control.

2.4. Antibacterial activity

An overview of the antibacterial testing strategy is illustrated in

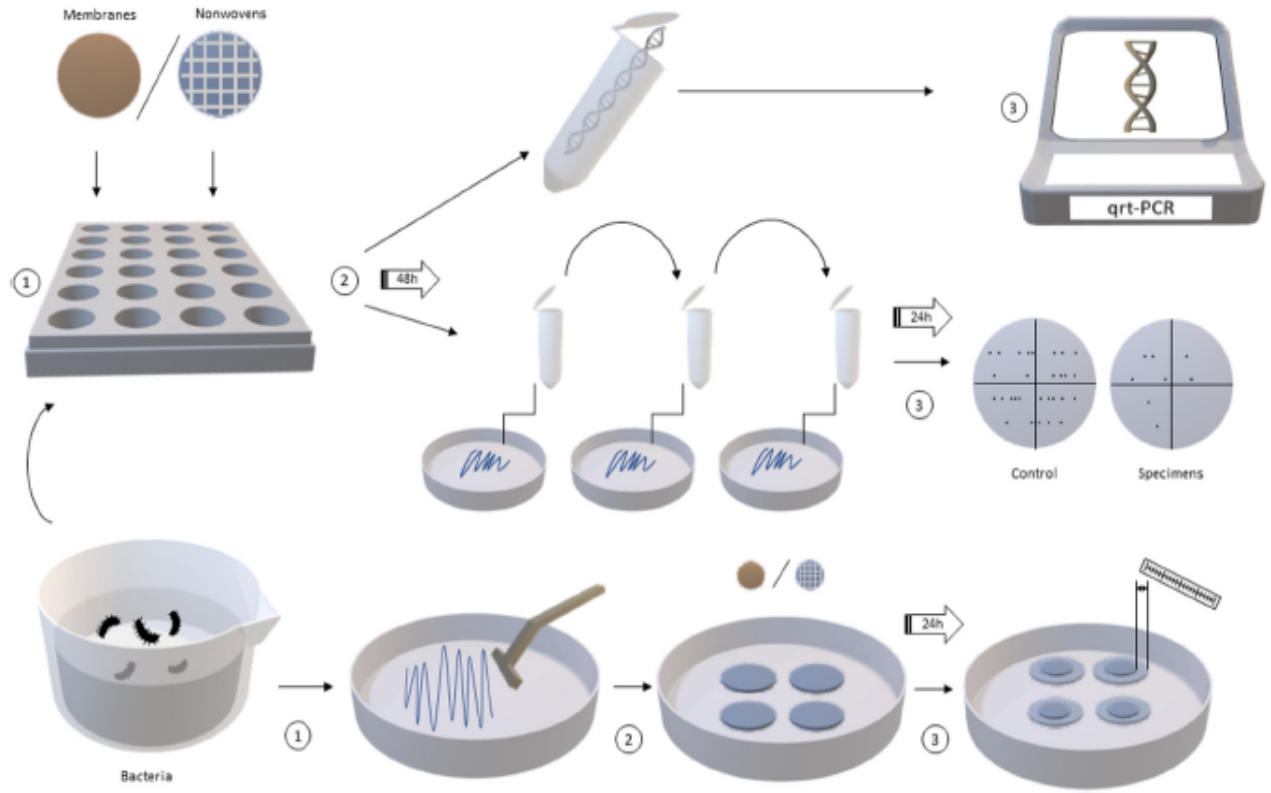

Fig. 1. Antibacterial testing strategy. Two structural forms of SF and SS materials, i.e., CMs and NWs were manufactured. 1. Materials were either placed in 24-well plates preincubated with bacterial mixed culture solution, or the materials were plated on blood agar plates previously incubated with bacterial mixed culture solution. 2. For the first test, an incubation time of 48 h, for the second test, an incubation time of 24 h was chosen. 3. Antibacterial activity was assessed through qrt-PCR, CFU analysis, and zone of inhibition (ZOI).

Fig. 1.

2.4.1. Antibacterial activity analysis of total and viable bacterial count

All specimens were stored in 70 v% ethanol (EtOH), consequently, specimens were considered sterile. A sample size of $n = 10$ specimens per structure (CM or NW) and functionalization, i. e., untreated SS/SF controls (CM-C, CM-SSC, NW-C), loaded with silver ions (CM-Ag, NW-Ag), and loaded with gentamicin (CM-G, NW-G), was incubated for 24 h in artificial saliva, which was comprised of a-amylase 1 mg/mL, mucin 0.85 mg/mL, and bovine serum albumin (BSA) 0.4 mg/mL.

Cultivation of bacterial strains and following treatment of the specimens was performed in anaerobic conditions at 37 °C in Whitley A35 Workstation (Whitley A35 Workstation Don Whitley Scientific, Bingley, United Kingdom).

In order to create a liquid bacterial mixed culture, anaerobic stains of early colonizing *Streptococcus mutans* (*Streptococcus mutans*, DSM 20523, German Collection of Microorganisms and Cell Cultures GmbH, Leibnitz, Germany), moderate colonizing *Actinomyces naeslundii* (*Actinomyces naeslundii*, DSM 17233, German Collection of Microorganisms and Cell Cultures GmbH, Leibnitz, Germany), *Fusobacterium nucleatum* (*Fusobacterium nucleatum*, DSM 15643, German Collection of Microorganisms and Cell Cultures GmbH, Leibnitz, Germany), and late colonizing *Porphyromonas gingivalis* (*Porphyromonas gingivalis*, DSM 20709, German Collection of Microorganisms and Cell Cultures GmbH, Leibnitz, Germany) were separately cultivated on blood agar plates. Subsequently, each strain was transferred into bacterial culture medium (CDC Anaerobe 5% Sheep Blood), and after sufficient observable growth (usually after 2–5 days), 1 mL of each strain was mixed into 20 mL CDC medium. Mixed bacterial culture optical density (OD) was 0.1.

Test membranes were placed onto 24-well plates. Each well was previously filled with 1.5 mL mixed bacterial culture suspension. After an incubation time of 48 h, membranes were separately moved into sterile 1.5 mL Eppendorf tubes, vortexed, and a total of 100 µL sample was taken from each Eppendorf tube for total and viable bacterial count analysis. Viable bacterial count was tested by inoculating blood agar plates with 50 µL sample in dilutions of 1:100, 1:1000, 1:10.000 and the Colony Forming Unit (CFU) was measured. Total bacterial DNA count was measured through Polymerase Chain Reaction (PCR) by processing 50 µL sample with DNA Isolation Kit (innuPREP DNA Isolation Kit, Analytik Jena AG, Jena, Germany) and quantifying the DNA amount with qrt-PCR (quantitative Real-Time-PCR, CFX96 Touch Real-Time PCR Detection System, Bio-Rad Laboratories, Berkeley, California, USA) utilizing a universal eubacterial 16S-rRNA primer (HDA1-GACTCCTACGGGAGGCAGCAGT, E1115RAGGGTTGCGCTCGTTGCGGG) and specific Primers (Table 2).

2.4.2. Direct antibacterial activity analysis

Direct antibacterial activity was evaluated in an agar diffusion test. For this purpose, five blood agar plates for each material and functionalization were inoculated with either mixed bacterial culture solution or isolated liquid culture of the bacterial strains, respectively. Two samples of each material and functionalization were directly taken from storage tubes, briefly drained, and placed on the agar plates. After an incubation time of 24 h, respective inhibition zones were measured with a micrometer screw gauge.

2.5. Data evaluation

For the cytocompatibility assays, the mean absorbance of the blank controls without cells was subtracted from the mean absorbances and

Table 2
Specific primer sequences for qrt-PCR and references of their applicability according to our former work [38].

Organism	Primer	Primer sequence	Reference of primer applicability
Porphyromonas gingivalis	CA-PG-F/R	AGGCAGCTTGCCATACTGCG ACTGTTAGCAACTACCGATGT	Carrouel F. et al., 2016 [39].
Streptococcus mutans	MKD-FV/RV	GGCACCACAACATTGGGAAGCTCAG GGAATGGCCGCTAAGTCAACAGG	Hoshino T. et al., 2004 [40].
Actinomyces species	ACT-174-F ACT-281-R	GGTCTCTGGGCCGTTACTGA GRCCCCCCACACCTAGTG	Ellerbrock B., 2010 [UKD].
Fusobacterium nucleatum	CA-FN-F/R	AGAGTTTGATCCTGGCTCAG GTCATCGTGCACACAGAATTGCTG	Carrouel F. et al., 2016 [39].

data was normalized to the negative control. Statistical analysis of the antibacterial tests was conducted using SAS 7.4 (SAS Institute Inc., Cary, North Carolina, USA). Mean bacterial DNA counts from qrt-PCR measurement and CFU analysis values were evaluated. For the qrt-PCR and CFU analysis results an exponential-linear model was chosen. *P*-values < 0.05 were considered statistically significant.

3. Results

3.1. Structural analysis

Fibroin nonwovens comprised a highly porous structure, created through highly intertwining fibers compared to the smooth surface of the SF and SS casted membranes. Cross-sectional imaging shows upheld continuity of fiber connections within the whole thickness of the NWs. Some CMs present a layered appearance in cross-section, presumably cutting artifacts.

The CM-C and CM-SSC present a rough topography distinguishable from gentamicin and silver CMs. Conversely, NW-C appear to have a smooth fiber surface texture, whereas the NW-Ag appear to present a more uneven fiber surface texture within 10,000× magnification imaging (Fig. 2).

3.2. Cytocompatibility

With the exception of the silver loaded materials (CM-Ag, NW-Ag), all membranes had sufficient cytocompatibility with viability values >70% of the negative control in the indirect assay which indicates the non-toxic range as defined in in current, international standards (DIN EN ISO 10993-5:2009, German Institute for Standardization, Berlin, Germany) (Fig. 3). The viability was similar (range 91%–108% of the negative control) for all materials except for the silver loaded specimens (4% of the negative control) ($p < 0.001$). Cytotoxicity values for all specimens were consistent – showing a similar range as the negative control (cells incubated with cell culture medium) for all materials except for the silver specimens, indicating low cytotoxicity (Fig. 4). Notably, silver specimens yielded negative values in the LDH assay, thus, silver ions were suspected to interfere with the assay. Therefore, assay interference testing was conducted. For this purpose, the LDH-assay was repeated with the material extracts omitting cells, resulting in negative extinction values for the silver loaded materials (data not shown). Additionally, the silver loaded materials were extracted together with the toxic control (RM-A) and the LDH-assay was repeated again, resulting in an apparent RM-A toxicity that was decreased by the

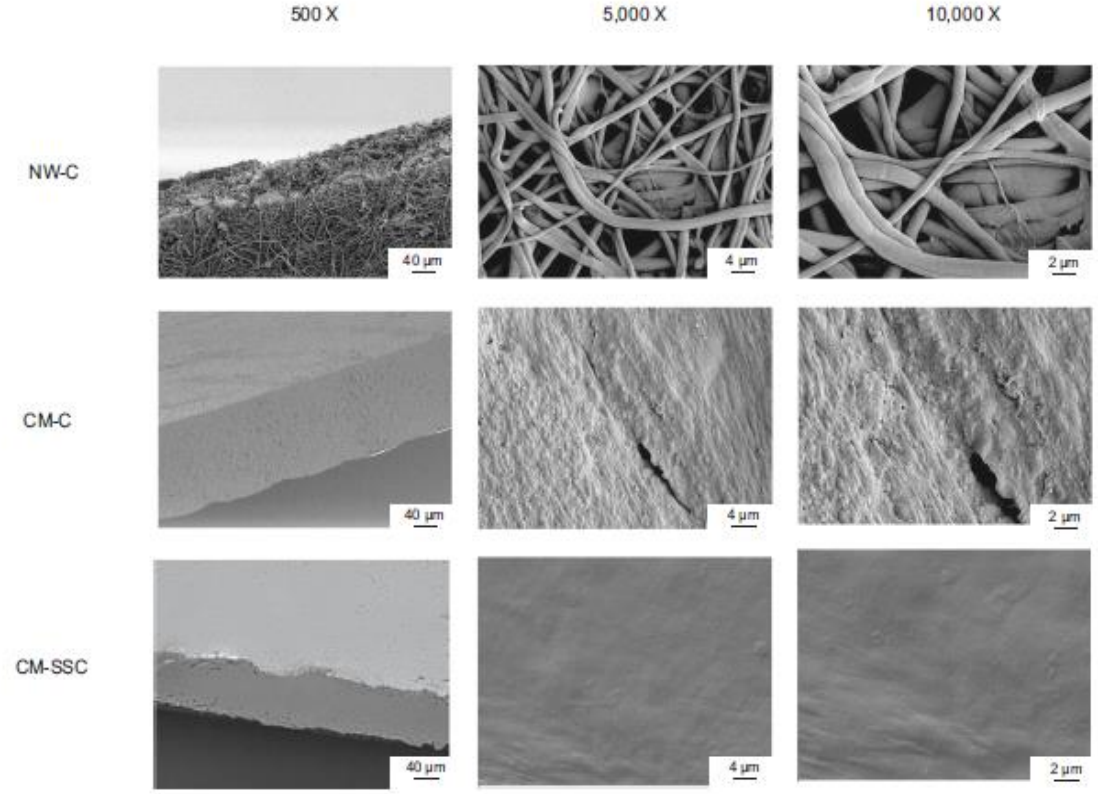

Fig. 2. SEM imaging of SF and SS materials with three magnifications (500×, 5000×, and 10,000×). Depicted are control CMs and NWs. Imaging of the other specimens (NW-G, NW-Ag, CM-G, CM-Ag, CM-SF-SS) can be found in the Supplementary data.

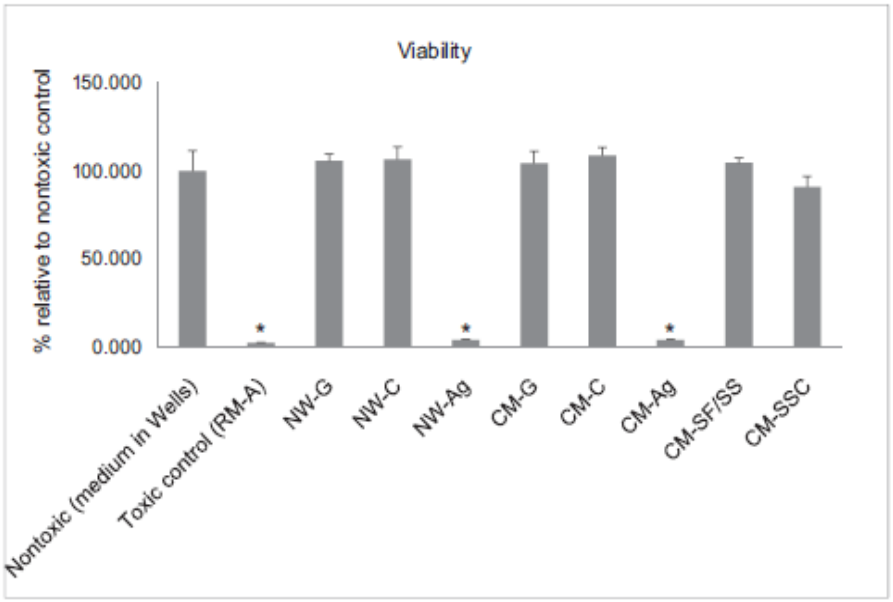

Fig. 3. Viability of L929 fibroblasts after extract application of SF and SS materials with/without active agents: gentamicin, silver, combined SF/SS, and control casted membranes (CM-G, CM-Ag, CM-SF/SS, CM-C, CM-SSC) and gentamicin, silver, and control NWs (NW-G, NW-Ag, NW-C); $n = 10$/group. Abbreviations according to Table 1. Data are expressed as MV + STD; *$p > 0.05$ compared to nontoxic control.

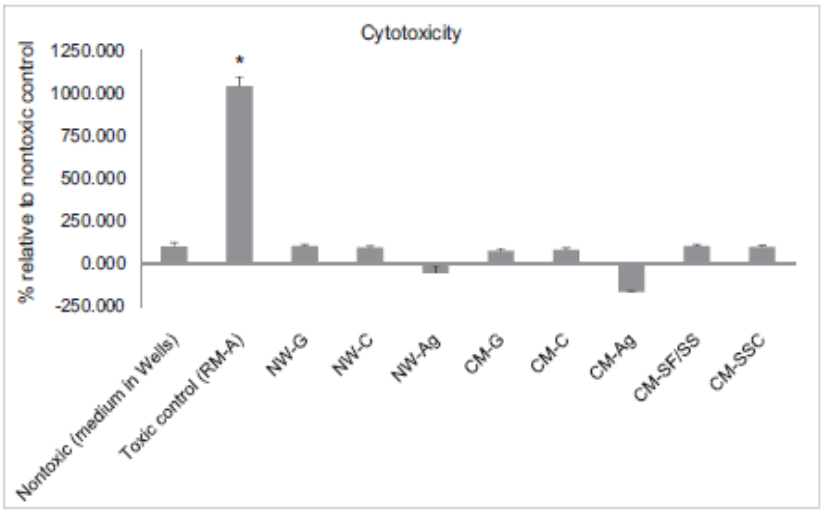

Fig. 4. Cytotoxicity assay with L929 fibroblasts after extract application of SF and SS materials with/without active agents: gentamicin, silver, combined SF/SS, and control casted membranes (CM-G, CM-Ag, CM-SF/SS, CM-C, CM-SSC) and gentamicin, silver, and control nonwovens (NW-G, NW-Ag, NW-C); $n = 10$/group. Abbreviations according to Table 1. Data are expressed as MV + STD; *$p > 0.05$ compared to nontoxic control.

same magnitude as the materials were suspected to interfere with the assay (not shown), strongly suggesting assay interference by the silver ions and thus false negative cytotoxicity values for the silver loaded materials.

Live-dead staining revealed large numbers of green fluorescein diacetate (FDA) positive vital cells with only sporadic red propidium iodide (PI) positive dead cells visible on all materials except for the silver loaded specimens which were covered with much fewer cells indicating weak attachment and/or cytotoxicity (Fig. 5). On all materials, with the exception of the silver loaded specimens, at least some spindle shaped cells, with fibroblast characteristic morphology were detected. The cells on the silver loaded specimens were rounded, suggesting weak attachment or cytotoxicity. The assessment of NW-Ag and NW-C was limited because these materials underwent a deformation process upon hydration after contact with the cell culture suspension. Overall, these results indicate that all materials except for the silver loaded specimens are cytocompatible.

3.3. Antibacterial activity

3.3.1. Viable bacterial count

CFU analysis showed significantly lowest colony growth for CM-Ag ($p < 0.0001$) compared to all other groups followed by CM-G and NW-G ($p < 0.02$) (Fig. 6). CM-Ag decreased bacterial DNA count by 3 log-reductions compared to the positive control (bacterial mixed culture solution), implying a reduction of 99.9%. No significant difference could

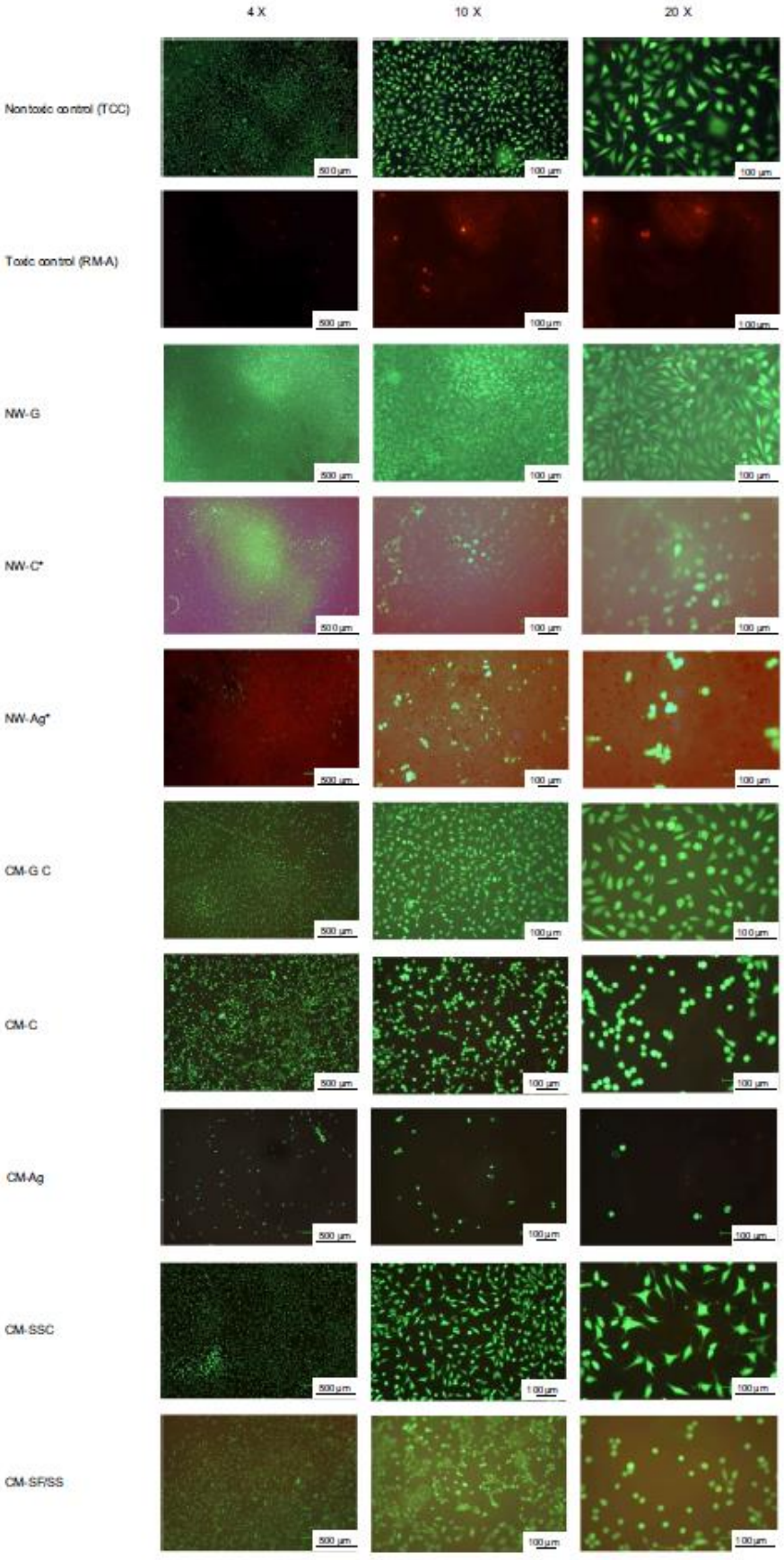

Fig. 5. Live-dead staining assay with L929 fibroblasts seeded on membranes with/without active agents: gentamicin, silver, combined fibroin-sericin, and control casted membranes (CM-G, CM-Ag, CM-SF/SS, CM-C, CM-SSC) and gentamicin, silver, and control nonwovens (NW-G, NW-Ag, NW-C); $n = 10$/group. Abbreviations according to Table 1.

*Specimens underwent a deformation process upon hydration after contact with the cell culture suspension impeding accurate imaging.

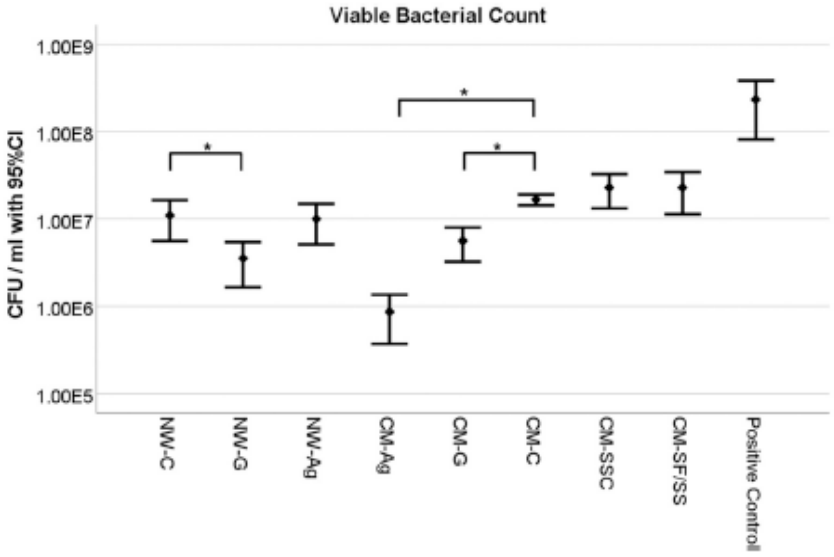

Fig. 6. Colony Forming Unit/mL of SF and SS materials after 48 h of specimen incubation on plated mixed bacterial culture solution. Mean values with 95% confidence interval are given in logarithmic scale unit. Results indicate viable bacterial count. n = 10/group. All groups were compared to each other (Section 3.3.1). For clarity, the parentheses indicate the results for the loaded nonwoven materials compared to the nonloaded nonwoven control (NW-C) and the results for the loaded membrane materials compared to the nonloaded casted membrane control (CM-C), $*p > 0.05$.

be detected between CM-G and NW-G. NW-Ag showed similar CFU values as the control NW-C ($p = 0.7$). CM-SF/SS and the controls CM-SSC and CM-C showed CFU-values of similar range with $p = 0.9$ and $p = 0.6$, respectively. All tested materials had significantly lower CFU values compared to the positive control (bacterial mixed culture solution) ($p < 0.0001$). In a sum, bacterial viability was inhibited in the following order from best to least effectivity: CM-Ag, NW-G, CM-G, NW-Ag, NW-C, CM-C, CM-SSC, and CM-SF/SS.

3.3.2. Total bacterial count

As presented in Fig. 7, all tested membranes had significantly lower bacterial DNA counts compared to the positive control ($p < 0.0001$) with the lowest DNA count for CM-Ag among all comparison groups ($p < 0.0001$). CM-Ag decreased bacterial DNA count by 3 log-reductions compared to the positive control implying a reduction of 99.9%. Consistent with CFU results, no statistical difference was found between the CMs-G and NW-G ($p = 0.1$). Notably different to CFU results, NW-Ag had significantly lower bacterial DNA copies compared to the control NW-C ($p < 0.005$), indicating a containment of total bacterial counts. According to the measurement with specific primers (data not shown), positive deflections of the PCR analysis in all membranes presented *S. mutans* and *F. nucleatum* as most prevalent bacterial colonies followed by small amounts of *P. gingivalis* and *A. neaslundii*. No significant intergroup differences were present. In a sum, total bacterial count was inhibited from best to least in the following order: CM-Ag, NW-G, CM-G, NW-Ag, NW-C, CM-C, CM-SSC, and CM-SF/SS.

3.3.3. Direct antibacterial activity

For both material types, casted membranes and nonwovens, the largest inhibition zone of 7–8 mm was found for gentamicin loaded samples (CM-G, NW-G) and the second largest inhibition zone of 2–3 mm was found for silver loaded samples (CM-Ag, NW-Ag). No inhibition zone was detected for the untreated controls (CM-C, CM-SSC, NW-C) (Fig. 8). Accordingly, the combined SF/SS membranes yielded no zone of inhibition, either. With the specialized agar diffusion test it could be shown that gentamicin loaded membranes show an antibacterial activity against strains of *A. neaslundii*, *F. nucleatum*, and *S. mutans*, in descending order, whereas silver loaded membranes present

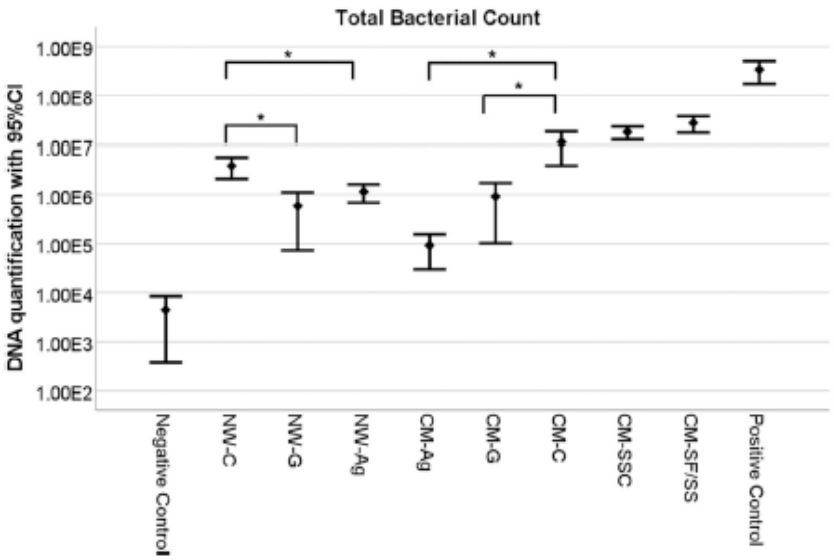

Fig. 7. Quantification of mean bacterial DNA copies measured by qrt-PCR (Universal Poly-Primer results) after 48 h for SF and SS membranes. Mean values with 95% confidence interval are given in logarithmic scale unit. qrt-PCR results indicate total bacterial count. $n = 10$/group. All groups were compared to each other (Section 3.3.2). For clarity, the parentheses indicate the results for the loaded nonwoven materials compared to the nonloaded nonwoven control (NW-C) and the results for the loaded membrane materials compared to the nonloaded casted membrane control (CM-C), $*p > 0.05$.

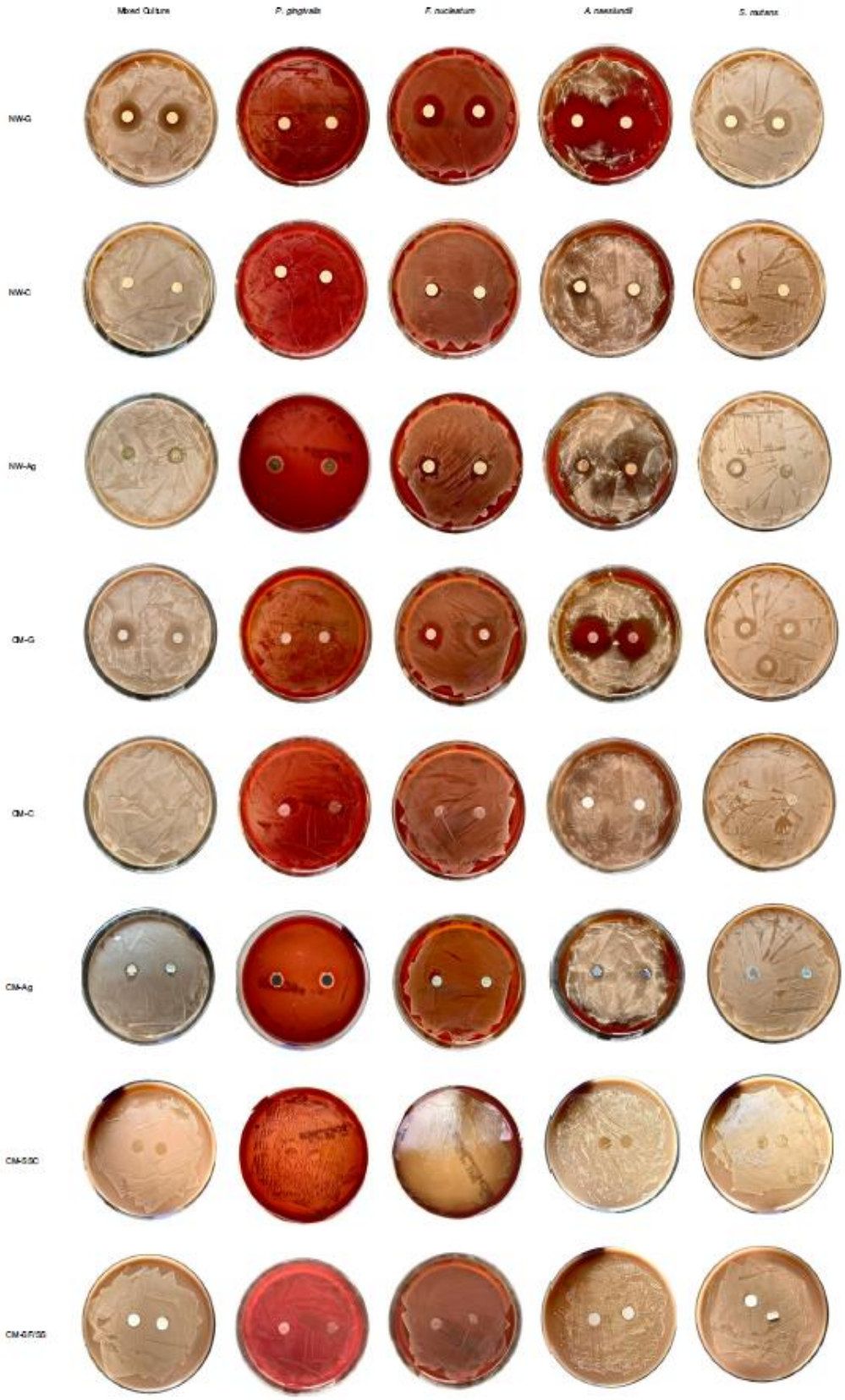

Fig. 8. Direct antibacterial activity assessment of SP and SS materials with agar diffusion test on bacterial mixed culture solution and selective bacterial strain solutions, respective zone of inhibition was measured with a micrometer after 24 h of incubation. n = 10/group.

antibacterial activity against *P. gingivalis* and *A. neaslundii* only. The CM-SF/SS and control membranes presented no inhibition zone, however, all test specimens prevented bacterial growth beneath the placement site.

In sum, the most pronounced direct antibacterial activity within all tested materials can be assigned to gentamicin loaded membranes followed by silver membranes.

4. Discussion

The healing of oral and maxillofacial wounds is a particularly challenging research area in the field of nanobiotechnology and tissue engineering. This importance can be attributed to specific features of the oral cavity [3], where a balance between pathogenic and commensal bacteria is needed to establish a state of homeostasis within the oral cavity [41]. Thus, a slight imbalance can lead to the development of caries, periodontitis, mucositis, and, eventually, to soft and hard tissue damage [42]. To avoid such impairments, the development of biomaterials able to inhibit the growth of pathogenic bacteria and, concurrently, to promote the wound healing process is needed [43]. In this context, the aim of this in vitro study was the characterization of antibacterial silk protein-based CMs and NWs for wound healing applications in oral and maxillofacial surgery and the implementation as wound coverages in plastic and reconstructive surgery.

The selection of a versatile biocompatible material is one of the most challenging points in the field of wound healing in oral and maxillofacial surgery due to the delicacy and sensitivity of the targeted tissue. So far, collagen, a promising biopolymer, has been broadly used to fabricate biodegradable wound dressing materials for surgical defects of the oral mucosa. For instance, in a clinical study by Rastogi et al., purified bovine collagen was employed to fabricate membranes for the treatment of secondary defects of the oral mucosa in 60 adult patients [44]. These defects appeared after excision of premalignant lesions and other conditions, such as incisional biopsy wounds. After using these membranes, the desirable levels of hemostasis, epithelialization and granulation were observed at the lesion sites. Accordingly, it was suggested that collagen membranes can be biologically acceptable wound graft materials for the oral mucosa. In another similar clinical studies, Omura et al., manufactured a bilayer membrane composed of silicone as the outer side, and dehydro-thermally cross-linked composites of collagen sponge as inner side [45]. Then, they put these membranes on oral mucosal defects in five patients after the surgery for cancers including Pleomorphic adenoma, Squamous cell carcinoma and Leukoplakia. It was observed that after 4–5 weeks, the collagen membrane formed a connective tissue after the migration of epithelial cells that made the repair effective. However, apart from the benefits, applying collagen as the membrane for wound healing has some challenging points. For instance, due to extraction from natural sources, collagen may cause immunogenicity. In addition, it may be subjected to gradual destruction during collagenolysis and inflammatory reactions. This procedure leads to weakening of the collagen membrane and mechanical instability of the graft within the oral cavity which may cause inconveniencies for the patients. Therefore, some research groups preferred to use other substitutes such as phospholipid [46], chitosan [47], polylactic galactic acid/polycaprolactone (PLGA/PCL) [48], carboxyvinyl polymer [49], hydrochloride gel [50], fibrin [51] etc., for the fabrication of membranes intended to heal mucosal wounds in the oral cavity. Focusing on the unique properties of silk proteins, we investigated the applicability of SF and SS membranes for intra-oral wound healing and thoroughly investigated nonwovens as well as casted membranes with respect to their antibacterial properties. It is well proved that silk nano-fibrous structures represent superior attachment and proliferation of fibroblast and keratinocytes, thus, improving the healing process of wounds in mucosal tissues [52,53]. Correspondingly, Tang et al. investigated the wound healing ability of electrospun SF matrices on buccal mucosa in rat models [54]. They concluded SF electrospun matrices promote the healing process and improve an anti-inflammatory host response. Also, they suggested that their developed mates can be a good substitute for ADMs. Similar results were reported in an in vivo study by Ge et al. in which SF scaffolds were applied on buccal defects in rat models [55]. For the application in wound healing, a vicinity of cells of the damaged tissue needs to be addressed and adequate biocompatibility is inevitable. In several studies, the good biocompatibility of silk-based scaffolds has been investigated [56,57]. In this experiment, we performed XTT, LDH, and *live/dead staining* assay on L929 mouse fibroblasts. The results of the XTT and LDH assay demonstrate sufficient cytocompatibility for all gentamicin-modified membranes. These findings illustrated a safe, tolerable usage dose of 10 mg/mL gentamicin for L929 mouse fibroblasts. Similar outcomes were obtained by Stevanović and colleagues [58], demonstrating well tolerable concentrations of gentamicin below 50 mg/mL on L929 cells. In contrast to this, CMs and NWs containing AgNPs decreased the L929 cell line in XTT assay and demonstrated cytotoxicity in LDH assay as well as in live/dead assay. According to our observations, we concluded that high concentrations of AgNPs corresponded with higher cytotoxicity, which was the case at 100 mg/L in this study. It is suggested that the cell toxicity of AgNPs and silver ions results from triggering oxidative stress in cells [59]. Indeed, AgNPs generate a high level of intracellular reactive oxygen species (ROS) and negatively affect the activity of antioxidant enzymes. These events disrupt normal cell function and cause disintegration of the cell membrane inducing apoptotic signaling pathways in cells [60]. Moreover, AgNPs can bind to functional groups of cell proteins and subsequently, trigger physicochemical interactions within cells [61]. Most studies report a safe, non-cytotoxic application of AgNPs at concentrations of $\leq$25 mg/L [62,63]. AgNP cytotoxicity might vary with the size of the nanoparticles in an inversely proportional fashion, yielding decreased cytotoxicity with bigger particle size due to lower surface area to volume ratio [64–67].

In this investigation, the main goal for the fabricated membranes with AgNPs and gentamicin was to induce antibacterial properties in these structures. The use of silver as an antibacterial substance in regenerative medicine has been investigated for decades [68,69]. The mode of antibacterial action of silver was found to be through membrane permeability disruption which results in the loss of intracellular K^+ ions, ATP and phospholipids. In addition, AgNPs cause oxidative damage by producing reactive oxygen species (ROS) and subsequently leaking intracellular metabolites through permeabilized membranes [70]. On the other hand, the aminoglycoside antibiotic, gentamicin, has a mechanism of action based on an oxygen-dependent entry into the bacterial cell and stasis of bacterial protein synthesis by binding to 30S ribosomal subunit [71]. These processes in turn lead to protein mistranslation and disintegration of the cytoplasmic membrane [72].

To assess the antibacterial potential of AgNPs and gentamicin loaded membranes, we performed a qrt-PCR, CFU assay, and agar diffusion tests. According to the review of Curtis et al., the gram-positive, facultative anaerobe, early colonizers *A. neaslundii* and *S. mutans* are the most prevalent bacteria within a healthy oral microbiota, thus, these strains were included in our investigation [60]. Furthermore, two anaerobe, gram-negative bacterial species were included: *F. nucleatum*, the second most prevalent intraoral microbe in health, and the periodontitis associated bacterial species *P. gingivalis* [73]. The utilization of artificial saliva provided optimal growth conditions for the bacteria with high similarity to natural clinical conditions of the oral cavity. The best antibacterial activity was observed for CM-Ag; consistently, the qrt-PCR results reflect the lowest bacterial DNA count for CM-Ag compared to all other material groups, indicating a reduced bacterial adhesion potential by 3log-steps compared to the control membranes (CM-C, CM-SSC, and NW-C). Similar results on sufficient antibacterial activity are reported by Dhas et al., showing Ag-loaded SF fibers with >90% inhibition against common skin infection associated with *P. aeruginosa* and *S. aureus* as well as ZOI results of >2 mm [74]. In another study, SS-based AgNP loaded films yielded ZOIs of >10 mm and markedly decreased colony

growth of *E. coli* and *S. aureus* compared to the non-functionalized controls [75]. Within the NWs group, the best antibacterial activity was shown in gentamicin-treated ones regarding viable and total bacterial count with a 2log-reduction in both categories (i.e., 99% reduction), and direct antibacterial activity with a ZOI of 7–8 mm. A possible explanation for the disparity between CM and NW findings lies within the manufacturing process of the SF and SS membranes. To functionalize CMs, aqueous AgNO3 or gentamicin were incorporated into the silk solution before the casting procedure. In contrast, for the modification of NWs, the active agents were incorporated into membranes after the electrospinning process. Another possible justification for the reduction in antibacterial activity can be the washing-out and/or interaction of silver ions (Ag ions) with components of the artificial saliva (e.g., BSA), culturing media (e.g., Hemin, Cysteine, Pepsin, etc.), or the PBS which used in the testing process. Ando et al. ascribed the compromise of the antibacterial activity of silver to components of the culturing media which contained fetal bovine serum (FBS) [76]. A main component of FBS is bovine serum albumin which was included in the artificial saliva of our tests (Section 2.4.1). On the other hand, gentamicin activity is shown to increase with the interaction of blood components (e.g., those included in CDC media), conforming with our results [76–78]. In many cases, the antibiotics entrapment can be affected by the internal conformation of polymer chains. In a study by Hassani Besheli et al. it was indicated that the loading of antibiotics can be enhanced by increasing the content of silk II (higher ß-sheet content) of matrices. Moreover, they proved that pH variations impact release kinetics of antibiotics from SF materials [79].

Some studies attribute an inherent bactericidal activity to the silk proteins fibroin and SS. For example, Bakhsheshi-Rad et al. found a ZOI of 3–3.5 mm for SS dressings on *E. coli* and *S. aureus* [80]. Other authors proved a positive correlation between colony growth inhibition and SS concentration [81]. SS mechanism of antibacterial action is supposed to be through membrane ballooning and bleb formation, which is a known mechanism for other antimicrobial peptides [82]. The inherent antibacterial property of SF is mainly reported as a result of its' barrier function as a wound dressing [83]. Additionally, SF has been associated with residual antimicrobial peptides (e.g., seroins) from the silk cocoons, which are natural protections of the silkworm against external pathogens [84]. Therefore, in this study, we assessed the possibility of an inherent antibacterial activity of the pristine silk proteins fibroin and sericin. Our results showed no antibacterial activity, neither with the SF and SS control membranes nor with the combined SF/SS membranes; however, they acted as a suitable mechanical barrier shown in the agar diffusion assay.

Our investigation has met different challenging points and limitations. In this study, we stored the samples in ethanol 70 v% solution and extracted them for an agar diffusion test. However, because of the antibacterial potency of the storage solution, we expected to have additional antibacterial effects and, subsequently, false-positive results. In order to eliminate errors associated with the storage conditions, we performed a simultaneous confirmatory test with a washing step in PBS before plating the samples onto the agar plate, which yielded similar results. Moreover, despite the oxygen dependent action of gentamicin, an anaerobic setting was necessary for proper bacterial colonization.

To sum up briefly, the investigated antibacterial silk protein-based membranes are promising substrates for wound healing applications in the field of oral and maxillofacial surgery. Future studies should be accomplished to further understand application specific material functionalization.

5. Conclusion

Silk proteins offer favorable characteristics that can be tailored to casted membranes or electro-spun nonwovens for the application as adherent/non-adherent wound dressings. The potential to alleviate infections can be realized through functionalization with antibacterial substances such as silver or gentamicin. The antibacterial activity of silver and silver loaded biomaterials has been described in literature thoroughly. In this study, we proved the antimicrobial effects of AgNPs and the aminoglycoside antibiotic gentamicin which was incorporated in silk protein membranes. Both functionalization methods proved containment of bacterial DNA count and colony growth of the common oral microbes *F. nucleatum*, *P. gingivalis*, *A. neaslundii*, and *S. mutans*. Prospective investigations should target on application specific material functionalization and understanding of in vivo effectivity in a suitable animal model.

Supplementary data to this article can be found online at https://doi.org/10.1016/j.bioadv.2022.212740.

CRediT authorship contribution statement

Schäfer S: bacterial analysis; design and planning of experiments; data collection; data analysis and interpretation of results; drafted the manuscript.

Smeets R: interpretation and critical revision; approval of the article.

Köpf M: idea and concept of the study; design and planning of experiments; interpretation of results; critical revision and approval of the article.

Drinic A: development of fabrication and functionalization methods for silk protein membranes as well as sample production; critical revision and approval of the article.

Kopp A: critical revision and approval of the article.

Kröger N: critical revision and approval of the article.

Hartjen P: cytocompatibility analysis; critical revision and approval of the article.

Assaf AT: interpretation; critical revision and approval of the article.

Aavani F: interpretation; critical revision and approval of the article.

Beikler T: critical revision and approval of the article.

Peters U: data collection, data analysis/interpretation.

Fiedler I: SEM analysis; data collection, critical revision and approval of the article.

Busse B: SEM analysis; data collection.

Stürmer EK: critical revision and approval of the article.

Vollkommer T: critical revision and approval of the article.

Gosau M: interpretation and critical revision; approval of the article.

Fuest S: interpretation; critical revision of the manuscript; approval of the article.

Declaration of competing interest

The authors declare that they have no conflict of interest to report.

Acknowledgements

The authors gratefully acknowledge Frank Fischer for his technical assistance culturing the bacterial strains, Thomas Derra for the graphical illustration of the antibacterial testing methods, and Eric Bibiza Freiwald for his assistance in the statistical data analysis.

References

[1] G. Broughton II, J.E. Janis, C.E. Attinger, The basic science of wound healing, Plast. Reconstr. Surg. 117 (7 Suppl) (2006) 12s–34s.
[2] G. Han, R. Ceilley, Chronic wound healing: a review of current management and treatments, Adv. Ther. 34 (3) (2017) 599–610.
[3] C. Politis, J. Schoenaers, R. Jacobs, J.O. Agbaje, Wound healing problems in the mouth, Front. Physiol. 7 (507) (2016).
[4] M. Waasdorp, B.P. Krom, F.J. Bikker, P.P. van Zuijlen, F.B. Niessen, S. Gibbs, The bigger picture: why oral mucosa heals better than skin, Biomolecules 11 (8) (2021) 1165.
[5] N. Funato, K. Moriyama, Y. Baba, T. Kuroda, Evidence for apoptosis induction in myofibroblasts during palatal mucoperiosteal repair, J. Dent. Res. 78 (9) (1999) 1511–1517.
[6] E.A. Yücel, O. Oral, V. Olgaç, C.K. Oral, Effects of fibrin glue on wound healing in oral cavity, J. Dent. 31 (8) (2003) 569–575.

[7] N.A.M. Barakat, M.A. Kanjwal, F.A. Sheikh, H.Y. Kim, Spider-net within the N6, PVA and PU electrospun nanofiber mats using salt addition: novel strategy in the electrospinning process, Polymer 50 (18) (2009) 4389–4396.
[8] R. Rauso, G.F. Nicoletti, E. Sesenna, C. Lo Faro, F. Chirico, R. Fragola, et al., Superficial temporal artery perforator flap: indications, surgical outcomes, and donor site morbidity, Dent. J. 8 (4) (2020) 117.
[9] F. Momen-Heravi, S.M. Peters, L. Garfinkle, P. Kang, Acellular dermal matrix as a barrier for guided bone regeneration of dehiscence defects around dental implants: a clinical and histological report, Implant. Dent. 27 (4) (2018) 521–524.
[10] K.C. Broussard, J.G. Powers, Wound dressings: selecting the most appropriate type, Am. J. Clin. Dermatol. 14 (6) (2013) 449–459.
[11] S. Alven, X. Nqoro, B.A. Aderibigbe, Polymer-based materials loaded with curcumin for wound healing applications, Polymers 12 (10) (2020) 2286.
[12] M. Rinastiti, Harijadi, A.L. Santoso, W. Sosroseno, Histological evaluation of rabbit gingival wound healing transplanted with human amniotic membrane, Int. J. Oral Maxillofac. Surg. 35 (3) (2006) 247–251.
[13] K. Ishikawa, Y. Ueyama, T. Mano, T. Koyama, K. Suzuki, T. Matsumura, Self-setting barrier membrane for guided tissue regeneration method: initial evaluation of alginate membrane made with sodium alginate and calcium chloride aqueous solutions, J. Biomed. Mater. Res. 47 (2) (1999) 111–115.
[14] Y. Ueyama, K. Ishikawa, T. Mano, T. Koyama, H. Nagatsuka, K. Suzuki, et al., Usefulness as guided bone regeneration membrane of the alginate membrane, Biomaterials 23 (9) (2002) 2027–2033.
[15] C. Xu, C. Lei, L. Meng, C. Wang, Y. Song, Chitosan as a barrier membrane material in periodontal tissue regeneration, J Biomed Mater Res B Appl Biomater 100 (5) (2012) 1435–1443.
[16] S. Zhang, Y. Huang, X. Yang, F. Mei, Q. Ma, G. Chen, et al., Gelatin nanofibrous membrane fabricated by electrospinning of aqueous gelatin solution for guided tissue regeneration, J. Biomed. Mater. Res. A 90 (3) (2009) 671–679.
[17] C. Holland, K. Numata, J. Rnjak-Kovacina, F.P. Seib, The biomedical use of silk: past, present, future, Adv. Healthc. Mater. 8 (1) (2019) 1800465.
[18] C. Sobajo, F. Behzad, X.F. Yuan, A. Bayat, Silk: a potential medium for tissue engineering, Eplasty 8 (2008), e47.
[19] P.P. Patil, M.R. Reagan, R.A. Bohara, Silk fibroin and silk-based biomaterial derivatives for ideal wound dressings, Int. J. Biol. Macromol. 164 (2020) 4613–4627.
[20] D. Chouhan, B.B. Mandal, Silk biomaterials in wound healing and skin regeneration therapeutics: from bench to bedside, Acta Biomater. 103 (2020) 24–51.
[21] M. Yonesi, M. Garcia-Nieto, G.V. Guinea, F. Panetsos, J. Pérez-Rigueiro, D. González-Nieto, Silk Fibroin: An Ancient Material for Repairing the Injured Nervous System, Pharmaceutics. 13 (3) (2021) 429, https://doi.org/10.3390/pharmaceutics13030429.
[22] M. Santin, A. Motta, G. Freddi, M. Cannas, In vitro evaluation of the inflammatory potential of the silk fibroin, J. Biomed. Mater. Res. 46 (3) (1999) 382–389.
[23] S. Napavichayanun, P. Aramwit, Effect of animal products and extracts on wound healing promotion in topical applications: a review, J. Biomater. Sci. Polym. Ed. 28 (8) (2017) 703–729.
[24] S.P. Miguel, D. Simões, A.F. Moreira, R.S. Sequeira, I.J. Correia, Production and characterization of electrospun silk fibroin based asymmetric membranes for wound dressing applications, Int. J. Biol. Macromol. 121 (2019) 524–535.
[25] M. Bienert, M. Hoss, M. Bartneck, S. Weinandy, M. Böbel, S. Jockenhövel, et al., Growth factor-functionalized silk membranes support wound healing in vitro, Biomed. Mater. 12 (4) (2017), 045023.
[26] Y. Zhang, L. Lu, Y. Chen, J. Wang, Y. Chen, C. Mao, et al., Polydopamine modification of silk fibroin membranes significantly promotes their wound healing effect, Biomaterials Science. 7 (12) (2019) 5232–5237.
[27] A. Oliveira, S. Simões, A. Ascenso, C.P. Reis, Therapeutic advances in wound healing, J. Dermatol. Treat. (2020) 1–21.
[28] L. Loomba, T. Scarabelli, Metallic nanoparticles and their medicinal potential. Part II: aluminosilicates, nanobiomagnets, quantum dots and cochleates, Ther. Deliv. 4 (9) (2013) 1179–1196.
[29] K.K. Wong, S.O. Cheung, L. Huang, J. Niu, C. Tao, C.M. Ho, et al., Further evidence of the anti-inflammatory effects of silver nanoparticles, ChemMedChem 4 (7) (2009) 1129–1135.
[30] Z.-m. Xiu, Q.-b. Zhang, H.L. Puppala, V.L. Colvin, P.J. Alvarez, Negligible particle-specific antibacterial activity of silver nanoparticles, Nano Lett. 12 (8) (2012) 4271–4275.
[31] E.M. Pritchard, T. Valentin, B. Panilaitis, F. Omenetto, D.L. Kaplan, Antibiotic-releasing silk biomaterials for infection prevention and treatment, Adv. Funct. Mater. 23 (7) (2013) 854–861.
[32] S.M. Dizaj, F. Lotfipour, M. Barzegar-Jalali, M.H. Zarrintan, K. Adibkia, Antimicrobial activity of the metals and metal oxide nanoparticles, Mater. Sci. Eng. C Mater. Biol. Appl. 44 (2014) 278–284.
[33] H.R. Rosen, A.P. Marczell, E. Czerwenka, M.O. Stierer, H. Spoula, H. Wasl, Local gentamicin application for perineal wound healing following abdominoperineal rectum excision, Am. J. Surg. 162 (5) (1991) 438–441.
[34] U. Gruessner, M. Clemens, P.V. Pahlplatz, P. Sperling, J. Witte, H.R. Rosen, et al., Improvement of perineal wound healing by local administration of gentamicin-impregnated collagen fleeces after abdominoperineal excision of rectal cancer, Am. J. Surg. 182 (5) (2001) 502–509.
[35] A. Kwong, J. Cogan, Y. Hou, R. Antaya, M. Hao, G. Kim, et al., Gentamicin induces laminin 332 and improves wound healing in junctional epidermolysis bullosa patients with nonsense mutations, Mol. Ther. 28 (5) (2020) 1327–1338.
[36] W. Zhou, Z. Jia, P. Xiong, J. Yan, Y. Li, M. Li, et al., Bioinspired and biomimetic AgNPs/gentamicin-embedded silk fibroin coatings for robust antibacterial and osteogenetic applications, ACS Appl. Mater. Interfaces 9 (31) (2017) 25830–25846.
[37] S. Schafer, H. Al-Qaddo, M. Gosau, R. Smeets, P. Hartjen, R.E. Friedrich, et al., Cytocompatibility of bone substitute materials and membranes, In Vivo 35 (4) (2021) 2035–2040.
[38] P. Gehrke, P. Hartjen, R. Smeets, M. Gosau, U. Peters, T. Beikler, et al., Marginal adaptation and microbial leakage at conometric prosthetic connections for implant-supported single crowns: an in vitro investigation, Int. J. Mol. Sci. 22 (2) (2021) 881.
[39] F. Carrouel, S. Viennot, J. Santamaria, P. Veber, D. Bourgeois, Quantitative molecular detection of 19 major pathogens in the interdental biofilm of periodontally healthy young adults, Front. Microbiol. 7 (2016) 840.
[40] T. Hoshino, M. Kawaguchi, N. Shimizu, N. Hoshino, T. Ooshima, T. Fujiwara, PCR detection and identification of oral streptococci in saliva samples using gtf genes, Diagn. Microbiol. Infect. Dis. 48 (3) (2004) 195–199.
[41] P.E. Kolenbrander, R.N. Andersen, D.S. Blehert, P.G. Egland, J.S. Foster, R. J. Palmer Jr., Communication among oral bacteria, Microbiol. Mol. Biol. Rev. 66 (3) (2002) 486–505, table of contents.
[42] B. Sampaio-Maia, I.M. Caldas, M.L. Pereira, D. Pérez-Mongiovi, R. Araujo, The oral microbiome in health and its implication in oral and systemic diseases, Adv. Appl. Microbiol. 97 (2016) 171–210.
[43] G.F. Rogers, A.A. Lim, J.B. Mulliken, B.L. Padwa, Effect of a syndromic diagnosis on mandibular size and sagittal position in Robin sequence, J. Oral Maxillofac. Surg. 67 (11) (2009) 2323–2331.
[44] S. Rastogi, M. Modi, B. Sathian, The efficacy of collagen membrane as a biodegradable wound dressing material for surgical defects of oral mucosa: a prospective study, J. Oral Maxillofac. Surg. 67 (8) (2009) 1600–1606.
[45] S. Omura, N. Mizuki, S. Horimoto, R. Kawabe, K. Fujita, A newly developed collagen/silicone bilayer membrane as a mucosal substitute: a preliminary report, Br. J. Oral Maxillofac. Surg. 35 (2) (1997) 85–91.
[46] D. Ryabova, N. Orlinskaya, S. Tsybusov, N. Homutinnikova, R. Lapshin, E. Durnovo, Application of polymer phospholipid matrix for closing open wounds on oral mucosa, СорбентныетехнологиивМедицине 8 (1 (eng)) (2016).
[47] Ç. Kılıç, E.G.G. Peker, F. Acartürk, S.M.S. Kılıçaslan, Ş.Ç. Cevher, Investigation of the effects of local glutathione and chitosan administration on incisional oral mucosal wound healing in rabbits, Colloids Surf. B: Biointerfaces 112 (2013) 499–507.
[48] S.A. Ballestas, T.C. Turner, A. Kamalakar, Y.C. Stephenson, N.J. Willett, S. L. Goudy, et al., Improving hard palate wound healing using immune modulatory autotherapies, Acta Biomater. 91 (2019) 209–219.
[49] Y.S. Lim, S.K. Kwon, J.H. Park, C.G. Cho, S.W. Park, W.K. Kim, Enhanced mucosal healing with curcumin in animal oral ulcer model, Laryngoscope 126 (2) (2016) E68–E73.
[50] S. Yaprak Karavana, P. Güneri, G. Ertan, Benzydamine hydrochloride buccal bioadhesive gels designed for oral ulcers: preparation, rheological, textural, mucoadhesive and release properties, Pharm. Dev. Technol. 14 (6) (2009) 623–631.
[51] G. Lis, J. Zarzecka, J. Litwin, E. Jasek, T. Cichocki, J. Zapala, Effect of cultured autologous oral keratinocyte suspension in fibrin glue on oral wound healing in rabbits, Int. J. Oral Maxillofac. Surg. 41 (9) (2012) 1146–1152.
[52] M. Gholipourmalekabadi, S. Sapru, A. Samadikuchaksaraei, R.L. Reis, D.L. Kaplan, S.C. Kundu, Silk fibroin for skin injury repair: where do things stand? Adv. Drug Deliv. Rev. 153 (2020) 28–53.
[53] N. Kasoju, U. Bora, Silk fibroin in tissue engineering, Adv. Healthc. Mater. 1 (4) (2012) 393–412.
[54] J. Tang, Y. Han, F. Zhang, Z. Ge, X. Liu, Q. Lu, Buccal mucosa repair with electrospun silk fibroin matrix in a rat model, Int. J. Artif. Organs 38 (2) (2015) 105–112.
[55] Z. Ge, Q. Yang, X. Xiang, K.Z. Liu, Assessment of silk fibroin for the repair of buccal mucosa in a rat model, Int. J. Oral Maxillofac. Surg. 41 (5) (2012) 673–680.
[56] P. Kamalathevan, P.S. Ooi, Y.L. Loo, Silk-based biomaterials in cutaneous wound healing: a systematic review, Adv. Skin Wound Care 31 (12) (2018) 565–573.
[57] Q. Wang, S. Zhou, L. Wang, R. You, S. Yan, Q. Zhang, et al., Bioactive silk fibroin scaffold with nanoarchitecture for wound healing, Compos. Part B 224 (2021) 109165.
[58] M. Stevanović, M. Djošić, A. Janković, V. Kojić, M. Vukašinović-Sekulić, J. Stojanović, et al., Antibacterial graphene-based hydroxyapatite/chitosan coating with gentamicin for potential applications in bone tissue engineering, J. Biomed. Mater. Res. A 108 (11) (2020) 2175–2189.
[59] K.K. Panda, V.M.M. Achary, R. Krishnaveni, B.K. Padhi, S.N. Sarangi, S.N. Sahu, et al., In vitro biosynthesis and genotoxicity bioassay of silver nanoparticles using plants, Toxicol. in Vitro 25 (5) (2011) 1097–1105.
[60] M.J. Piao, K.A. Kang, I.K. Lee, H.S. Kim, S. Kim, J.Y. Choi, et al., Silver nanoparticles induce oxidative cell damage in human liver cells through inhibition of reduced glutathione and induction of mitochondria-involved apoptosis, Toxicol. Lett. 201 (1) (2011) 92–100.
[61] M. Skłodanowski, P. Golińska, K. Rudnicka, H. Dahm, M. Rai, Evaluation of cytotoxicity, immune compatibility and antibacterial activity of biogenic silver nanoparticles, Med. Microbiol. Immunol. 205 (6) (2016) 603–613.
[62] H. He, G. Tao, Y. Wang, R. Cai, P. Guo, L. Chen, et al., In situ green synthesis and characterization of sericin-silver nanoparticle composite with effective antibacterial activity and good biocompatibility, Mater. Sci. Eng. C Mater. Biol. Appl. 80 (2017) 509–516.
[63] X. Lv, H. Wang, A. Su, Y. Chu, A novel approach for sericin-conjugated silver nanoparticle synthesis and their potential as microbicide candidates, J. Microbiol. Biotechnol. 28 (8) (2018) 1367–1375.

[64] A. Gao, H. Chen, A. Hou, K. Xie, Efficient antimicrobial silk composites using synergistic effects of violacein and silver nanoparticles, Mater. Sci. Eng. C Mater. Biol. Appl. 103 (2019) 109821.
[65] M. Guzman, J. Dille, S. Godet, Synthesis and antibacterial activity of silver nanoparticles against gram-positive and gram-negative bacteria, Nanomedicine 8 (1) (2012) 37–45.
[66] L.D. Koh, J. Yeo, Y.Y. Lee, Q. Ong, M. Han, B.C. Tee, Advancing the frontiers of silk fibroin protein-based materials for futuristic electronics and clinical wound-healing (invited review), Mater. Sci. Eng. C Mater. Biol. Appl. 86 (2018) 151–172.
[67] M.D. Scherer, J.C.V. Sposito, W.F. Falco, A.B. Grisolia, L.H.C. Andrade, S.M. Lima, et al., Cytotoxic and genotoxic effects of silver nanoparticles on meristematic cells of Allium cepa roots: a close analysis of particle size dependence, Sci. Total Environ. 660 (2019) 459–467.
[68] H.J. Klasen, Historical review of the use of silver in the treatment of burns. I. Early uses, Burns 26 (2) (2000) 117–130.
[69] X. Lv, Z. Li, S. Chen, M. Xie, J. Huang, X. Peng, et al., Structural and functional evaluation of oxygenating keratin/silk fibroin scaffold and initial assessment of their potential for urethral tissue engineering, Biomaterials 84 (2016) 99–110.
[70] V. Gopinath, S. Priyadarshini, M. Loke, J. Arunkumar, E. Marsili, D. MubarakAli, et al., Biogenic synthesis, characterization of antibacterial silver nanoparticles and its cell cytotoxicity, Arab. J. Chem. 10 (2017) 1107–1117.
[71] X. Pan, S. Chen, D. Li, W. Rao, Y. Zheng, Z. Yang, et al., The synergistic antibacterial mechanism of gentamicin-loaded CaCO3 nanoparticles, Front. Chem. 5 (2018) 130.
[72] A.W. Serio, T. Keepers, L. Andrews, K.M. Krause, Aminoglycoside revival: review of a historically important class of antimicrobials undergoing rejuvenation, EcoSal Plus 8 (1) (2018).
[73] M.A. Curtis, P.I. Diaz, T.E. Van Dyke, The role of the microbiota in periodontal disease, Periodontol. 83 (1) (2020) 14–25.
[74] S.P. Dhas, S. Anbarasan, A. Mukherjee, N. Chandrasekaran, Biobased silver nanocolloid coating on silk fibers for prevention of post-surgical wound infections, Int. J. Nanomedicine 10 (Suppl. 1) (2015) 159–170.
[75] Y. Wang, R. Cai, G. Tao, P. Wang, H. Zuo, P. Zhao, et al., A novel AgNPs/sericin/agar film with enhanced mechanical property and antibacterial capability, Molecules 23 (7) (2018).
[76] Y. Ando, H. Miyamoto, I. Noda, F. Miyaji, T. Shimazaki, Y. Yonekura, et al., Effect of bacterial media on the evaluation of the antibacterial activity of a biomaterial containing inorganic antibacterial reagents or antibiotics, Biocontrol Sci. 15 (1) (2010) 15–19.
[77] A. Hostacká, Serum sensitivity and cell surface hydrophobicity of Klebsiella pneumoniae treated with gentamicin, tobramycin and amikacin, J. Basic Microbiol. 38 (5–6) (1998) 383–388.
[78] Y. Wang, J. Wang, S. Huang, C. Liu, Y. Fu, Evaluating the effect of aminoglycosides on the interaction between bovine serum albumins by atomic force microscopy, Int. J. Biol. Macromol. 134 (2019) 28–35.
[79] N. Hassani Besheli, F. Mottaghitalab, M. Eslami, M. Gholami, S.C. Kundu, D. L. Kaplan, et al., Sustainable release of vancomycin from silk fibroin nanoparticles for treating severe bone infection in rat tibia osteomyelitis model, ACS Appl. Mater. Interfaces 9 (6) (2017) 5128–5138.
[80] H.R. Bakhsheshi-Rad, A.F. Ismail, M. Aziz, M. Akbari, Z. Hadisi, M. Omidi, et al., Development of the PVA/CS nanofibers containing silk protein sericin as a wound dressing: in vitro and in vivo assessment, Int. J. Biol. Macromol. 149 (2020) 513–521.
[81] S. Gilotra, D. Chouhan, N. Bhardwaj, S.K. Nandi, B.B. Mandal, Potential of silk sericin based nanofibrous mats for wound dressing applications, Mater. Sci. Eng. C Mater. Biol. Appl. 90 (2018) 420–432.
[82] R. Xue, Y. Liu, Q. Zhang, C. Liang, H. Qin, P. Liu, et al., Shape changes and interaction mechanism of Escherichia coli cells treated with sericin and use of a sericin-based hydrogel for wound healing, Appl. Environ. Microbiol. 82 (15) (2016) 4663–4672.
[83] W. Zhang, L. Chen, J. Chen, L. Wang, X. Gui, J. Ran, et al., Silk fibroin biomaterial shows safe and effective wound healing in animal models and a randomized controlled clinical trial, Adv. Healthc. Mater. 6 (10) (2017).
[84] X. Guo, Z. Dong, Y. Zhang, Y. Li, H. Liu, Q. Xia, et al., Proteins in the cocoon of silkworm inhibit the growth of Beauveria bassiana, PLoS One 11 (3) (2016), e0151764.

Received: 31 May 2022 | Revised: 25 August 2022 | Accepted: 6 September 2022

DOI: 10.1111/wrr.13049

Wound Repair and Regeneration — WILEY

SYSTEMATIC REVIEW

Silk proteins in reconstructive surgery: Do they possess an inherent antibacterial activity? A systematic review

Sogand Schäfer MD[1] | Farzaneh Aavani MSc[1] | Marius Köpf PhD[2] | Aleksander Drinic MSc[2] | Ewa K. Stürmer MD[3] | Sandra Fuest MSc[1] | Audrey Laure Céline Grust MD[1,4] | Martin Gosau MD, DMD[4] | Ralf Smeets MD, DMD[1,4]

[1]Department of Oral and Maxillofacial Surgery, Division of Regenerative Orofacial Medicine, University Hospital Hamburg-Eppendorf, Hamburg, Germany

[2]Fibrothelium GmbH, Aachen, Germany

[3]Department of Vascular Medicine, University Heart Centre, Translational Wound Research, University Medical Centre Hamburg-Eppendorf, Hamburg, Germany

[4]Department of Oral and Maxillofacial Surgery, University Medical Centre Hamburg-Eppendorf, Hamburg, Germany

Correspondence
Sogand Schäfer, Department of Oral and Maxillofacial Surgery, Division of Regenerative Orofacial Medicine, University Hospital Hamburg-Eppendorf, 20251 Hamburg, Germany.
Email: sog.schaefer@uke.de

Abstract

The field of reconstructive surgery encompasses a wide range of surgical procedures and regenerative approaches to treat various tissue types. Every surgical procedure is associated with the risk of surgical site infections, which are not only a financial burden but also increase patient morbidity. The surgical armamentarium in this area are biomaterials, particularly natural, biodegradable, biocompatible polymers, including the silk proteins fibroin (SF) and sericin (SS). Silk is known to be derived from silkworms and is mainly composed of 60–80% fibroin, which provides the structural form, and 15–35% sericin, which acts as a glue-like substance for the SF threads. Silk proteins possess most of the desired properties for biomedical applications, including biocompatibility, biodegradability, minimal immunogenicity, and tunable biomechanical behaviour. In an effort to alleviate or even prevent infections associated with the use of biomaterials in surgery, antibacterial/antimicrobial properties have been investigated in numerous studies. In this systematic review, the following question was addressed: Do silk proteins, SF and SS, possess an intrinsic antibacterial property and how could these materials be tailored to achieve such a property?

KEYWORDS
antibacterial properties, reconstructive surgery, regenerative medicine, silk fibroin

1 | INTRODUCTION

Reconstructive surgery, which includes plastic surgery, oral and maxillofacial surgery, and a variety of other surgical specialties, strives to repair, restore, and replace bone and/or soft tissue imperfections. Biomaterials are a component of the surgical armamentarium in this approach. They promote host cell adhesion, proliferation, and migration at the defect location, resulting in native tissue regeneration. The application of biomaterials includes a broad patient population, various etiologies, and intervention risks, ranging from the treatment of chronic wounds and burns, nerve and cartilage repair, breast reconstruction after mastectomy, and replacement of diseased or fractured bone.[1] It must be taken into account that all of these procedures carry the risk of surgical site infections (SSI), leading to additional postoperative hospitalisation, a second surgical procedure, ICU treatment, and higher mortality rates. According to released data from the

U.S. Centres of Disease Control (CDC), SSIs are the most economically burdensome healthcare-associated infections, with an estimated annual cost of $3.3 billion and one million additional hospital days.[2] However, the CDC also reports a declining trend in infections associated with improved surveillance measures, such as improved operating room ventilation, sterilisation methods, improved surgical techniques, and availability of antimicrobial prophylaxis.[2] Application of antibacterial systems provides a chance to rely on recent advances in biomaterials design. In this term, biomaterials attract great deals of attentions in reconstructive surgery. Depending on the intended function and target sites these substances can originate from a variety of sources, for example, autogenic, allogenic, xenogenic, and synthetic (Table 1), and designed in a variety of forms (membranes, matrices, three-dimensional scaffolds, gels, etc.).[3] Silk proteins, that is, silk fibroin (SF) and silk sericin (SS), are currently trending natural biopolymers which can be extracted from the cocoons of mulberry silkworms (e.g., *Bombyx mori*), non-mulberry silkworms (e.g., *Antheraea mylitta*, *Antheraea pernyi*, *Antheraea yamamai*, and *Philosamia ricini*), or as threads from other arthropods, for example, spiders or scorpions.[3] Silk is composed of 60–80% fibroin, which provides the structural form, 15–35% sericin, which contributes as a glue-like material to the SF threads, and 1–5% non-sericin components in the cocoon of *Bombyx mori* (B. Mori)[3,4] (Figure 1). Fibroin exists mainly in two secondary conformations: α-Helix, which is found in the silk gland, and ß-fold, which is formed by the silkworm during the spinning process. Sericin, on the other hand, exists predominantly in random coil form and contains a number of different amino acids, most of which are hydrophilic: Serine (33.43%), aspartic acid (16.71%), and glycine (13.49%).[6,7] The hydrophobic repeating domains of glycine and alanine (e.g., [GAGAGS]n and [GAGAGY]n) are included in the SF structure and are responsible for its mechanical strength.[3] Threads made of original silk, that is, a mixture of SS and SF, have caused a type I hypersensitivity reaction since the ancient use of silk threads in surgery.[6] Therefore, such combination threads have been replaced by threads consisting of individual protein components.[1] Silk proteins are proven to be biocompatible and facilitate adhesion and proliferation of various cell types. They also exhibit minimal immunogenicity and anti-inflammatory behaviour after implantation. However, they have been shown to exhibit a different biomechanical behaviour.[4,8] Isolated SF is characterised by its controllable biodegradability, mechanical strength, and oxygen and water vapour permeability, while SS is characterised by its fragile and amorphous nature that allows moisture retention, showing a high affinity for biomolecules while acting as an antioxidant, and most importantly, its antibacterial activity.[7,9] Napavichayanun et al.,[10] published a review including three clinical randomised controlled trials with a total of 89 SS wound dressings (including controls), all of which showed a decrease in healing time, pain scores, and wound size in all intervention groups, suggesting that SS dressings are suitable for successful wound healing. An example of the successful application of SF is the FDA-approved surgical scaffold SERI, which is based on B. mori SF. The scaffold showed promising performance in plastic surgery related applications but its use was questioned after the occurrence of postoperative infections.[5] As mentioned earlier, SSIs are among the most severe types of trauma which require complicated therapeutic care. Therefore, an additional antibacterial activity tailored to the beneficial properties of silk proteins could improve the biomaterials' usage for regenerative and reconstructive applications. For this reason, we investigated whether (1) silk proteins possess an inherent antimicrobial activity and (2) whether there are ways to add/adapt these properties to the materials. The primary objective of this systematic review was to examine the literature on the inherent antibacterial activity of the silk proteins fibroin and sericin. The secondary endpoint was to evaluate current approaches to antibacterial functionalization. With this review, we attempt to answer the question of whether silk proteins possess an inherent antibacterial property and how such a property can be developed. In addition, we attempt to inform the reader about current applications in reconstructive surgery.

2 | MATERIALS AND METHODS

2.1 | Literature review

The terms ([silk fibroin] OR [silk sericin] OR [silk protein]) AND ([antibacterial] OR [antimicrobial] OR [bactericidal]) were searched in PubMed, a literature database maintained by the National Library of Medicine. On 1 January 2021, the search was performed in the following order: Titles were checked first for content match, then abstracts, and finally full texts. The admissibility of references from included papers was also checked.

2.2 | Inclusion criteria

The inclusion criteria for this study were as follows:

1. Original studies (preclinical and clinical)
2. Tested materials should aim at clinical application
3. Test materials must at least partly include silk fibroin or silk sericin
4. Comprehensive definition of the antibacterial analysis
5. Control group without an antibacterial functionalization

The research strategy is outlined in Figure 2.

3 | RESULTS

3.1 | Literature search

The initial search yielded a total 218 results, of which three articles were published in a language other than English or German (i.e., Chinese, Russian, and Norwegian). After title screening, 23 articles were excluded because they did not meet the content criteria for this search. 195 abstracts were screened, excluding articles that analysed spider silk materials, review articles, and articles with substantial differences from the defined endpoints. As a result, 133 full-text articles

TABLE 1 Selection of commercially available silk-based products

Application	Origin	Source/Composition	Trade name	Company	Form
Soft Tissue Repair/Reconstruction (e.g., wound healing, muscle flap reinforcement, breast reconstruction)	Allogenic	Human	AlloDerm TheraSkin Alloskin AmnioBioGraft Tutoplast	LifeCell Corp. USA LifeNet Health, USA AlloSource, USA Alamo Tissue Service, USA RTI Surgical Inc., USA	Membrane Membrane Mesh Membrane Membrane
	Xenogenic	Porcine	Medeor Matrix Strattice	Kensey Nash, US. LifeCell Corp., USA	Mesh Mesh
		Bovine	Surgimend	Integra LifeScience Inc., USA	Membrane
		Equine	PROcuff PROankle PROxxx (TBD)	Synovis Orthopaedic	Mesh
		B. mori - Silk Fibroin	SERI surgical	Allergan, Inc., USA.	Scaffold Mesh
	Synthetic	Polylactide glycolic acid/Polylactide acid Polypropylene Polytetrafluoroethylene	VICRYL X-REPAIR PROLENE GORE-TEX	Ethicon, Inc., USA Synthasome, Inc., USA Ethicon, Inc., USA W.L. Gore & Associates, Inc., USA	Mesh Mesh 3D patch Mesh
	Composite	Bovine/polyglycolic acid	Endoform	Aroa biosurgery, New Zealand.	Mesh
Nerve Repair/Reconstruction (e.g., in peripheral nerve injuries)	Biologic allogenic	Human	Avance	AxoGen, USA	Scaffold/conduit
	Xenogenic	Porcine	SURGISIS	Mark Bleyer, President, Cook Biotech, Inc., USA	Scaffold/conduit
		Bovine	NeuraGen	Integra LifeSciences Corp., USA.	Scaffold/conduit
		Chitosan	Reaxon	MEDOVENT Gmbh, Germany	Scaffold/conduit
	Synthetic	Poly (DL-lactide-co-s-caprolactone)	Neurolac	Polyganics BV, Netherlands	Scaffold/conduit
Cartilage Repair/ Reconstruction	Biologic Allogenic	Human	CARTISTEM	Medipost Inc., USA	Suspension
	Xenogenic	Porcine	Chondro-Gide	Geistlich Pharma, Switzerland.	Membrane
		Bovine	NeoCart	Histogenics, USA	Membrane
	Synthetic	Monomer p-dioxanone	PDS	Ethicon, Inc., USA	Film
	Composite	Polyglycolic acid/ hyaluronic acid	Chondrotissue	BioTissue, USA	Membrane
Bone repair/reconstruction (e.g., oral, cranio−/ maxillofacial, or orthopaedic bony defects)	Biologic Allogenic	Human	AlloDerm OraGraft	LifeCell Corp., USA LifeNet Health, USA	Fenestrated, Mesh, Non-mesh Particle
	Xenogenic	Porcine	Strattice	LifeCell Corp., USA	Mesh
		Bovine	BioOss SurgiMend	TEI Biosciences Inc., USA	Granules
		Equine	EquiMatrix	NIBEC CO., Ltd, South Korea.	Granules
	Synthetic	Bioglass β-tricalcium phosphate	Perioglass PolyBone	NovaBone Products, USA Kyungwon Medical Ltd., USA	Granules Scaffold
	Composite	Calcium phosphate/ collagen Hyaluronic acid/bio glass/glycerol	VITOss Confirm Bioactive	Orthova, Inc., USA Globus Medical Inc., USA	Scaffold Putty, Gel, Crunch

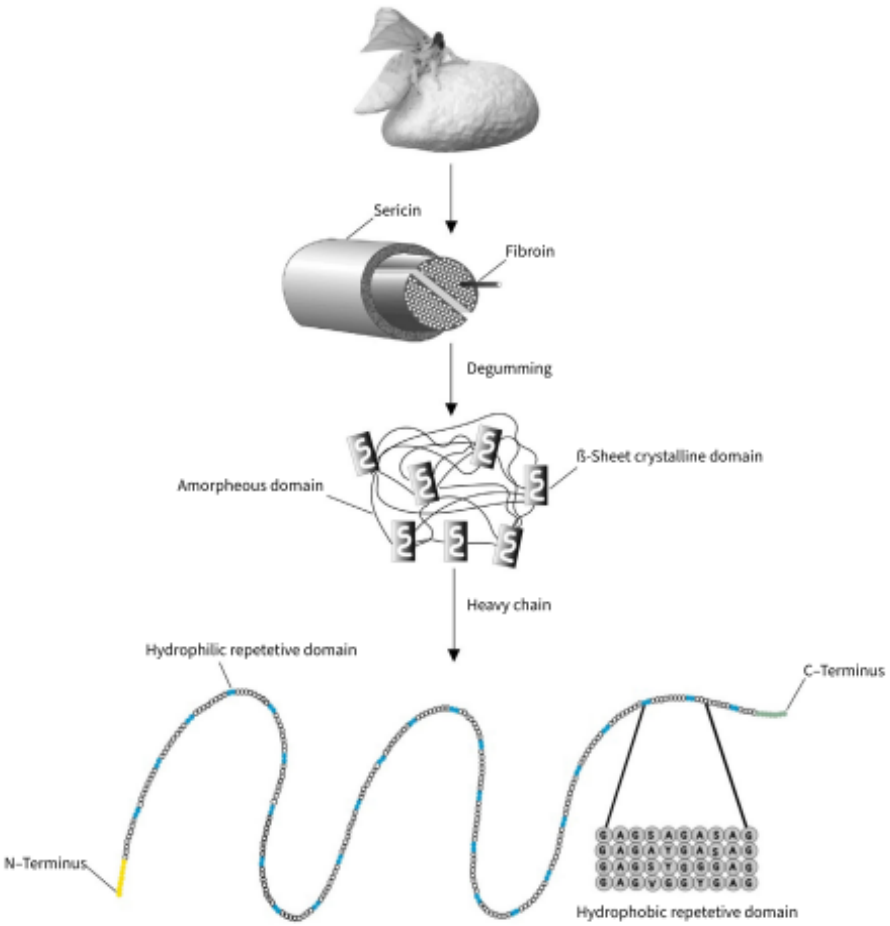

FIGURE 1 Illustration of silk fibres produced by silkworms. Silk is a natural polymeric fibre produced by the silkworm *Bombyx mori*. Two fibroin fibres covered with a sericin coat are the constitutes of a silk fibre. The degumming process sets the fibroin fibres free from the sericin coat. Fibroin fibres consist of β-sheet crystalline domains embedded in an amorphous matrix. The heavy chain (H-chain) includes hydrophobic and hydrophilic repetitive domains. Each hydrophobic subdomain is comprised of different repeating units of hexapeptides[5]

were examined. Of the total 47 included articles, 30 studies examined silk fibroin- based materials and 17 studies examined silk sericin-based materials. Accordingly, 86 articles were excluded from this review because they did not meet the above inclusion criteria. All included articles were preclinical studies. The silk proteins used in the antibacterial tests were all from *B. mori*, except in three studies that used SF from the silkworm *Anthera Assama*. A categorization was made indicating the best antibacterial functionalization in terms of efficacy compared to the respective control groups of each study. Therefore, the included articles were classified into four groups: inherent activity, metals (i.e., nanoparticles of metallic elements), drugs (i.e., antibiotics), and others (i.e., antimicrobial peptides, polymers, etc.) (Tables 2 and 3). The antibacterial activity against the tested bacterial strains is shown in Figures 3 and 4.

3.2 | Articles on silk fibroin

The categorization of materials based on SF is shown in Table 2. All 30 preclinical articles evaluated examined the test materials in vitro; five studies additionally used in vivo models, including four rat models[23,25,38] and one mouse model.[15] Three articles were assigned the best or equal antibacterial activity without additional functionalization (see Section 3.4). The in vitro methods used were agar diffusion/inhibition zone analysis (AD /ZOI), colony number/colony forming unit analysis (CC/CFU), minimum inhibitory/minimum bactericidal concentration (MIC/MBC) assessment, optical density assessment (OD), or scanning electron microscopy (SEM) in 15, 15, 2, 5, and 6 articles, respectively. Eight of nine articles testing metallic agents were assigned to the metal group that achieved the best antibacterial activity with their respective functionalization. One article described the superior activity of gentamicin compared with silver nanoparticles (AgNPs)[30] and one article concluded that zinc nanoparticles (ZnNPs) and chitosan performed equally well.[36] Within the metal group, the active ingredient consisted of AgNPs in five cases, ZnNPs in two cases, and transition metal dichalcogenides (TMDs) in one case. Efficacy against Gram-negative *E. coli* ($n = 5$) and *P. aeruginosa* ($n = 1$) and Gram-positive *S. aureus* ($n = 6$), MRSA ($n = 1$), and other bacterial strains (i.e., *M. tuberculosis*, *B. subtilis*, and *P. mirabilis*) ($n = 3$) was reported (Figure 3). Twelve studies included materials containing antibiotics of the fluoroquinolone type (i.e., levofloxacin and ciprofloxacin) ($n = 2$), the ss-lactam type (i.e., amoxicillin) ($n = 4$), aminoglycoside-

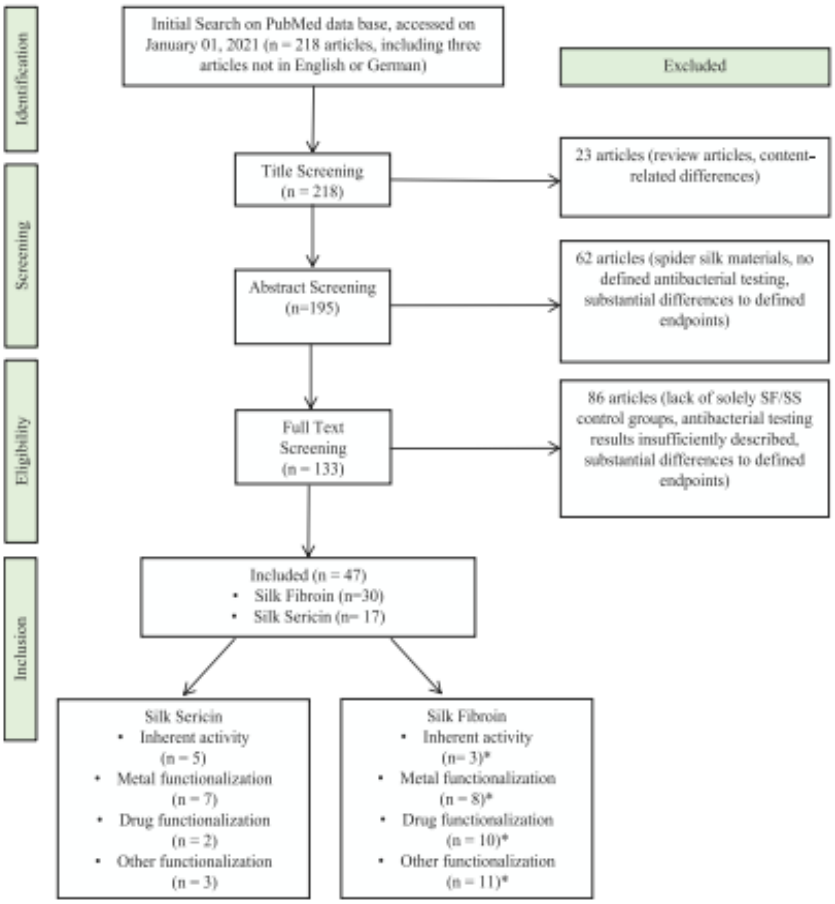

FIGURE 2 Literature review flowchart. *Articles categorised based on best antimicrobial performance, therefore, similar performances are counted twice to the respective group

type (e.g., gentamicin) ($n = 4$), glycopeptide-type (e.g., vancomycin) ($n = 1$), and tricyclic-type (e.g., doxycycline) (n = 1). Of these, two articles with functionalization of AgNPs were found to be superior compared to kanamycin/amoxicillin[19] and ciprofloxacin[14]; the best performance for drug-loaded materials was reported in 10 articles, accordingly, these articles were assigned to this group. Here, antibacterial activity against strains of *S. aureus* ($n = 8$) was reported, followed by *E. coli* ($n = 4$), and one report each for *MRSA* and *K. pneumoneae* was also indicated. The last group, consisting of the best performances for other functional agents, included 10 articles out of a total of 12 articles that investigated a range of agents: from the incorporation of calcium ions into the material or of natural polymers, such as chitosan and colistin, to the use of oregano essential oil as an antimicrobial agent. In this group, compared to the others, more studies were found with tested activity against Gram-negative *P. aeruginosa* and other Gram-positive microbes, for example, *S. anguinis*, *A. naeslundii*, *S. gordnoni*, and *S. epidermidis*, but with a consistent number of reports of activity against *E. coli* ($n = 9$) and *S. aureus* ($n = 7$). For the other two articles, gentamicin and amoxicillin showed better antibacterial activity than chitosan[20,27]; in one case, SF alone was as adequate as the polypropylene-based agent.[11]

Across all groups, the most commonly produced structural forms were films/dressings and electrospun mats; likewise, wound healing and bone regeneration were the most common intended applications.

3.3 | Articles on silk sericin

The categorization of the SS-based materials is shown in Table 3. A total of 17 articles were identified that met the inclusion criteria. All articles were generated using an in vitro method. Five articles were assigned to the best antibacterial activity without additional functionalization (see Section 3.4). Antibacterial activity was assessed in 8, 6, 2, 6, and one articles, respectively, using agar diffusion/inhibition zone analysis (AD/ZOI), colony number/colony forming unit analysis (CC/CFU), minimum inhibitory/minimum bactericidal concentration (MIC/MBC) assessment, optical density assessment (OD), or scanning electron microscopy (SEM). Functionalization with metals was performed in a total of nine studies, out of which three studies used ZnNPs and six used AgNPs. Six studies showed the best activity when loaded with metals. Among them, the materials showed an efficacy against *E. coli* ($n = 6$), *S. aureus* ($n = 7$) and *MRSA* ($n = 1$) (Figure 4). In one study, the active ingredient violacein showed a higher antibacterial activity compared to AgNPs[52] and in another study, chlorhexidine was superior to AgNPs.[54] The best efficacy for drug-loaded materials was determined in two articles using tetracycline and gentamicin. These articles demonstrated an efficacy against *E. coli* ($n = 2$), *S. aureus* ($n = 2$), and *P. aeruginosa* ($n = 1$) (Figure 4). Four articles contained a functional agent associated with other approaches to functionalization, that is, chlorhexidine, violacein, cecropin-B, and chitosan. However, the

TABLE 2 Silk fibroin-based materials with respective antibacterial functional agents, categorised according to best antibacterial performance

Antibacterial functionalization	Study type	Material/form	Antibacterial test	Intended application	References
Inherent activity					
SF only (Polypropylene)[a]	In vitro	Suture	AD/ZOI	Surgery	11
SF only (Transgenic *B. mori*)	In vitro	N/A	CC/CFU	Universal	12
SF only (Transgenic *B. mori*)	In vitro	N/A	CC/CFU	Universal	13
Metals					
AgO_2NP (Ciprofloxacin)[b]	In vitro	Film/Dressing	AD/ZOI	Wound healing	14
ZnO	In vitro/In vivo	Suture	CC/CFU	Surgery	15
AgNP	In vitro	Fibres	CC/CFU	Wound healing	16
AgNP	In vitro	Solution	MIC/MBC, SEM	Universal	17
Transition metal dichalcogenide	In vitro/In vivo	Film/Dressing	CC/CFU, OD, SEM	Wound healing	18
AgNP (Kanamycin/Amoxicillin)[b]	In vitro	3D Scaffold	MIC/MBC, CC/CFU	Osseous regeneration	19
ZnNP (Chitosan)[b]	In vitro	Film/Dressing	AD/ZOI	Wound healing	20
AgNP	In vitro	Electrospun mats	AD/ZOI	Osseous regeneration	21
Drugs					
Levofloxacin	In vitro	Implant coating	CC/CFU, SEM	Osseous regeneration	22
Amoxicillin	In vitro/In vivo	Suture	AD/ZOI	Surgery	23
Doxycycline[b]	In vitro	Electrospun mat	AD/ZOI	Universal	24
Vancomycin	In vitro/In vivo	3D Scaffold	AD/ZOI	Osseous regeneration	25
Amoxicillin	In vitro	Electrospun mat	AD/ZOI, OD	Soft tissue regeneration	26
Gentamicin (Chitosan)[b]	In vitro	3D Scaffold	AD/ZOI	Cartilage regeneration	20
Amoxicillin (Chitosan)[b]	In vitro	Yarn	AD/ZOI	Universal	27
Gentamicin	In vitro	Implant coating	CC/CFU, SEM	Osseous regeneration	28
Gentamicin	In vitro	Screw	CC/CFU, SEM	Osseous regeneration	29
Gentamicin (AgNP)[b]	In vitro	Implant coating	CC/CFU, SEM	Osseous regeneration	30
Other					
Chitosan	In vitro	Electrospun mats	OD	Wound healing	31
Polyethyleneimine	In vitro	Electrospun mats	CC/CFU	Universal	32
SF only (Polypropylene)[a]	In vitro	Suture	AD/ZOI	Surgery	11
4-Hexylresorcinol	In vitro	Sutures	AD/ZOI	Surgery	33
Oregano essential oil	In vitro	Electrospun mats	AD/ZOI, OD	Wound healing	34
Calcium peroxide	In vitro	Film/Dressing	AD/ZOI	Urethral regeneration	35
ZnNP(+Chitosan)[a]	In vitro	Film/Dressing	AD/ZOI	Wound healing	36
Cys-KR12	In vitro	Electrospun mats	CC/CFU	Wound healing	37
Colistin	In vitro/In vivo	Membrane	CC/CFU	Wound healing	38
Calcium	In vitro	3D Scaffold	CC/CFU, OD	Wound healing	20
Chitooligosaccharide	In vitro	Membrane	CC/CFU	Universal	39

Abbreviations: AD, agar diffusion; CC, colony count; CFU, colony forming unit; MBC, minimum bactericidal concentration; MIC, minimum inhibitory concentration; OD, optical density; SEM, scanning electron microscopy; ZOI, zone of inhibition.

[a]Both forms of functionalization were similarly effective.

[b]Two functionalization agents were tested—the agent with the best performance is listed, the second agent is indicated in parenthesis.

article that tested chitosan concluded that ZnNPs exhibited a better activity[49] and was therefore assigned to the metal group. In the group of other functional materials, only the activity against *A. baumannii* and *B. subtilis* was tested.[54] Similar to the materials of SF, films/dressings were frequently produced to be used for wound healing, but novel forms, such as hydrogels, were also introduced.

3.4 | Inherent antibacterial activity of SF and SS

The information of an inherent antibacterial activity of SF or SS was rarely mentioned directly in the reviewed articles; hence, it was necessary to conclude the evidence from the respective results and discussions. As a result, for the best or equal antibacterial activity compared

TABLE 3 Silk sericin-based materials with respective antibacterial functional agents, categorised according to best antibacterial performance

Antibacterial functionalization	Study type	Material/Form	Antibacterial Test	Intended Application	References
Inherent activity					
SS only	In vitro	Implant coating	OD	Dentistry	9
SS only	In vitro	Electrospun mats	OD	Wound healing	40
SS only	In vitro	Hydrogel	CC/CFU, SEM	Wound healing	41
SS only	In vitro	Hydrogel	OD	Wound healing	42
SS only	In vitro	Implant coating	CC/CFU	Dentistry	43
Metals					
ZnNP	In vitro	Film/dressing	CC/CFU	Wound healing	44
ZnNP	In vitro/	3D Scaffold	CC/CFU	Wound healing	45
AgNP	In vitro	Sutures	AD/ZOI	General surgery	46
AgNP	In vitro	Solution	CC/CFU, MIC/MBC	Universal	47
AgNP	In vitro	Solution	OD	Universal	48
ZnNP (Chitosan)[a]	In vitro	Film/dressing	AD/ZOI, OD	Wound healing	49
AgNP	In vitro	Film/dressing	AD/ZOI	Wound healing	50
Drugs					
Tetracycline	In vitro	Film/dressing	AD/ZOI	Wound healing	51
Gentamicin	In vitro	Hydrogel	AD/ZOI	Wound healing	9
Other					
Chlorhexidine (AgNP)[a]	In vitro	Film/dressing	AD/ZOI, OD	Wound healing	41
Violacein (AgNP)[a]	In vitro	Fibre	AD/ZOI, CC/CFU	Universal	52
Cecropin-B	In vitro	Film/dressing	AD/ZOI, MIC/MBC	Wound healing	53

Abbreviations: AD, agar diffusion; CC, colony count; CFU, colony forming unit; MBC, minimum bactericidal concentration; MIC, minimum inhibitory concentration; SEM, scanning electron microscopy; OD, optical density; ZOI, zone of inhibition.
[a]Two functionalization agents were tested—the agent with the best performance is listed, the second agent is indicated in parenthesis.

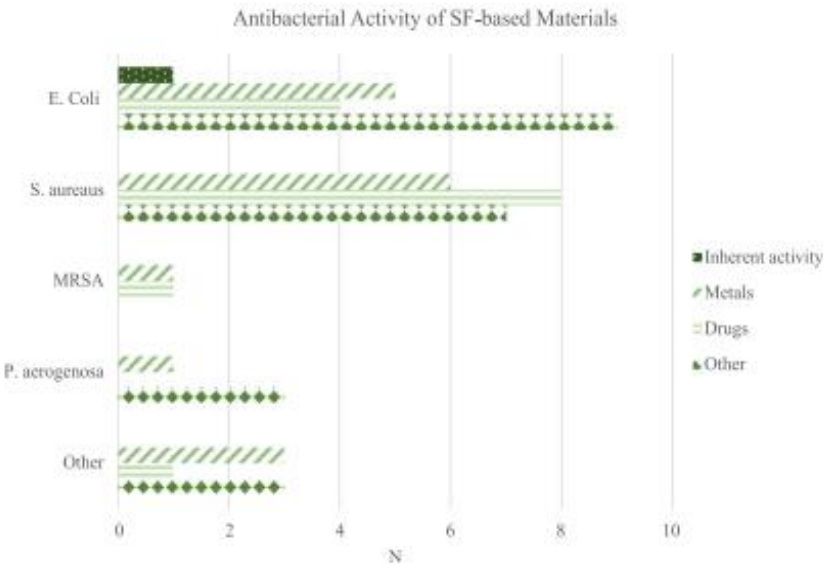

FIGURE 3 Specified antibacterial activity of silk fibroin-based materials and respective functionalization groups. *N* = number of articles reporting an antimicrobial effect regarding to the tested bacterial strain. Only groups of similar or best antimicrobial performance are counted to *N* (s. Table 2)

to the respective control groups, three out of 30 studies based on SF and five out of 17 studies based on SS could be found (Tables 2 and 3). However, the indication for overall inherent antibacterial activity was given in five out of 30 (5:30 or 16.67%) for SF and six out of 17 (6:17 or 35.29%) for SS. In studies indicating best performance for SF, only one of three studies investigated an additional functional agent, that is, polypropylene + SF, as a comparison concluded that agar diffusion analysis showed equivalent antimicrobial activity of

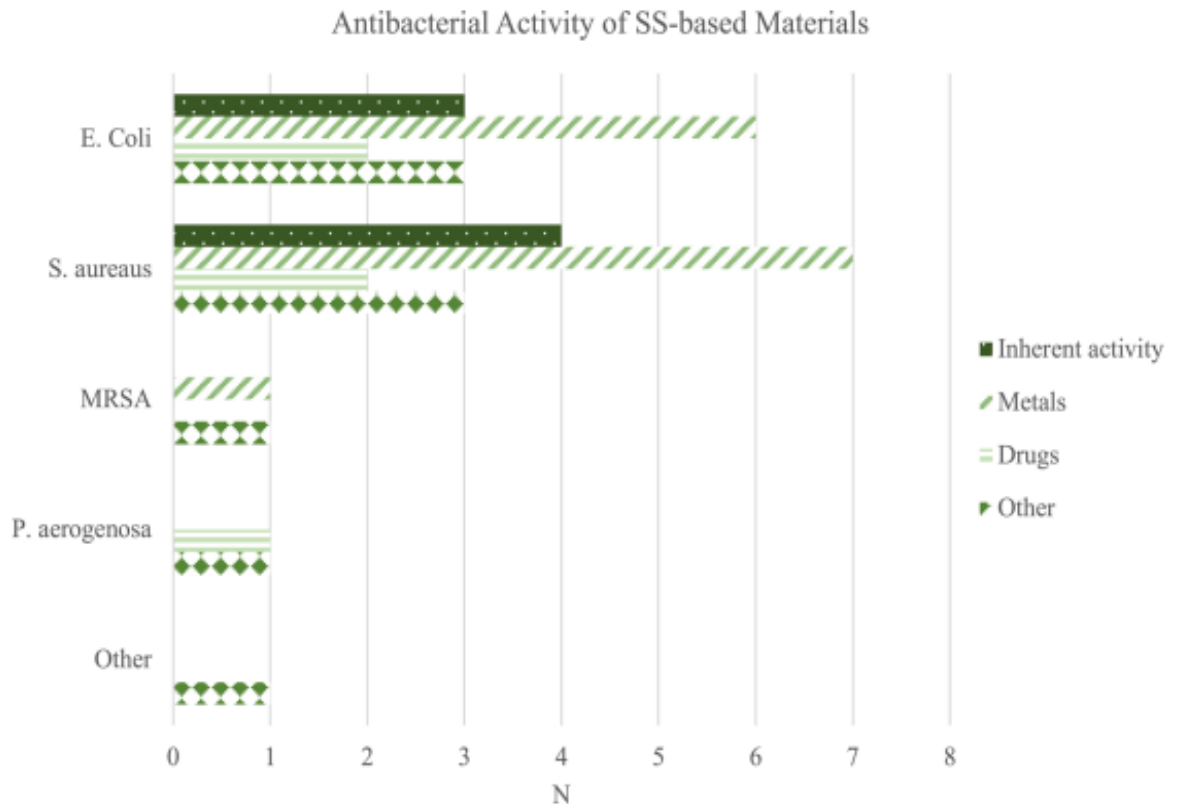

FIGURE 4 Specified antibacterial activity of silk sericin-based materials and respective functionalization groups. *N* = number of articles reporting an antimicrobial effect regarding to the tested bacterial strain. Only groups of similar or best antimicrobial performance are counted to *N* (s. Table 3)

sutures consisting of only SF against *E. coli*.[16] The other two articles attributed an inherent antibacterial property to SF. The silk proteins in these studies were from transgenic silkworms.[13,53] Both studies took advantage of the antimicrobial peptide cecropin, which is naturally secreted by the silkworm to defend against pathogens. Li et al.,[12] introduced the cecropin gene into the fibroin L-chain gene of *B. mori* by homologous recombination, while Saviane et al.,[13] induced a germline transformation in *B. mori* that resulted in an overexpression of the antimicrobial peptides cecropin B and moricin. In both studies, the produced cocoons showed enhanced antibacterial properties and the resulting silk fibre was able to inhibit bacterial growth of *E. coli*. The results of the two other studies showed an antibacterial activity for SF, however, the authors disagreed with the application of pristine SF for antibacterial purposes.[11,51] For SS, five studies reported best or equal antibacterial activity for materials composed of or with additional SS; however, none of these studies tested an additional comparable antibacterial agent (Table 3). Two studies implemented SS implant coatings for dental/oral surgery applications and demonstrated reduced growth of *S. aureus* and *S. epidermidis* strains through OD evaluation and CC/CFU analysis.[9,43] Despite this finding, Zhang et al. attributed the reduction of bacterial counts to the anti-adhesive properties of the surfaces rather than bactericidal properties.[43] Three studies produced SS materials for wound healing, including films/dressings and hydrogels and tested for *E. coli* and *S. aureus* colonisation by OD evaluation, CC/CFU analysis, and SEM, yielding promising bactericidal results.

4 | DISCUSSION

Open wounds created during surgical intervention constitute a general risk of infection with microorganisms such as bacteria, fungi, and viruses.[32] Nowadays, many promising strategies have been introduced to prevent infection during and after surgery. An ideal measure of prevention would be the development of advanced biomaterials inhibiting bacterial colonisation or even resisting bacterial adhesion.[36] Silk proteins have gained attention due to their desirable properties as natural, biodegradable, and biocompatible polymers. With this review, our aim was to find evidence for the commonly expressed hypothesis of an inherent antibacterial property of silk fibroin and silk sericin. From the literature reviewed, SF was found to have an inherent antibacterial activity in 16.67% (5:30 ratio) and SS in 35.29% (6:17 ratio) of respective studies. The other articles determined a superior antibacterial activity for the active agent and found no effect for the original silk material in comparison. Nevertheless, the current literature offers a wide variety of functional agents, for example, metallic

nanoparticles, antibiotics, antimicrobial peptides and many more, to tailor this desired effect to silk proteins.

In literature, SS is known as a biopolymer which offers unique properties such as antioxidant, anticancer, and antiwrinkle activity. In addition, a notable, however conversely discussed, antibacterial activity has been attributed to SS throughout literature.[55]

The antibacterial mechanism of action of SS is due to to the structural accumulation of hydrophilic amino acid residues such as serine, aspartic acid, and glycine. These amino acids have amine groups (-NH2) which convert to protonated amino groups (-NH3+) through a pronation process in the microenvironment. Subsequently, positively charged groups interact with negatively charged subunits of bacterial cell membranes such as the lipopolysaccharides of Gram-negative bacteria. As a result of this interaction, the permeability of the bacterial cell membrane changes, leading to leakage of internal proteins or carbohydrates, restriction of bacterial metabolism, increase in internal cellular pressure, and formation of internal vesicles. All these processes lead to growth inhibition or death of the pathogens.[41,42] In many reports, the antibacterial activity of SS is also attributed to the presence of specific small domains that include seroins and protease inhibitors. These proteins are mixed with SS during the secretion process from the silkworm gland. The reason why the silkworm synthesises seroins instead of antimicrobial peptides for defence remains unknown.[56] To date, three types of seroins have been discovered: seroin 1, seroin 2, and seroin 3. Seroin 1 is secreted in both SF and SS. In contrast, seroin 2 is mainly detectable in the outermost SS layer and seroin 3 is solely found in SS. In a study, Dong et al. demonstrated that the distribution of seroin 3 on the surface of SS allows it to directly contact pathogens in the environment and play a more efficient antimicrobial role.[57] They also demonstrated that seroin 1 has a dual function in silk: it prevents microbial invasion and participates as a molecular chaperone in the formation of the silk fibroin complex. Xue et al. examined healthy *E. coli* cells by SEM and visualised smooth surfaces and rod-shaped bacteria from 0.5 to 1.5 μm in size.[41] After treatment with SS, cell shrinkage and detachment from the membrane surfaces of *E. coli* cells were observed. From the values of OD, the percentage of *E. coli* decreased according to the increase of sericin concentration from 10 g/L to 40 g/L reaching a growth inhibition of 62% to 93%, respectively.

In our review of the current literature, we found in six out of 17 studies examined an indication for SS antibacterial activity (Section 3.4). Five of these reported best or equal antibacterial activity for the pristine SS material. In one study examining antimicrobial dressings, Bakhsheshi-Rad et al. found a ZOI of 3.5 mm for SS alone against bacterial strains of *E. coli* and *S. aureus*, yet, they attributed the best efficacy to tetracycline-containing dressings and the observed inherent activity of SS was not discussed.[51] Overall, this analysis sums up to a ratio of 6:17 or 35.29% articles indicating an inherent antibacterial effect of SS to articles disagreeing with this hypothesis. The interaction and efficacy of sericin against bacterial cells is not only considered to be dose-dependent, but also varies with the structural features after manufacturing. The latter is an inevitable consideration regarding the intended application. It has been observed that structures such as membranes or films made of pure SS are fragile, especially in dry stage due to the variable distribution of molecular weight.[58] They also swell in water-based solutions and can be dissolved at high temperatures. In this regard, there are some challenges in the application of SS for soft tissue or osseous regeneration such as for guided bone regeneration (GBR) or guided tissue regeneration (GTR) which require a scaffold or occlusive membrane to temporarily provide space, support, and guidance for host cell adhesion and proliferation.[58] Other applications come with different demands, for example, the use as a wound dressing requires the material to isolate the wound from environmental pathogens, while the use as a coating material for implants, such as orthopaedic or dental implants, requires protection from biofilm formation. The SS nanocomposite hydrogel tested by Yang et al. restrains bacterial growth by adsorbing bacteria onto the hydrogel surface.[42] Through SEM imaging they found that *E. coli* and *S. aureus* cells adhered abundantly to the surface of the hydrogel composite. The adherence of bacteria to the hydrogel surface is attributed to the charge interaction of SS with the bacterial cell membrane. Indeed, adhering bacteria to the hydrogel helped to keep the bacteria away from the wound surface and can subsequently prevent from infection. They hypothesized that a denser hydrogel surface layer would make it much more difficult for bacteria to penetrate the internal pores. They also suggested that micromolecular sericin can detach from the hydrogel form and enter the bacterial cell to adsorb anion materials, with similar effects on Gram-positive (e.g., *S. aureus*) or Gram-negative (e.g., *E. coli*) bacteria. In contrast, Zhang et al. reported non-adhesive properties that prevent biofilm formation by *S. aureus* and *S. epidermidis* on titanium implant surfaces coated with SS.[43] Another report found that microbial penetration through the SS nanofiber mats was negligible after 14 days, indicating favourable barrier properties. The various amino, hydroxyl, and carboxyl functional groups of sericin enable its successful co-polymerisation, crosslinking, or blending with other polymers, leading to improved mechanical properties and extensive applications.[48]

Unlike SS, SF is not commonly known as a polymer with a bactericidal activity. Instead, many reports describe mechanical anti-adhesive and bacterial barrier properties as the mechanism of antibacterial action, preventing bacteria from penetration.[32] For instance, Zhang et al. conducted a multipart study set up investigating a novel SF film/dressing for wound healing applications comparing it to commercial wound dressings, among others, Sidaiyi SF composite scaffold. The study was comprised of an in vitro assessment in which the SF film could mechanically prevent bacterial penetration due to its unique nonporous structure and an in vivo rabbit full-thickness skin defect model showing the SF film effectively reduces the average wound healing time with better skin regeneration compared to the commercial wound dressing. A subsequent assessment in a porcine model confirmed its long-term safety and effectiveness for full-thickness skin defects. In addition, in a randomised, single blind, clinical trial with 71 patients, the silk fibroin film significantly reduced the wound healing time and incidence of adverse events, that is, postsurgical infections.[8] In our review of the current literature, we found in five out of 30 studies examined an indication for SF antibacterial activity. Yet,

three studies ascribed best or similar antibacterial activity to SF compared to the control group. Two of these studies investigated genetically transformed silkworms producing antibacterial peptides and one study reported similar antibacterial activity of pristine SF compared to polypropylene + SF (Section 3.4). Among the other two studies, a study by Arpaçay et al. investigated antimicrobial implant coatings for improved bone regeneration.[22] They assigned levofloxacin-coated implants the best antibacterial effect against *S. aureus* biofilm formation. However, reduced biofilm formation was also observed in the implants coated exclusively with SF compared to uncoated ones, with a lower number of colony-forming units identified. Nonetheless, the authors discouraged the use of pristine SF for antibacterial use, rather, they recommended using SF drug delivery properties to load it with antibacterial substances. In another study by Babu et al.,[14] a ZOI of 2 mm was found for planar SF scaffolds designed to facilitate cartilage regeneration, with the best antibacterial effect for gentamicin-loaded scaffolds.[20] Overall, this analysis sums up to a ratio of 5:30 or 16.67% articles indicating an inherent antibacterial effect of SF to articles disagreeing with this hypothesis. Apart from this, SF biomaterials provide exceptional properties such as biodegradability, biocompatibility, and depending on the structure and manufacturing process, desirable mechanical properties that can be tailored to the target application. The abundance of structural forms for SF (i.e., gels, 3D scaffolds, electrospun mats, etc.) allows for a wide range of application in the field of reconstructive surgery. In vivo studies include soft tissue regeneration (e.g., for wound healing), nerve regeneration, cartilage regeneration, and bone regeneration, for example, as GBR/GTR membrane.[8]

In agreement with the results presented in this review, silk protein materials loaded with different kinds of antibiotics show strong efficacy,[12] but the mode of drug release and the respective concentrations must be sufficient, which on the other hand is associated with an increasing risk of antimicrobial resistance. In addition, there is evidence of biofilm formation due to treatment with antibiotics at subinhibitory concentrations, presumably by promoting the production of extracellular polymeric substances. For example, Hoffman et al.,[59] reported that subinhibitory concentrations of the aminoglycoside tobramycin induce biofilm formation by *P. aeruginosa* and *E. coli* as a consecutive defensive response to the presence of an antimicrobial agent. Novel antimicrobial agents such as polymers, lipids, peptides, or approaches to bind the agents directly to the silkworm or silk proteins have emerged as alternatives to currently available antibiotics and metallic nanoparticles.[33–35,37,39,60] However, these agents face challenges such as bioavailability and high product cost.

5 | CONCLUSION

This systematic review searched the PubMed literature database for evidence of intrinsic antimicrobial properties of both silk proteins fibroin and sericin. Our results show an indication for fibroin- and sericin-based materials confirming this hypothesis. However, caveats to consider in this regard are that none of the studies reviewed intended to investigate the hypotheses of an inherent antibacterial property of SF or SS, thus, we had to draw the answer to this question from the respective results and discussions. Rather, the desired form and functional properties of the silk proteins were extended with antimicrobial additives and investigated within the studies presented. Since antibiotics are associated with tissue reactions and undesirable resistance reactions, we suggest silk proteins loaded with metals, such as silver or zinc nanoparticles, are the best studied alternatives at the current state of research. Nevertheless, novel natural approaches such as oregano essential oil or chitosan offer particularly high biocompatibility and superior antibacterial activity to pristine silk proteins. Future studies comparing the antibacterial efficacy of different active agents manufactured to SF or SS may complement the current data and bring closer to answering the question of an inherent antibacterial property of these biomaterials.

AUTHOR CONTRIBUTIONS

Sogand Schäfer: design and planning of the review; data collection; data analysis and interpretation of results; drafted the manuscript. Farzaneh Aavani: interpretation; critical revision and approval of the article. Marius Köpf: interpretation; critical revision and approval of the article. Aleksander Drinic: interpretation; critical revision and approval of the article. Ewa K. Stürmer: critical revision and approval of the article. Sandra Fuest: critical revision of the manuscript; approval of the article. Audrey Laure Céline Grust: critical revision and approval of the article. Martin Gosau: critical revision; approval of the article. Ralf Smeets: interpretation and critical revision; approval of the article.

ACKNOWLEDGMENT

Open Access funding enabled and organized by Projekt DEAL.

CONFLICT OF INTEREST

The authors declare no conflict of interest.

DATA AVAILABILITY STATEMENT

Data sharing not applicable: no new data generated.

ORCID

Sogand Schäfer https://orcid.org/0000-0001-5877-5931

REFERENCES

1. Sun W, Gregory DA, Tomeh MA, Zhao X. Silk fibroin as a functional biomaterial for tissue engineering. *Int J Mol Sci*. 2021;22(3):1499.
2. CDC. *Surgical Site Infection Event (SSI)*. Center for Disease Control and Prevention; 2021.
3. Chouhan D, Mandal BB. Silk biomaterials in wound healing and skin regeneration therapeutics: from bench to bedside. *Acta Biomater*. 2020;103:24-51.
4. Jao D, Mou X, Hu X. Tissue regeneration: a silk road. *J Funct Biomater*. 2016;7(3):22.
5. van Turnhout A, Franke CJJ, Vriens-Nieuwenhuis EJC, van der Sluis WB. The use of SERI™ surgical scaffolds in direct-to-implant reconstruction after skin-sparing mastectomy: a retrospective study on surgical outcomes and a systematic review of current literature. *J Plast Reconstr Aesthet Surg*. 2018;71(5):644-650.

6. Kunz RI, Brancalhão RM, Ribeiro LF, Natali MR. Silkworm sericin: properties and biomedical applications. *Biomed Res Int*. 2016;2016:8175701.
7. Tao G, Wang Y, Cai R, et al. Design and performance of sericin/poly (vinyl alcohol) hydrogel as a drug delivery carrier for potential wound dressing application. *Mater Sci Eng C Mater Biol Appl*. 2019;101:341-351.
8. Zhang W, Chen L, Chen J, et al. Silk fibroin biomaterial shows safe and effective wound healing in animal models and a randomized controlled clinical trial. *Adv Healthc Mater*. 2017;6(10):1700121.
9. Ghensi P, Bettio E, Maniglio D, et al. Dental implants with anti-biofilm properties: a pilot study for developing a new Sericin-based coating. *Materials (Basel)*. 2019;12(15):2429.
10. Napavichayanun S, Ampawong S, Harnsilpong T, Angspatt A, Aramwit P. Inflammatory reaction, clinical efficacy, and safety of bacterial cellulose wound dressing containing silk sericin and polyhexamethylene biguanide for wound treatment. *Arch Dermatol Res*. 2018;310(10):795-805.
11. Gogoi D, Choudhury AJ, Chutia J, et al. Development of advanced antimicrobial and sterilized plasma polypropylene grafted muga (Antheraea assama) silk as suture biomaterial. *Biopolymers*. 2014;101(4):355-365.
12. Li Z, Jiang Y, Cao G, Li J, Xue R, Gong C. Construction of transgenic silkworm spinning antibacterial silk with fluorescence. *Mol Biol Rep*. 2015;42(1):19-25.
13. Saviane A, Romoli O, Bozzato A, et al. Intrinsic antimicrobial properties of silk spun by genetically modified silkworm strains. *Transgenic Res*. 2018;27(1):87-101.
14. Babu PJ, Doble M, Raichur AM. Silver oxide nanoparticles embedded silk fibroin spuns: microwave mediated preparation, characterization and their synergistic wound healing and anti-bacterial activity. *J Colloid Interface Sci*. 2018;513:62-71.
15. Cao F, Zeng B, Zhu Y, et al. Porous ZnO modified silk sutures with dual light defined antibacterial, healing promotion and controlled self-degradation capabilities. *Biomater Sci*. 2020;8(1):250-255.
16. Dhas SP, Anbarasan S, Mukherjee A, Chandrasekaran N. Biobased silver nanocolloid coating on silk fibers for prevention of post-surgical wound infections. *Int J Nanomedicine*. 2015;10(Suppl 1):159.
17. Fei X, Jia M, Du X, et al. Green synthesis of silk fibroin-silver nanoparticle composites with effective antibacterial and biofilm-disrupting properties. *Biomacromolecules*. 2013;14(12):4483-4488.
18. Huang X-W, Wei J-J, Liu T, Zhang X-L, Bai S-M, Yang H-H. Silk fibroin-assisted exfoliation and functionalization of transition metal dichalcogenide nanosheets for antibacterial wound dressings. *Nanoscale*. 2017;9(44):17193-17198.
19. Patil S, Singh N. Antibacterial silk fibroin scaffolds with green synthesized silver nanoparticles for osteoblast proliferation and human mesenchymal stem cell differentiation. *Colloids Surf B Biointerfaces*. 2019;176:150-155.
20. Mehta AS, Singh BK, Singh N, et al. Chitosan silk-based three-dimensional scaffolds containing gentamicin-encapsulated calcium alginate beads for drug administration and blood compatibility. *J Biomater Appl*. 2015;29(9):1314-1325.
21. Sheikh FA, Woo JH, Mi Moon B, et al. Facile and highly efficient approach for the fabrication of multifunctional silk nanofibers containing hydroxyapatite and silver nanoparticles. *J Biomed Mater Res A*. 2014;102(10):3459-3469.
22. Arpaçay P, Türkan U. Development of antibiotic-loaded silk fibroin/hyaluronic acid polyelectrolyte film coated CoCrMo alloy. *Biomed Tech (Berl)*. 2016;61(5):463-474.
23. Choudhury AJ, Gogoi D, Chutia J, et al. Controlled antibiotic-releasing Antheraea assama silk fibroin suture for infection prevention and fast wound healing. *Surgery*. 2016;159(2):539-547.
24. Dadras Chomachayi M, Solouk A, Akbari S, Sadeghi D, Mirahmadi F, Mirzadeh H. Electrospun nanofibers comprising of silk fibroin/gelatin for drug delivery applications: thyme essential oil and doxycycline monohydrate release study. *J Biomed Mater Res A*. 2018;106(4):1092-1103.
25. Hassani Besheli N, Mottaghitalab F, Eslami M, et al. Sustainable release of vancomycin from silk fibroin nanoparticles for treating severe bone infection in rat tibia osteomyelitis model. *ACS Appl Mater Interfaces*. 2017;9(6):5128-5138.
26. Liu Z, Zhu X, Tang R. Electrospun scaffold with sustained antibacterial and tissue-matched mechanical properties for potential application as functional mesh. *Int J Nanomedicine*. 2020;15:4991-5004.
27. Ojah N, Deka J, Haloi S, et al. Chitosan coated silk fibroin surface modified by atmospheric dielectric-barrier discharge (DBD) plasma: a mechanically robust drug release system. *J Biomater Sci Polym Ed*. 2019;30(13):1142-1160.
28. Sharma S, Bano S, Ghosh AS, et al. Silk fibroin nanoparticles support in vitro sustained antibiotic release and osteogenesis on titanium surface. *Nanomed Nanotechnol Biol Med*. 2016;12(5):1193-1204.
29. Shi C, Pu X, Zheng G, et al. An antibacterial and absorbable silk-based fixation material with impressive mechanical properties and biocompatibility. *Sci Rep*. 2016;6(1):1-12.
30. Zhou W, Jia Z, Xiong P, et al. Bioinspired and biomimetic AgNPs/gentamicin-embedded silk fibroin coatings for robust antibacterial and osteogenetic applications. *ACS Appl Mater Interfaces*. 2017;9(31):25830-25846.
31. Cai Z-X, Mo X-M, Zhang K-H, et al. Fabrication of chitosan/silk fibroin composite nanofibers for wound-dressing applications. *Int J Mol Sci*. 2010;11(9):3529-3539.
32. Çalamak S, Erdoğdu C, Özalp M, Ulubayram K. Silk fibroin based antibacterial bionanotextiles as wound dressing materials. *Mater Sci Eng C*. 2014;43:11-20.
33. Jo Y-Y, Kim D-W, Choi J-Y, Kim S-G. 4-Hexylresorcinol and silk sericin increase the expression of vascular endothelial growth factor via different pathways. *Sci Rep*. 2019;9(1):1-11.
34. Khan AUR, Nadeem M, Bhutto MA, et al. Physico-chemical and biological evaluation of PLCL/SF nanofibers loaded with oregano essential oil. *Pharmaceutics*. 2019;11(8):386.
35. Lv X, Li Z, Chen S, et al. Structural and functional evaluation of oxygenating keratin/silk fibroin scaffold and initial assessment of their potential for urethral tissue engineering. *Biomaterials*. 2016;84:99-110.
36. Patil PP, Bohara RA, Meshram JV, Nanaware SG, Pawar SH. Hybrid chitosan-ZnO nanoparticles coated with a sonochemical technique on silk fibroin-PVA composite film: a synergistic antibacterial activity. *Int J Biol Macromol*. 2019;122:1305-1312.
37. Song DW, Kim SH, Kim HH, Lee KH, Ki CS, Park YH. Multi-biofunction of antimicrobial peptide-immobilized silk fibroin nanofiber membrane: implications for wound healing. *Acta Biomater*. 2016;39:146-155.
38. Steinstraesser L, Rittig A, Hirsch T, Kesting MR, Steinau H-U, Jacobsen F. Colistin-loaded silk membranes against wound infection with Pseudomonas aeruginosa. *Plast Reconstr Surg*. 2011;127(5):1838-1846.
39. Zhou Q, Cui L, Ren L, et al. Preparation of a multifunctional fibroin-based biomaterial via laccase-assisted grafting of chitooligosaccharide. *Int J Biol Macromol*. 2018;113:1062-1072.
40. Gilotra S, Chouhan D, Bhardwaj N, Nandi SK, Mandal BB. Potential of silk sericin based nanofibrous mats for wound dressing applications. *Mater Sci Eng C*. 2018;90:420-432.
41. Xue R, Liu Y, Zhang Q, et al. Shape changes and interaction mechanism of Escherichia coli cells treated with sericin and use of a sericin-based hydrogel for wound healing. *Appl Environ Microbiol*. 2016;82(15):4663-4672.
42. Yang C, Xue R, Zhang Q, et al. Nanoclay cross-linked semi-IPN silk sericin/poly(NIPAm/LMSH) nanocomposite hydrogel: an outstanding

antibacterial wound dressing. *Mater Sci Eng C Mater Biol Appl*. 2017;81:303-313.
43. Zhang F, Zhang Z, Zhu X, Kang E-T, Neoh K-G. Silk-functionalized titanium surfaces for enhancing osteoblast functions and reducing bacterial adhesion. *Biomaterials*. 2008;29(36):4751-4759.
44. Ai L, Wang Y, Tao G, et al. Polydopamine-based surface modification of ZnO nanoparticles on sericin/polyvinyl alcohol composite film for antibacterial application. *Molecules*. 2019;24(3):503.
45. Ai L, He H, Wang P, et al. Rational design and fabrication of ZnONPs functionalized sericin/PVA antimicrobial sponge. *Int J Mol Sci*. 2019;20(19):4796.
46. Gallo AL, Pollini M, Paladini F. A combined approach for the development of novel sutures with antibacterial and regenerative properties: the role of silver and silk sericin functionalization. *J Mater Sci Mater Med*. 2018;29(8):1-13.
47. Chaisabai W, Khamhaengpol A, Siri S. Sericins of mulberry and non-mulberry silkworms for eco-friendly synthesis of silver nanoparticles. *Artif Cells Nanomed Biotechnol*. 2018;46(3):536-543.
48. He H, Tao G, Wang Y, et al. In situ green synthesis and characterization of sericin-silver nanoparticle composite with effective antibacterial activity and good biocompatibility. *Mater Sci Eng C*. 2017;80:509-516.
49. Liu L, Cai R, Wang Y, et al. Polydopamine-assisted silver nanoparticle self-assembly on Sericin/agar film for potential wound dressing application. *Int J Mol Sci*. 2018;19(10):2875.
50. Wang Y, Cai R, Tao G, et al. A novel AgNPs/sericin/agar film with enhanced mechanical property and antibacterial capability. *Molecules*. 2018;23(7):1821.
51. Bakhsheshi-Rad HR, Ismail AF, Aziz M, et al. Development of the PVA/CS nanofibers containing silk protein sericin as a wound dressing: in vitro and in vivo assessment. *Int J Biol Macromol*. 2020;149:513-521.
52. Gao A, Chen H, Hou A, Xie K. Efficient antimicrobial silk composites using synergistic effects of violacein and silver nanoparticles. *Mater Sci Eng C Mater Biol Appl*. 2019;103:109821.
53. Thomas DS, Manoharan C, Rasalkar S, Mishra RK, Gopalapillai R. Recombinant expression of sericin-cecropin fusion protein and its functional activity. *Biotechnol Lett*. 2020;42(9):1673-1682.
54. Ampawong S, Aramwit P. A study of long-term stability and antimicrobial activity of chlorhexidine, polyhexamethylene biguanide, and silver nanoparticle incorporated in sericin-based wound dressing. *J Biomater Sci Polym Ed*. 2017;28(13):1286-1302.
55. Zhao R, Li X, Sun B, et al. Electrospun chitosan/sericin composite nanofibers with antibacterial property as potential wound dressings. *Int J Biol Macromol*. 2014;68:92-97.
56. Yang W, Cheng T, Ye M, et al. Functional divergence among silkworm antimicrobial peptide paralogs by the activities of recombinant proteins and the induced expression profiles. *PLoS One*. 2011;6(3):e18109.
57. Dong Z, Song Q, Zhang Y, et al. Structure, evolution, and expression of antimicrobial silk proteins, seroins in Lepidoptera. *Insect Biochem Mol Biol*. 2016;75:24-31.
58. Makvandi P, Ali GW, Della Sala F, Abdel-Fattah WI, Borzacchiello A. Hyaluronic acid/corn silk extract based injectable nanocomposite: a biomimetic antibacterial scaffold for bone tissue regeneration. *Mater Sci Eng C Mater Biol Appl*. 2020;107:110195.
59. Hoffman LR, D'Argenio DA, MacCoss MJ, Zhang Z, Jones RA, Miller SI. Aminoglycoside antibiotics induce bacterial biofilm formation. *Nature*. 2005;436(7054):1171-1175.
60. Tian W, Wang Y, Xu J, et al. Evaluation of the biomedical properties of a Ca+-conjugated silk fibroin porous material. *Mater Sci Eng C*. 2019;104:110003.

How to cite this article: Schäfer S, Aavani F, Köpf M, et al. Silk proteins in reconstructive surgery: Do they possess an inherent antibacterial activity? A systematic review. *Wound Rep Reg*. 2023;31(1):99-110. doi:10.1111/wrr.13049

scientific reports

Check for updates

OPEN

Doping of casted silk fibroin membranes with extracellular vesicles for regenerative therapy: a proof of concept

Sandra Fuest[1]✉, Amanda Salviano-Silva[2], Cecile L. Maire[2], Yong Xu[3], Christian Apel[3], Audrey Laure Céline Grust[1], Arianna Delle Coste[1], Martin Gosau[4], Franz L. Ricklefs[2] & Ralf Smeets[1,4]

Bioactive material concepts for targeted therapy have been an important research focus in regenerative medicine for years. The aim of this study was to investigate a proof-of-concept composite structure in the form of a membrane made of natural silk fibroin (SF) and extracellular vesicles (EVs) from gingival fibroblasts. EVs have multiple abilities to act on their target cell and can thus play crucial roles in both physiology and regeneration. This study used pH neutral, degradable SF-based membranes, which have excellent cell- and tissue-specific properties, as the carrier material. The characterization of the vesicles showed a size range between 120 and 180 nm and a high expression of the usual EV markers (e.g. CD9, CD63 and CD81), measured by nanoparticle tracking analysis (NTA) and single-EV flow analysis (IFCM). An initial integration of the EVs into the membrane was analyzed using scanning and transmission electron microscopy (SEM and TEM) and vesicles were successfully detected, even if they were not homogeneously distributed in the membrane. Using direct and indirect tests, the cytocompatibility of the membranes with and without EVs could be proven and showed significant differences compared to the toxic control ($p < 0.05$). Additionally, proliferation of L929 cells was increased on membranes functionalized with EVs ($p > 0.05$).

Extracellular vesicles (EVs) have emerged in recent years as an important mediator of intercellular communication. They possess multiple capabilities to act on their target cells and can thus play critical roles in both physiology and pathology[1]. EVs carry complex biological information consisting of soluble and transmembrane proteins, RNAs and miRNAs, DNA, and lipids[2]. They can be taken up by recipient cells and release their bioactive contents, which can subsequently significantly alter the phenotype of the recipient cell. EVs released from mesenchymal stem cells have a similar therapeutic effect as the cells from which they are derived of[3,4]. Thus, they show remarkable effect on promoting regeneration on different types of tissues. The use of EVs has been shown to be more beneficial than the use of mesenchymal stem cells themselves for several reasons[2,4]. EVs are not limited by viability, cannot replicate, and therefore cannot degenerate. They also express limited major histocompatibility markers (MHC) and have immunomodulatory properties that reduce the risk of negative immune responses while preserving beneficial regenerative properties[5,6]. In addition, a key advantage is that unlike cells, EVs can be stored for longer periods of time[7]. Thus, they can be frozen and thawed or even lyophilized without major functional losses[8]. EVs are considered as promising in diagnostics and as new tools for various therapeutic approaches, including regenerative therapies and drug delivery, for anti-tumor therapy, and in the context of vaccination strategies[9–21]. The beneficial effects of EVs from mesenchymal stem cells on wound healing and tissue regeneration have already been demonstrated in various cell culture experiments and animal models, and were manifested by improved re-epithelialization, accelerated collagen deposition and angiogenesis among others[22–24]. In particular, EVs derived from dental pulp stem cells promote endothelial cell proliferation

[1]Department of Oral and Maxillofacial Surgery, Division of Regenerative Orofacial Medicine, University Medical Center Hamburg-Eppendorf, 20246 Hamburg, Germany. [2]Department of Neurosurgery, University Medical Center Hamburg-Eppendorf, 20246 Hamburg, Germany. [3]Department of Biohybrid and Medical Textiles (BioTex), AME - Institute of Applied Medical Engineering, Helmholtz Institute of RWTH Aachen University and Hospital, 52074 Aachen, Germany. [4]Department of Oral and Maxillofacial Surgery, University Medical Center Hamburg-Eppendorf, 20246 Hamburg, Germany. ✉email: s.fuest@uke.de

through the expression of proangiogenic factors and have hence been shown to drive angiogenesis[22,25]. Huang et al. demonstrated that EVs derived from dental pulp stem cells induce odontogenic differentiation both in vitro and in vivo[26]. Liu et al.[23] further demonstrated the efficacy of EVs in periodontal tissue regeneration. As a result, there is a growing interest in exploring the use of EVs for regenerative treatments, particularly in the head and neck region. However, one of the major challenges for the therapeutic application of EVs is that free EVs are rapidly excreted in the bloodstream and ultimately digested by macrophages[27]. The clinically very relevant problem of keeping the EVs at the site of action for a longer period of time or enabling a controlled release of these can be achieved by immobilizing the EVs in a suitable carrier structure. Various research groups have already shown that the integration of EVs into different biomaterial-based carrier structures such as hydrogels, hydrogel patches, and 3D scaffolds proved to be more effective than direct injection of EVs into the defect[22,28–31]. As a novel approach, the biomaterial silk fibroin (SF), which is extracted from the cocoon of the mulberry silkworm *Bombyx mori* (*B. mori*), can be used as a carrier material. SF as a medical carrier material is increasingly becoming the focus of research for new biomedical applications, such as wound dressings, because silk fibroin is an ideal starting material due to the dissolution of silk fibers in an aqueous solution, which can be formed into almost any shape by incorporating numerous available textile techniques (e.g. weaving, knitting and braiding)[32–34]. The advantages of SF as a biomaterial are its high strength, moisture retention, flexibility, biocompatibility, bioresorbability, oxygen permeability, and hemostatic ability[33–36]. Furthermore, the degradation and release kinetics of silk fibroin products can be precisely controlled. Especially in the broad field of oral and maxillofacial surgery, the use of regenerative biomaterials after trauma, surgical procedures or aesthetic applications is a standard procedure. Bone substitute materials and collagen membranes for instance are used in the field of guided bone and soft tissue regeneration (guided bone regeneration (GBR)/ guided tissue regeneration (GTR)), which, however, still have material-specific shortcomings due to their manufacturing chain[37]. SF can be processed by the electrospinning method, in which fibers in the size range of micro- to nanometers are obtained from a polymer solution by applying an electrical force[33]. Nonwoven structures can also be fabricated in this way. Fibroin-based films, nonwovens and also 3D scaffolds are excellent for biomedical applications such as wound dressings due to their mechanical properties and porous structure, which promotes cell infiltration and vascular sprouting[32]. In the present study we tested the hypothesis that EVs can be successfully incorporated into SF-membranes during the production process. EVs were isolated from the supernatant of an immortalized Gingiva-Fibroblast (GF) cell line and analyzed by NTA and ICFM analysis and subsequently incorporated into the SF-membranes. Scanning electron microscopy was used to examine the surface structures as well as cross-sections of the membranes, and transmission electron microscopy was used to demonstrate evidence of EVs in the membranes. The membranes were further examined with regards to cytotoxicity and proliferation both macroscopically and in cell culture, see Fig. 1.

Results

Characterization of the EVs

The size distribution of EVs was determined by Nanoparticle Tracking Analysis (NTA), presented by six biological replicates (EV1–EV6) isolated from an immortalized gingiva-fibroblast cell line. The majority of EVs from gingvia fibroblasts, 88.9%, had a size below 250 nm with a peak at 147 nm, which falls within the particle size range of small EVs, previously known as exosomes. A second peak was observed at 289 nm, representing only 0.05% of EVs, and a mere 0.007% of EVs were above 500 nm (Fig. 2A). Additionally, the majority of secreted EVs exhibited high expression of common EV markers (i.e. CD9, CD63 and CD81), as characterized by Imaging Flow Cytometry (IFCM) (Fig. 2B). Out of those markers, CD81 showed the highest abundancy (78.33%) on gingiva-fibroblast EVs, a tetraspanine known for its importance of EV functionality, as it facilitates interactions with target cells and contributes to their role in intercellular communication and cargo delivery. To further analyze the molecular profile of gingival fibroblast-derived EVs, we employed a multiplex bead-based assay, enabling the simultaneous assessment of 39 surface proteins (Fig. 2C). In addition to confirming our IFCM results by detecting high levels of CD9, CD63 and CD81, this assay revealed elevated levels of CD105, CD29, CD142 and CD44 on our EVs. These markers, associated with diverse cellular processes, indicate the multifaceted nature of gingiva-fibroblast EV functions. The presence of CD105, CD29, CD142, and CD44 on EV surfaces suggest potential contributions to intercellular communications, tissue homeostasis, and responses to physiological cues. This comprehensive characterization enhances our understanding of the molecular cargo carried by gingival fibroblast-derived EVs and emphasizes their versatility in mediation various cellular processes.

Structural analysis of the SF-membranes

Figure 3 demonstrates on the left side (A) the air-dried membranes with (w) (A, C) and without (w/o) (B, D) EVs in cross-section and top view. With the achieved resolution, no EVs in the form of round shape structures could be detected in the SF-substrate material. Both membranes show a homogeneous and amorphous surface structure, however, membrane A shows a more pronounced line structure than membrane B. In cross-section, both membranes seem to behave similarly. No pore structure can be visualized, the membrane with EVs shows many small particles in the cross section, which are assumed to be fibroin residues due to their size. The membrane without EVs (D) presents as flat and homogeneous in the core, the outer regions however show scale-like fibroin residues. The right side of figure B shows the same arrangement as in A, with the difference that the membranes were freeze-dried to better display EVs. Again, homogeneous amorphous SF structures were clearly revealed in the top-view, representing a uniform membrane structure. In cross-section, the membranes appear to be less SF-particulate in contrast to the air-dried membranes. Especially the outer regions show smooth structures. Further information on EVs in the SF-drawn membranes cannot be made from these images.

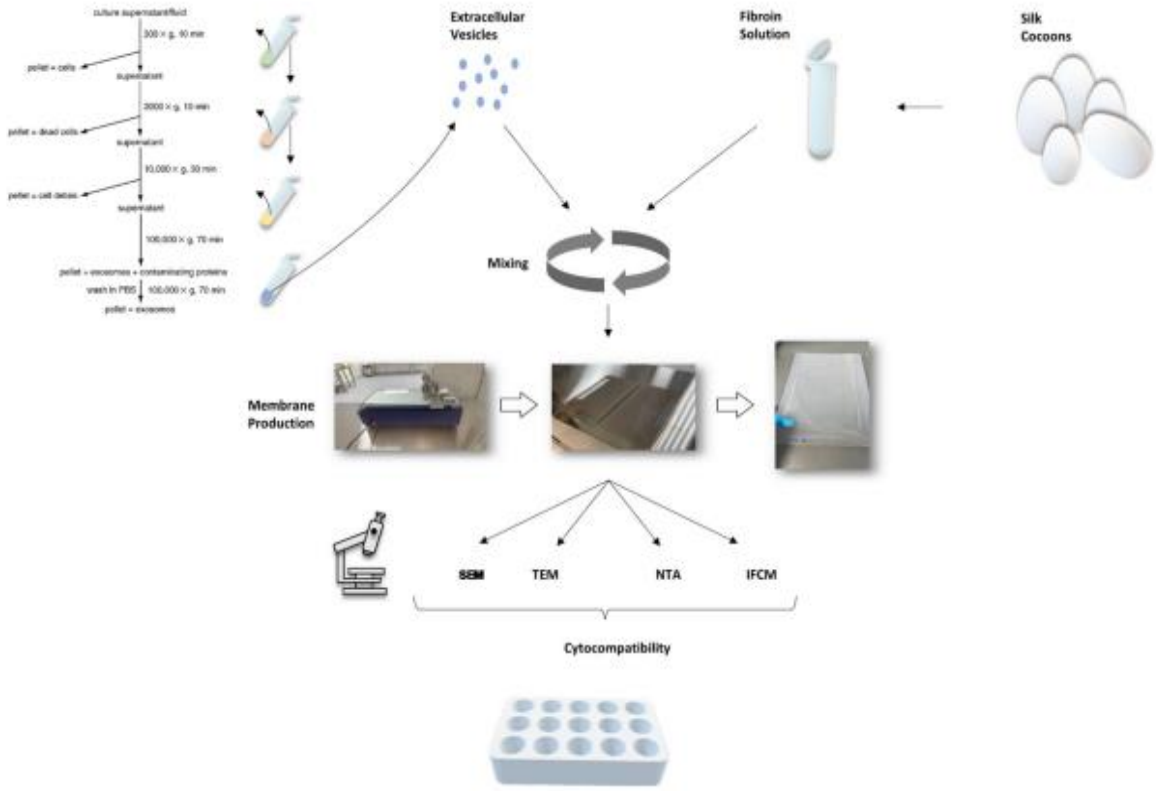

Figure 1. Schematic representation of the experiments carried out in this study.

Close inspection of the TEM images in Figure A and B reveals EVs at both 16.700 × magnification and 60.000 ×, see Fig. 4. The yellow arrows visualize the detection of EVs. The vesicles in the form of small round spheres with a darker rim and lighter core are not homogeneously distributed in the SF membrane.

Cell proliferation assay (XTT)

In this study, we performed a XTT-Assay on L929 cells to assess cell viability and metabolic activity on different days (2, 4, 6 and 8 days (d)), see Fig. 5. These cell lines are commonly used due to their availability and relevance for various research areas such as toxicology, pharmacology, and cell biology. By measuring the metabolic activity of these cells, researchers can evaluate the impact of treatments, test substances, or drugs on their viability and overall functionality. The XTT assay serves as a valuable tool for proliferation, drug screening, and understanding cellular responses to different experimental conditions.

The number of cells in the experimental group with EVs was higher after five days than in the control group without EVs. From day 5, the non-functionalized membrane proliferates better and peaks on day 8. The membrane loaded with EVs also peaks on day 8, but to a lesser extent than the control membrane. There were no statistical differences among the experimental groups. The control group consisting of pure cells proliferates much better than the two membrane types, but reaches its peak already on day 6. However, it is important to note that while the XTT assay provides a valuable indication of cell viability, additional experiments and analyses, such as cytotoxicity assays and molecular investigations, should be performed to validate and better understand the underlying mechanisms of the observed protective effects.

Lactate dehydrogenase assay (LDH)

An LDH assay was also performed on L929 and MC3T3 cells to allow for the evaluation of cytotoxicity, cell damage, comparative analysis, and drug screening. This assay provides valuable insights into the effects of various treatments or interventions on cell viability and membrane integrity, aiding in understanding cellular responses and informing the development of potential therapies.

We could report SF w EVs and SF w/o EVs exhibited slightly higher cell toxicity on L929 cells compared to MC3T3 cells, as indicated by the LDH assay results. In the LDH assay, both SF w EVs and SF w/o EVs demonstrated significantly higher viability compared to the toxic control group ($p < 0.05$). In L929 cells, both samples showed a modest but not statistically significant increase in LDH activity compared to the corresponding non-toxic control group ($p > 0.05$) (Fig. 6). This suggests a mild toxic effect of SF w EVs (MV = 22.4540; SD = 9.42404) and SF w/o EVs (MV = 27.0078; SD = 10.49305) on L929 cells. However, a trend in the LDH assay on L929 cells can be identified which shows that SF w EVs achieves a lower toxicity than SF w/o EVs. Due to the small number

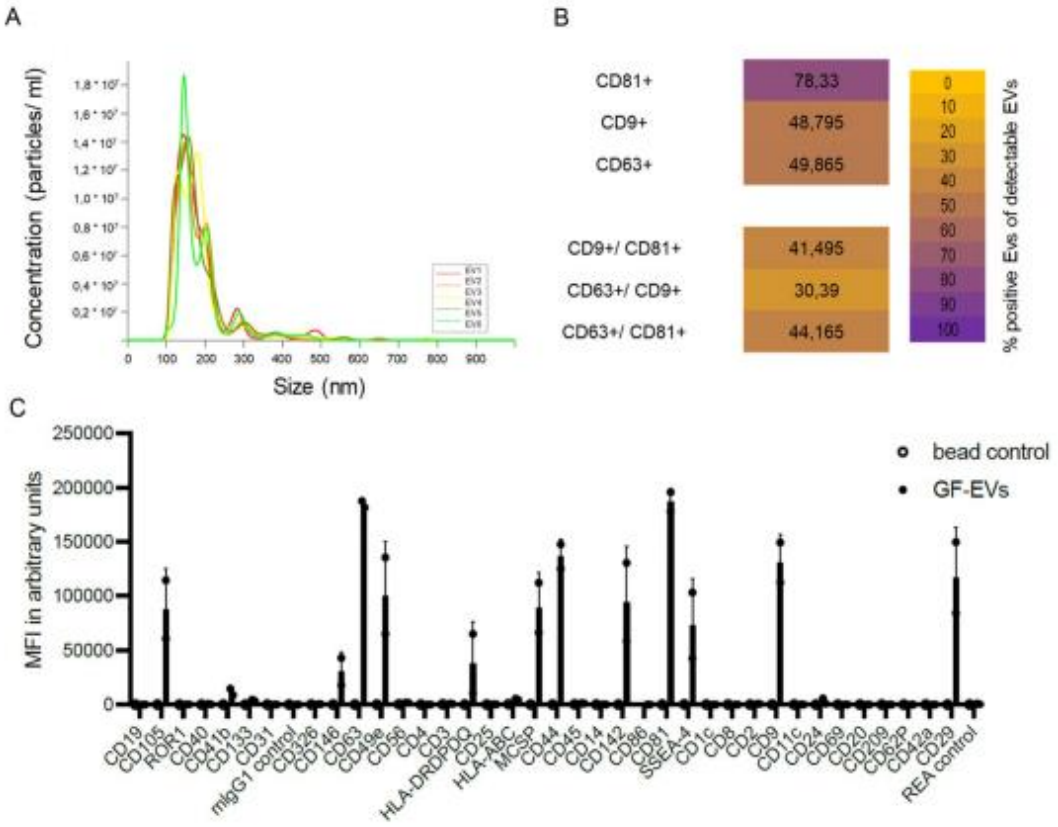

Figure 2. (**A**) Representative NTA Graph of six biological replicates (EV1–EV6); (**B**) IFCM analysis on EVs stained with antibodies against CD9, CD63 and CD81 described in[38]; (**C**) Phenotypical characterization of EVs using MACSPlex Exosome kit (Miltenyi) as described in the material and methods section.

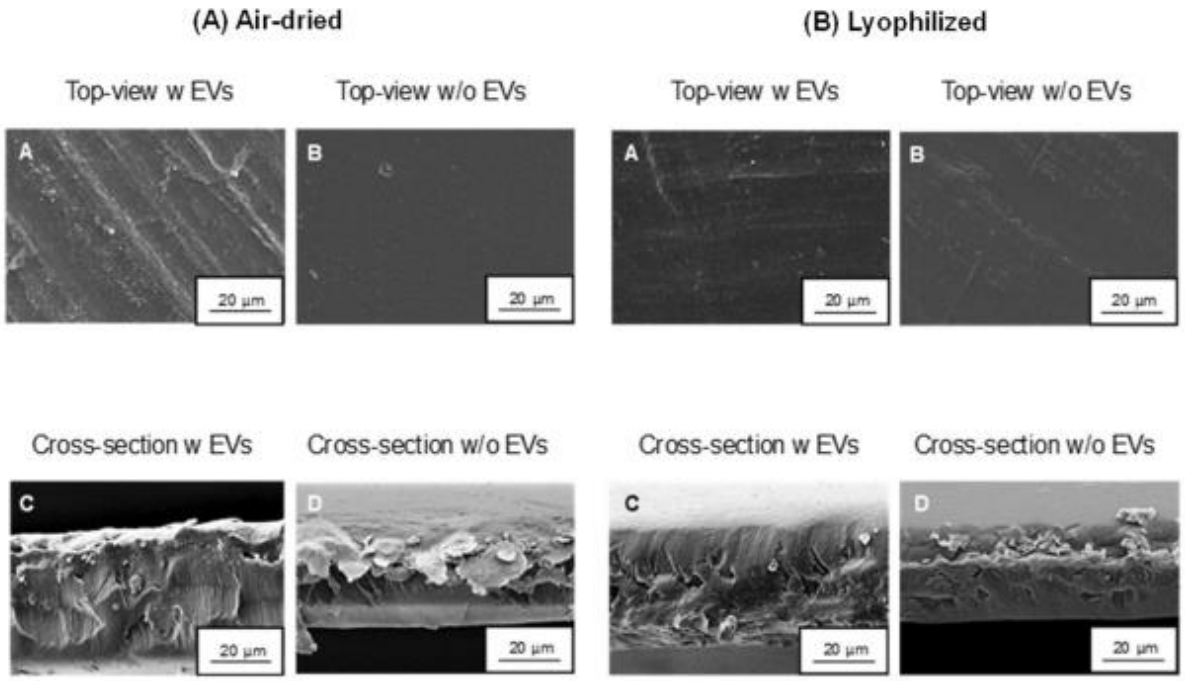

Figure 3. SEM-images of SF-membranes in 40 µm diameter with (w) and without (w/o) vesicles after different drying processes. (**A**) Air-dried membranes: top-view (**A**, **B**) and cross-section (**C**, **D**); (**B**) Lyophilized membranes: top-view (**A**, **B**) and cross-section (**C**, **D**) in 1000 × magnification.

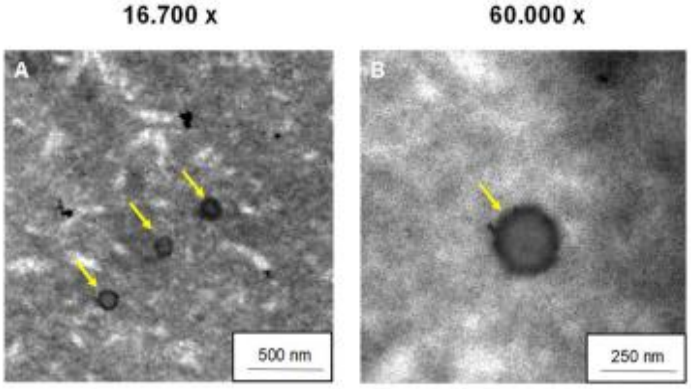

Figure 4. TEM-images of SF-membranes w EVs in 16.700 x (**A**) and 60.000 x (**B**) magnification.

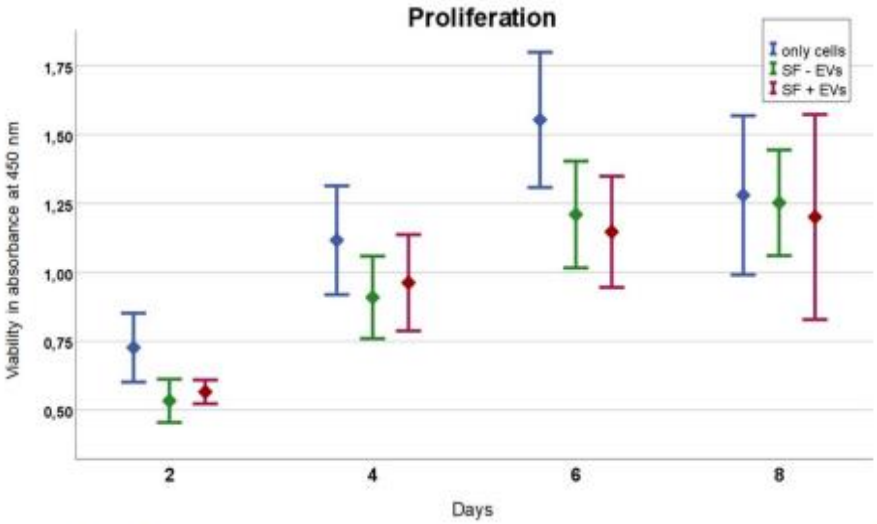

Figure 5. The Proliferation-Assay was performed on L929 cells treated with SF w EVs and SF w/o EVs and only cells. The cell proliferation was characterized using XTT on 2, 4, 6 and 8 days. Data are presented as mean ± SD.

of cases, this hypothesis can however not be proven substantially. Interestingly, when tested on MC3T3 cells, SF w EVs and SF w/o EVs displayed a relatively lower LDH activity, indicating a reduced toxic impact compared to L929 cells (Fig. 7). Nevertheless, this difference did not reach statistical significance ($p > 0.05$). In general, these findings suggest that L929 cells may be more susceptible to the toxic effects of SF w EVs and w/o EVs compared to MC3T3 cells. The different responses in cell toxicity between L929 and MC3T3 cells may be attributed to inherent variations in cellular characteristics, sensitivity, or metabolic processes. Further investigations are required to elucidate the underlying mechanisms responsible for the observed differences in toxicity profiles. These results highlight the importance of considering cell line-specific responses in assessing cellular toxicity and understand the need for comprehensive toxicity evaluations using multiple cell lines to ensure robust and reliable conclusions.

Live/ Dead-staining

After live/dead staining with a L929-mouse fibroblast cell line, an almost equal number of vital (green stained) and well-distributed spindle-shaped cells were detected in both the SF-membranes with (w) EVs and the SF-membranes without (w/o) EVs and the negative control (Tissue Culture Coverslips, Sarstedt, Germany (TCC)). The absence of dead (red-stained) cells confirmed the assumption that no toxicity is associated with these two variants, while the toxic positive control (Polyurethan Film with 0,1% zinc diethyldithiocarbamate (ZDEC), Hatano Research Institute, Food and Drug Safety Center, Japan (RMA)) only sporadically showed cells on the tested surfaces (Fig. 8). In conclusion, both indirect and direct cytotoxicity testing indicated a good biological response of the SF-membranes, without any signs of cytotoxic potential.

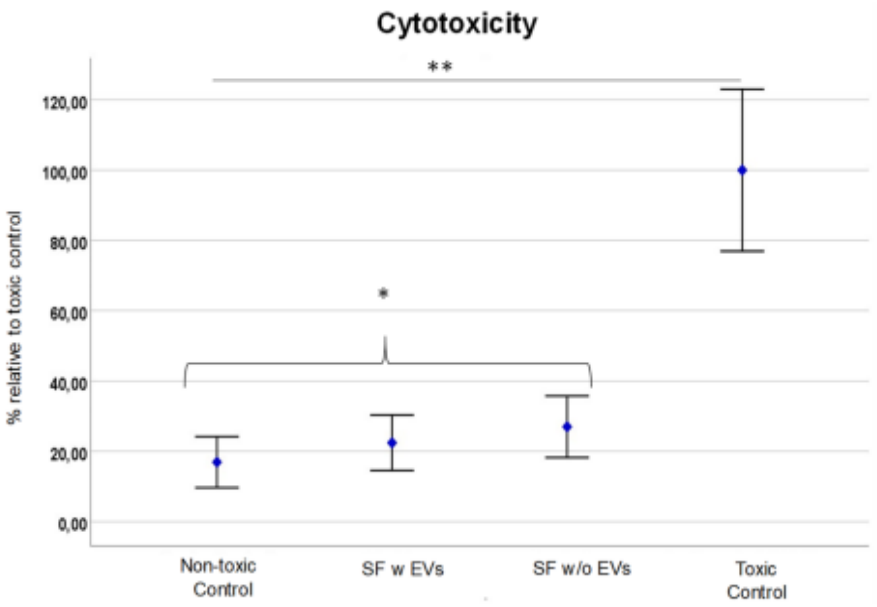

Figure 6. LDH activity in L929 cells treated with SF w EVs and SF w/o EVs, toxic control, and non-toxic control. Data is represented as mean ± standard deviation (SD) of three independent experiments. Statistical significance was determined using one-way analysis of variance (ANOVA) followed by LSD post-hoc test. *$p > 0.05$ indicates non statistic significances between the tested groups; and **$p < 0.05$ indicates a significant difference compared to the toxic control group.

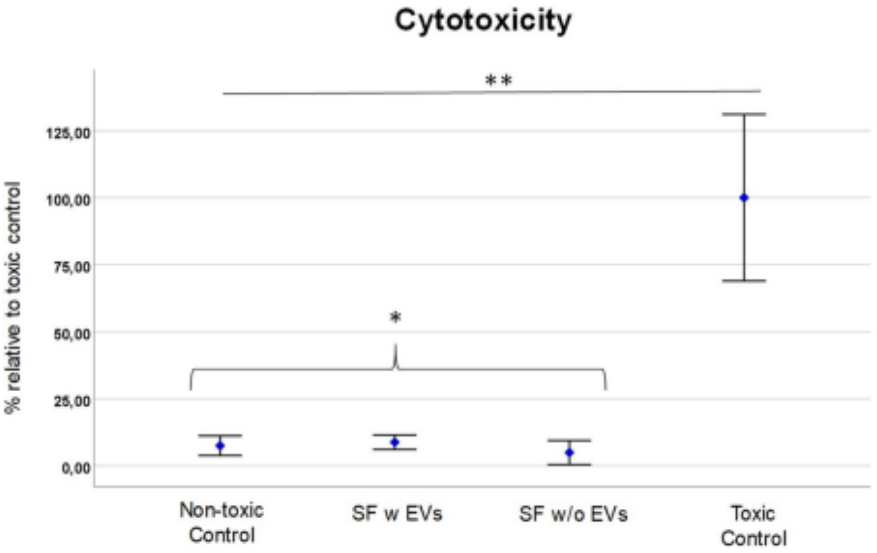

Figure 7. LDH activity in MC3T3 cells treated with SF w EV, SF w/o EVs, toxic control, and non-toxic control. The results demonstrate that both SF w EVs and SF w/o EVs induced a slightly higher LDH activity compared to the non-toxic control group, suggesting a mild toxicity effect. However, LDH activity was significantly lower in both samples than the toxic control group, indicating their non-toxic nature. Statistical significance was determined using one-way analysis of variance (ANOVA) followed by LSD post-hoc test. *$p > 0.05$ indicates non statistic significances between the tested groups; **$p < 0.05$ indicates a significant difference compared to the toxic control group.

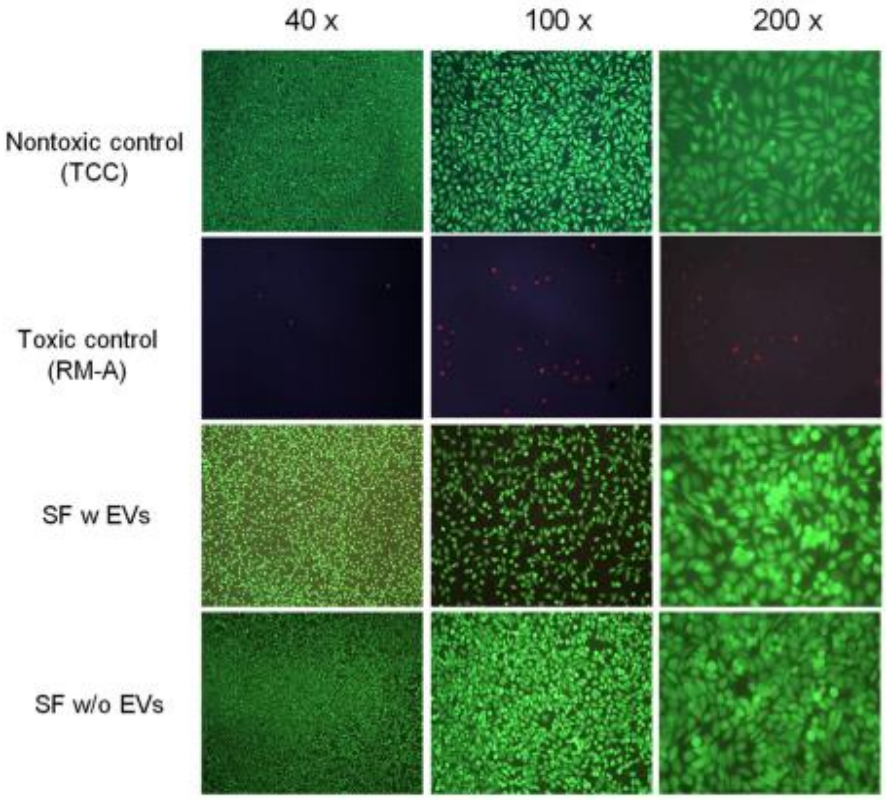

Figure 8. Results of the cytotoxicity testing with L929-mouse fibroblasts (live/ dead-staining) in direct contact with the fibroin membranes with (w) and without (w/o) EVs in different magnificnations (40×,100× and 200×).

Discussion

Silk fibroin as a biomaterial of natural origin has already been used for years in the field of medical technology, among other things as a suture material[39]. The excellent biological and mechanical properties of fibroin combined with its outstanding adjustable biodegradability have made its application the focus of regenerative therapy approaches for many years[40]. Due to the advantage of the fibroin's versatile shape, a wide variety of silk shapes can be created by various techniques using electrospinning, casting, or freeze–thaw processes[40]. Especially for regenerative approaches, it is essential to generate a suitable scaffold with the aim of implanting this at the target site and to create a suitable microenvironment that closely resembles the host tissue to induce the desired cellular responses[41]. The silk fibroin structure chosen in this study represents a fibroin membrane drawn on a Poly-Tetra-Fluor-Ethylen (PTFE) plate, which combines transparent and flexible properties. Previous studies have shown that post-treatment techniques using water vapor or methanol for insolubility causes a brittle character in fibroin films[42–44]. By adding plasticizers such as sorbitol or glycerol at an early stage, such a complex post-treatment step can become obsolete and excellent flexible and transparent films can be produced, as shown by Srivastava et al.[45]. EVs are also drawing significant attention in the biomaterials field due to their distinct characteristics and broad potential applications in various biomedical areas. These membranous particles, which are enclosed by a bi-lipid membrane, carry a diverse cargo comprising proteins, lipids, nucleic acids, and other bioactive molecules. This cargo can be transferred to recipient cells, thus influencing their behavior and functions. In our study, EVs derived from an immortalized gingiva-fibroblast cell line demonstrated an anticipated size range of 120–180 nm. Multimodal protein analysis further revealed high expression of common EV markers, including CD9 and CD63, along with elevated levels of CD105, CD29, CD142, and CD44 on our EVs. These markers, associated with a range of cellular processes, underscore the diverse functions of gingiva-fibroblast EVs. The presence of CD105, CD29, CD142, and CD44 on EV surfaces suggests potential contributions to intercellular communication, tissue homeostasis, and responses to physiological cues.

A noteworthy finding is the significant abundance of CD81 on gingiva-fibroblast EVs, indicating its potential significance in facilitating interactions with target cells. This heightened presence of CD81 suggests a crucial role in intercellular communication and cargo delivery. The characteristics and molecular profile of gingiva-fibroblast EVs, as revealed by this study, highlight their potential in biomaterial applications. The multifaceted nature of their functions, coupled with the specific markers identified, suggests a promising role in influencing cellular behavior, maintaining tissue homeostasis, and responding to physiological cues. Nevertheless, it should be noted

that, based on the isolation method, the group of EVs contains different subpopulations (also visible in Fig. 1A) that can carry different surface markers and can also have different biological effects in principle.

The main challenge to enable a controlled release of EVs and to keep them at the site of action for a longer period of time, if possible, can be enabled by incorporation into a suitable biomaterial. Previous studies have already shown that the integration of EVs into different carrier structures proved to be more efficient than a direct application into the respective defect[12,22,28,29,31,46]. Shi et al.[29] for example showed that hybrid 3D scaffolds of silk and chitosan, which were loaded with EVs derived from gingival mesenchymal stem cells, exhibited improved wound healing in diabetic rats.

Interestingly, there are no published approaches on the formulation of an already EV-loaded silk fibroin solution, which is ultimately processed into a support structure e.g. in the form of a membrane. In previously published studies, only a subsequent loading of e.g. already spun fibers was performed, which does not sufficiently enable a continuous release of EVs into the wound defect during the entire degradation process of the biomaterial[47,48]. The structure of a drawn fibroin membrane used here, in which the EVs have already been incorporated into the protein solution, thus represents an innovative approach to preserving the biological native function of the EVs and, moreover to unify them with a novel biomaterial. In this study, SEM images were taken both in the top view and in cross-section in order to detect vesicles. Although the freeze-drying process was used in addition to air-dried membranes, it was not possible to detect EVs satisfactorily. This may be due on the one hand to the vanishingly small size of the vesicles, and on the other hand to the fibroin structure used in this case. Here, more macro porous structures such as 3D scaffolds may be more suitable, in which the EVs could be embed better and adhere within the pores[49,50]. Using transmission electron microscopy, it was finally possible to identify EVs within the silk membrane, according to Ricklefs et al.[38].

Conversely, by pulling the membrane on the PTFE mould, a homogeneous distribution of the EVs in the membrane could not be achieved. A more even distribution of additives could possibly be achieved by means of further alternative processing options such as electrospinning or gas-foaming processes[49,50]. Future research should therefore investigate which fibroin structures represent a more sensible alternative as a bioactive cell carrier in order to be able to guarantee an ideal and homogeneously distributed release behaviour for subsequent application in the field of regeneration and wound healing. Additional in vitro tests were performed to further evaluate the biocompatibility of fibroin the membranes. No cytotoxic effects could be observed, neither in the functionalized membranes with EVs nor in the control group. Similar results could already be presented in previous studies from our research group[33,51]. The enhanced viability observed for L929 cells in both SF with EVs and SF without EVs compared to the toxic control group suggests a potential protective effect against the tested toxic agent. The higher viability values indicate that these samples have the ability to mitigate the toxic effects induced by the control substance. In general, these results suggest that L929 cells may be more susceptible to the toxic effects of SF w EVs and w/o EVs compared to MC3T3 cells. This interesting effect has also been described by others comparing the cytotoxic effects of different materials on these two cell lines[52–54]. Therefore, it may be beneficial to include more than one cell line in the assessment of potential cytotoxic effects of materials or medical devices. This finding suggests that SF with EVs and SF without EVs may contain compounds or factors that promote cellular survival and counteract the toxicity. These results indicate that further investigation into the composition and mechanism of action of SF with EVs and SF without EVs are required. The functionalized and non-functionalized fibroin membranes showed good proliferation in the first 5 days. From day 5, the peak is exceeded and the number of cells decrease. On the other hand, studies according to Mandal et al.[55] show that proliferation in silk structures is particularly dependent on their porosity and pore size. In a next step, the release kinetics of the EVs from the carrier material will also be analyzed, which can presumably be adjusted by the porosity of the SF structure. Since the membrane used here is a pore-free fibroin structure, this could be a limiting factor for a more pronounced proliferation of the cells[55,56]. In addition, the test is dependent on the position of the vesicles in the membrane. However, due to the shrinking process of the membrane during drying, it is possible that some of the vesicles have attached themselves to the surface of the membrane and have a positive effect on the proliferation of the cells. Since a cell type-specific morphology and a high cell density were detected on the pure and the functionalized fibroin membranes during live/dead staining, we assume that the pure fibroin structure has a high potential for use as a bioactive material. Similar results could also be obtained from Kopp et al.[33].

Materials and methods

Production of PureSilk solution

The silk fibroin aqueous solution was obtained using *PureSilk* technology (Fibrothelium GmbH, Aachen, Germany) enabling medical grade quality on an industrial scale for a broad range of concentrations. Briefly, fibroin was separated from sericin by degumming it in hot alkali solution before dissolving it in a proprietary non-toxic solvent system based on Ajisawa's reagent. The dissolved fibroin was fully dialyzed against VE water within 8 h using tailored extraction processing. The fibroin concentration used within this study was adjusted to 3 wt% and stored at 4 °C.

Cell culture, Isolation and Characterization of EVs

Immortalized human gingival fibroblasts (P10866, Innoprot, Derio (Bizkaia), Spain) were cultivated in α-MEM depleted of exosomes for 72 h after the last change of medium. Exosome-depleted α-MEM was produced by ultracentrifugation at 110,000 × g for 5 h. The supernatant was then accumulated as conditioned medium (CM). EVs were recovered from the CM by differential centrifugation in cell culture passages 2–7. In brief, dead cells, cell debris, and large vesicles were extracted by centrifugation at 300 × g for 10 min, 2000 × g for 20 min, and 10,000 × g for 40 min. The supernatant was pooled, and EVs were then pelleted by ultracentrifugation in an

Optima LE-80 K ultracentrifuge equipped with a SW 32 Ti rotor (Beckman Coulter, Chaska, MN, USA) at 110,000 × g for 90 min. The pellet was rinsed with PBS and a second run of ultracentrifugation was performed as described above. Total protein content of EVs was measured using a BCA Protein Assay Kit (Thermo Fisher Scientific, Waltham, MA, USA). Afterwards, the EVs were analyzed by Nanoparticle Tracking Analysis (NTA) and Imaging Flow Cytometry (IFCM) analysis described in detail in Ricklefs et al.[38].

For the phenotypical characterization of SF EVs, we used the MACSPlex Exosome kit (Miltenyi). This bead-based assay allows the simultaneous detection of 37 surface markers to determine the cellular origin of the EVs. In brief, EVs were incubated overnight with antibody-coated capture beads, washed, and incubated with tetraspanin CD9/CD81/CD63 antibodies provided in the kit. The measurements were done at FACSCanto II (BD Biosciences).

Preparation of fibroin films

Flexible SF films were obtained by adding glycerol to 10 ml SF solution The initial quantity of EVs was 248 µg. For functionalization, the fibroin solution was priorly mixed with 24.8 µg EVs/ml SF solution (SF w| w/o EVs). The solution was then stirred for 5 min to ensure homogeneous mixture of glycerol and SF. Following that, the SF solution was casted on a PTFE mold. After drying for 24 h at 21 °C under a laminar hood, the final fibroin membrane had a thickness of approximately 200 µm bevor drying and 40 µm after drying process. The thickness was determined by a digital micrometer (Micromar 40 ER, Mahr GmbH, Germany). The films were then stored in press-seal bags at 4 °C until further use.

Scanning electron microscopy

The surface morphology of the samples was characterized by SEM (Crossbeam 340, Zeiss, Oberkochen, Germany). Before imaging, the specimens were dried under a laminar soil hood for seven days. For cross-sectional imaging, a clear cut was made through the midline of the specimens using a scalpel. The samples were then mounted on a sample holder and subsequently coated with gold to ensure electron stability (Sputter Coater S150B, Edwards, London, UK). Imaging was accomplished in secondary electron (SE) mode at an excitation voltage of 5 kV, a scanning distance of 5 mm, and magnifications ranging from 500 × to 10,000 ×. Subsequently, a part of the membranes was air-dried and another part was lyophilized to better detect differences under SEM.

Transmission electron microscopy

Membranes were fixed in 3% glutaraldehyde in PBS. Samples were washed in 0.1 M Soerensen's phosphate buffer (Merck, Darmstadt, Germany), post-fixed in 1% OsO4 (Roth, Karlsruhe, Germany) in 25 mM sucrose buffer (Merck, Darmstadt, Germany) and dehydrated by ascending ethanol series (30, 50, 70, 90 and 100%) for 10 min each. Last step was repeated 3 times. Dehydrated specimens were incubated in propylene oxide (Serva, Heidelberg, Germany) for 30 min, in a mixture of Epon resin (Serva, Heidelberg, Germany) and propylene oxide (1:1) for 1 h and finally in pure Epon for 1 h. Samples were embedded in pure Epon. Epon polymerization was performed at 90 °C for 2 h. Ultrathin sections (70–100 nm) were picked up on Cu/Rh grids (HR23 Maxtaform, Plano, Wetzlar, Germany). Contrast was enhanced by staining with 0.5% uranyl acetate and 1% lead citrate (both EMS, Munich, Germany). Samples were examined using a TEM LEO 906 (Carl Zeiss, Oberkochen, Germany), operating at an acceleration voltage of 60 kV.

Cytocompatibility and Proliferation

In vitro cytocompatibility testing was performed as previously described[57] using indirect viability and cytotoxicity assays. L929-mouse fibroblasts were purchased from the European Collection of Cell Culture, ECACC (Salisbury, United Kingdom). L929 mouse fibroblasts were obtained from the European Collection of Cell Culture, ECACC (Salisbury, UK). Cells were incubated in MEM supplemented with 10% foetal bovine serum, glutamine to a final concentration of 4 mM and penicillin/streptomycin (100 U/ml each) (all from Life Technologies, Carlsbad, USA), hereafter referred to as cell culture medium, at 37 °C, 5% CO2 and 95% humidity (cell culture conditions). The cells were passaged when they had achieved approximately 80% confluence. MC3T3 cells were referred from MC3T3-E1 cell line from the American Type Culture Collection (ATCC, United States of America). Cells were cultured in MEM-alpha that was supplemented with 10% fetal bovine serum and penicillin/streptomycin (100 U/ml each) (all from Life Technologies, Carlsbad, USA), hereafter referred to as cell culture medium, at 37 °C, 5% CO2 and 95% humidity (cell culture conditions). The cells were passaged when they had grown to approximately 80% confluence. Briefly, for indirect assays, three samples of each specimen type and toxic control samples were isolated under cell culture conditions (37 °C, 5% CO2, and 95% humidity) with cell culture medium at a ratio of 3 cm^2/ml, whereas cell culture medium incubated under the same conditions functioned as a negative control. The extracts underwent centrifugation at 14.000 rpm for 10 min, and the supernatants were used as medium for cell culture for 24 h. Subsequently, the Cytotoxicity and Proliferation were measured using LDH-Assay (BioVision, Milpitas, USA) and XTT-Assay (Cell Proliferation Kit II, Roche Diagnostics, Mannheim, Germany) assay kits following the manufacturer's instructions. The cell growth on the surface of the material was observed under a microscope at two, four, six and eight days respectively. The optical density (OD) values of the supernatants were measured at 450 nm and a reference wavelength of 650 nm.

Live-dead-staining Assay

The Assay was carried out after an incubation time of 24 h under cell culture conditions with L929-mouse fibroblasts. To stain the surfaces of the samples with live and dead cells, 60 µl per ml of medium of propidium iodide (PI) stock solution (50 µg/ml in PBS) and 500 µl per ml of medium of fresh fluorescein diacetate (FDA) working solution (20 µg/ml in PBS from 5 mg/ml FDA in acetone stock solution) were dispensed into each well.

The live-dead staining assay was performed at a surface-to-volume ratio of 5.65 cm^2/ml and the stained specimens were then visualized using an upright fluorescence microscope (Eclipse Ti-S/L100, Nikon, Düsseldorf, Germany) fitted with a red and green fluorescence parallel detection filter. Pictures were taken using a 40×, 100× and 200× magnification.

Statistics

Statistical analysis was performed using SPSS 21 (IBM, Armonk, NY, USA). The significance of differences in viability and toxicity was assessed using one-way analysis of variance (ANOVA) followed by LSD post-hoc test. $^{**}p < 0.05$ indicates a significant difference for all tested groups.

Data availability

The datasets generated during and/or analyzed used in this manuscript are available from the corresponding author upon reasonable request.

Received: 15 December 2023; Accepted: 7 February 2024
Published online: 12 February 2024

References

1. Stevic, I., Buescher, G. & Ricklefs, F. L. Monitoring therapy efficiency in cancer through extracellular vesicles. *Cells* **9**(1), 130. https://doi.org/10.3390/cells9010130 (2020).
2. Babuta, M. & Szabo, G. Extracellular vesicles in inflammation: Focus on the microRNA cargo of EVs in modulation of liver diseases. *J. Leukoc. Biol.* **111**(1), 75–92. https://doi.org/10.1002/JLB.3MIR0321-156R (2021).
3. Batsali, A. K. *et al.* The role of bone marrow mesenchymal stem cell derived extracellular vesicles (MSC-EVs) in normal and abnormal hematopoiesis and their therapeutic potential. *J. Clin. Med.* **9**(3), 856. https://doi.org/10.3390/jcm9030856 (2020).
4. Del Fattore, A. *et al.* Differential effects of extracellular vesicles secreted by mesenchymal stem cells from different sources on glioblastoma cells. *Expert Opin. Biol. Ther.* **15**(4), 495–504. https://doi.org/10.1517/14712598.2015.997706 (2015).
5. Zheng, G. *et al.* Mesenchymal stromal cell-derived extracellular vesicles: Regenerative and immunomodulatory effects and potential applications in sepsis. *Cell Tissue Res.* **374**(1), 1–15. https://doi.org/10.1007/s00441-018-2871-5 (2018).
6. Dabrowska, S., Andrzejewska, A., Janowski, M. & Lukomska, B. Immunomodulatory and regenerative effects of mesenchymal stem cells and extracellular vesicles: Therapeutic outlook for inflammatory and degenerative diseases. *Front. Immunol.* https://doi.org/10.3389/fimmu.2020.591065 (2021).
7. Görgens, A. *et al.* Identification of storage conditions stabilizing extracellular vesicles preparations. *J. Extracell. Vesicles* https://doi.org/10.1002/jev2.12238 (2022).
8. Trenkenschuh, E. *et al.* Enhancing the stabilization potential of lyophilization for extracellular vesicles. *Adv. Healthc. Mater.* **11**(5), 2100538. https://doi.org/10.1002/adhm.202100538 (2022).
9. Alcaraz, M. J., Compañ, A. & Guillén, M. I. Extracellular vesicles from mesenchymal stem cells as novel treatments for musculoskeletal diseases. *Cells* **9**(1), 98. https://doi.org/10.3390/cells9010098 (2019).
10. Colao, I. L., Corteling, R., Bracewell, D. & Wall, I. Manufacturing exosomes: A promising therapeutic platform. *Trends Mol. Med.* **24**(3), 242–256. https://doi.org/10.1016/j.molmed.2018.01.006 (2018).
11. Gardiner, C. *et al.* Techniques used for the isolation and characterization of extracellular vesicles: Results of a worldwide survey. *J. Extracell. Vesicles* **5**(1), 32945. https://doi.org/10.3402/jev.v5.32945 (2016).
12. Li, P., Kaslan, M., Lee, S. H., Yao, J. & Gao, Z. Progress in exosome isolation techniques. *Theranostics* **7**(3), 789–804. https://doi.org/10.7150/thno.18133 (2017).
13. Momen-Heravi, F. *et al.* Current methods for the isolation of extracellular vesicles. *bchm* **394**(10), 1253–1262. https://doi.org/10.1515/hsz-2013-0141 (2013).
14. Patel, G. K. *et al.* Comparative analysis of exosome isolation methods using culture supernatant for optimum yield, purity and downstream applications. *Sci. Rep.* **9**(1), 5335. https://doi.org/10.1038/s41598-019-41800-2 (2019).
15. Phinney, D. G. & Pittenger, M. F. Concise review: MSC-derived exosomes for cell-free therapy. *Stem Cells* **35**(4), 851–858. https://doi.org/10.1002/stem.2575 (2017).
16. Ramasubramanian, L., Kumar, P. & Wang, A. Engineering extracellular vesicles as nanotherapeutics for regenerative medicine. *Biomolecules* **10**(1), 48. https://doi.org/10.3390/biom10010048 (2019).
17. Riazifar, M., Pone, E. J., Lötvall, J. & Zhao, W. Stem cell extracellular vesicles: Extended messages of regeneration. *Annu. Rev. Pharmacol. Toxicol.* **57**(1), 125–154. https://doi.org/10.1146/annurev-pharmtox-061616-030146 (2017).
18. Théry, C. *et al.* Minimal information for studies of extracellular vesicles 2018 (MISEV2018): A position statement of the international society for extracellular vesicles and update of the MISEV2014 guidelines. *J. Extracell. Vesicles* **7**(1), 1535750. https://doi.org/10.1080/20013078.2018.1535750 (2018).
19. Willis, G. R., Kourembanas, S. & Mitsialis, S. A. Toward exosome-based therapeutics: Isolation, heterogeneity, and fit-for-purpose potency. *Front. Cardiovasc. Med.* https://doi.org/10.3389/fcvm.2017.00063 (2017).
20. Witwer, K. W. *et al.* Standardization of sample collection, isolation and analysis methods in extracellular vesicle research. *J. Extracell. Vesicles* **2**(1), 20360. https://doi.org/10.3402/jev.v2i0.20360 (2013).
21. Zhu, X. *et al.* Comprehensive toxicity and immunogenicity studies reveal minimal effects in mice following sustained dosing of extracellular vesicles derived from HEK293T cells. *J. Extracell. Vesicles* **6**(1), 1324730. https://doi.org/10.1080/20013078.2017.1324730 (2017).
22. Zhang, S. *et al.* Extracellular vesicles-loaded fibrin gel supports rapid neovascularization for dental pulp regeneration. *Int. J. Mol. Sci.* **21**(12), 4226. https://doi.org/10.3390/ijms21124226 (2020).
23. Liu, Y. *et al.* Exosomes derived from stem cells from apical papilla promote craniofacial soft tissue regeneration by enhancing Cdc42-mediated vascularization. *Stem Cell Res. Ther.* **12**(1), 76. https://doi.org/10.1186/s13287-021-02151-w (2021).
24. Qian, Z. *et al.* A moisturizing chitosan-silk fibroin dressing with silver nanoparticles-adsorbed exosomes for repairing infected wounds. *J. Mater. Chem. B* **8**(32), 7197–7212. https://doi.org/10.1039/D0TB01100B (2020).
25. Xian, X., Gong, Q., Li, C., Guo, B. & Jiang, H. Exosomes with highly angiogenic potential for possible use in pulp regeneration. *J. Endod.* **44**(5), 751–758. https://doi.org/10.1016/j.joen.2017.12.024 (2018).
26. Huang, C.-C., Narayanan, R., Alapati, S. & Ravindran, S. Exosomes as biomimetic tools for stem cell differentiation: Applications in dental pulp tissue regeneration. *Biomaterials* **111**, 103–115. https://doi.org/10.1016/j.biomaterials.2016.09.029 (2016).
27. Wiklander, O. P. B. *et al.* Extracellular vesicle in vivo biodistribution is determined by cell source, route of administration and targeting. *J. Extracell. Vesicles* **4**(1), 26316. https://doi.org/10.3402/jev.v4.26316 (2015).
28. Han, C. *et al.* Delivery of miR-675 by stem cell-derived exosomes encapsulated in silk fibroin hydrogel prevents aging-induced vascular dysfunction in mouse hindlimb. *Mater. Sci. Eng. C* **99**, 322–332. https://doi.org/10.1016/j.msec.2019.01.122 (2019).

29. Shi, Q. *et al.* GMSC-derived exosomes combined with a chitosan/silk hydrogel sponge accelerates wound healing in a diabetic rat skin defect model. *Front. Physiol.* https://doi.org/10.3389/fphys.2017.00904 (2017).
30. Liu, X. *et al.* Integration of stem cell-derived exosomes with in situ hydrogel glue as a promising tissue patch for articular cartilage regeneration. *Nanoscale* **9**(13), 4430–4438. https://doi.org/10.1039/C7NR00352H (2017).
31. Xu, N. *et al.* Wound healing effects of a Curcuma zedoaria polysaccharide with platelet-rich plasma exosomes assembled on chitosan/silk hydrogel sponge in a diabetic rat model. *Int. J. Biol. Macromol.* **117**, 102–107. https://doi.org/10.1016/j.ijbiomac.2018.05.066 (2018).
32. Patil, P. P., Reagan, M. R. & Bohara, R. A. Silk fibroin and silk-based biomaterial derivatives for ideal wound dressings. *Int. J. Biol. Macromol.* **164**, 4613–4627. https://doi.org/10.1016/j.ijbiomac.2020.08.041 (2020).
33. Kopp, A. *et al.* Effect of process parameters on additive-free electrospinning of regenerated silk fibroin nonwovens. *Bioact. Mater.* **5**(2), 241–252. https://doi.org/10.1016/j.bioactmat.2020.01.010 (2020).
34. Kopp, A. *et al.* Production and characterization of porous fibroin scaffolds for regenerative medical application. *In Vivo (Brooklyn)* **33**(3), 757–762. https://doi.org/10.21873/invivo.11536 (2019).
35. Chouhan, D. & Mandal, B. B. Silk biomaterials in wound healing and skin regeneration therapeutics: From bench to bedside. *Acta Biomater.* **103**, 24–51. https://doi.org/10.1016/j.actbio.2019.11.050 (2020).
36. Thangavel, P., Ramachandran, B., Kannan, R. & Muthuvijayan, V. Biomimetic hydrogel loaded with silk and <scp>l</scp> -proline for tissue engineering and wound healing applications. *J. Biomed. Mater. Res. Part B Appl. Biomater.* **105**(6), 1401–1408. https://doi.org/10.1002/jbm.b.33675 (2017).
37. Buser, D., Brägger, U., Lang, N. P. & Nyman, S. Regeneration and enlargement of jaw bone using guided tissue regeneration. *Clin. Oral Implants Res.* **1**(1), 22–32. https://doi.org/10.1034/j.1600-0501.1990.010104.x (1990).
38. Ricklefs, F. L. *et al.* Imaging flow cytometry facilitates multiparametric characterization of extracellular vesicles in malignant brain tumours. *J. Extracell. Vesicles* **8**(1), 1588555. https://doi.org/10.1080/20013078.2019.1588555 (2019).
39. Tajirian, A. L. & Goldberg, D. J. A review of sutures and other skin closure materials. *J. Cosmet. Laser Ther.* **12**(6), 296–302. https://doi.org/10.3109/14764172.2010.538413 (2010).
40. Chen, K., Li, Y., Li, Y., Pan, W. & Tan, G. Silk fibroin combined with electrospinning as a promising strategy for tissue regeneration. *Macromol. Biosci.* **23**(2), 2200380. https://doi.org/10.1002/mabi.202200380 (2023).
41. Kundu, B., Rajkhowa, R., Kundu, S. C. & Wang, X. Silk fibroin biomaterials for tissue regenerations. *Adv. Drug Deliv. Rev.* **65**(4), 457–470. https://doi.org/10.1016/j.addr.2012.09.043 (2013).
42. Chen, C., Chuanbao, C., Xilan, M., Yin, T. & Hesun, Z. Preparation of non-woven mats from all-aqueous silk fibroin solution with electrospinning method. *Polymer (Guilalf)* **47**(18), 6322–6327. https://doi.org/10.1016/j.polymer.2006.07.009 (2006).
43. Ha, S. W., Tonelli, A. E. & Hudson, S. M. Structural studies of Bombyx mori silk fibroin during regeneration from solutions and wet fiber spinning. *Biomacromolecules* **6**(3), 1722–1731. https://doi.org/10.1021/bm050010y (2005).
44. Bayraktar, O., Malay, O., Ozgarip, Y. & Batigun, A. Silk fibroin as a novel coating material for controlled release of theophylline. *Eur. J. Pharm. Biopharm.* **60**(3), 373–381. https://doi.org/10.1016/j.ejpb.2005.02.002 (2005).
45. Srivastava, C. M., Purwar, R., Kannaujia, R. & Sharma, D. Flexible silk fibroin films for wound dressing. *Fibers Polym.* **16**(5), 1020–1030. https://doi.org/10.1007/s12221-015-1020-y (2015).
46. Song, Y. *et al.* Silk sericin patches delivering miRNA-29-enriched extracellular vesicles-decorated myoblasts (SPEED) enhances regeneration and functional repair after severe skeletal muscle injury. *Biomaterials* **287**, 121630. https://doi.org/10.1016/j.biomaterials.2022.121630 (2022).
47. Cunnane, E. M. *et al.* Extracellular vesicles enhance the remodeling of cell-free silk vascular scaffolds in rat aortae. *AC S Appl. Mater. Interfaces* **12**(24), 26955–26965. https://doi.org/10.1021/acsami.0c06609 (2022).
48. Kyung Kim, D., Lee, S., Kim, M., Jeong, Y. & Lee, S. Exosome-coated silk fibroin 3D-scaffold for inducing osteogenic differentiation of bone marrow derived mesenchymal stem cells. *Chem. Eng. J.* **406**, 127080. https://doi.org/10.1016/j.cej.2020.127080 (2021).
49. Wang, Z. *et al.* Engineered multifunctional Silk fibroin cryogel loaded with exosomes to promote the regeneration of annulus fibrosus. *Appl. Mater. Today* **29**, 101632. https://doi.org/10.1016/j.apmt.2022.101632 (2022).
50. Zhang, X., Cao, C., Ma, X. & Li, Y. Optimization of macroporous 3-D silk fibroin scaffolds by salt-leaching procedure in organic solvent-free conditions. *J. Mater. Sci. Mater. Med.* https://doi.org/10.1007/s10856-011-4476-3 (2012).
51. Kopp, A. *et al.* Influence of the casting concentration on the mechanical and optical properties of Fa/CaCl2-derived silk fibroin membranes. *Int. J. Mol. Sci.* **21**(18), 1–17. https://doi.org/10.3390/ijms21186704 (2020).
52. Shin, H., Ko, H. & Kim, M. Cytotoxicity and biocompatibility of Zirconia (Y-TZP) posts with various dental cements. *Restor. Dent. Endod.* **41**(3), 167. https://doi.org/10.5395/rde.2016.41.3.167 (2016).
53. Wang, M. O. *et al.* Evaluation of the in vitro cytotoxicity of cross-linked biomaterials. *Biomacromolecules* **14**(5), 1321–1329. https://doi.org/10.1021/bm301962f (2013).
54. Brackett, M. G. *et al.* Cytotoxic response of three cell lines exposed in vitro to dental endodontic sealers. *J. Biomed. Mater. Res. Part B Appl. Biomater.* **95B**(2), 380–386. https://doi.org/10.1002/jbm.b.31727 (2010).
55. Mandal, B. B. & Kundu, S. C. Cell proliferation and migration in silk fibroin 3D scaffolds. *Biomaterials* **30**(15), 2956–2965. https://doi.org/10.1016/j.biomaterials.2009.02.006 (2009).
56. Jiang, S. *et al.* Effects of different aperture-sized type I collagen/silk fibroin scaffolds on the proliferation and differentiation of human dental pulp cells. *Regen. Biomater.* https://doi.org/10.1093/rb/rbab028 (2021).
57. Jung, O. *et al.* Improved in vitro test procedure for full assessment of the cytocompatibility of degradable magnesium based on ISO 10993-5/-12. *Int. J. Mol. Sci.* https://doi.org/10.3390/ijms20020255 (2019).

Acknowledgements

The authors thank Alexander Kopp and Aleksander Drinic from Fibrothelium GmbH, Aachen regarding the silk technology and providing the silk fibroin solution (PureSilk). Further we thank Eric Bibiza and Thomas Derra for support of the statistical evaluation and technical drawing. Special thanks to Miriam Buhl for taking the TEM pictures at Electron Microscopy Facility, Institute of Pathology, RWTH Aachen University Hospital

Author contributions

Conceptualization, S.F., C.A. and R.S.; methodology, validation and formal analysis, S.F., A.S.S., C.L.M., Y.X. and A.D.C.; project administration and resources, R.S., F.L.R. and C.A.; data curation S.F., A.S.S., F.L.R and Y.X.; writing—original draft, S.F., F.L.R and C.A.; writing—review and editing, R.S., A.L.C.G.; supervision, C.A., F.L.R, R.S. and M.G.; all authors have read and agreed to the final version of the manuscript.

Funding

Open Access funding enabled and organized by Projekt DEAL. The authors thank the German Research Foundation (Deutsche Forschungsgemeinschaft, DFG) for its financial support within the research project "EVs for

functionalization of polymers—new biohybrid materials for regenerative medicine in the head and neck surgery" 516860159 (AP 94/3-1 | RI 2616/ 5-1 | SM 214/8-1).

Competing interests

The authors declare no competing interests.

Additional information

Correspondence and requests for materials should be addressed to S.F.

Reprints and permissions information is available at www.nature.com/reprints.

Publisher's note Springer Nature remains neutral with regard to jurisdictional claims in published maps and institutional affiliations.

9 Auszeichnungen und Vorträge

9.1 Preise & Auszeichnungen

10/2023 **2. Platz Implant Dentistry Award** 2023 – Deutsche Gesellschaft für zahnärztliche Implantologie

07/2023 **Tagungspreis** für das beste wissenschaftliche Poster auf der 19. Jahreskongress der Deutschen Gesellschaft für Orale Implantologie, 7. – 8. Juli 2023, Hamburg

10/2021 **Tagungspreis** für das beste Poster auf der 2. ImpAct Masterleague der Deutschen Gesellschaft für Orale Implantologie, Seeheim

9.2 Vorträge & Poster

05/2024 **Vortrag** 72. Jahrestagung der Arbeitsgemeinschaft für Oral- und Kieferchirurgie: *Schichtweise Ablagerung von regeneriertem Seidenfibroin - ein Ansatz zur Oberflächenbeschichtung von biomedizinischen Implantatmaterialien*

02/2024 **Poster** 28. Jahreskongress der Österreichischen Gesellschaft für Mund-, Kiefer- und Gesichtschirurgie: *Einsatz von resorbierbaren Barriere-Membranen auf Seidenfibroin- und Kollagenbasis in der GBR/GTR-Technik – ein in-vivo-Vergleich*

01/2024 **Poster** Arbeitsgemeinschaft für Grundlagenforschung: *Biofunktionalisierung von Seidenfibroin-Scaffolds mit Schmelzmatrixprotein und injizierbarem plättchenreichem Fibrin (iPRF) in ovo*

01/2024 **Poster** Arbeitsgemeinschaft für Grundlagenforschung: *Antibakteriell beladene Magnesiumdrähte für den Einsatz in der Parodontitis- und Periimplantitistherapie*

09/2023 **Vortrag** Deutsche Gesellschaft für Biomaterialien: *Assessment of corrosion, cytocompatibility and immunological effects in vitro of magnesium-based biomaterials for regenerative applications in oral surgery*

09/2023 **Poster** Deutsche Gesellschaft für Biomaterialien: *Antibacterial Properties of Functionalized Silk Fibroin and Sericin Membranes for Wound Healing Applications in Oral and Maxillofacial Surgery*

09/2023 **Vortrag** Additive Manufacturing Meets Medicine: *3D-printed silk fibroin as a resorbable biomaterial in wound healing*

07/2023 **Poster** Deutsche Gesellschaft für Orale Implantologie: *Eine resorbierbare GBR/ GTR-Membran aus Fibroin*

06/2023 **Vortrag** Deutsche Gesellschaft für Mund-, Kiefer- und Gesichtschirurgie: *Eine resorbierbare GBR/ GTR-Membran aus Fibroin*

05/2023 **Vortrag** 71. Jahrestagung der Arbeitsgemeinschaft für Oral- und Kieferchirurgie: *Seidenmatrices als Trägermaterial für extrazelluläre Vesikel in der regenerativen Medizin – ein proof-of-concept*

11/2022 **Poster** Deutsche Gesellschaft für Implantologie: *In vitro-Beurteilung von Magnesium-basierten Biomaterialien in der dentalen Implantologie*

10/2021 **Poster** Deutsche Gesellschaft für Orale Implantologie: *In-vitro Analyse einer Glasmatrix-Oberfläche auf Keramikproben mittels humanen Pulpa-Zellen und L929-Mausfibroblasten*

10 Lebenslauf

1) Persönliche Daten

Name:	Fuest
Vorname:	Sandra
Geburtstag:	13. Januar 1995
Geschlecht:	weiblich
Derzeitige Position:	wissenschaftliche Mitarbeiterin, M.Sc., MBA, Promovendin
Institutsanschrift:	Universitätsklinikum Hamburg-Eppendorf Klinik und Poliklinik für Mund-, Kiefer- und Gesichtschirurgie Martinistraße 52, 20251 Hamburg
Telefon:	015789650692
E-Mail-Adresse:	s.fuest@uke.de

2) Akademische Laufbahn

seit 07/2021	**PhD-Programm** für Nicht-MedizinerInnen, UKE Hamburg-Eppendorf, Doktorvater: Univ.-Prof. Dr. Dr. Ralf Smeets
05/2021 – 01/2023	Masterstudium **Master of Business Administration**, IU Internationale Hochschule,
09/2018 – 01/2020	**Masterstudium** Biomedical Engineering FH Aachen
09/2015 – 07/2018	**Bachelorstudium** Biomedizinische Technik FH Aachen
09/2013 – 03/2015	Bachelorstudium Maschinenbau RWTH Aachen

3) Wissenschaftliche Laufbahn

seit 02/2020	**wissenschaftliche Mitarbeiterin** und Promovendin in der Sektion für „Regenerative orofaziale Medizin“ in der Klinik und Poliklinik für Mund-, Kiefer- und Gesichtschirurgie des Universitätsklinikums Hamburg-Eppendorf
08/2018 – 12/2019	wissenschaftliche Mitarbeiterin der Fibrothelium GmbH
10/2016 – 01/2018	studentische Mitarbeiterin am Institut für angewandte Medizintechnik an der RWTH Aachen

4) Tätigkeiten und Auszeichnungen

10/2023	**Implant Dentistry Award** 2023 (2. Platz) – Deutsche Gesellschaft für Zahnärztliche Implantologie
07/2023	**Tagungspreis** (1. Platz) für das beste wissenschaftliche Poster auf der 19. Jahreskongress der Deutschen Gesellschaft für Orale Implantologie, 7. – 8. Juli 2023, Hamburg
10/2021	**Tagungspreis** (1. Platz) für das beste Poster auf der 2. ImpAct Masterleague der Deutschen Gesellschaft für Orale Implantologie, Seeheim
06/2020	**Erfinderbenennung Patent** WO2020/109222 A1 *„Implant device comprising magnesium and fibroin“*
02/2019 – 12/2019	**Ehrenamtliche Mitarbeitern** an der Sprachenakademie Aachen
11/2018	Best Exhibitor Award 1st Place NRW Nano Conference
09/2015 – 07/2016	DAAD Sprachenzertifikat Level C1 Englisch
07/2010 – 09/2010	Auslandsaufenthalt Australien, Noosa Heads – Sunshine Beach State High-School

11 Literaturverzeichnis

Agarwal, S., Wendorff, J. H. and Greiner, A. (2008) ‘Use of electrospinning technique for biomedical applications’, *Polymer*, 49(26), pp. 5603–5621. doi: 10.1016/j.polymer.2008.09.014.

Ajisawa, A. (1997) ‘Dissolution aqueous of silk fibroin with calciumchloride / ethanol solution’, *The Journal of Sericultural Science of Japan*, 67(2), pp. 91–94.

Alcaraz, M. J., Compañ, A. and Guillén, M. I. (2019) ‘Extracellular Vesicles from Mesenchymal Stem Cells as Novel Treatments for Musculoskeletal Diseases’, *Cells*, 9(1), p. 98. doi: 10.3390/cells9010098.

Altman, G. H. *et al.* (2003) ‘Silk-based biomaterials’, *Biomaterials*, 24(3), pp. 401–416. doi: 10.1016/S0142-9612(02)00353-8.

Amiraliyan, N., Nouri, M. and Kish, M. H. (2009) ‘Effects of Some Electrospinning Parameters on Morphology of Natural Silk-Based Nanofibers’, *Journal of Applied Polymer Science*, 113, pp. 226–234. doi: 10.1002/app.

Andersson, M., Johansson, J. and Rising, A. (2016) ‘Silk Spinning in Silkworms and Spiders’, *International Journal of Molecular Sciences*, 17(8), p. 1290. doi: 10.3390/ijms17081290.

ANDO, Y. *et al.* (2010) ‘Effect of Bacterial Media on the Evaluation of the Antibacterial Activity of a Biomaterial Containing Inorganic Antibacterial Reagents or Antibiotics’, *Biocontrol Science*, 15(1), pp. 15–19. doi: 10.4265/bio.15.15.

Anitha, R. (2011) ‘Indian Silk Industry in the Global Scenario’, *EXCEL International Journal of Interdisciplinary Management Studies*, 1(3).

Aramwit, P., Siritientong, T. and Srichana, T. (2012) ‘Potential applications of silk sericin, a natural protein from textile industry by-products’, *Waste Management and Research*, 30(3), pp. 217–224. doi: 10.1177/0734242X11404733.

Arnon, H. *et al.* (2015) ‘Development of polysaccharides-based edible coatings for citrus fruits: A layer-by-layer approach’, *Food Chemistry*, 166, pp. 465–472. doi: 10.1016/j.foodchem.2014.06.061.

Arpaçay, P. and Türkan, U. (2016) ‘Development of antibiotic-loaded silk fibroin/hyaluronic acid polyelectrolyte film coated CoCrMo alloy’, *Biomedical Engineering / Biomedizinische Technik*, 61(5). doi: 10.1515/bmt-2015-0061.

Asakura, T. *et al.* (2007) ‘Some observations on the structure and function of the spinning apparatus in the silkworm bombyx mori’, *Biomacromolecules*, 8(1), pp. 175–181.

Ayutsede, Jonathan; Gandhi, Milind; Ko, Frank; Micklus, Michael; sukigara, S. (2003) *Regeneration of Bombyx mori silk by electrospinning. Part 1*. Polymer. Bd. 44.

Bakhsheshi-Rad, H. R. *et al.* (2020) ‘Development of the PVA/CS nanofibers containing silk protein sericin as a wound dressing: In vitro and in vivo assessment’, *International Journal of Biological Macromolecules*, 149, pp. 513–521. doi: 10.1016/j.ijbiomac.2020.01.139.

Baumann, K. (2017) *Strukturierungsmethoden für Seidenfibroin-Scaffolds*. Julius-Maximilians-Universität Würzburg.

Bayraktar, O. *et al.* (2005) ‘Silk fibroin as a novel coating material for controlled release of theophylline’, *European Journal of Pharmaceutics and Biopharmaceutics*, 60(3), pp. 373–381. doi: 10.1016/j.ejpb.2005.02.002.

Bhardwaj, N. *et al.* (2015) ‘Silk fibroin–keratin based 3D scaffolds as a dermal substitute for skin tissue

engineering', *Integrative Biology*, 7(1), pp. 53–63. doi: 10.1039/C4IB00208C.
Biggi, S. *et al.* (2020) 'Characterization of Physical, Mechanical, and Biological Properties of SilkBridge Nerve Conduit after Enzymatic Hydrolysis', *ACS Applied Bio Materials*, 3(12), pp. 8361–8374. doi: 10.1021/acsabm.0c00613.
Brackett, M. G. *et al.* (2010) 'Cytotoxic response of three cell lines exposed in vitro to dental endodontic sealers', *Journal of Biomedical Materials Research Part B: Applied Biomaterials*, 95B(2), pp. 380–386. doi: 10.1002/jbm.b.31727.
Bridges, A. W. and García, A. J. (2008) 'Anti-Inflammatory Polymeric Coatings for Implantable Biomaterials and Devices', *Journal of Diabetes Science and Technology*, 2(6), pp. 984–994. doi: 10.1177/193229680800200628.
Broussard, K. C. and Powers, J. G. (2013) 'Wound Dressings: Selecting the Most Appropriate Type', *American Journal of Clinical Dermatology*, 14(6), pp. 449–459. doi: 10.1007/s40257-013-0046-4.
Brown, B. N. and Badylak, S. F. (2014) *Biocompatibility and immune response to biomaterials*, *Regenerative Medicine Applications in Organ Transplantation*. Elsevier Inc. doi: 10.1016/B978-0-12-398523-1.00011-2.
Bunn, H. F., Ransil, B. J. and Chao, A. (1971) 'The Interaction between Erythrocyte Organic Phosphates, Magnesium Ion, and Hemoglobin', *Journal of Biological Chemistry*, 246(17), pp. 5273–5279. doi: 10.1016/S0021-9258(18)61903-9.
Cao, Y. and Wang, B. (2009) 'Biodegradation of silk biomaterials', *International Journal of Molecular Sciences*, pp. 1514–1524. doi: 10.3390/ijms10041514.
Chandrasekaran, N. *et al.* (2015) 'Biobased silver nanocolloid coating on silk fibers for prevention of post-surgical wound infections', *International Journal of Nanomedicine*, p. 159. doi: 10.2147/IJN.S82211.
Chao, P.-H. G. *et al.* (2010) 'Silk hydrogel for cartilage tissue engineering', *Journal of Biomedical Materials Research Part B: Applied Biomaterials*, 95B(1), pp. 84–90. doi: 10.1002/jbm.b.31686.
Chen, C. *et al.* (2006) 'Preparation of non-woven mats from all-aqueous silk fibroin solution with electrospinning method', *Polymer*, 47(18), pp. 6322–6327. doi: 10.1016/j.polymer.2006.07.009.
Chen, J. *et al.* (2018) 'Enhanced physical and biological properties of silk fibroin nanofibers by layer-by-layer deposition of chitosan and rectorite', *Journal of Colloid and Interface Science*, 523, pp. 208–216. doi: 10.1016/j.jcis.2018.03.093.
Cheng, G. *et al.* (2018) 'Advanced Silk Fibroin Biomaterials for Cartilage Regeneration', *ACS Biomaterials Science & Engineering*, 4(8), pp. 2704–2715. doi: 10.1021/acsbiomaterials.8b00150.
Chopra, S. and Gulrajani, M. L. (1994) 'Comparative evaluation of the various methods of degumming silk', *Indian Journal of Fibre & Textile Research*, 19(June), pp. 76–3.
Chouhan, D. and Mandal, B. B. (2020) 'Silk biomaterials in wound healing and skin regeneration therapeutics: From bench to bedside', *Acta Biomaterialia*, 103, pp. 24–51. doi: 10.1016/j.actbio.2019.11.050.
Colao, I. L. *et al.* (2018) 'Manufacturing Exosomes: A Promising Therapeutic Platform', *Trends in Molecular Medicine*, 24(3), pp. 242–256. doi: 10.1016/j.molmed.2018.01.006.
Colomban, P. and Jauzein, V. (2018) 'Silk: fibers, films, and composites - types, processing, structure, and mechanics', in *Handbook of Properties of Textile and Technical Fibres*. Elsevier, pp. 137–183. doi:

10.1016/B978-0-08-101272-7.00005-5.
Curtis, M. A., Diaz, P. I. and Van Dyke, T. E. (2020) 'The role of the microbiota in periodontal disease', *Periodontology 2000*. Edited by R. J. Mariano, 83(1), pp. 14–25. doi: 10.1111/prd.12296.
Drinic, A. (2019) *Entwicklung einer nadellos elektrogesponnenen Seidenfibroin Membran zur Separierung von Gewebearten*. Universität Stuttgart.
Echeverry-Rendón, M. *et al.* (2017) 'Modification of titanium alloys surface properties by plasma electrolytic oxidation (PEO) and influence on biological response', *Journal of Materials Science: Materials in Medicine*, 28(11), p. 169. doi: 10.1007/s10856-017-5972-x.
Emara, A. and Shah, R. (2021) 'Recent update on craniofacial tissue engineering', *Journal of Tissue Engineering*, 12, p. 204173142110037. doi: 10.1177/20417314211003735.
Fang, S.-M. *et al.* (2015) 'Comparative analysis of the silk gland transcriptomes between the domestic and wild silkworms', *BMC Genomics*, 16(1), p. 60. doi: 10.1186/s12864-015-1287-9.
Farahani, M. and Shafiee, A. (2021) 'Wound Healing: From Passive to Smart Dressings', *Advanced Healthcare Materials*, 10(16). doi: 10.1002/adhm.202100477.
Farè, S. *et al.* (2013) 'In vitro study on silk fibroin textile structure for Anterior Cruciate Ligament regeneration', *Materials Science and Engineering C*, 33(7), pp. 3601–3608. doi: 10.1016/j.msec.2013.04.027.
Fibrothelium GmbH (2022). Available at: https://www.fibrothelium.com/.
Fitzpatrick, V. *et al.* (2021) 'Functionalized 3D-printed silk-hydroxyapatite scaffolds for enhanced bone regeneration with innervation and vascularization', *Biomaterials*, 276, p. 120995. doi: 10.1016/j.biomaterials.2021.120995.
Flanagan, M. (2000) 'The physiology of wound healing', *Journal of Wound Care*, 9(6), pp. 299–300. doi: 10.12968/jowc.2000.9.6.25994.
Franz, S. *et al.* (2011) 'Immune responses to implants - A review of the implications for the design of immunomodulatory biomaterials', *Biomaterials*, 32(28), pp. 6692–6709. doi: 10.1016/j.biomaterials.2011.05.078.
Frich, L. H. *et al.* (1997) 'Bone strength and material properties of the glenoid', *Journal of Shoulder and Elbow Surgery*, 6(2), pp. 97–104. doi: 10.1016/S1058-2746(97)90029-X.
Fu, C., Shao, Z. and Fritz, V. (2009) 'Animal silks: their structures, properties and artificial production', *Chemical Communications*, (43), p. 6515. doi: 10.1039/b911049f.
Fuest, S. *et al.* (2023) 'Layer-by-Layer Deposition of Regenerated Silk Fibroin─An Approach to the Surface Coating of Biomedical Implant Materials', *ACS Biomaterials Science & Engineering*. doi: 10.1021/acsbiomaterials.3c00852.
Fuest, S. *et al.* (2024) 'Doping of casted silk fibroin membranes with extracellular vesicles for regenerative therapy: a proof of concept', *Scientific Reports*, 14(1), p. 3553. doi: 10.1038/s41598-024-54014-y.
Gailani, D. and Renné, T. (2007) 'Intrinsic Pathway of Coagulation and Arterial Thrombosis', *Arteriosclerosis, Thrombosis, and Vascular Biology*, 27(12), pp. 2507–2513. doi: 10.1161/ATVBAHA.107.155952.
Gamal, A. Y. and Iacono, V. J. (2013) 'Enhancing Guided Tissue Regeneration of Periodontal Defects by Using a Novel Perforated Barrier Membrane', *Journal of Periodontology*, 84(7), pp. 905–913. doi:

10.1902/jop.2012.120301.
Garcia-Fuentes, M. *et al.* (2008) 'The effect of hyaluronic acid on silk fibroin conformation', *Biomaterials*, 29(6), pp. 633–642. doi: 10.1016/j.biomaterials.2007.10.024.
Gardiner, C. *et al.* (2016) 'Techniques used for the isolation and characterization of extracellular vesicles: results of a worldwide survey', *Journal of Extracellular Vesicles*, 5(1), p. 32945. doi: 10.3402/jev.v5.32945.
Gardner, A. B. *et al.* (2013) 'Biomaterials-Based Modulation of the Immune System', *BioMed Research International*, 2013, pp. 1–7. doi: 10.1155/2013/732182.
Gautam, R., Jain, A. and Kapoor, S. (2017) 'Silk Protein based Novel Matrix for Tissue Engineering Applications', *Indian Journal of Science and Technology*, 10(31), pp. 1–7. doi: 10.17485/ijst/2017/v10i31/113863.
Ge, Z. *et al.* (2012) 'Assessment of silk fibroin for the repair of buccal mucosa in a rat model', *International Journal of Oral and Maxillofacial Surgery*, 41(5), pp. 673–680. doi: 10.1016/j.ijom.2011.11.016.
Gholipourmalekabadi, M. *et al.* (2020) 'Silk fibroin for skin injury repair: Where do things stand?', *Advanced Drug Delivery Reviews*, 153, pp. 28–53. doi: 10.1016/j.addr.2019.09.003.
Ghumatkar, A. *et al.* (2016) 'Influence of adherend surface roughness on the adhesive bond strength', *Latin American Journal of Solids and Structures*, 13(13), pp. 2356–2370. doi: 10.1590/1679-78253066.
Gil, E. S. *et al.* (2011) 'Response of Human Corneal Fibroblasts on Silk Film Surface Patterns', *Macromol. Biosci.*, 10(6), pp. 664–673. doi: 10.1002/mabi.200900452.Response.
Gilotra, S. *et al.* (2018) 'Potential of silk sericin based nanofibrous mats for wound dressing applications', *Materials Science and Engineering: C*, 90, pp. 420–432. doi: 10.1016/j.msec.2018.04.077.
Gonzalez, A. C. de O. *et al.* (2016) 'Wound healing - A literature review', *Anais Brasileiros de Dermatologia*, 91(5), pp. 614–620. doi: 10.1590/abd1806-4841.20164741.
Gopinath, V. *et al.* (2017) 'Biogenic synthesis, characterization of antibacterial silver nanoparticles and its cell cytotoxicity', *Arabian Journal of Chemistry*, 10(8), pp. 1107–1117. doi: 10.1016/j.arabjc.2015.11.011.
Gregor Lang (2015) *Herstellung und Charakterisierung von Fasern aus rekombinanten Spinnenseidenproteinen und deren potentielle Applikationen*. Universität Bayreuth. Available at: https://epub.uni-bayreuth.de/id/eprint/2038/1/Dissertation_Lang.pdf.
Gruessner, U. *et al.* (2001) 'Improvement of perineal wound healing by local administration of gentamicin-impregnated collagen fleeces after abdominoperineal excision of rectal cancer', *The American Journal of Surgery*, 182(5), pp. 502–509. doi: 10.1016/S0002-9610(01)00762-0.
Guo, X. *et al.* (2016) 'Proteins in the Cocoon of Silkworm Inhibit the Growth of Beauveria bassiana', *PLOS ONE*. Edited by E. Ling, 11(3), p. e0151764. doi: 10.1371/journal.pone.0151764.
Guo, Y. *et al.* (2019) 'Tightly adhered silk fi broin coatings on Ti6Al4V biometals for improved wettability and compatible mechanical properties', *Materials & Design*, 175, p. 107825. doi: 10.1016/j.matdes.2019.107825.
Ha, S. W., Tonelli, A. E. and Hudson, S. M. (2005) 'Structural studies of Bombyx mori silk fibroin during regeneration from solutions and wet fiber spinning', *Biomacromolecules*, 6(3), pp. 1722–1731. doi: 10.1021/bm050010y.

Haghi, A.; Zaikov, G. E. (2011) 'Electrospinning process and nanofiber research', *New York: Noca Science Publishers*.

Han, C. *et al.* (2019) 'Delivery of miR-675 by stem cell-derived exosomes encapsulated in silk fibroin hydrogel prevents aging-induced vascular dysfunction in mouse hindlimb', *Materials Science and Engineering: C*, 99, pp. 322–332. doi: 10.1016/j.msec.2019.01.122.

Hanken, H. *et al.* (2016) 'Attachment, Viability and Adipodifferentiation of Pre-adipose Cells on Silk Scaffolds with and Without Co-expressed FGF-2 and VEGF', *In Vivo*, 30(5), pp. 567–572.

Hardy, J. G. and Scheibel, T. R. (2010) 'Composite materials based on silk proteins', *Progress in Polymer Science (Oxford)*, 35(9), pp. 1093–1115. doi: 10.1016/j.progpolymsci.2010.04.005.

Harkin, D. G. *et al.* (2011a) 'Silk fibroin in ocular tissue reconstruction', *Biomaterials*, 32(10), pp. 2445–2458. doi: 10.1016/j.biomaterials.2010.12.041.

Harkin, D. G. *et al.* (2011b) 'Silk fibroin in ocular tissue reconstruction', *Biomaterials*, 32(10), pp. 2445–2458. doi: 10.1016/j.biomaterials.2010.12.041.

Hassani Besheli, N. *et al.* (2017) 'Sustainable Release of Vancomycin from Silk Fibroin Nanoparticles for Treating Severe Bone Infection in Rat Tibia Osteomyelitis Model', *ACS Applied Materials & Interfaces*, 9(6), pp. 5128–5138. doi: 10.1021/acsami.6b14912.

He, H. *et al.* (2017) 'In situ green synthesis and characterization of sericin-silver nanoparticle composite with effective antibacterial activity and good biocompatibility', *Materials Science and Engineering: C*, 80, pp. 509–516. doi: 10.1016/j.msec.2017.06.015.

He, J.-H. *et al.* (2008) 'BioMimic fabrication of electrospun nanofibers with high-throughput', *Chaos, Solitons & Fractals*, 37(3), pp. 643–651. doi: 10.1016/j.chaos.2007.11.028.

Hodgkinson, A. T. and Bayat, A. (2014) *Silk for dermal tissue engineering*, *Silk Biomaterials for Tissue Engineering and Regenerative Medicine*. Woodhead Publishing Limited. doi: 10.1533/9780857097064.3.456.

Hofmann, S. *et al.* (2014) 'Effect of sterilization on structural and material properties of 3-D silk fibroin scaffolds', *Acta Biomaterialia*, 10(1), pp. 308–317. doi: 10.1016/j.actbio.2013.08.035.

Horan, R. L. *et al.* (2005) 'In vitro degradation of silk fibroin', *Biomaterials*. doi: 10.1016/j.biomaterials.2004.09.020.

Hu, X. *et al.* (2011) 'Regulation of Silk Material Structure by Temperature-Controlled Water Vapor Annealing', *Biomacromolecules*, 12(5), pp. 1686–1696. doi: 10.1021/bm200062a.

Huang, W. *et al.* (2012) 'Regenerative potential of silk conduits in repair of peripheral nerve injury in adult rats', *Biomaterials*, 33(1), pp. 59–71. doi: 10.1016/j.biomaterials.2011.09.030.

Huang, W. *et al.* (2018) 'Silkworm silk-based materials and devices generated using bio-nanotechnology', *Chemical Society Reviews*, 47(17), pp. 6486–6504. doi: 10.1039/C8CS00187A.

Jaya Prakash, N., Wang, X. and Kandasubramanian, B. (2023) 'Regenerated silk fibroin loaded with natural additives: a sustainable approach towards health care', *Journal of Biomaterials Science, Polymer Edition*, 34(10), pp. 1453–1490. doi: 10.1080/09205063.2023.2170137.

Jiang, C. *et al.* (2007) 'Mechanical properties of robust ultrathin silk fibroin films', *Advanced Functional Materials*, 17(13), pp. 2229–2237. doi: 10.1002/adfm.200601136.

Jiang, S. *et al.* (2021) 'Effects of different aperture-sized type I collagen/silk fibroin scaffolds on the proliferation and differentiation of human dental pulp cells', *Regenerative Biomaterials*, 8(4). doi:

10.1093/rb/rbab028.
Jin, H.-J. *et al.* (2005) 'Water-Stable Silk Films with Reduced β-Sheet Content', *Advanced Functional Materials*, 15(8), pp. 1241–1247. doi: 10.1002/adfm.200400405.
Jindal, S. K. *et al.* (2014) *Silk scaffolds for dental tissue engineering*, *Silk Biomaterials for Tissue Engineering and Regenerative Medicine*. Woodhead Publishing Limited. doi: 10.1533/9780857097064.3.403.
Jo, Y.-Y. *et al.* (2019) '4-Hexylresorcinol and silk sericin increase the expression of vascular endothelial growth factor via different pathways', *Scientific Reports*, 9(1), p. 3448. doi: 10.1038/s41598-019-40027-5.
Juncos Bombin, A. D., Dunne, N. J. and McCarthy, H. O. (2020) 'Electrospinning of natural polymers for the production of nanofibres for wound healing applications', *Materials Science and Engineering: C*, 114, p. 110994. doi: 10.1016/j.msec.2020.110994.
Karageorgiou, V. *et al.* (2006) 'Porous silk fibroin 3-D scaffolds for delivery of bone morphogenetic protein-2 in vitro and in vivo', *Journal of Biomedical Materials Research Part A*, 78A(2), pp. 324–334. doi: 10.1002/jbm.a.30728.
Kasoju, N., Bhonde, R. R. and Bora, U. (2009) 'Fabrication of a novel micro–nano fibrous nonwoven scaffold with Antheraea assama silk fibroin for use in tissue engineering', *Materials Letters*, 63(28), pp. 2466–2469. doi: 10.1016/j.matlet.2009.08.037.
Kasoju, N. and Bora, U. (2012a) 'Fabrication and characterization of curcumin-releasing silk fibroin scaffold', *Journal of Biomedical Materials Research Part B: Applied Biomaterials*, 100B(7), pp. 1854–1866. doi: 10.1002/jbm.b.32753.
Kasoju, N. and Bora, U. (2012b) 'Silk fibroin in tissue engineering', *Advanced Healthcare Materials*, 1(4), pp. 393–412. doi: 10.1002/adhm.201200097.
Kasoju, N. and Bora, U. (2012c) 'Silk Fibroin in Tissue Engineering', *Advanced Healthcare Materials*, 1(4), pp. 393–412. doi: 10.1002/adhm.201200097.
Khan, A. ur R. *et al.* (2019) 'Physico-Chemical and Biological Evaluation of PLCL/SF Nanofibers Loaded with Oregano Essential Oil', *Pharmaceutics*, 11(8), p. 386. doi: 10.3390/pharmaceutics11080386.
Khan, M. M. R. and Tsukada, M. (2014) *Electrospun silk sericin nanofibers for biomedical applications*, *Silk Biomaterials for Tissue Engineering and Regenerative Medicine*. Woodhead Publishing Limited. doi: 10.1533/9780857097064.1.125.
Kim, J.-Y. *et al.* (2014) 'Comparable efficacy of silk fibroin with the collagen membranes for guided bone regeneration in rat calvarial defects', *The Journal of Advanced Prosthodontics*, 6(6), p. 539. doi: 10.4047/jap.2014.6.6.539.
Kim, J. *et al.* (2010) 'Comparison of methods for the repair of acute tympanic membrane perforations: Silk patch vs. paper patch', *Wound Repair and Regeneration*, 18(1), pp. 132–138. doi: 10.1111/j.1524-475X.2009.00565.x.
Kim, S. H. *et al.* (2003) 'Silk Fibroin Nanofiber. Electrospinning, Properties, and Structure', *Polymer Journal*, 35(2), pp. 185–190. doi: 10.1295/polymj.35.185.
Klasen, H. J. (2000) 'Historical review of the use of silver in the treatment of burns. I. Early uses', *Burns*, 26(2), pp. 117–130. doi: 10.1016/S0305-4179(99)00108-4.
Koh, L. D. *et al.* (2015a) 'Structures, mechanical properties and applications of silk fibroin materials',

Progress in Polymer Science, 46, pp. 86–110. doi: 10.1016/j.progpolymsci.2015.02.001.
Koh, L. D. *et al.* (2015b) 'Structures, mechanical properties and applications of silk fibroin materials', *Progress in Polymer Science*, 46, pp. 86–110. doi: 10.1016/j.progpolymsci.2015.02.001.
Koh, T. J. and DiPietro, L. A. (2011) 'Inflammation and wound healing: the role of the macrophage', *Expert Reviews in Molecular Medicine*, 13, p. e23. doi: 10.1017/S1462399411001943.
Kopp, A. *et al.* (2019a) 'Production and characterization of porous fibroin scaffolds for regenerative medical application', *In Vivo*, 33(3), pp. 757–762. doi: 10.21873/invivo.11536.
Kopp, A. *et al.* (2019b) 'Production and characterization of porous fibroin scaffolds for regenerative medical application', *In Vivo*, 33(3), pp. 757–762. doi: 10.21873/invivo.11536.
Kopp, A., Smeets, R., *et al.* (2020) 'Effect of process parameters on additive-free electrospinning of regenerated silk fibroin nonwovens', *Bioactive Materials*, 5(2), pp. 241–252. doi: 10.1016/j.bioactmat.2020.01.010.
Kopp, A., Schunck, L., *et al.* (2020) 'Influence of the casting concentration on the mechanical and optical properties of Fa/CaCl2-derived silk fibroin membranes', *International Journal of Molecular Sciences*, 21(18), pp. 1–17. doi: 10.3390/ijms21186704.
Kuboyama, N. *et al.* (2013) 'Silk fibroin-based scaffolds for bone regeneration', *Journal of Biomedical Materials Research - Part B Applied Biomaterials*, 101 B(2), pp. 295–302. doi: 10.1002/jbm.b.32839.
Kundu, B. *et al.* (2013a) 'Silk fibroin biomaterials for tissue regenerations', *Advanced Drug Delivery Reviews*, 65(4), pp. 457–470. doi: 10.1016/j.addr.2012.09.043.
Kundu, B. *et al.* (2013b) 'Silk fibroin biomaterials for tissue regenerations', *Advanced Drug Delivery Reviews*, pp. 457–470. doi: 10.1016/j.addr.2012.09.043.
Kundu, B. *et al.* (no date) 'Silk fibroin biomaterials for tissue regnerations', *Advanced Drug Delivery Reviews*, 65(4), pp. 457–470. doi: https://doi.org/10.1016/j.addr.2012.09.043.
Kwong, A. *et al.* (2020) 'Gentamicin Induces Laminin 332 and Improves Wound Healing in Junctional Epidermolysis Bullosa Patients with Nonsense Mutations', *Molecular Therapy*, 28(5), pp. 1327–1338. doi: 10.1016/j.ymthe.2020.03.006.
Kyung Kim, D. *et al.* (2021) 'Exosome-coated silk fibroin 3D-scaffold for inducing osteogenic differentiation of bone marrow derived mesenchymal stem cells', *Chemical Engineering Journal*, 406, p. 127080. doi: 10.1016/j.cej.2020.127080.
Kzhyshkowska, J. *et al.* (2015) 'Macrophage responses to implants: prospects for personalized medicine', *Journal of Leukocyte Biology*, 98(6), pp. 953–962. doi: 10.1189/jlb.5VMR0415-166R.
Lamboni, L. *et al.* (2015) 'Silk sericin: A versatile material for tissue engineering and drug delivery', *Biotechnology Advances*, 33(8), pp. 1855–1867. doi: 10.1016/j.biotechadv.2015.10.014.
Lehmann, T. *et al.* (2022) 'Silk Fibroin-Based Therapeutics for Impaired Wound Healing', *Pharmaceutics*, 14(3), p. 651. doi: 10.3390/pharmaceutics14030651.
Li, H. *et al.* (2023) 'A pilot study of stable isotope fractionation in Bombyx mori rearing', *Scientific Reports*, 13(0123456789), pp. 1–11. doi: 10.1038/s41598-023-33790-z.
Li, M. and Li, J. (2014) 'Biodegradation behavior of silk biomaterials', *Silk Biomaterials for Tissue Engineering and Regenerative Medicine*, pp. 330–348. doi: 10.1533/9780857097064.2.330.
Li, P. *et al.* (2017) 'Progress in Exosome Isolation Techniques', *Theranostics*, 7(3), pp. 789–804. doi: 10.7150/thno.18133.

Li, Z. H. *et al.* (2013) 'Silk fibroin-based scaffolds for tissue engineering', *Frontiers of Materials Science*, 7(3), pp. 237–247. doi: 10.1007/s11706-013-0214-8.

Liivak, O. *et al.* (1998) 'A Microfabricated Wet-Spinning Apparatus To Spin Fibers of Silk Proteins. Structure−Property Correlations', *Macromolecules*, 31(9), pp. 2947–2951. doi: 10.1021/ma971626l.

Liu, X. *et al.* (2017) 'Integration of stem cell-derived exosomes with in situ hydrogel glue as a promising tissue patch for articular cartilage regeneration', *Nanoscale*, 9(13), pp. 4430–4438. doi: 10.1039/C7NR00352H.

Liu, Y. *et al.* (2021) 'Exosomes derived from stem cells from apical papilla promote craniofacial soft tissue regeneration by enhancing Cdc42-mediated vascularization', *Stem Cell Research & Therapy*, 12(1), p. 76. doi: 10.1186/s13287-021-02151-w.

Lu, Q. *et al.* (2008) 'Preparation of three-dimensional fibroin/collagen scaffolds in various pH conditions', *Journal of Materials Science: Materials in Medicine*. doi: 10.1007/s10856-007-3180-9.

Lu, S. *et al.* (2015) 'A novel silk fibroin nanofibrous membrane for guided bone regeneration: A study in rat calvarial defects', *American Journal of Translational Research*, 7(11), pp. 2244–2253.

Luo, Z. *et al.* (2015) 'Effect of pore size on the biodegradation rate of silk fibroin scaffolds', *Advances in Materials Science and Engineering*, 2015, pp. 1–8. doi: 10.1155/2015/315397.

Luthringer, B. J. C., Feyerabend, F. and Römer, R. W. (2014) 'Magnesium-Based Implants: A Mini-Review', *Magnesium Research*, 27(4), pp. 142–154. doi: 10.1684/mrh.2015.0375.

Lv, X. *et al.* (2016) 'Structural and functional evaluation of oxygenating keratin/silk fibroin scaffold and initial assessment of their potential for urethral tissue engineering', *Biomaterials*, 84, pp. 99–110. doi: 10.1016/j.biomaterials.2016.01.032.

Lv, X. *et al.* (2018) 'A Novel Approach for Sericin-Conjugated Silver Nanoparticle Synthesis and Their Potential as Microbicide Candidates', *Journal of Microbiology and Biotechnology*, 28(8), pp. 1367–1375. doi: 10.4014/jmb.1802.02054.

Makaya, K. *et al.* (2009) 'Comparative study of silk fibroin porous scaffolds derived from salt/water and sucrose/hexafluoroisopropanol in cartilage formation', *Journal of Bioscience and Bioengineering*, 108(1), pp. 68–75. doi: 10.1016/j.jbiosc.2009.02.015.

Makvandi, P. *et al.* (2020) 'Hyaluronic acid/corn silk extract based injectable nanocomposite: A biomimetic antibacterial scaffold for bone tissue regeneration', *Materials Science and Engineering: C*, 107, p. 110195. doi: 10.1016/j.msec.2019.110195.

Mandal, B. B. and Kundu, S. C. (2009) 'Cell proliferation and migration in silk fibroin 3D scaffolds', *Biomaterials*, 30(15), pp. 2956–2965. doi: 10.1016/j.biomaterials.2009.02.006.

Meinel, L. and Kaplan, D. L. (2012) 'Silk constructs for delivery of musculoskeletal therapeutics', *Advanced Drug Delivery Reviews*, 64(12), pp. 1111–1122. doi: 10.1016/j.addr.2012.03.016.

Melke, J. *et al.* (2016) 'Silk fibroin as biomaterial for bone tissue engineering', *Acta Biomaterialia*, 31, pp. 1–16. doi: 10.1016/j.actbio.2015.09.005.

Meng, X., Zhu, F. and Chen, K. (2017) 'Silkworm: A promising model organism in life science', *Journal of Insect Science*, 17(5). doi: 10.1093/jisesa/iex064.

Min, B. M. *et al.* (2004) 'Electrospinning of silk fibroin nanofibers and its effect on the adhesion and spreading of normal human keratinocytes and fibroblasts in vitro', *Biomaterials*, 25(7–8), pp. 1289–1297. doi: 10.1016/j.biomaterials.2003.08.045.

Mingo, B. *et al.* (2018) 'Influence of sealing post-treatments on the corrosion resistance of PEO coated AZ91 magnesium alloy', *Applied Surface Science*, 433, pp. 653–667. doi: 10.1016/j.apsusc.2017.10.083.

Molinnus, D. *et al.* (2021) 'Towards a flexible electrochemical biosensor fabricated from biocompatible Bombyx mori silk', *Biosensors and Bioelectronics*, 183, p. 113204. doi: 10.1016/j.bios.2021.113204.

Momen-Heravi, F. *et al.* (2013) 'Current methods for the isolation of extracellular vesicles', *bchm*, 394(10), pp. 1253–1262. doi: 10.1515/hsz-2013-0141.

Monroe, D. M. and Hoffman, M. (2006) 'What Does It Take to Make the Perfect Clot?', *Arteriosclerosis, Thrombosis, and Vascular Biology*, 26(1), pp. 41–48. doi: 10.1161/01.ATV.0000193624.28251.83.

Napavichayanun, S. and Aramwit, P. (2017) 'Effect of animal products and extracts on wound healing promotion in topical applications: a review', *Journal of Biomaterials Science, Polymer Edition*, 28(8), pp. 703–729. doi: 10.1080/09205063.2017.1301772.

Naskar, D., Barua, R. R., *et al.* (2014) *Introduction to silk biomaterials*, *Silk Biomaterials for Tissue Engineering and Regenerative Medicine*. Woodhead Publishing Limited. doi: 10.1533/9780857097064.1.3.

Naskar, D., Barua, R.R., *et al.* (2014) 'Silk Biomaterials for Tissue Engineering and Regenerative Medicine', *Silk Biomaterials for Tissue Engineering and Regenerative Medicine*, pp. xiii–xvii. Available at: http://www.sciencedirect.com/science/article/pii/B9780857096999500239.

Nazarov, Rina; Jin, Hyoung-Joon; kaplan, D. L. (2004) 'Porous 3-D Scaffolds from Regenerated Silk Fibroin', *Biomacromolecules*, 5(3), pp. 718–726.

Nazarov, R., Jin, H.-J. and Kaplan, D. L. (2004) 'Porous 3-D Scaffolds from Regenerated Silk Fibroin', *Biomacromolecules*, 5(3), pp. 718–726. doi: 10.1021/bm034327e.

Nguyen, T. P. *et al.* (2019) 'Silk Fibroin-Based Biomaterials for Biomedical Applications: A Review', *Polymers*, 11(12), p. 1933. doi: 10.3390/polym11121933.

Ninan, N. *et al.* (2015) 'Natural Polymer/Inorganic Material Based Hybrid Scaffolds for Skin Wound Healing', *Polymer Reviews*, 55(3), pp. 453–490. doi: 10.1080/15583724.2015.1019135.

Noosak, C. *et al.* (2022) 'Dual-functional bioactive silk sericin for osteoblast responses and osteomyelitis treatment', *PLOS ONE*. Edited by J. Xu, 17(3), p. e0264795. doi: 10.1371/journal.pone.0264795.

Numata, K. (2014) *Silk hydrogels for tissue engineering and dual-drug delivery*, *Silk Biomaterials for Tissue Engineering and Regenerative Medicine*. Woodhead Publishing Limited. doi: 10.1533/9780857097064.3.503.

Nwekwo, C. W. (2015) *Antimicrobial Activity of Silk Fibroin Microparticles*. The Graduate School of Applied Sciences of Near East University.

Omenetto, F. G. and Kaplan, D. L. (2010) 'New opportunities for an ancient material', *Science*, 329(5991), pp. 528–531. doi: 10.1126/science.1188936.

Page, M. J. *et al.* (2021) 'The PRISMA 2020 statement: An updated guideline for reporting systematic reviews', *PLOS Medicine*, 18(3), p. e1003583. doi: 10.1371/journal.pmed.1003583.

Panda, K. K. *et al.* (2011) 'In vitro biosynthesis and genotoxicity bioassay of silver nanoparticles using plants', *Toxicology in Vitro*, 25(5), pp. 1097–1105. doi: 10.1016/j.tiv.2011.03.008.

Panilaitis, B. *et al.* (2003) 'Macrophage responses to silk', 24, pp. 3079–3085. doi: 10.1016/S0142-9612(03)00158-3.

Parivatphun, T. *et al.* (2022) 'Biphasic scaffolds of polyvinyl alcohol with silk fibroin for oral and maxillofacial surgery based on mimicking materials design: fabrication, characterization, properties', *Journal of Materials Science*, 57(3), pp. 2131–2148. doi: 10.1007/s10853-021-06718-z.

Park, Y. R. *et al.* (2018) 'NF-κB signaling is key in the wound healing processes of silk fibroin', *Acta Biomaterialia*, 67, pp. 183–195. doi: 10.1016/j.actbio.2017.12.006.

Patil, P. P., Reagan, M. R. and Bohara, R. A. (2020) 'Silk fibroin and silk-based biomaterial derivatives for ideal wound dressings', *International Journal of Biological Macromolecules*, 164, pp. 4613–4627. doi: 10.1016/j.ijbiomac.2020.08.041.

Piao, M. J. *et al.* (2011) 'Silver nanoparticles induce oxidative cell damage in human liver cells through inhibition of reduced glutathione and induction of mitochondria-involved apoptosis', *Toxicology Letters*, 201(1), pp. 92–100. doi: 10.1016/j.toxlet.2010.12.010.

Pins, G. D. *et al.* (1997) 'Self-assembly of collagen fibers. Influence of fibrillar alignment and decorin on mechanical properties', *Biophysical Journal*, 73(4), pp. 2164–2172. doi: 10.1016/S0006-3495(97)78247-X.

Qian, C. *et al.* (2020) 'Vascularized silk electrospun fiber for promoting oral mucosa regeneration', *NPG Asia Materials*, 12(1), p. 39. doi: 10.1038/s41427-020-0221-z.

Qian, Z. *et al.* (2020) 'A moisturizing chitosan-silk fibroin dressing with silver nanoparticles-adsorbed exosomes for repairing infected wounds', *Journal of Materials Chemistry B*, 8(32), pp. 7197–7212. doi: 10.1039/D0TB01100B.

Ramadass, S. K. *et al.* (2019) 'Type I collagen peptides and nitric oxide releasing electrospun silk fibroin scaffold: A multifunctional approach for the treatment of ischemic chronic wounds', *Colloids and Surfaces B: Biointerfaces*, 175, pp. 636–643. doi: 10.1016/j.colsurfb.2018.12.025.

Rasouli, R., Barhoum, A. and Uludag, H. (2018) 'A review of nanostructured surfaces and materials for dental implants: surface coating, patterning and functionalization for improved performance', *Biomaterials Science*, 6(6), pp. 1312–1338. doi: 10.1039/C8BM00021B.

Recum, A. F. Van and Laberge, M. (1995) 'Educational Goals for Biomaterials Science and Engineering : Prospective View', 6, pp. 137–144.

Reeves, A. R. D. *et al.* (2015) 'Controlled release of cytokines using silk-biomaterials for macrophage polarization', *Biomaterials*, 73, pp. 272–283. doi: 10.1016/j.biomaterials.2015.09.027.

Rentsch, C. *et al.* (2012) 'Knochenersatz', *Der Unfallchirurg*, 115(10), pp. 938–949. doi: 10.1007/s00113-012-2238-4.

Rockwood, Danielle N., Gil, E. S., *et al.* (2011) 'Ingrowth of human mesenchymal stem cells into porous silk particle reinforced silk composite scaffolds: An in vitro study', *Acta Biomaterialia*, 7(1), pp. 144–151. doi: 10.1016/j.actbio.2010.07.020.

Rockwood, Danielle N *et al.* (2011) 'Materials fabrication from Bombyx mori silk fibroin', *Nature Protocols*, 6(10), pp. 1612–1631. doi: 10.1038/nprot.2011.379.

Rockwood, Danielle N., Preda, R. C., *et al.* (2011) 'Materials fabrication from Bombyx mori silk fibroin', *Nature Protocols*, 6(10), pp. 1612–1631. doi: 10.1038/nprot.2011.379.

Roh, D.-H. *et al.* (2006) 'Wound healing effect of silk fibroin/alginate-blended sponge in full thickness skin defect of rat', *Journal of Materials Science: Materials in Medicine*, 17(6), pp. 547–552. doi: 10.1007/s10856-006-8938-y.

Roh, D. H. *et al.* (2006) 'Wound healing effect of silk fibroin/alginate-blended sponge in full thickness skin defect of rat', *Journal of Materials Science: Materials in Medicine*. doi: 10.1007/s10856-006-8938-y.

Rosen, H. R. *et al.* (1991) 'Local gentamicin application for perineal wound healing following abdominoperineal rectum excision', *The American Journal of Surgery*, 162(5), pp. 438–441. doi: 10.1016/0002-9610(91)90256-D.

Rouabhia, M. and Allaire, P. (2010) 'Gingival mucosa regeneration in athymic mice using in vitro engineered human oral mucosa', *Biomaterials*, 31(22), pp. 5798–5804. doi: 10.1016/j.biomaterials.2010.04.004.

Saha, S., Pramanik, K. and Biswas, A. (2019) 'Silk fibroin coated TiO2 nanotubes for improved osteogenic property of Ti6Al4V bone implants', *Materials Science and Engineering: C*, 105, p. 109982. doi: 10.1016/j.msec.2019.109982.

Santin, M. *et al.* (1999) 'In vitro evaluation of the inflammatory potential of the silk fibroin', *Journal of Biomedical Materials Research*, 46(3), pp. 382–389. doi: 10.1002/(SICI)1097-4636(19990905)46:3<382::AID-JBM11>3.0.CO;2-R.

Saris, N. E. L. *et al.* (2000) 'Magnesium: An update on physiological, clinical and analytical aspects', *Clinica Chimica Acta*, 294(1–2), pp. 1–26. doi: 10.1016/S0009-8981(99)00258-2.

Schäfer, S. *et al.* (2022) 'Antibacterial properties of functionalized silk fibroin and sericin membranes for wound healing applications in oral and maxillofacial surgery', *Biomaterials Advances*, 135, p. 212740. doi: 10.1016/j.bioadv.2022.212740.

Schäfer, S. *et al.* (2023) 'Silk proteins in reconstructive surgery: Do they possess an inherent antibacterial activity? A systemativ review', *Wound Repair and Regeneration*, 31(1), pp. 99–110. doi: 10.1111/wrr.13049.

Seo, Y. K. *et al.* (2007) 'The Biocompatibility of Silk Scaffold for Tissue Engineered Ligaments', *Key Engineering Materials*, 342–343, pp. 73–76. doi: 10.4028/www.scientific.net/KEM.342-343.73.

Serio, A. W. *et al.* (2018) 'Aminoglycoside Revival: Review of a Historically Important Class of Antimicrobials Undergoing Rejuvenation', *EcoSal Plus*. Edited by K. Bush, 8(1). doi: 10.1128/ecosalplus.ESP-0002-2018.

Shah, J. B. (2011) 'The History of Wound Care', *The Journal of the American College of Certified Wound Specialists*, 3(3), pp. 65–66. doi: 10.1016/j.jcws.2012.04.002.

Shao, Z. and Vollrath, F. (2002) 'Surprising strength of silkworm silk', *Nature*, 418(6899), pp. 741–741. doi: 10.1038/418741a.

Sheikh, Z. *et al.* (2015) 'Macrophages, Foreign Body Giant Cells and Their Response to Implantable Biomaterials', *Materials*, 8(9), pp. 5671–5701. doi: 10.3390/ma8095269.

Shen, T. *et al.* (2018) 'Dissolution behavior of silk fibroin in a low concentration CaCl2-methanol solvent: From morphology to nanostructure', *International Journal of Biological Macromolecules*, 113, pp. 458–463. doi: 10.1016/j.ijbiomac.2018.02.022.

Shi, Q. *et al.* (2017) 'GMSC-Derived Exosomes Combined with a Chitosan/Silk Hydrogel Sponge Accelerates Wound Healing in a Diabetic Rat Skin Defect Model', *Frontiers in Physiology*, 8. doi: 10.3389/fphys.2017.00904.

Shin, H., Ko, H. and Kim, M. (2016) 'Cytotoxicity and biocompatibility of Zirconia (Y-TZP) posts with

various dental cements', *Restorative Dentistry & Endodontics*, 41(3), p. 167. doi: 10.5395/rde.2016.41.3.167.

Sideratou, Z. *et al.* (2022) 'Antibiotic-Loaded Hyperbranched Polyester Embedded into Peptide-Enriched Silk Fibroin for the Treatment of Orthopedic or Dental Infections', *Nanomaterials*, 12(18), p. 3182. doi: 10.3390/nano12183182.

Silva, A. S. *et al.* (2022) 'Silk Sericin: A Promising Sustainable Biomaterial for Biomedical and Pharmaceutical Applications', *Polymers*, 14(22), p. 4931. doi: 10.3390/polym14224931.

Singh, S., Young, A. and McNaught, C.-E. (2017) 'The physiology of wound healing', *Surgery (Oxford)*, 35(9), pp. 473–477. doi: 10.1016/j.mpsur.2017.06.004.

Składanowski, M. *et al.* (2016) 'Evaluation of cytotoxicity, immune compatibility and antibacterial activity of biogenic silver nanoparticles', *Medical Microbiology and Immunology*, 205(6), pp. 603–613. doi: 10.1007/s00430-016-0477-7.

Smeets, R. *et al.* (2014) 'Knochenersatzmaterialien', *Der Freie Zahnarzt*, 58(10), pp. 78–88. doi: 10.1007/s12614-014-1989-4.

Smeets, R., Henningsen, A., *et al.* (2017) 'Allogene Knochenersatzmaterialien', *Der Freie Zahnarzt*, 61(9), pp. 74–82. doi: 10.1007/s12614-017-6767-7.

Smeets, R., Knabe, C., *et al.* (2017) 'Novel silk protein barrier membranes for guided bone regeneration', *Journal of Biomedical Materials Research - Part B Applied Biomaterials*, 105(8), pp. 2603–2611. doi: 10.1002/jbm.b.33795.

Smeets, R., Henningsen, A., *et al.* (2022) 'New and innovative biomaterials, techniques and therapy concepts: Biologization in maxillofacial surgery, oral surgery and dentistry is in full swing. PRF, PRGF, PRP, blood plasma-stabilized augmentations, supplementation of micronutrients and vitamins -', *GMS Interdisciplinary plastic and reconstructive surgery DGPW*, 11, p. Doc05. doi: 10.3205/iprs000166.

Smeets, R., Tauer, N., *et al.* (2022) 'Tissue Adhesives in Reconstructive and Aesthetic Surgery—Application of Silk Fibroin-Based Biomaterials', *International Journal of Molecular Sciences*, 23(14), p. 7687. doi: 10.3390/ijms23147687.

Smeets, R. *et al.* (2023) 'Regenerative Verfahren in der Mund-, Kiefer- und Gesichtschirurgie', *wissen kompakt*, 17(2), pp. 77–90. doi: 10.1007/s11838-023-00173-z.

Sobajo, C. *et al.* (2008) 'Silk : A Potential Medium for Tissue Engineering', *Journal of Plastic Surgery*, 8(47), pp. 438–446.

Song, D. W. *et al.* (2016) 'Multi-biofunction of antimicrobial peptide-immobilized silk fibroin nanofiber membrane: Implications for wound healing', *Acta Biomaterialia*, 39, pp. 146–155. doi: 10.1016/j.actbio.2016.05.008.

Song, Y. *et al.* (2022) 'Silk sericin patches delivering miRNA-29-enriched extracellular vesicles-decorated myoblasts (SPEED) enhances regeneration and functional repair after severe skeletal muscle injury', *Biomaterials*, 287, p. 121630. doi: 10.1016/j.biomaterials.2022.121630.

Srivastava, C. M. *et al.* (2015) 'Flexible Silk Fibroin Films for Wound Dressing', *Fibers and Polymers*, 16(5), pp. 1020–1030. doi: 10.1007/s12221-015-1020-y.

Stevanović, M. *et al.* (2020) 'Antibacterial graphene-based hydroxyapatite/chitosan coating with gentamicin for potential applications in bone tissue engineering', *Journal of Biomedical Materials Research Part A*, 108(11), pp. 2175–2189. doi: 10.1002/jbm.a.36974.

Sugihara, A. *et al.* (2000) ‘Promotive Effects of a Silk Film on Epidermal Recovery from Full-Thickness Skin Wounds’, *Proceedings of the Society for Experimental Biology and Medicine*, 225(1), pp. 58–64. doi: 10.1046/j.1525-1373.2000.22507.x.

Sugihara, A. *et al.* (2008) ‘Promotive Effects of a Silk Film on Epidermal Recovery from Full-Thickness Skin Wounds’, *Proceedings of the Society for Experimental Biology and Medicine*, 225(1), pp. 58–64. doi: 10.1111/j.1525-1373.2000.22507.x.

Sultan, T., Lee, O. J. and Kim, S. H. (2018) ‘Silk Fibroin in Wound Healing Process’.

Sun, K. *et al.* (2014) ‘Silk fibroin/collagen and silk fibroin/chitosan blended three-dimensional scaffolds for tissue engineering’, *European Journal of Orthopaedic Surgery and Traumatology*, 25(2), pp. 243–249. doi: 10.1007/s00590-014-1515-z.

Sun, W. *et al.* (2021) ‘Silk Fibroin as a Functional Biomaterial for Tissue Engineering’, *International Journal of Molecular Sciences*, 22(3), p. 1499. doi: 10.3390/ijms22031499.

Sutherland, T. D. *et al.* (2010) ‘Insect Silk: One Name, Many Materials’, *Annual Review of Entomology*, 55(1), pp. 171–188. doi: 10.1146/annurev-ento-112408-085401.

Takeda, S. (2009) *Bombyx mori*. Second Edi, *Encyclopedia of Insects*. Second Edi. Elsevier Inc. doi: 10.1016/B978-0-12-374144-8.00040-0.

Tanaka, K., Inoue, S. and Mizuno, S. (1999) ‘Hydrophobic interaction of P25, containing Asn-linked oligosaccharide chains, with the H-L complex of silk fibroin produced by Bombyx mori’, *Insect Biochemistry and Molecular Biology*, 29(3), pp. 269–276. doi: 10.1016/S0965-1748(98)00135-0.

Tang, J. *et al.* (2015) ‘Buccal mucosa repair with electrospun silk fibroin matrix in a rat model’, *International Journal of Artificial Organs*, 38(2), pp. 105–112. doi: 10.5301/ijao.5000392.

Tang, L., Thevenot, P. and Hu, W. (2008) ‘Surface Chemistry Influences Implant Biocompatibility’, *Current Topics in Medicinal Chemistry*, 8(4), pp. 270–280. doi: 10.2174/156802608783790901.

Tao, H., Kaplan, D. L. and Omenetto, F. G. (2012) ‘Silk materials - A road to sustainable high technology’, *Advanced Materials*, 24(21), pp. 2824–2837. doi: 10.1002/adma.201104477.

Terada, D. *et al.* (2016) ‘The outermost surface properties of silk fibroin films reflect ethanol-treatment conditions used in biomaterial preparation’, *Materials Science and Engineering C*, 58, pp. 119–126. doi: 10.1016/j.msec.2015.07.041.

Thangavel, P. *et al.* (2017) ‘Biomimetic hydrogel loaded with silk and <scp>l</scp> -proline for tissue engineering and wound healing applications’, *Journal of Biomedical Materials Research Part B: Applied Biomaterials*, 105(6), pp. 1401–1408. doi: 10.1002/jbm.b.33675.

Thurber, A. E., Omenetto, F. G. and Kaplan, D. L. (2015) ‘In vivo bioresponses to silk proteins’, *Biomaterials*, 71, pp. 145–157. doi: 10.1016/j.biomaterials.2015.08.039.

Tian, W. *et al.* (2019) ‘Evaluation of the biomedical properties of a Ca+-conjugated silk fibroin porous material’, *Materials Science and Engineering: C*, 104, p. 110003. doi: 10.1016/j.msec.2019.110003.

Toffler, M. (2014) ‘Guided bone regeneration (GBR) using cortical bone pins in combination with leukocyte- and platelet-rich fibrin (L-PRF)’, *Compendium of continuing education in dentistry (Jamesburg, N.J. : 1995)*, 35(3), pp. 192–198.

Ude, A. U. *et al.* (2014) ‘Bombyx mori silk fibre and its composite: A review of contemporary developments’, *Materials and Design*, 57, pp. 298–305. doi: 10.1016/j.matdes.2013.12.052.

Um, I. C. *et al.* (2001) ‘Structural characteristics and properties of the regenerated silk fibroin prepared

from formic acid', *International Journal of Biological Macromolecules*, 29(2), pp. 91–97. doi: 10.1016/S0141-8130(01)00159-3.
Unger, R. E. *et al.* (2004) 'Endothelialization of a non-woven silk fibroin net for use in tissue engineering: growth and gene regulation of human endothelial cells', *Biomaterials*, 25(21), pp. 5137–5146. doi: 10.1016/j.biomaterials.2003.12.040.
Üstündağ Okur, N. *et al.* (2019) 'An alternative approach to wound healing field; new composite films from natural polymers for mupirocin dermal delivery', *Saudi Pharmaceutical Journal*, 27(5), pp. 738–752. doi: 10.1016/j.jsps.2019.04.010.
Vollrath, F. and Knight, D. P. (2001) 'Liquid crystalline spinning of spider silk', *Nature*, 410(6828), pp. 541–548. doi: 10.1038/35069000.
Wadbua, P. *et al.* (2010) 'Different properties of electrospun fibrous scaffolds of separated heavy-chain and light-chain fibroins of Bombyx mori', *International Journal of Biological Macromolecules*, 46(5), pp. 493–501. doi: 10.1016/j.ijbiomac.2010.03.007.
Wang, D., Liu, H. and Fan, Y. (2017) 'Silk fibroin for vascular regeneration', *Microscopy Research and Technique*, 80(3), pp. 280–290. doi: 10.1002/jemt.22532.
Wang, H.-Y. and Zhang, Y.-Q. (2013) 'Effect of regeneration of liquid silk fibroin on its structure and characterization', *Soft Matter*, 9(1), pp. 138–145. doi: 10.1039/C2SM26945G.
Wang, M. *et al.* (2004) 'Mechanical Properties of Electrospun Silk Fibers', *Macromolecules*, 37(18), pp. 6856–6864. doi: 10.1021/ma048988v.
Wang, M. *et al.* (2023) 'Engineering functional natural polymer-based nanocomposite hydrogels for wound healing', *Nanoscale Advances*, 5(1), pp. 27–45. doi: 10.1039/D2NA00700B.
Wang, M. O. *et al.* (2013) 'Evaluation of the In Vitro Cytotoxicity of Cross-Linked Biomaterials', *Biomacromolecules*, 14(5), pp. 1321–1329. doi: 10.1021/bm301962f.
Wang, X. *et al.* (2005) 'Biomaterial Coatings by Stepwise Deposition of Silk Fibroin', *Langmuir*, 21(24), pp. 11335–11341. doi: 10.1021/la051862m.
Wang, X. *et al.* (2016) 'Comparative transcriptome analysis of Bombyx mori spinnerets and Filippi's glands suggests their role in silk fiber formation', *Insect Biochemistry and Molecular Biology*, 68, pp. 89–99.
Wang, X. *et al.* (2017) 'In vivo effects of metal ions on conformation and mechanical performance of silkworm silks', *Biochimica et Biophysica Acta - General Subjects*, 1861(3), pp. 567–576. doi: 10.1016/j.bbagen.2016.11.025.
Wang, X. *et al.* (2020) 'Osteoimmune Modulation and Guided Osteogenesis Promoted by Barrier Membranes Incorporated with S-Nitrosoglutathione (GSNO) and Mesenchymal Stem Cell-Derived Exosomes', *International Journal of Nanomedicine*, Volume 15, pp. 3483–3496. doi: 10.2147/IJN.S248741.
Wang, Y.-C. *et al.* (2018) 'Evaluation of a series of silk fibroin protein-based nonwoven mats for use as an anti-adhesion patch for wound management in robotic surgery', *Journal of Biomedical Materials Research Part A*, 106(1), pp. 221–230. doi: 10.1002/jbm.a.36225.
Wang, Y. *et al.* (2008) 'In vivo degradation of three-dimensional silk fibroin scaffolds', *Biomaterials*. doi: 10.1016/j.biomaterials.2008.05.002.
Wang, Y. *et al.* (2010) 'The synergistic effects of 3-D porous silk fibroin matrix scaffold properties and

hydrodynamic environment in cartilage tissue regeneration', *Biomaterials*, 31(17), pp. 4672–4681. doi: 10.1016/j.biomaterials.2010.02.006.

Wang, Y. *et al.* (2015) 'Flexible silk fibroin films modified by genipin and glycerol', *RSC Advances*, 5(123), pp. 101362–101369. doi: 10.1039/c5ra19754f.

Wang, Z. *et al.* (2022) 'Engineered multifunctional Silk fibroin cryogel loaded with exosomes to promote the regeneration of annulus fibrosus', *Applied Materials Today*, 29, p. 101632. doi: 10.1016/j.apmt.2022.101632.

Wenk, E., Merkle, H. P. and Meinel, L. (2011) 'Silk fibroin as a vehicle for drug delivery applications', *Journal of Controlled Release*, 150(2), pp. 128–141. doi: 10.1016/j.jconrel.2010.11.007.

Wigger-Alberti, W. *et al.* (2009) 'Using a novel wound model to investigate the healing properties of products for superficial wounds', *Journal of Wound Care*, 18(3), pp. 123–131. doi: 10.12968/jowc.2009.18.3.39813.

Witte, F. *et al.* (2005) 'In vivo corrosion of four magnesium alloys and the associated bone response', *Biomaterials*, 26(17), pp. 3557–3563. doi: 10.1016/j.biomaterials.2004.09.049.

Witwer, K. W. *et al.* (2013) 'Standardization of sample collection, isolation and analysis methods in extracellular vesicle research', *Journal of Extracellular Vesicles*, 2(1), p. 20360. doi: 10.3402/jev.v2i0.20360.

Wöltje, M. *et al.* (2021) 'A Fast and Reliable Process to Fabricate Regenerated Silk Fibroin Solution from Degummed Silk in 4 Hours'.

Wong, J., Chan, H. K. and Chrzanowski, W. (2014) *Silk for pharmaceutical and cosmeceutical applications*, *Silk Biomaterials for Tissue Engineering and Regenerative Medicine*. Woodhead Publishing Limited. doi: 10.1533/9780857097064.3.519.

Wray, L. S. *et al.* (2011) 'Effect of processing on silk-based biomaterials: Reproducibility and biocompatibility', *Journal of Biomedical Materials Research Part B: Applied Biomaterials*, 99B(1), pp. 89–101. doi: 10.1002/jbm.b.31875.

Xu, N. *et al.* (2018) 'Wound healing effects of a Curcuma zedoaria polysaccharide with platelet-rich plasma exosomes assembled on chitosan/silk hydrogel sponge in a diabetic rat model', *International Journal of Biological Macromolecules*, 117, pp. 102–107. doi: 10.1016/j.ijbiomac.2018.05.066.

Yamada, H. *et al.* (2001) 'Preparation of undegraded native molecular fibroin solution from silkworm cocoons', *Materials Science and Engineering: C*, 14(1), pp. 41–46. doi: 10.1016/S0928-4931(01)00207-7.

Yamada, H. *et al.* (2004) 'Identification of fibroin-derived peptides enhancing the proliferation of cultured human skin fibroblasts', *Biomaterials*, 25(3), pp. 467–472. doi: 10.1016/S0142-9612(03)00540-4.

Yang, C. *et al.* (2017) 'Nanoclay cross-linked semi-IPN silk sericin/poly(NIPAm/LMSH) nanocomposite hydrogel: An outstanding antibacterial wound dressing', *Materials Science and Engineering: C*, 81, pp. 303–313. doi: 10.1016/j.msec.2017.08.008.

Yang, Y. *et al.* (2007) 'Development and evaluation of silk fibroin-based nerve grafts used for peripheral nerve regeneration', *Biomaterials*, 28(36), pp. 5526–5535. doi: 10.1016/j.biomaterials.2007.09.001.

Yerra, A. and Dadala, M. M. (2022) 'Silk fibroin electrospun nanofiber blends with antibiotics and polyvinyl alcohol for burn wound healing', *Journal of Applied Polymer Science*, 139(15). doi: 10.1002/app.51930.

Yin, Z. *et al.* (2021) 'Biomimetic Mechanically Enhanced Carbon Nanotube Fibers by Silk Fibroin Infiltration', *Small*, 17(19). doi: 10.1002/smll.202100066.

Yoo, C.-K. *et al.* (2016) 'Cell attachment and proliferation of osteoblast-like MG63 cells on silk fibroin membrane for guided bone regeneration', *Maxillofacial Plastic and Reconstructive Surgery*, 38(1), p. 17. doi: 10.1186/s40902-016-0062-4.

Yu, X. *et al.* (2021) 'Conjugation of CMCS to silk fibroin for tuning mechanical and swelling behaviors of fibroin hydrogels', *European Polymer Journal*, 150, p. 110411. doi: 10.1016/j.eurpolymj.2021.110411.

Zaitoon, A. and Lim, L.-T. (2020) 'Effect of poly(ethylene oxide) on the electrospinning behavior and characteristics of ethyl cellulose composite fibers', *Materialia*, 10, p. 100649. doi: 10.1016/j.mtla.2020.100649.

Zhang, D. *et al.* (2019) 'Helicobacter pylori Ribosomal Protein-A2 Peptide/Silk Fibroin Nanofibrous Composites as Potential Wound Dressing', *Journal of Biomedical Nanotechnology*, 15(3), pp. 507–517. doi: 10.1166/jbn.2019.2707.

Zhang, S. *et al.* (2020) 'Extracellular Vesicles-Loaded Fibrin Gel Supports Rapid Neovascularization for Dental Pulp Regeneration', *International Journal of Molecular Sciences*, 21(12), p. 4226. doi: 10.3390/ijms21124226.

Zhang, W. *et al.* (2017) 'Silk Fibroin Biomaterial Shows Safe and Effective Wound Healing in Animal Models and a Randomized Controlled Clinical Trial', *Advanced Healthcare Materials*, 6(10), p. 1700121. doi: 10.1002/adhm.201700121.

Zhang, W. and Yelick, P. C. (2018) 'Craniofacial Tissue Engineering', *Cold Spring Harbor Perspectives in Medicine*, 8(1), p. a025775. doi: 10.1101/cshperspect.a025775.

Zhang, X. *et al.* (2012) 'Optimization of macroporous 3-D silk fibroin scaffolds by salt-leaching procedure in organic solvent-free conditions', *Journal of Materials Science: Materials in Medicine*. doi: 10.1007/s10856-011-4476-3.

Zhou, C.-Z. *et al.* (2001) 'Silk fibroin: Structural implications of a remarkable amino acid sequence', *Proteins: Structure, Function, and Genetics*, 44(2), pp. 119–122. doi: 10.1002/prot.1078.

Zhou, Q. *et al.* (2018) 'Preparation of a multifunctional fibroin-based biomaterial via laccase-assisted grafting of chitooligosaccharide', *International Journal of Biological Macromolecules*, 113, pp. 1062–1072. doi: 10.1016/j.ijbiomac.2018.03.042.

Zhou, W. *et al.* (2017) 'Bioinspired and Biomimetic AgNPs/Gentamicin-Embedded Silk Fibroin Coatings for Robust Antibacterial and Osteogenetic Applications', *ACS Applied Materials & Interfaces*, 9(31), pp. 25830–25846. doi: 10.1021/acsami.7b06757.

Zhu, H. *et al.* (2011) 'Preparation and characterization of bioactive mesoporous calcium silicate-silk fibroin composite films', *Journal of Biomedical Materials Research Part B: Applied Biomaterials*, 98B(2), pp. 330–341. doi: 10.1002/jbm.b.31856.

Zhu, M. *et al.* (2014) 'Fabrication of highly interconnected porous silk fibroin scaffolds for potential use as vascular grafts', *Acta Biomaterialia*, 10(5), pp. 2014–2023. doi: 10.1016/j.actbio.2014.01.022.

Zuo, B., Dai, L. and Wu, Z. (2006) 'Analysis of structure and properties of biodegradable regenerated silk fibroin fibers', *Journal of Materials Science*, 41(11), pp. 3357–3361. doi: 10.1007/s10853-005-5384-z.

12 Eidesstattliche Versicherung

Ich versichere ausdrücklich, dass ich die Arbeit selbständig und ohne fremde Hilfe verfasst, andere als die von mir angegebenen Quellen und Hilfsmittel nicht benutzt und die aus den benutzten Werken wörtlich oder inhaltlich entnommenen Stellen einzeln nach Ausgabe (Auflage und Jahr des Erscheinens), Band und Seite des benutzten Werkes kenntlich gemacht habe.
Ferner versichere ich, dass ich die Dissertation bisher nicht einem Fachvertreter an einer anderen Hochschule zur Überprüfung vorgelegt oder mich anderweitig um Zulassung zur Promotion beworben habe.
Ich erkläre mich einverstanden, dass meine Dissertation vom Dekanat der Medizinischen Fakultät mit einer gängigen Software zur Erkennung von Plagiaten überprüft werden kann.

Unterschrift: .....